



University College London

Department of Chemistry

Studies Towards Novel Aldolase Mimics

A thesis presented by

Yumiko Kato

**In Partial Fulfilment of The Requirements For The Award of The
Degree of**

Doctor of Philosophy

of

University College London

**University College London
Department of Chemistry
20 Gordon Street
London
WC1H 0AJ**

Declaration

I hereby declare that the research described in this thesis is my own work and that, to the best of my knowledge and belief, it contains no material previously published or written by another person nor material which has been accepted for the award of any other degree or diploma of the university or other institute of higher learning, except where due acknowledgment has been made in the text.

Abstract

The present thesis is concerned with a novel approach towards the design of artificial aldolase mimics.

The introductory chapter provides an overview of previous strategies and approaches that have been employed in the design and synthesis of artificial enzyme systems.

Following on from a brief introduction to previous work within our own group, Chapter 2 presents and discusses the preparation and reactivity of a number of novel polymeric systems which are capable of catalysing the aldol reaction. The strategy adopted consisted of the preparation of regiochemically defined alternating co-polymers wherein each of the two monomers, an *N*-alkylated maleimide and a *para* carboxamide styrene possessed either a carboxylic acid or an amino group and were hence capable of functioning as Class I aldolase mimetics.

A complementary strategy has also been undertaken wherein both functional groups involved in catalysis are attached to a single monomer, and subsequently subjected to ring opening metathesis polymerisation. This approach guaranteed attachment of these two groups in a fixed 1:1 ratio and had the added advantage of acting as organocatalysts in their own right. For this purpose, systems based on 7-azabicyclo[2.2.1]hept-2-ene, tropane alkaloid like derivatives and a functionalised norbornene were studied. Preliminary work towards functionalised bispidinone derivatives were also considered within this framework.

Chapter 3 provides a formal description of the detailed experimental results and procedures used.

Contents

Declaration	2
Abstract	3
Contents	4
Abbreviations	9
Acknowledgements	13
Chapter 1: Introduction	15
1.1 Introduction	15
1.2 Principles of Enzyme Catalysis	16
1.2.1 Transition State Theory	16
1.2.2 Determinant Factors in Enzyme Catalysis	19
1.3 The Aldol Reaction and Natural Aldolases	25
1.3.1 The Aldol Reaction	25
1.3.2 Zimmerman Traxler Model	25
1.3.3 Natural Aldolases	27
1.4 L-Proline as Class I ‘Micro-Aldolase’	30
1.4.1 Polymeric Systems Containing L-Proline	32
1.4.2 Peptides Containing L-Proline	35
1.4.3 L-Proline Derivatives as Efficient Organocatalysts	36
1.5 Previous Approaches to Artificial Enzymes	38
1.5.1 The Design Approach	38
1.5.1.1 β -Cyclodextrins as Class I Aldolase Mimics	39
1.5.1.2 Cyclophanes as Enzyme Mimics	42
1.5.1.3 Self-Assembled Molecular Capsules as Catalysts	45
1.5.1.4 Metal Complexes as Class II Aldolase Mimics	48
1.5.1.5 Cyclic Metalloporphyrin Trimers as Artificial Diels-Alderases	49
1.5.2 Transition State Analogue Selection Approach	51

1.5.2.1 Catalytic Antibodies as Class I Aldolase Mimics	51
1.5.2.2 Molecular Imprinted Polymers (MIPs) as Class II Aldolase Mimics	56
1.5.2.3 Imprinting an Artificial Proteinase	58
1.5.2.4 Bioimprinting	60
1.5.2.5 Dynamic Combinatorial Libraries	63
1.5.3 The Catalytic Activity Selection Approach	68
1.5.3.1 Combinatorial Polymers as Enzyme Mimics	68
1.5.3.2 Dendrimers Containing L-Proline as Aldolase Mimics	71
1.5.4 Directed Evolution of Enzymes	73
1.6 Conclusion	77
Chapter 2: Results and Discussion	80
2.1 Previous Research Within our Group	80
2.2 Objectives of the Current Research Programme	86
2.3 Alternating Co-polymers as Aldolase Mimics	88
2.3.1 Synthesis of Functionalised Maleimide Monomer with Proline	89
2.3.2 Synthesis of Functionalised Maleimide Monomer with Flexible Carboxylic Acid Group	92
2.3.3 Functionalised Styrene Monomers	93
2.3.3.1 Synthesis of Functionalised Styrene Monomer with Flexible Carboxylic Acid Group	94
2.3.3.2 Functionalised Styrene Monomer with Chiral Dicarboxylic Acid Group (L-Aspartic Acid)	95
2.3.3.3 Synthesis of Functionalised Styrene Monomer with Thiourea Binding Group	95
2.3.3.4 Functionalised Styrene Monomer with L-Proline	98
2.3.4 Polymerisation of Functionalised Maleimide and Styrene Monomers	99
2.3.5 The Aldol Reaction using 4-Nitrobenzaldehyde and Acetone	102
2.3.6 Type II Aldolase Mimics	108

2.3.7	Summary	115
2.4	A Complementary Approach to the Synthesis of Regiochemically Defined Polymers: - The Organocatalytic Route	117
2.4.1	Systems Based on a 7-Azabicyclo[2.2.1]hept-2-ene Core	118
2.4.2	Synthesis of [4+2] Cycloaddition Adducts	120
2.4.3	Systems Based Around the Tropane Alkaloid Core	123
2.4.4	Aldolase Mimics Based on Norbornene Derivatives	131
2.4.4.1	Ring Opening Metathesis Polymerisation (ROMP) of Norbornene Derivative	136
2.5	Functionalised Bispidinone Derivatives as Organocatalysts	139
2.6	Conclusions and Perspectives	143
 Chapter 3: Experimental		 148
3.1	(<i>R</i>)-4-Hydroxy-4-(4-nitrophenyl)butan-2-one (15)	151
3.2	<i>N</i>-<i>tert</i>-Butoxy(6-hydroxyhexyl)carbamate (96)	151
3.3	<i>N</i>-<i>tert</i>-Butoxy(2-aminoethyl)carbamate (99)	152
3.4	2,5-Dioxo-2,5-dihydro-pyrrole-1-carboxylic acid methyl ester (101)	153
3.5	<i>N</i>-<i>tert</i>-Butoxy[2-(2,5-dioxo-2,5-dihydro-pyrrol-1-yl)ethyl] carbamate (102)	154
3.6	(<i>S</i>)-2-[2-(2,5-Dioxo-2,5-dihydropyrrol-1-yl)ethylcarbamoyl] pyrrolidine-1-carboxylic acid <i>tert</i>-butyl ester (104)	155
3.7	6-(2,5-Dioxo-2,5-dihydropyrrol-1-yl)hexanoic acid (106)	156
3.8	6-Aminohexanoic acid methyl ester hydrochloride (108)	157
3.9	6-(4-Vinylbenzoylamino)hexanoic acid (109)	158
3.10	Aspartic acid dimethyl ester (111)	159
3.11	(<i>S</i>)- 2-(4-Vinyl-benzoylamino)succinic acid dimethyl ester (112)	160
3.12	(<i>S</i>)- 2-(4-Vinyl-benzoylamino)succinic acid (113)	161
3.13	1-(2-Aminoethyl)-3-phenylthiourea (118)	162

3.14	<i>N</i> -[2-(3-Phenylthioureido)ethyl]-4-vinylbenzamide (119)	163
3.15	(<i>S</i>)-2-Pyrrolidine-2-carboxylic acid [2-(4-vinyl-benzoylamino)ethyl]amide (124)	164
3.16	Maleic Anhydride – Styrene Co-polymer (132)	166
3.17	Functionalised Maleimide (104) – Styrene Co-polymer (133)	166
3.18	Functionalised Maleimide (104) – 4-vinylbenzoic acid Co-polymer (134)	167
3.19	Functionalised Maleimide (104) – 3-vinyl-benzoic acid Co-polymer (135)	168
3.20	Functionalised Maleimide (104) – Functionalised Styrene (109) Co-polymer (136)	169
3.21	Functionalised Maleimide (104) – Functionalised Styrene (119) Co-polymer (137)	170
3.22	Functionalised Maleimide (104) – Functionalised Styrene (113) Co-polymer (138)	171
3.23	<i>N</i> -Methyl Maleimide – Functionalised Styrene (109) Co-polymer (139)	172
3.24	Functionalised Maleimide (106) – Functionalised Styrene (124) Co-polymer (140)	173
3.25	4-Benzenesulfonyl-benzaldehyde (142)	174
3.26	(<i>R</i>)-4-Hydroxy-4-(4-trifluoromethyl-phenyl)butan-2-one (143)	175
3.27	(<i>R</i>)-4-Hydroxy-4-(4-benzenesulfonyl-phenyl)butan-2-one (144)	176
3.28	1-(4-Fluoro-benzenesulfonyl)-1 <i>H</i> -pyrrole (177)	177
3.29	4-(1 <i>H</i> -Pyrrol-1-ylsulfonyl)- <i>N</i> -(2-aminoethyl)benzenamine (178)	178
3.30	1,1,3,3-Tetrabromopropan-2-one (190)	178
3.31	Pyrrole-1-carboxylic acid <i>tert</i> -butyl ester (196)	179
3.32	2-Methoxy-2-methyl-[1,3]dioxan-5-one (197)	180
3.33	2-Triisopropylsilanyloxypropenal (198)	180
3.34	7-Oxabicyclo[2.2.1]heptene-endo-2,3-dicarboxylic anhydride (211)	181
3.35	<i>N</i> -Methyl-2,6-endimino-8,11-endomethylen-bicyclo[5.4.0]	

	undecen-(9)-on-(4) (212)	182
3.36	<i>N</i> -(5-Aminopentan-1-ol)-2,6-endimino-8,11-endomethylen-bicyclo[5.4.0]undecen-(9)-on-(4) (213)	183
3.37	Reductive Amination Product of 213 (214)	185
3.38	Tropane Alkaloid Derivative (215)	186
3.39	(1 <i>R</i> , 2 <i>S</i> , 6 <i>R</i> , 7 <i>R</i>)-4-Oxa-tricyclo[5.2.1.0 ^{2,6}]dec-8-ene-3,5-dione (218)	187
3.40	7-Oxabicyclo[2.2.1]heptene-endo-2,3-dicarboxylic anhydride (221)	188
3.41	3-(2- <i>tert</i> -Butoxycarbonylamino-ethylcarbamoylethyl)bicyclo[2.2.1]hept-5-ene-2-carboxylic acid (222)	189
3.42	6-([3-(2- <i>tert</i> -Butoxycarbonylamino-ethylcarbamoylethyl)bicyclo[2.2.1]hept-5-ene-2-carbonyl]amino)hexanoic acid methyl ester (224)	190
3.43	(2 <i>S</i>)-2-(2-([3-(5-Methoxycarbonyl-pentylcarbamoylethyl)bicyclo[2.2.1]hept-5-ene-2-carbonyl]amino)ethylcarbamoylethyl)pyrrolidino-1-carboxylic acid <i>tert</i> -butyl ester (225)	191
3.44	3-(5-Methoxycarbonyl-pentylcarbamoylethyl)bicyclo[2.2.1]hept-5-ene-2-carboxylic acid (226)	193
3.45	(<i>S</i>)-(9 <i>H</i> -Fluoren-9-yl)methyl-2-([2-(<i>tert</i> -butoxycarbonyl)ethyl]carbamoylethyl)pyrrolidine-1-carboxylate (227)	194
3.46	(2 <i>S</i>)-2-6-([3-(2-([Pyrrolidine-2-carbonyl]amino)ethylcarbamoylethyl)bicyclo[2.2.1]hept-5-ene-2-carbonyl]amino)hexanoic acid methyl ester (229)	195
3.47	(2 <i>S</i>)-2-6-([3-(2-([Pyrrolidine-2-carbonyl]-amino)ethylcarbamoylethyl)bicyclo[2.2.1]hept-5-ene-2-carbonyl]amino)hexanoic acid; hydrochloride (230)	197
3.48	1,1-Dimethyl-4-oxo-piperidinium iodide (240)	198
3.49	[2-(4-Oxo-piperidin-1-yl)-ethyl]carbamic acid <i>tert</i> -butyl ester (241)	199
3.50	7-Benzyl-9-oxo-3,7-diaza-bicyclo[3.3.1]nonane-3-carboxylic acid <i>tert</i> -butyl ester (244)	200

Abbreviations

Ab	antibodies
Ac	acetyl
AIBN	2,2'-azobisisobutyronitrile
AMP	adenosine monophosphate
ANEH	<i>Aspergillus niger</i> epoxide hydrolase
Ar	aromatic
Asp	aspartic acid
ATP	adenosine triphosphate
BAS	5-bromoacetylsalicylate
B-FIT	B-factor iterative test
Bn	benzyl
Boc	<i>tert</i> -butoxycarbonyl
br	broad
CA	6-aminocaproic acid
CAST	combinatorial active site saturation test
Cbz	benzyloxycarbonyl
CD	cyclodextrin
CI	chemical ionisation
CLIP	crosslinked imprinted protein
CPMO	cyclopentanone monooxygenase
C _q	quaternary carbon
CSA	camphor-10-sulfonic acid
d	doublet
DBM	dibenzoylmethane
DCC	<i>N,N'</i> -dicyclohexylcarbodiimide
DCL	dynamic combinatorial library
DCM	dichloromethane
DEAD	diethyl azodicarboxylate
DHAP	dihydroxyacetone phosphate

DHP	dihydropyridine
DIAD	diisopropyl azodicarboxylate
DIC	diisopropylcarbodiimide
DMAP	dimethylaminopyridine
DMF	dimethylformamide
DMSO	dimethyl sulfoxide
DNA	deoxyribonucleic acid
E	enzyme
EDC	1-[3-(dimethylamino)propyl]-3-ethylcarbodiimide hydrochloride
<i>ee</i>	enantiomeric excess
EI	electron impact
EP	enzyme-product complex
epPCR	error-prone polymerase chain reaction
ES	enzyme-substrate complex
ESI	electrospray ionisation
ESR	electron spin resonance
Et	ethyl
FAB	fast atom bombardment
FAD	flavin adenine dinucleotide
FBP	D-fructose 1,6-bis(phosphate)
FG	functional group
Fmoc	9-fluorenylmethoxycarbonyl
FruA	D-fructose 1,6-bisphosphate aldolase
FT-IR	fourier transform infrared
FucA	L-fuculose-1-phosphate aldolase
G3P	D-glyceraldehyde 3-phosphate
Glu	glutamate
Gly	glycine
GPE	glycidyl phenyl ether
GPX	glutathione peroxidase
HATU	O-(7-azabenzotriazol-1-yl)- <i>N,N,N',N'</i> -tetramethyluronium hexafluorophosphate

His	histidine
HMPA	hexamethylphosphoramide
HPLC	high performance liquid chromatography
HRMS	high resolution mass spectrometry
ISM	iterative saturation mutagenesis
Lys	lysine
m	multiplet
Me	methyl
MIP	molecular imprinted polymer
m.p.	melting point
NADH	nicotineamide adenine dinucleotide
NMM	<i>N</i> -methyilmorpholine
NMR	nuclear magnetic resonance
NOESY	nuclear Overhauser enhancement spectroscopy
Nu	nucleophile
P	product
PAA	poly(allylamine)
PAD	poly(aminomethylstyrene-co-divinylbenzene)
PAL	<i>pseudomonas aeruginosa</i> lipase
PBS	phosphate buffered saline
PDC	pyridinium dichromate
PEG	poly(ethyleneglycol)
PEI	poly(ethylenimine)
PFG	pulsed field gradient
Ph	phenyl
ppm	parts per million
Pr	propyl
Pro	proline
Py	pyridine
qn	quintet
RCM	ring closing metathesis
R _f	retention factor

RNA	ribonucleic acid
ROMP	ring opening metathesis polymerisation
RT	room temperature
s	singlet
S	substrate
Sal	salicylate
Ser	serine
t	triplet
Tf	triflate
TFA	trifluoroacetic acid
T _g	glass transition temperature
ThDP	thiamine diphosphate
THF	tetrahydrofuran
TIPS	triisopropyl silyl
t.l.c	thin layer chromatography
TMS	tetramethylsilane
Ts	tosyl
TSA	transition state analogue
Tyr	tyrosine
UV	ultraviolet
VCL	virtual combinatorial library

Acknowledgements

First and foremost I would like to thank my supervisor Professor Willie Motherwell for the opportunity to carry out my PhD in his research group. I will be eternally grateful for his brilliant and somewhat crazy ideas as well as his amusing anecdotes.

I would also like to thank Steve Hilton, the most selfless person I know, who always took care of me when I needed him. It is ok to say 'No' sometimes! Tom Sheppard, aaaahh Tom. What can I say! A brilliant mind, an exceptional chemist and a fascinating human being. It was great having a walking encyclopaedia for three years. Thank you so much for all your advice. As I'm still on the subject of postdocs, I'd like to thank Helen Chapman too, who seems to be the lab 'ho' in terms of chemistry, hopping from one project to another. I will reminisce on our short affair with fondness. Ela Smiljanic, without whom this project may not have existed. Your electronic advice has been invaluable.

Moussa Sehailia, need I say more, and of course I can't mention Moussa without Chi Tang, you two made one heck of a duo! Talking of duos, Phil Gray and Burt Waller, collectively known as Philburt...you two were inseparable, bonded together with the love you had for Sunhill. I will cherish the moments I shared with both of you. Chris Phang, although you were only in the lab for a few weeks, I'd like to think that I gained a friend for life...your continuous string of insults will be remembered with fondness.

My year buddies, Sandra Luengo Arratta and Laure Jerome. I love you both for your eccentricities. Lorna, I never thought you'd leave but you did eventually. Thanks for introducing me to 'Ciao Bella' – it's so GOOOD! Alex Cayley, as a fellow IC, it seemed like we both adopted the no. 1 rule of antisocialism. It was nice sharing those rare moments of rap madness with you – keep it real (!!!).

Thierry de Merode – there is so much I could say about you but I think I’ll just say ‘Woooo Hooooo’, ‘Yeeee Haaa’.

And now my dear Josie Arendorf. I consider you to be one of my closest friends and I will always remember our fumehood shenanigans. Keep on Flip-Flopping! Not forgetting the lovely Mr. Penny who replaced the gap left by Philburt. It’s down to you to carry on the light side legacies. James Galman, another peep not within my research group but a vital part of my PhD. I couldn’t have gotten all my *ees* on time without you. I O U big time! The same goes for my housemate Alan Lobo, who’s had to put up with my endless whinging during my write-up. Thanks for keeping me sane. Oh and to add a bit of mystery...Chris (Eel) Foster...you know who you are – cheers for being you ;p

I cannot end the acknowledgements without thanking John and Lisa from mass spec. as well as Abil Aliev from NMR. Without you guys there would be no experimental section...well at least half! Last but not least, Dr. Robyn Motherwell - thank you so much for buying all those expensive chemicals and for allowing me to whinge and whine in the process.

Each and every one of you mentioned on these two pages has had a great impact on my life as well as my PhD. So a one last BIG FAT THANK YOU!!!

Finally, this thesis is dedicated to my mum, who’s been always been there for me. I love you xxx

Chapter 1: Introduction

1.1 Introduction

Enzymes are biomolecules that have been developed by nature over billions of years to catalyse chemical reactions which would proceed too slowly on their own to sustain life. They are able to carry out these reactions with extraordinary regio- and stereoselectivity and thus have inspired chemists to explore synthetic equivalents. In order to achieve this, a better understanding of the principles behind enzyme catalysis is required so that novel artificial enzymes can be developed which rival natural enzymes in terms of rate accelerations, turnover and specificity. Furthermore, research into artificial enzymes provides an opportunity to design catalysts for reactions for which there are no natural enzyme equivalents.

Since the present thesis is concerned with the design and synthesis of artificial enzymes, it is therefore appropriate to provide a discussion of the main principles behind enzyme catalysis and an overview of the previous approaches which have been taken towards the creation of artificial enzymes. As implied in the title of the thesis, the artificial enzymes selected for investigation are related to those that catalyse the aldol reaction, and therefore, when appropriate, previous methods used in artificial aldolases will be exemplified. A brief overview of the mechanisms of natural aldolases as well as recent studies undertaken using L-proline and its derivatives, which can be considered as a ‘micro-aldolase’ system, will also be discussed.

1.2 Principles of Enzyme Catalysis

Enzymes are renowned for their remarkable ability to catalyse highly specific chemical reactions of biological importance. They differ from ordinary synthetic chemical catalysts in several ways. Firstly the rates of reactions catalysed by enzymes are typically factors of 10^6 to 10^{12} greater than those of the corresponding uncatalysed reaction and at least several orders of magnitude larger than those that are chemically catalysed. Secondly the reactions occur under very mild conditions, with temperatures generally below $100\text{ }^\circ\text{C}$ under atmospheric pressure and at nearly neutral pH. Thirdly, they have a greater degree of specificity for their substrates and the products formed, in comparison to chemical catalysts which often produce unwanted side products or incomplete reactions, limiting the efficiency of these chemical transformations.¹ It is therefore highly relevant to appreciate those factors which are considered to be responsible for such exquisite catalytic success.

1.2.1 Transition State Theory

The transition state theory is derived mainly from the work by Eyring (1935), and relates the rates of chemical reactions to thermodynamic properties of a transition state.

The reaction pathway between an enzyme (E) and a substrate (S) can be represented by the following equation (**Equation 1.1**).² The first step involves the formation of an enzyme-substrate complex (ES), which undergoes a series of chemical transformations to give the activated complex (ES*). The substrate is then converted to the final product, still bound to the enzyme (EP), before being released to give the product (P) and the unbound enzyme (E).



Equation 1.1: Representation of the enzymic reaction pathway.

In 1948, Pauling proposed that catalysis occurs due to the ability of the enzyme to stabilise the transition state structure for the reaction relative to that of the ground state of the substrate.³ Since the transition state of a chemical reaction is the point of highest free energy on the reaction coordinate, catalysts act by lowering the activation barrier for the reaction, allowing the chemical transformation to take place under milder conditions and at an accelerated rate. The following free energy diagram can be used to illustrate this process for a unimolecular reaction (**Figure 1.1**):

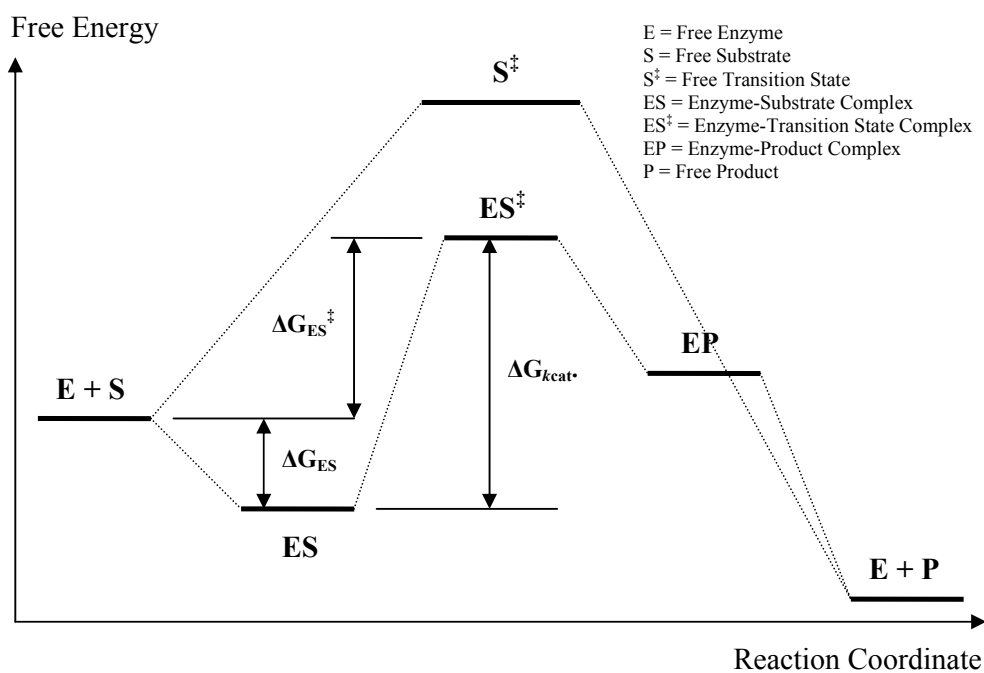


Figure 1.1: Energy diagram of an enzyme-catalysed reaction and the corresponding uncatalysed chemical reaction.

In the absence of an enzyme, product formation must take place by overcoming the high energy barrier required to reach the transition state S^\ddagger . In the presence of an enzyme, the reaction first proceeds *via* the ES complex, an intermediate along the reaction pathway that is not available in the uncatalysed reaction. Here the binding energy associated with ES complex formation can, to some degree, be

used to drive the formation of the transition state. Once binding has occurred, molecular forces in the bound molecule destabilises the ground state configuration of the bound substrate molecule, favouring the formation of the transition state. This means that complex ES^\ddagger occurs at a lower energy than the free S^\ddagger state.

The reaction next proceeds *via* another intermediate state, the enzyme-product complex (EP) before the final product (P) is released to give the free enzyme (E). It is worth noting that the initial and final states are energetically identical in the catalysed and uncatalysed reactions. However the overall activation energy barrier has been substantially reduced in the enzyme catalysed case.

ΔG_{ES^\ddagger} is the overall activation energy and is composed of ΔG_{ES} and ΔG_{kcat} . ΔG_{kcat} is the amount of energy required to reach the transition state, while ΔG_{ES} refers to the net energy gain associated with the enzyme-substrate binding energy. This reduction in activation barrier is the basis for acceleration of reaction rate in the presence of an enzyme.²

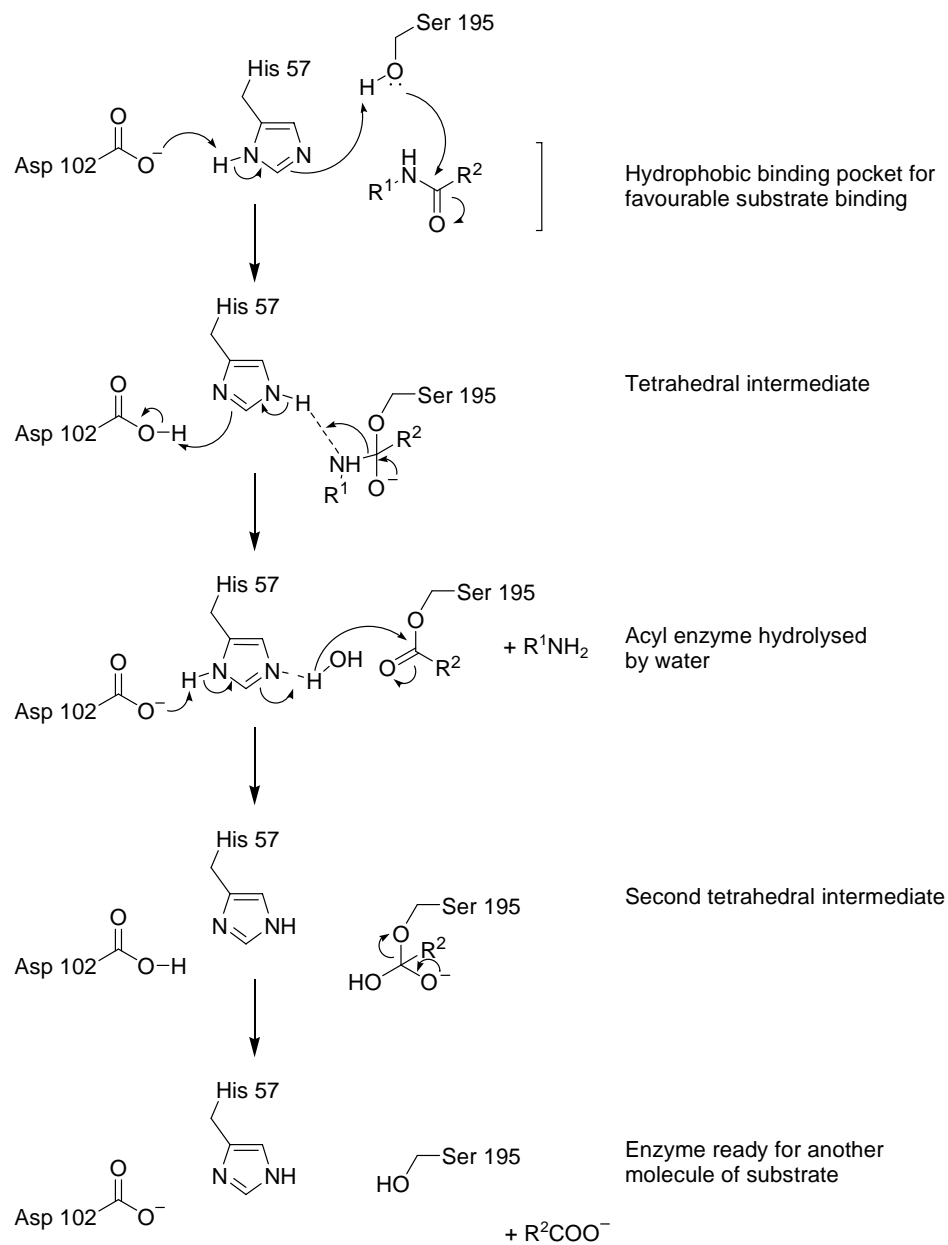
In order to gain a fuller picture of catalysis, the system also needs to exhibit turnover which is defined as the number of reaction processes that each active site catalyses per unit time. This will only occur efficiently if the enzyme-substrate complex is lower in energy than the enzyme-product complex. If the opposite was to take place, then product inhibition of the enzyme would be displayed. In summary, this picture of enzyme action requires both the transition state stabilisation and thermodynamically favourable release of the product to be considered when designing the active site of an enzyme mimic.

It should be appreciated however that the transition state theory is a simplification of the real situation and therefore in more complex cases of enzyme catalysis, for example in those involving bimolecular processes or covalent catalysis, the above model of transition state stabilisation becomes much more complex and requires further factors to be taken into account.

1.2.2 Determinant Factors in Enzyme Catalysis

In simplistic terms, four main factors are thought to contribute towards catalytic activity of enzymes. Firstly relevant functional groups are required to polarise key bonds to atoms, thus facilitating the proton transfer processes which occur throughout the reaction pathway. Secondly a binding site must be present which is able to immobilise the substrate at the active site. Thirdly, the substrate must be in the correct and precise orientation within the enzyme so that each reaction step involves only a small rotation about a single bond to align the attacking groups near to optimal directions. Finally, the activation energy must be lowered by reducing the energy of enzyme-substrate complex at the transition state. It should be noted that these factors cannot be separated from one another and the combination of these effects contributes towards the efficient function of the enzyme as a catalyst.

These can be illustrated by considering the classical activity of α -chymotrypsin which catalyses the hydrolysis of peptide bonds in protein foods.⁴ The mechanism involves a catalytic triad within the active site, composed of serine, histidine and aspartic acid residues in a charge relay system (**Scheme 1.1**).⁴



Scheme 1.1: Mode of hydrolysis in α -chymotrypsin.

The mode of hydrolysis is initiated by the polarisation of the imidazole ring of His-57 by buried Asp-102 with an associated negative charge, which induces a positive charge adjacent to it. The inherent excess negative charge left on the imidazole ring thus strengthens the hydrogen bonding between His-57 and Ser-195, facilitating the proton transfer from Ser-195 to His-57. The Ser-195 is then

left with a reactive alkoxide which is able to attack the amide bond of the substrate nestled within the hydrophobic pocket of the active site, in the correct geometry and orientation for attack. The tetrahedral intermediate which is stabilised by hydrogen bond formation between the carbonyl group of the substrate and the amide hydrogen of Ser-195 and Gly-193 lowers the activation energy and facilitates the collapse of this transition state to give an acyl enzyme, which is hydrolysed by water, since there is no proton available, linking His-57 and Ser-195. Subsequent nucleophilic attack by water allows the formation of another tetrahedral intermediate, which eliminates a carboxylic acid to regain the enzyme.^{4,5}

Although this gives an overview of how transition state stabilisation *via* hydrogen bonding lowers the activation energy of the reaction for efficient catalysis, a better understanding of how enzymes achieve selective binding of the transition state must also be discussed. These come in the form of intermolecular forces which include hydrogen bonding,⁶ electrostatic forces,⁷ hydrophobic interactions,⁶ Van der Waals forces⁷ and π -stacking.⁸ Since enzymes operate in water, the effects of desolvation must also be taken into account.

Hydrogen bonding and electrostatic forces contribute significantly to the total binding affinity between a substrate and an enzyme and are a major determinant of specificity in enzyme catalysis. However these reactions generally take place in water and therefore these effects are often moderated by solvation.⁹ Fersht however managed to quantify the contribution of hydrogen bonding by studying the coupling of tyrosine to adenosine triphosphate (ATP) to give tyrosyl adenosine monophosphate (AMP) which is catalysed by tyrosyl-transfer RNA synthase ($tRNA^{Tyr}$). By analysing the three-dimensional structure of the enzyme *via* X-ray crystallography, it was found that eleven possible hydrogen bonds could be formed between the amino acid side chains of the enzyme and the substrate. By systematically mutating these residues, the contributions of these side chains to binding were calculated. When a side chain which formed strong hydrogen bonds with an uncharged group on the substrate was removed, the binding energy

was weakened by $0.5 - 1.5 \text{ kcal mol}^{-1}$.¹⁰ This meant that binding was only increased by a factor of $2.5 - 15$. If however a side chain which formed hydrogen bonds with a charged group on the substrate was removed, the binding energy was weakened by $\sim 3.5 - 4.5 \text{ kcal mol}^{-1}$. This has much more of a significant effect and increased binding by a factor of 1000. It has therefore been suggested that the role of hydrogen bonding is to determine ligand specificity by creating an energy penalty for binding the wrong ligand.

Electrostatic interactions often occur between charged side chains of amino acid residues on the enzyme and a charged group on the substrate. During mitochondrial electron transfer cascade, electrons are transferred from the protein cytochrome c to an enzyme cytochrome oxidase, to reduce oxygen to water during cellular respiration. This process can only occur if the two species form a complex which is tight enough to allow electrons to jump from the protein to the enzyme. The crystal structure of cytochrome c revealed a large number of positively charged lysine residues and the corresponding binding site within cytochrome oxidase contained a high density of glutamic and aspartic acid residues. From this, it was assumed that the formation of the close-fit complex arose from the electrostatic interactions which were formed between the charged amino acid residues.²

The hydrophobic effect in selective binding has also been highlighted as an important interaction within an enzyme-substrate complex.⁶ This stabilisation arises from the transfer of a hydrocarbon surface out of water and into a hydrophobic region of an enzyme receptor. The favourable interaction and positive change in free energy, as ordered water molecules surrounding the hydrophobic surfaces are released into bulk water, provides a driving force for this process. Removal of the hydrophobic surface area from water into a hydrophobic region within a receptor site is worth $0.68 \text{ kcal mol}^{-1}$ which is approximately a 3.2-fold increase in binding constant per methyl group. It is well known that hydrophobic interactions often play a vital role in drug design by concept of an 'induced fit' in which the receptor site undergoes a conformational

change to optimise the hydrophobic interactions with the substrate. This notion can be exemplified by looking at the interactions involved in the complexes of **1** and **2** which act as inhibitors of the matrix metalloproteinase stromelysin (**Figure 1.2**).¹¹

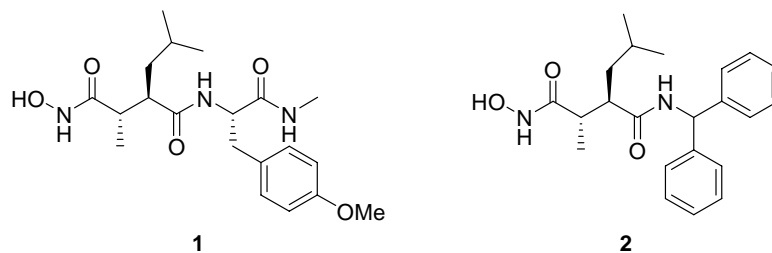


Figure 1.2: Structures of the inhibitors of matrix metalloproteinase stromelysin.

It was found that while the 4-methoxybenzyl group of **1** and the phenyl group of **2** showed similar binding conformations, replacing the *N*-methyl amide group in **1** by a phenyl group in **2** induced an unexpected conformational shift within the loop region of the enzyme. This meant that the two complexes showed major differences in the interactions that stabilised them within the protein. While complex **1** showed favourable hydrogen bonding to the backbone of stromelysin, **2** was bound by favourable Van der Waals and hydrophobic interactions. This demonstrated the profound ability of an enzyme to undergo conformational changes due to its flexibility to accomplish optimal binding.

Van der Waals forces contribute approximately 1 kcal mol⁻¹ to binding stabilisation. Although in certain situations, where a large number of Van der Waals forces are formed, they can collectively stabilise the enzyme-substrate complex, these do not alter the binding equilibrium to any significant degree.² This is due to the fact that Van der Waals forces between the first and second rows of the periodic table are insensitive to the nature of the atoms involved. As a result, there is no significant change on replacing solvent-ligand contacts with solvent-solvent or enzyme-ligand contacts.⁷

π -stacking interactions have also received attention due to their possible

involvement in ion selectivity in potassium channels. It is thought that a cation- π interaction between the side chains of phenylalanine, tyrosine or tryptophan and those of lysine or arginine may have a significant role in the functioning of potassium channels. The numerous aromatic residues found within the channel pore seem to form numerous cation- π interactions which are thought to be key factors in their ion selectivity.^{8;12;13} The magnitude of these interactions can be quite significant, for example in the case between a potassium ion and a benzene ring, it can be as high as 19 kcal mol^{-1} . Therefore these forces should not be ruled out when examining the factors which contribute to enzyme catalysis.

All of the intermolecular interactions discussed above involve binding between a discrete ligand and a receptor site. However this does not take into account the interactions that occur at the active site of the enzyme between the transition state of a substrate and the host, since the bonding interactions in this case are dynamic in nature. These binding phenomena termed ‘dynamic binding’ interactions distinguish between an active artificial enzyme and a synthetic receptor. This concept was illustrated by Kirby using serine proteases (**Figure 1.3**).¹⁴

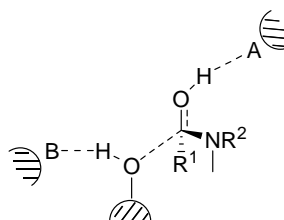


Figure 1.3: Representation of dynamic binding for amide bond cleavage in serine protease.

The transition state involves at least six bonds being made or broken during the amide cleavage process, where it is difficult to identify when transition binding starts and finishes. The key point of this is that simple molecular recognition is not enough to explain the binding interactions involved between the transition state and the enzyme. These partially formed or broken covalent bonds or ‘dynamic binding’ can be far greater than the individual interactions involved in ordinary molecular recognition and can have a major effect on the efficiency of

the catalytic process.

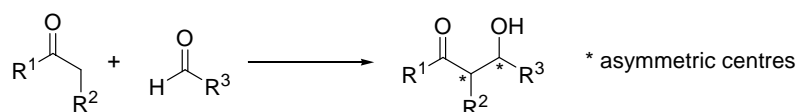
All of the factors discussed above contribute to the overall picture of how enzymes stabilise transition states and achieve selective binding. Combining this information allows for the creation of effective enzyme mimics and provides a solid basis for understanding the true nature by which enzymes perform catalysis.

1.3 The Aldol Reaction and Natural Aldolases

Within the context of the present thesis, the interplay of many of the above contributions can also be seen in the aldolase group of enzymes which have evolved to catalyse this key carbon – carbon bond forming reaction.

1.3.1 The Aldol Reaction

The catalytic asymmetric variant of this reaction is, of course, not only a fundamental method for carbon – carbon bond formation in organic chemistry but also allows the absolute configuration of the two newly formed stereogenic centres to be controlled.



Scheme 1.2: General aldol reaction.

1.3.2 Zimmerman Traxler Model

In 1957, Zimmerman and Traxler explained how enolate geometry controlled the stereochemical outcome of the aldol reaction using a model, now known as the Zimmerman Traxler model (**Figure 1.4**).¹⁵

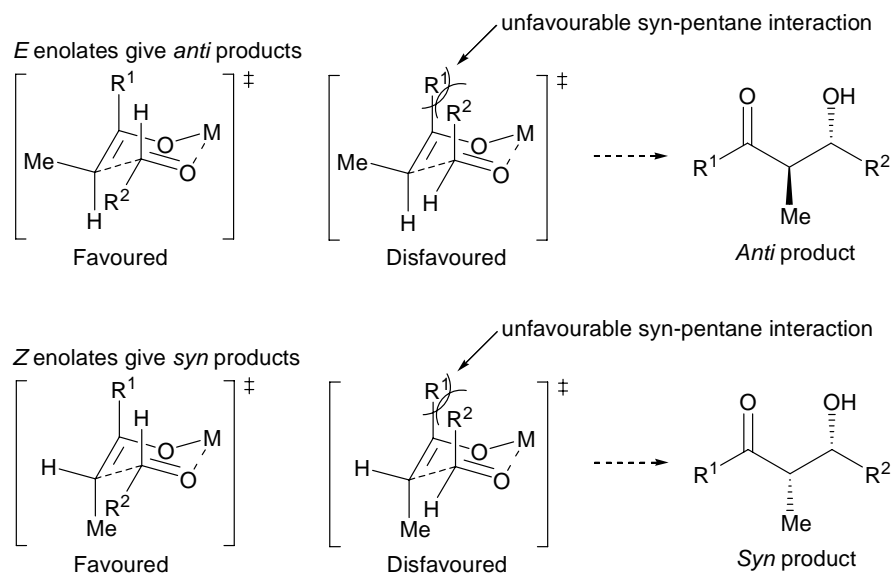


Figure 1.4: Zimmerman Traxler model for the aldol reaction.

They proposed that aldol reactions occur *via* a six-membered ring transition state where the ring adopts a chair conformation. As the diagram suggests, *E* enolates give rise to *anti* products whereas the *Z* enolates give *syn* products. This selectivity arises from the preference for placing the substituents equatorially in the six-membered transition state and thus avoiding the unfavourable *syn*-pentane interactions. It is worth noting that only some metals such as lithium or boron reliably follow this model and therefore the reaction may have unpredictable outcomes.

In terms of the asymmetric aldol reaction, the absolute configuration of the two stereogenic centres formed is dependent not only on the Zimmerman Traxler model but also in the approach of the aldehyde to either the *si* or the *re* face of the planar enolate.

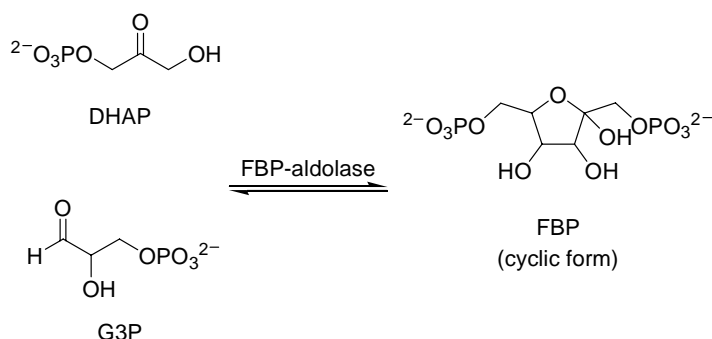
In nature, enzymes often have a cluster of amino acid residues which assist the active catalytic group to carry out this aldol reaction to ensure high selectivity and enantioselectivity, relying on the intermolecular interactions and polarisation of key bonds.

1.3.3 Natural Aldolases

Aldolases are a group of enzymes which are able to catalyse the aldol reaction in a reversible manner. Like all enzymes, this occurs with great regio- and stereoselectivity, under very mild conditions.⁹

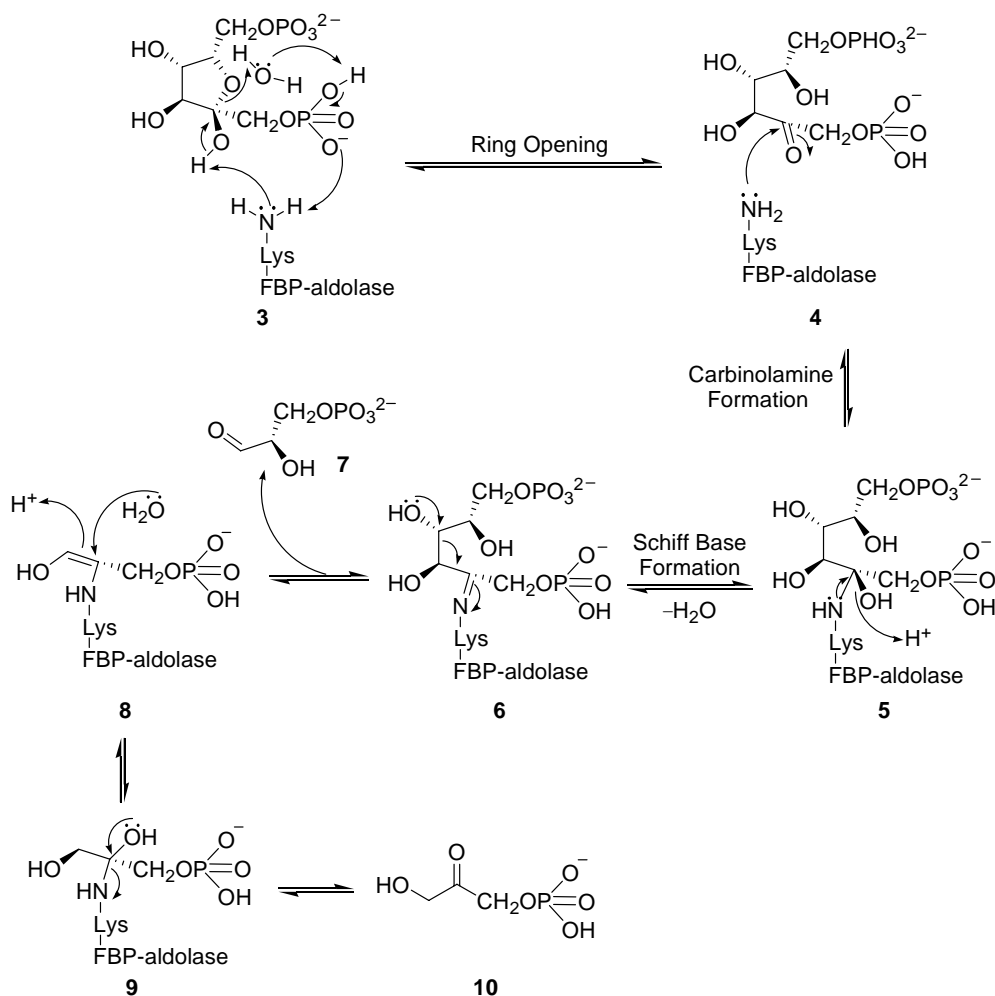
There are two types of aldolases, Class I and Class II, which are classified by their mode of catalysis. Class I aldolases utilise the ϵ -amino group of a lysine residue in the active site *via* an enamine mechanism and are found naturally in animals and plants. Class II aldolases are metalloenzymes that facilitate enolate formation by coordination to the substrate's carbonyl oxygen. This process is most commonly mediated by using a zinc cofactor and they are found in yeasts, bacteria and fungi. This difference in reactivity can be illustrated by using fructose 1,6-bis(phosphate) aldolase (FBP-aldolase, EC 4.1.2.13) as an example, which exists as both homotetrameric Class I and homodimeric Class II aldolases.

FBP-aldolase is a natural aldolase which catalyses the cleavage of D-fructose 1,6-bis(phosphate) (FBP) to dihydroxyacetone phosphate (DHAP) and D-glyceraldehyde 3-phosphate (G3P) and the reverse formation of FBP from DHAP and G3P (**Scheme 1.3**).¹⁶



Class I FBP-aldolase contains a lysine residue in the active site which becomes covalently linked with the substrate to form a Schiff base during catalysis

(Scheme 1.4).¹⁷

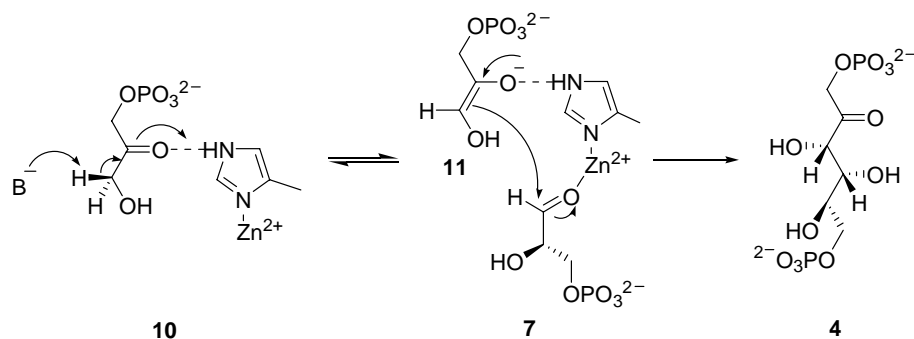


Scheme 1.4: Proposed reaction mechanism for Schiff base formation in Class I FBP-aldolase.

The first step of the mechanism involves ring opening of the substrate **3** to produce the acyclic FBP **4**. Nucleophilic attack on the carbonyl group by the Lys residue of the FBP-aldolase then forms the carbinolamine intermediate **5**. Subsequently, a proton is donated to the carbinolamine, followed by dehydration to yield the Schiff base **6**. The key retro-aldol reaction then takes place to give G3P **7** and the enolate **8**, which undergoes nucleophilic attack by water to give **9**. Finally elimination of the FBP-aldolase gives DHAP **10**. Since all of these reactions are reversible, the same mechanistic steps would also apply to the

formation of FBP from G3P and DHAP, in which an aldol reaction would yield the key Schiff base **6**.

In contrast to Class I FBP-aldolase, the Class II counterpart contains a divalent Zn^{2+} ion which is coordinated by three histidine (His) residues. It is believed that the Zn^{2+} ion facilitates catalysis by polarising the carbonyl group of D-glyceraldehyde 3-phosphate when bound to the enzyme (**Scheme 1.5**).¹⁸



Scheme 1.5: Proposed reaction mechanism for Class II FBP-aldolase.

The mechanism involves proton abstraction of the substrate **10** by a base (B^-) to form the enolate **11**, followed by an aldol reaction which is facilitated by coordination of the substrates to a Zn^{2+} ion and a histidine (His) residue to yield the product **4**.

It is worth noting that the mechanisms shown for both type I and type II aldolases are in fact much more complex in reality than those described, and involve the interplay of the surrounding amino acid residues and the intermolecular interactions which are formed within the active site. This makes it significantly more difficult to design and synthesise chemical equivalents by trying to re-create the exact environment of these enzymes. As a result, chemists have turned to small organic molecules, which are able to catalyse the aldol reaction by exploiting the key aspects of the reaction, such as imine and iminium ion formation. Amino acids fulfil this criteria, and in particular, L-proline, which contains a secondary amine and is therefore able to form more stable imine and

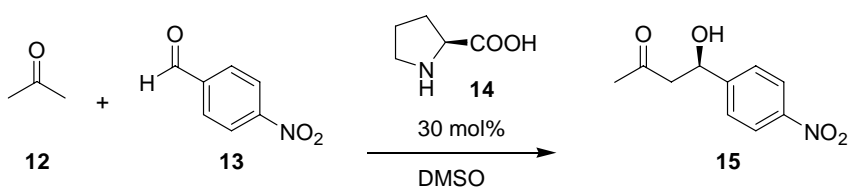
iminium species, has received great attention due to its efficiency in catalysing the aldol reaction. It is therefore only apt to summarise the evolution of L-proline as a ‘micro-aldolase’.

1.4 L-Proline as Class I ‘Micro-Aldolase’

Proline is the first example of a non-metallic, small-molecule catalyst which was able to undergo direct intermolecular aldol reactions. There are many advantages associated with the use of proline. It is non-toxic, inexpensive and readily available in both enantiomeric forms. The reaction does not require inert conditions and can be run at room temperature. No prior modification of the carbonyl substrates such as deprotonation or silylation is required. The catalyst is also water soluble and therefore readily removed by aqueous extraction. Potentially the reactions may also be run on an industrial scale.

List first reported that the amino acid L-proline could be used as an effective catalyst for direct, asymmetric aldol reaction between acetone and a variety of aldehydes with good yields and high enantioselectivities.¹⁹

Their initial study between acetone **12** and 4-nitrobenzaldehyde **13** using L-proline **14** (30 mol%) furnished the aldol product (*R*)-**15** in 68% yield and with 76% *ee* (Scheme 1.6).



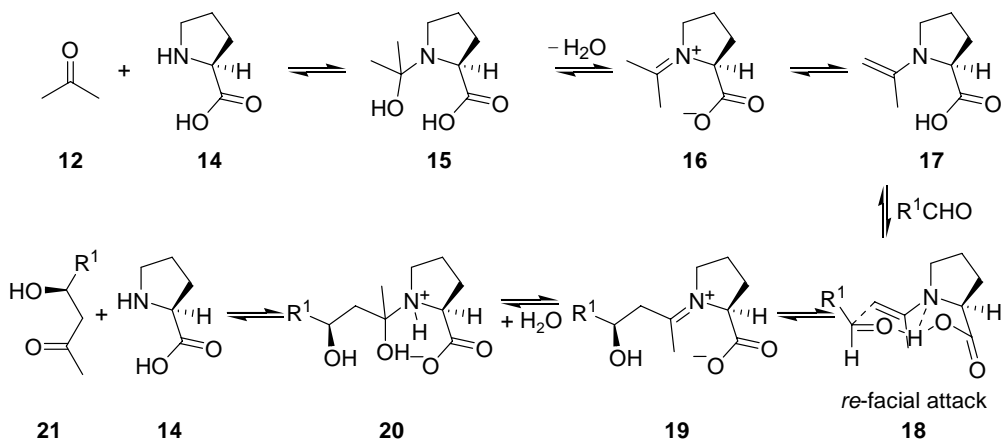
Scheme 1.6: Aldol reaction between acetone and 4-nitrobenzaldehyde catalysed by L-proline.

What is impressive about this transformation is that the high concentration of acetone suppresses any side reactions which may normally occur. For example it

is known that acetone can undergo self-aldolisation²⁰ and aromatic aldehydes can condense with proline to form azomethine ylides that undergo further 1,3-dipolar cycloaddition reactions.²¹ However the only significant side product is the α,β -unsaturated ketone. During their studies, DMSO was found to be the most suitable solvent with respect to both reaction time and enantioselectivity. Also since primary and acyclic secondary amino acids failed to give significant amount of desired product, it was concluded that the pyrrolidine ring and the carboxylate are essential for efficient catalysis to occur.

L-proline functions as a 'micro-aldolase', catalysing the reaction *via* an enamine mechanism as in natural Class I aldolases (**Scheme 1.7**).¹⁹ It provides both the nucleophilic amino group and an acid/base co-catalyst in the form of the carboxylic acid. This co-catalyst is thought to facilitate each individual step of the mechanism.

Although there were various speculations about the mechanism of L-proline-catalysed aldol reactions, calculations by Houk²² and density functional theory study by Domingo²³ also support the following mechanism.

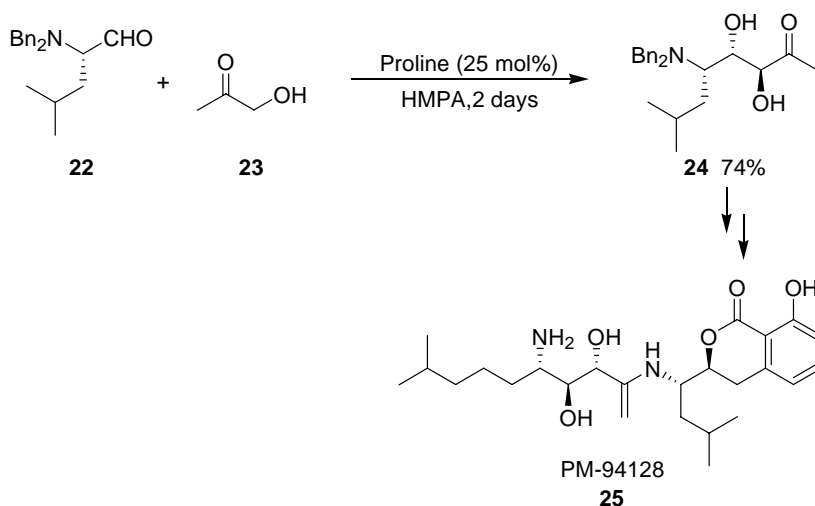


Scheme 1.7: The proposed enamine mechanism of the proline-catalysed asymmetric aldol reaction.

The first step of the mechanism involves nucleophilic attack by L-proline **14** on

the carbonyl group of acetone **12**, to give the carbinolamine intermediate **15**. Dehydration of this intermediate leads to the iminium species **16** which undergoes carboxylate-assisted deprotonation to yield **17**. This is followed by the key aldol reaction which occurs on the *re*-face to give **19**. Finally, hydrolysis of the iminium-aldol intermediate furnishes the aldol product **21** and regenerates proline **14**. The enantioselectivity is clearly shown by the tricyclic hydrogen bonded framework on **18** which resembles a metal free version of the Zimmerman-Traxler type transition state.

Since this discovery, L-proline has been applied to many direct asymmetric aldol reactions. Ma²⁴ recently reported the use of L-proline to provide the major aldol product of hydroxyacetone **23** with *N,N*-dibenzyl isoleucinal **22** to afford the intermediate **24** for the assembly of PM-94128 **25**, an anti-tumour agent originally synthesised by Vallee (**Scheme 1.8**).²⁵



Scheme 1.8: The key aldol reaction catalysed by L-proline used in the total synthesis of the anti-tumour agent PM-94128.

1.4.1 Polymeric Systems Containing L-Proline

In further developments of this concept, Cozzi reported a poly(ethyleneglycol)-supported proline (PEG-Pro) which exploited the solubility profile of PEG to give

the catalyst an added advantage of being soluble in many organic solvents, and insoluble in others (**Figure 1.5**). This allowed the reaction to proceed under homogeneous conditions, but also facilitated easy recovery and rendered the catalyst readily recyclable, as if working under heterogeneous conditions. Being an organic catalyst, this eliminated any complications of metal leaching. Also the polymer backbone acted as the peptide skeleton and L-proline as the catalytic site. These catalysts were found to catalyse various enantioselective aldol and iminoaldol reactions.²⁶

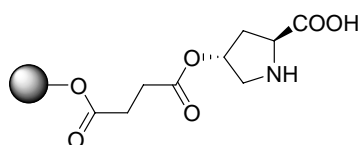


Figure 1.5: PEG-Pro developed by Cozzi.

Tao²⁷ also reported new recyclable L-proline-based linear polystyrene anchored catalysts for aldol reaction in the presence of water (**Figure 1.6**).

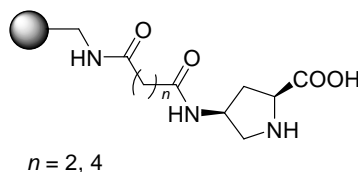
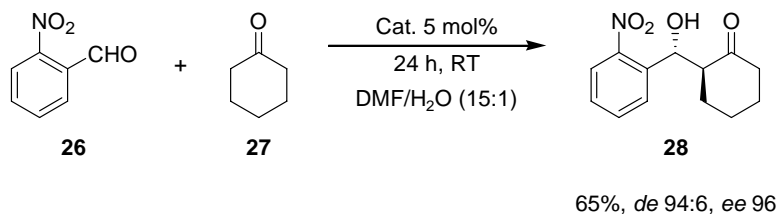


Figure 1.6: L-proline-based polystyrene anchored catalyst developed by Tao.

These were tested in the reaction between *o*-nitrobenzaldehyde **26** and cyclohexanone **27** in the presence of 5 mol% catalyst to yield the product **28** (**Scheme 1.9**).



Scheme 1.9: Asymmetric aldol reaction between *o*-nitrobenzaldehyde and cyclohexanone.

The best result was obtained using DMF/H₂O in a ratio of 15:1. It was proposed

that an interaction between water and the hydrophilic L-proline moiety increased the amphiphilic property of the catalysts. This meant that the hydrophilic catalytic moiety avoided the hydrophobic main chains, allowing it to interact with the substrates more efficiently. The improvement in diastereoselectivity and enantioselectivity in the presence of small amounts of water was attributed to the possible participation of water in the transition state during the catalytic aldol condensation. When the performance of the catalysts were evaluated, it was found that they could be re-used at least five times without any obvious decrease in diastereoselectivity or enantioselectivity although the reactivity decreased somewhat after repeating the reaction for the fourth time.

In terms of their scope for substrates, these catalysts were able to perform the aldol reaction between cyclohexanone and other aromatic aldehydes containing electron withdrawing groups.

Similarly Pericas²⁸ reported various polymeric systems in which L-proline was bonded to polystyrene through a 1,2,3-triazole linker as an efficient aldolase mimic for the reaction between cyclic ketones and a variety of aromatic aldehydes in water with excellent yield, diastereoselectivities and enantioselectivities (**Figure 1.7**). It is thought that in this case, the particular functional arrangement in the monomer as well as the linker ensemble in the resin appeared to have facilitated the establishment of hydrogen bond-based aqueous macrophase around the hydrophilic resin, which in turn played a fundamental role in its catalytic activity.

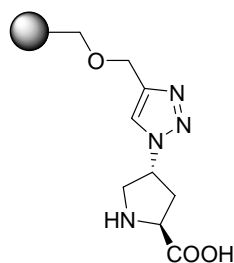


Figure 1.7: Polymeric L-proline-based catalyst with a 1,2,3-triazole linker developed by Pericas.

Other examples include novel prolinamide-supported polystyrene catalysts developed by Gruttadauria which catalysed the direct aldol reaction between cyclic and non-cyclic ketones and various aromatic aldehydes (**Figure 1.8**).²⁹

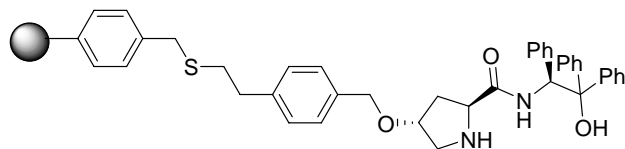
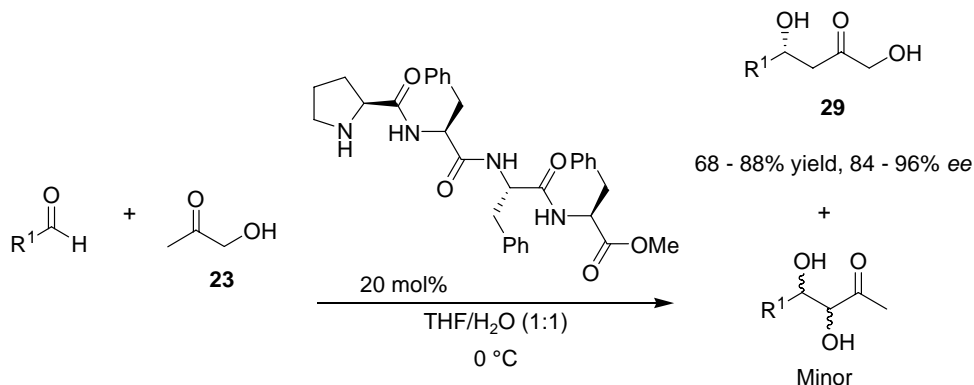


Figure 1.8: Polystyrene-supported prolinamide synthesised by Gruttadauria.

1.4.2 Peptides Containing L-Proline

A similar idea has also been applied to the synthesis of L-proline amides and dipeptides acting as efficient catalysts for asymmetric aldol reactions, due to their structures resembling the chiral non-covalent bonding environment in enzymes.³⁰

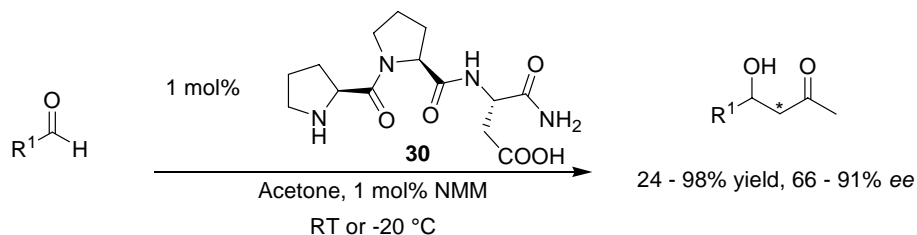
Gong developed L-proline-based small peptides as efficient catalysts for the asymmetric aldol reactions of hydroxyacetone **23** with aldehydes. Chiral 1,4-diols **29** which are disfavoured products in similar aldol reactions catalysed by L-proline or aldolases, were obtained in high yields and enantioselectivities (**Scheme 1.10**).³⁰



Scheme 1.10: Asymmetric direct aldol reactions of hydroxyacetone with aldehydes using an L-proline-based peptide.

This is a unique method for obtaining chiral 1,4-dihydroxy-1,2-ones directly from aldehydes and 2-hydroxyl ketones.

Wennemers also reported an H-Pro-Pro-Asp-NH₂ peptide as an efficient organocatalyst for direct asymmetric aldol reaction (**Scheme 1.11**).³¹



Scheme 1.11: Aldol reaction catalysed by H-Pro-Pro-Asp-NH₂.

It was found that peptide **30** was able to catalyse the aldol reaction between acetone and several aldehydes in high yields and enantioselectivities, using just 1 mol% of the catalyst.

This catalyst relies on both the *N*-terminal secondary amine and the carboxylic acid group in the side chain of the aspartic acid residue for efficient catalysis.

1.4.3 L-Proline Derivatives as Efficient Organocatalysts

The scope of the L-proline-catalysed direct enantioselective aldol reactions between aldehydes and ketones was fairly narrow until a few years ago. However more substrates, especially functionalised aldehydes and ketones have been explored in recent years and its application has been expanded for the synthesis of many useful chemicals. This can be illustrated by the flourishing number of L-proline derivatives that have been developed to encompass a greater range of substrates. Some of these are shown below (**Figure 1.9**) and all include L-proline at their core but also contain various ancillary substituents and groups to enhance enantio- and diastereoselectivity.³²⁻³⁸

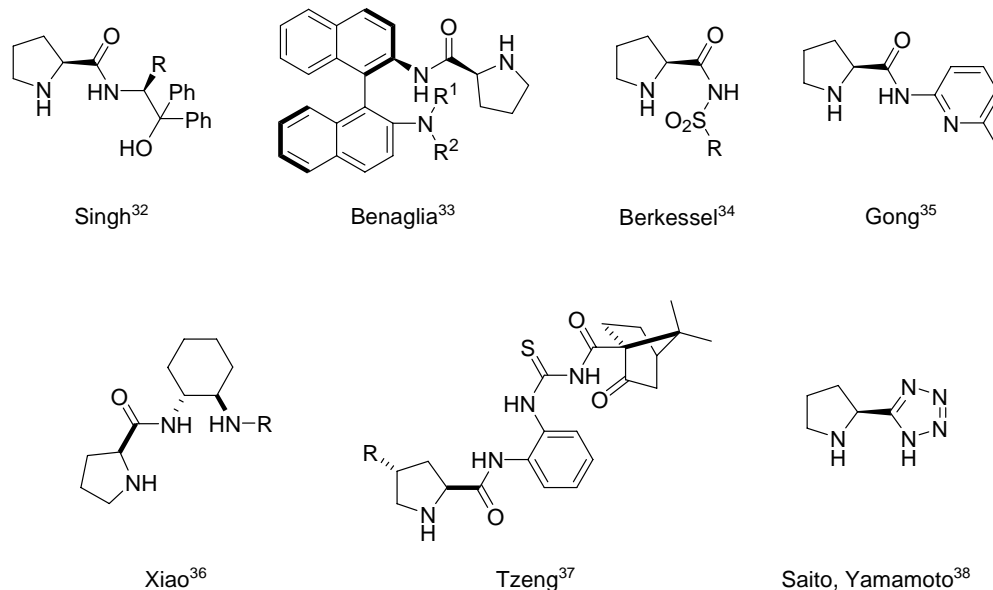


Figure 1.9: L-proline derivatives as efficient organocatalysts.

The entire area of organocatalysis is still expanding rapidly and this has been illustrated by the entire August 2004 issue of the *Accounts of Chemical Research* as well as work by McMillan.³⁹

Although this section has focused on L-proline-based aldol reactions, it is worth mentioning that due to the inherent versatility of the L-proline molecule, it has recently found application in many other types of reactions. L-Proline has been used as a ligand in asymmetric transition-metal catalysis, a chiral modifier in heterogeneously catalysed hydrogenations and as an effective organocatalyst by itself of several asymmetric transformations such as Mannich and Michael additions⁴⁰ It is worth noting just how powerful and remarkable a tool the L-proline molecule actually is in modern organic chemistry.

Although the foregoing discussion of L-proline as a ‘micro-aldolase’ is appropriate to our own studies, the major focus of the current thesis necessitates an overview of previous approaches to artificial enzymes.

1.5 Previous Approaches to Artificial Enzymes

Traditional approaches to the synthesis of artificial enzymes were focused on rational design and involved the synthesis of complex molecules *via* laborious synthetic routes. Although some impressive results were achieved using this process, they were often time consuming, both in conception and practice, and more importantly, the smallest flaw in design led to catastrophic consequences. In light of this fact, with the addition of recent advances in the fields of molecular biology, biochemistry, combinatorial and polymer chemistry, the field of artificial enzymes was able to evolve, combining expertise from both chemistry and biology to develop novel artificial enzymes. Recent strategies have concentrated on the idea of selection, either through binding or directly by catalytic activity. In general terms, these can be divided into three categories; the design approach, the transition state analogue selection approach and catalytic activity selection approach. Each will be discussed in more detail in the following sections.

1.5.1 The Design Approach

This involves the design of macromolecular receptors which have the appropriate functionality to mimic the binding, catalytic activity and microenvironment of the active site of the enzyme. These are often inspired by the natural enzymes, and evolve from examination of the amino residues which may be involved in catalysis for a particular reaction. A great deal of the work in this field has focused on the design and synthesis using functionalised cyclodextrins as an aromatic ring acceptor.⁴¹⁻⁴⁶ However, more recently, those based on cyclophanes,⁴⁷ and covalent conjugation⁴⁸ have yielded some remarkable results, and provided a more versatile alternative to cyclodextrins. The realisation of ideas in such a process however tend to be arduous and although some impressive successes have been reported, efficient catalysis which rivals that of the natural enzyme in terms of selective binding, rate accelerations and turnover still seems a long way off.

1.5.1.1 β -Cyclodextrins as Class I Aldolase Mimics

Cyclodextrins also known as Schardinger dextrins, cycloamyloses or cycloglucoamylases, comprise a family of cyclic oligosaccharides obtained from starch by enzymatic degradation. They were discovered by Villiers in 1891⁴⁹ but the first detailed description of the preparation and isolation of cyclodextrins was reported in 1903 by Schardinger.⁵⁰ The most common cyclodextrins consist of α -, β -, γ -, and δ -cyclodextrins which are comprised of six, seven, eight and nine glucose units respectively. However those with 10-13 glucose units have also been identified by chromatographic methods.

Out of these, β -cyclodextrins (β -CD) have received most attention in the field of artificial enzymes. As their appearance suggests, in the β -cyclodextrin molecule, the glucose units are all arranged in the C1 chair conformation and are linked by $\alpha(1\rightarrow4)$ glycosyl bonds (**Figure 1.10**).

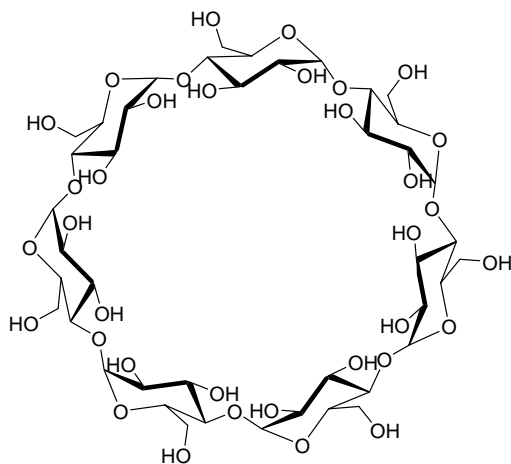


Figure 1.10: Structure of β -cyclodextrin

This geometry inherently gives the molecule an overall shape of a truncated cone with the wider side formed by the secondary 2- and 3-hydroxyl groups and the narrower side by the primary 6-hydroxyl groups. The cavity is lined by the hydrogen atoms and the glycosidic oxygen bridges (**Figure 1.11**).

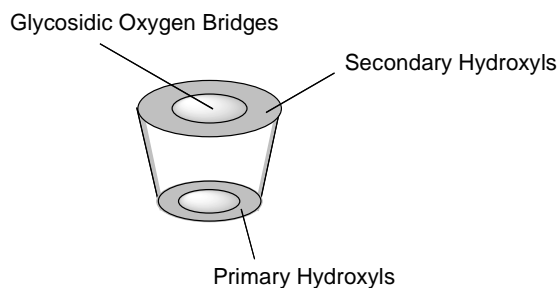


Figure 1.11: Functional structural scheme of β -cyclodextrin.

The non-bonding electron pairs of the glycosidic oxygen bridges are directed toward the inside of the cavity, producing a high electron density environment and lending it some Lewis base character. As a result of this unique arrangement of the functional groups in the β -CD molecule, the cavity is relatively hydrophobic compared to water while the external faces are hydrophilic. In the β -CD molecule, a ring of hydrogen bonds is also formed intramolecularly between the 2-hydroxyl and the 3-hydroxyl groups of adjacent glucose units. This hydrogen bonding ring gives β -CD a remarkably rigid structure.⁵¹

These features allow the binding of hydrophobic substrates, especially an aromatic ring, in their cavities, and permit facile modification for attachment of catalytic functional groups *via* the hydroxyl groups,⁵² making them attractive building blocks for the assembly of artificial enzymes and biomimetic materials. As well as this, they are readily available,⁵³ non-toxic, cheap, stable under basic conditions, and water soluble. Therefore it is not surprising that scientists have studied these molecules as potential enzyme mimics for the last few decades. These have included bimolecular⁵⁴ or intramolecular⁵⁵ Diels-Alder reactions, ester hydrolysis,⁵⁶ epoxidation of cyclohexene⁵⁷⁻⁶⁰ and benzoin condensation.^{61;62} Since this thesis is concerned with the aldol reaction, only the example relevant to this field will be discussed in detail.

A β -CD which was designed to mimic the ribonuclease A (RNA) was synthesised by attaching two imidazole rings to the primary face of β -CD (**Figure 1.12**). When the two imidazoles were in different geometries, this allowed for reactions

which required simultaneous acid-base proton transfers, such as aldol reactions.⁶³

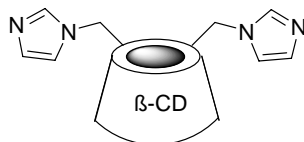
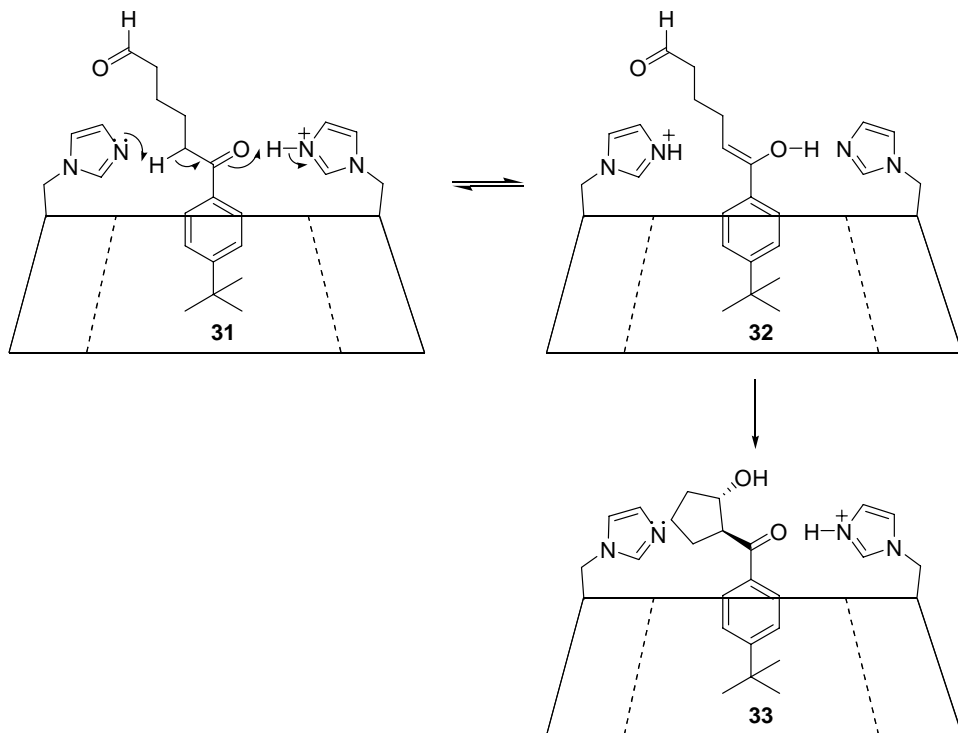


Figure 1.12: Representation of β-cyclodextrin functionalised with two imidazole groups.

Breslow utilised these imidazole-bearing CD molecules in an intramolecular aldol cyclisation of the keto aldehyde **31**, to yield exclusively the *trans*-keto alcohol **33** (Scheme 1.12).⁵³ This mechanism below illustrates the importance of both the imidazole and imidazolium ion in catalysis.



Scheme 1.12: Proposed reaction mechanism of β-cyclodextrin functionalised with two imidazole groups acting as an aldolase mimic.

β-CD containing other amino moieties were also found to mimic Class I aldolases by a Schiff base mechanism to catalyse crossed aldol condensations.⁵³

Using cyclodextrins as aldolase mimics does however have certain disadvantages. They are susceptible to acid hydrolysis and their rigidity can often limit the range of aromatic substrates that can be accommodated within them. These problems to an extent have been overcome by the introduction of cyclophanes as an alternative.

1.5.1.2 Cyclophanes as Enzyme Mimics

Although there is no uniformly accepted definition of a cyclophane, in general terms, it refers to an aromatic unit, primarily a benzene ring, bridged with hydrocarbon chains between non-adjacent positions of the ring. The most commonly used form of cyclophanes are those based on [n,n']paracyclophanes (**Figure 1.13**):⁶⁴

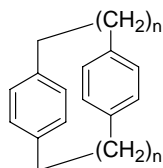


Figure 1.13: General structure of [n,n']paracyclophane.

As the structure illustrates, by altering the length of the hydrocarbon chains and the nature of the aromatic rings employed, the flexibility and cavity size can be tailored to fit the necessary spatial requirements. Therefore these features allow more versatility compared to cyclodextrins.

An impressive example of the application of cyclophanes as enzyme mimics was reported by Diederich^{65;66} who employed the design approach to create a pyruvate oxidase mimic, which utilises thiamine diphosphate (ThDP) and flavin adenine dinucleotide (FAD) as coenzymes. (**Figure 1.14**)

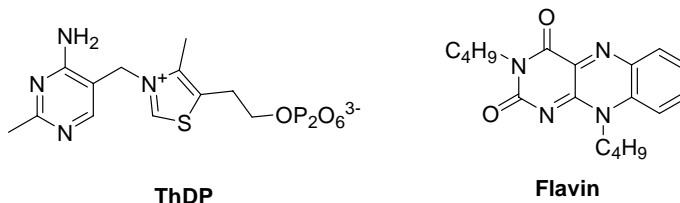
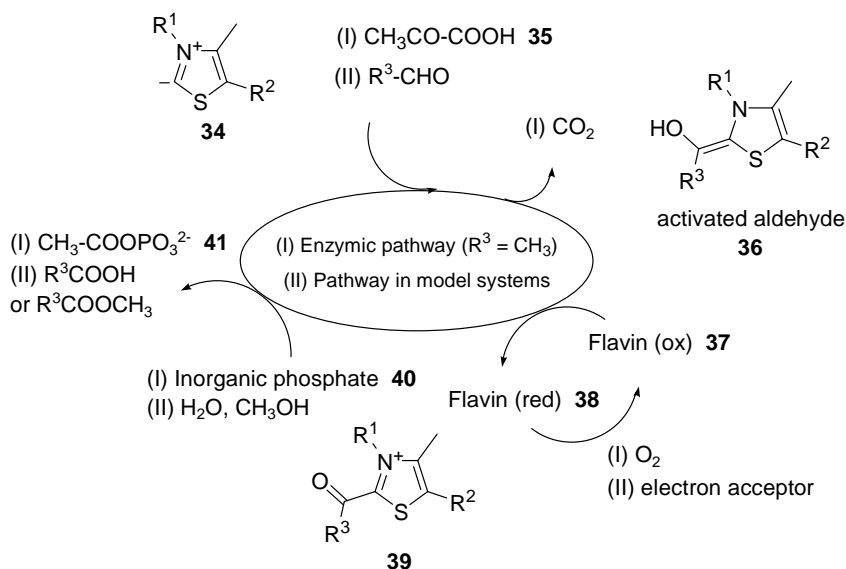


Figure 1.14: Structures of the coenzymes Flavin and ThDP employed by pyruvate oxidase.

This enzyme catalyses the transformation of pyruvate **35** to acetyl phosphate **41** (**Scheme 1.13**). The first step involves decarboxylation of pyruvate **35** which is mediated by ThDP **34** to generate an active aldehyde **36**. This is in turn oxidised by FAD **37**, to give the reduced form of flavin **38**, (FADH₂) which is re-oxidised by dioxygen. Oxidation of the active aldehyde produces the 2-acetylthiazolium intermediate **39**, which is attacked by the inorganic phosphate nucleophile **40** to give acetyl phosphate **41** and regenerate the thiazolium ylide **34**.



Scheme 1.13: Catalytic cycle for the conversion of pyruvate to acetyl phosphate catalysed by pyruvate oxidase. (I) Enzymic pathway. (II) Pathway in model systems.

In a similar fashion, thiazolium ions in the presence of flavin catalysed the oxidation of aldehydes in either water or alcohols to carboxylic acids or esters respectively.

Diederich synthesised a model of pyruvate oxidase using a functionalised cyclophane which contained a well defined binding site in addition to flavin and

thiazolium groups attached in a covalent manner (**Figure 1.15**).^{65,66}

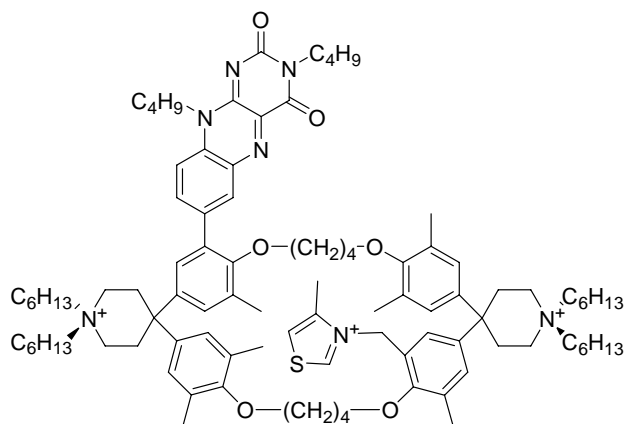
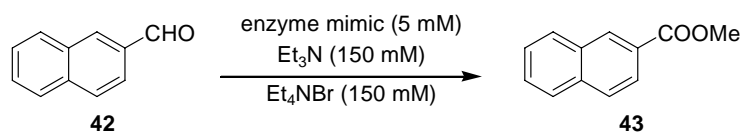


Figure 1.15: Pyruvate oxidase mimic by Diederich.

It was thought that the proximity of the flavin and thiazolium groups to the binding site would be an improvement relative to the previous system which did not incorporate a covalently bonded flavin moiety.⁶⁷ It was also more likely to mimic the natural pyruvate oxidase more closely where the two coenzymes are covalently bound within the active site of the enzyme.

This catalyst was indeed found to be active in an oxidation reaction to transform naphthalene-2-carbaldehyde **42** to naphthalene-2-carboxylate **43** under basic conditions in methanol with a k_{cat} of 0.22 s^{-1} . (**Scheme 1.14**).



MeOH, Ar atmosphere, 308 K, 16 h
working electrode: Pt foil
counter electrode: Pt foil
E = -0.3 V vs Ag/AgCl

Scheme 1.14: Transformation of naphthalene-2-carbaldehyde to naphthalene-2-carboxylate using a pyruvate oxidase mimic.

This rate enhancement is thought to be a result of macrocyclic binding and a favourable intramolecular, enzyme-like environment of the binding site. Since the

flavin moiety could not be re-oxidised under aerobic conditions due to the sensitive nature of the thiazolium unit, the oxidation of flavin was achieved using an electrode potential of -0.3 C vs. Ag/AgCl without affecting the thiazolium moiety.

The efficient intramolecular trapping of the active aldehyde formed in the catalytic cycle by the flavin unit allowed the reaction to be performed on a preparative scale with a turnover of up to 100 catalytic cycles.

Cyclophanes have also been utilised by Breslow in the form of a manganese-porphyrin unit linked to four cyclophane binding groups as a novel cytochrome P-450 mimic.⁶⁸ These were found to catalyse the hydroxylation of steroids with a turnover of approximately 70 catalytic cycles. To the best of our knowledge however, the cyclophane framework has yet to be used in a model aldolase.

Other macromolecules have also been employed for use as vessels to carry out catalytic transformations. A unique example of this comes in the form of molecular capsules as catalysts.

1.5.1.3 Self-Assembled Molecular Capsules as Catalysts

Rebek has previously investigated the use of a designed cavity to increase the rate of a Diels-Alder reaction. No catalytic groups were used in this process⁶⁹ and furthermore, although a natural Diels-Alderase has previously been reported,^{70;71} no natural enzyme catalyst has yet been isolated or is available for synthetic applications. Therefore this makes the artificial Diels-Alderase even more attractive.

For this purpose, a polycyclic system **44** which exists as a dimer, held together by 16 hydrogen bonds was chosen as a suitable vessel. Since these intermolecular forces resembled that of stitches found along the seam of a softball that hold the two pieces together, and due to the dimer having a pseudo-spherical shell, the

name ‘hydroxy softball’ was given to these species. Since these hydrogen bonds were dynamic in nature, they were able to form and dissipate on a millisecond timescale, allowing complementary molecules to form temporary bonds within the receptacle. The microenvironment found within the cavity provided some unusual physical constraints and chemical behaviours on the imposed molecules held within and thus were investigated for their potential as catalysts (**Figure 1.16**).

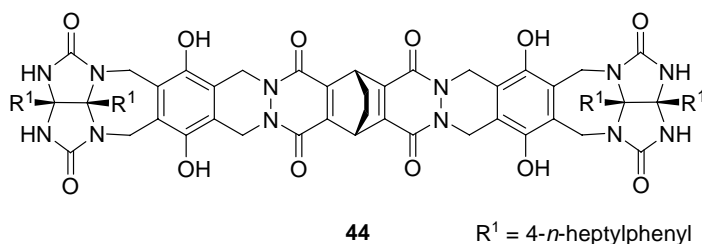
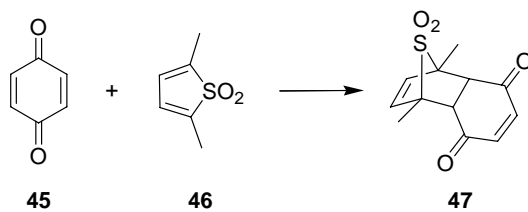


Figure 1.16: Polycyclic system used to construct the dimeric ‘hydroxy softball’ capsule.

An earlier observation that the cavity was able to accommodate two molecules of solvent benzene led to the idea of the capsule being used for certain bimolecular reactions. The studies focused on the Diels-Alder reaction between *p*-benzoquinone **45** and thiophene dioxide derivative **46** in *p*-xylene (**Scheme 1.15**).



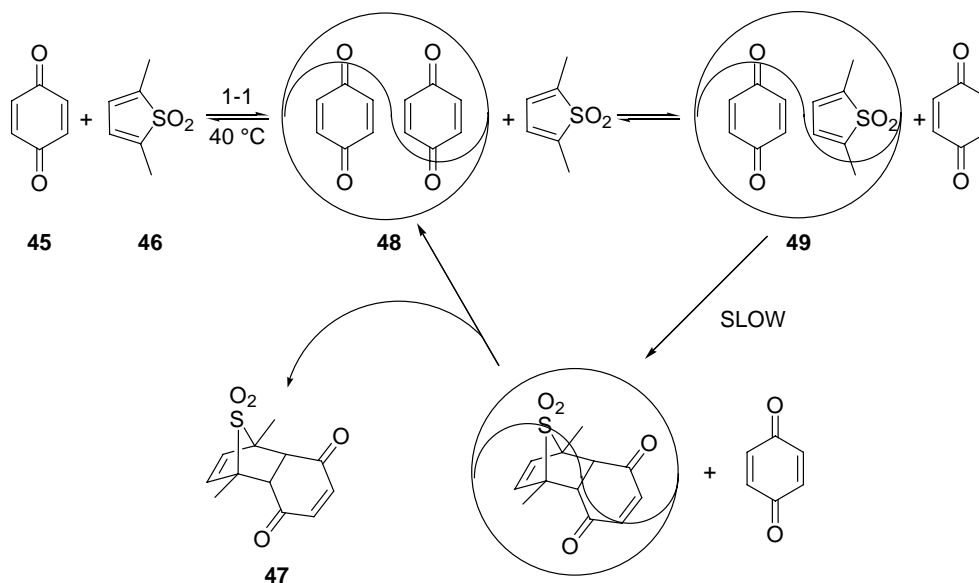
Scheme 1.15: Diels-Alder reaction between *p*-benzoquinone and thiophene dioxide derivative.

It was found that when a large excess of *p*-benzoquinone **45** was present and high temperatures were used, the adduct **47** lost SO₂ and aromatised to give a naphthalene skeleton. Although it was hoped that this would result in an unfavourable product whose dimensions could no longer be accommodated by the cavity of the softball, this was not observed due to the unconventional way that

the hydroxy softball catalysed the reaction.

By carrying out binding affinity studies between the softball cavity and adduct **47**, the association constant, K_a for this process could be calculated. This was found to be 155 M^{-1} and it could therefore be concluded that the adduct **47** was an unwelcome guest to the softball and was driven out by *p*-benzoquinone which had a much higher binding affinity to the cavity. This allowed the softball to act as an efficient catalyst for this Diels-Alder reaction and exhibit catalytic turnover.

In order to confirm that the reaction was indeed taking place within the capsule, a reference reaction using an isomer of the polycyclic species **44**, which was unable to form a dimer was used. This exhibited no catalytic activity, proving that the presence of **44** alone was not enough to catalyse the reaction. Furthermore the addition of [2,2]*p*-cyclophane which is known to be an excellent guest, showed competitive inhibition of the reaction, re-affirming that the Diels-Alder reaction did indeed take place within the capsule. The proposed catalytic cycle for this process is shown in **Scheme 1.16**:



Scheme 1.16: Proposed catalytic cycle for the Diels-Alder reaction between *p*-benzoquinone and thiophene dioxide.

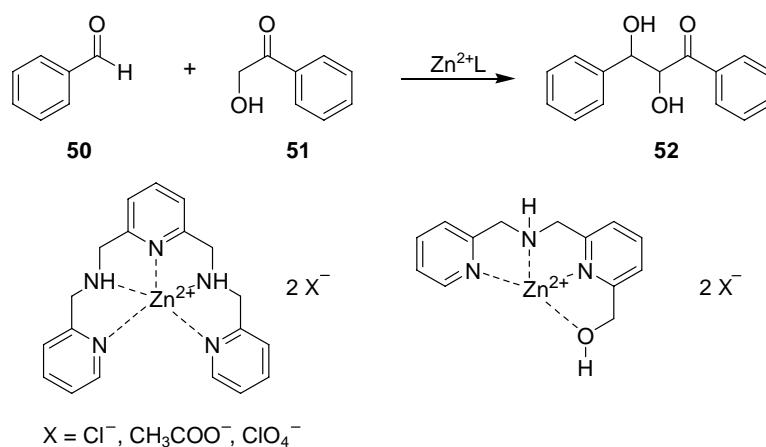
The resting state of the capsule **48** is thought to contain two quinones, one of which is occasionally displaced by the thiophene oxide to give the ‘Michaelis’ complex **49**. The Diels-Alder reaction then ensues to give the cycloadduct **47** which is immediately displaced by two *p*-benzoquinone molecules. The rate determining step in this case is thought to be the formation of the cycloadduct **47**.

Although rate enhancement based on a background reaction only showed a moderate 10-fold increase, the use of molecular capsules as catalytic reaction chambers offers great promise.

1.5.1.4 Metal Complexes as Class II Aldolase Mimics

Another aspect of the design approach utilises the formation of metal complexes to act as artificial enzymes. Here the focus will be on those that mimic the Class II aldolase. These generally consist of metallic catalysts containing a Lewis acidic metal for aldehyde activation and a Brønsted base for enolate generation to form the active complex.

Inspired by Zn^{2+} coordination site in the active site of Class II aldolases, Darbre developed novel catalysts for direct aldol condensation of benzaldehyde **50** with 2-hydroxyacetophenone **51** to give the product **52** (Scheme 1.17).⁷²



Scheme 1.17: Aldol reaction catalysed by Class II aldolase mimic based on Zn^{2+} ion complexes.

These utilised Zn^{2+} complexes containing ligands with nitrogen binding sites (N_5 and N_3O). The complexes catalysed the reaction in yields of up to 60%.

1.5.1.5 Cyclic Metalloporphyrin Trimers as Artificial Diels-Alderases

Another example of an artificial Diels-Alderase comes in the form of a cyclic metalloporphyrin trimer developed by Sanders. These possess flexible hydrophobic cavities, a feature lacking in cyclodextrins, which have a fixed dimension and hence can only accommodate substrates of a certain size.⁷³⁻⁷⁵ These systems were designed to act as templates for the Diels-Alder reaction by having convergent binding sites positioned in the correct orientation to recognise the two different substrates and to hold them in close proximity (**Figure 1.17**).

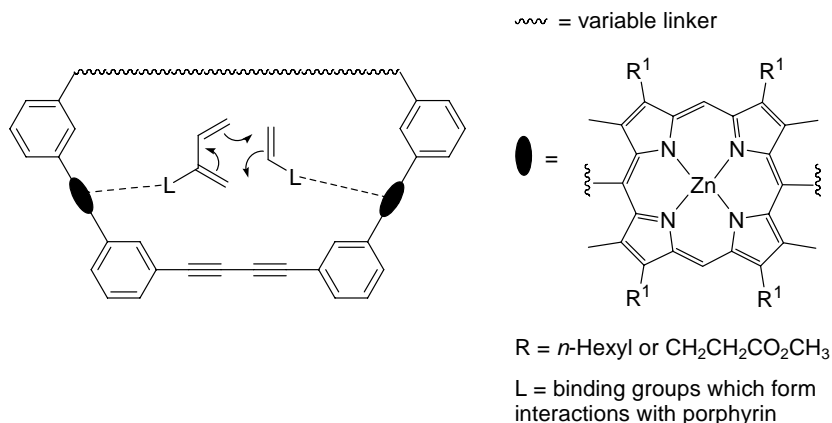
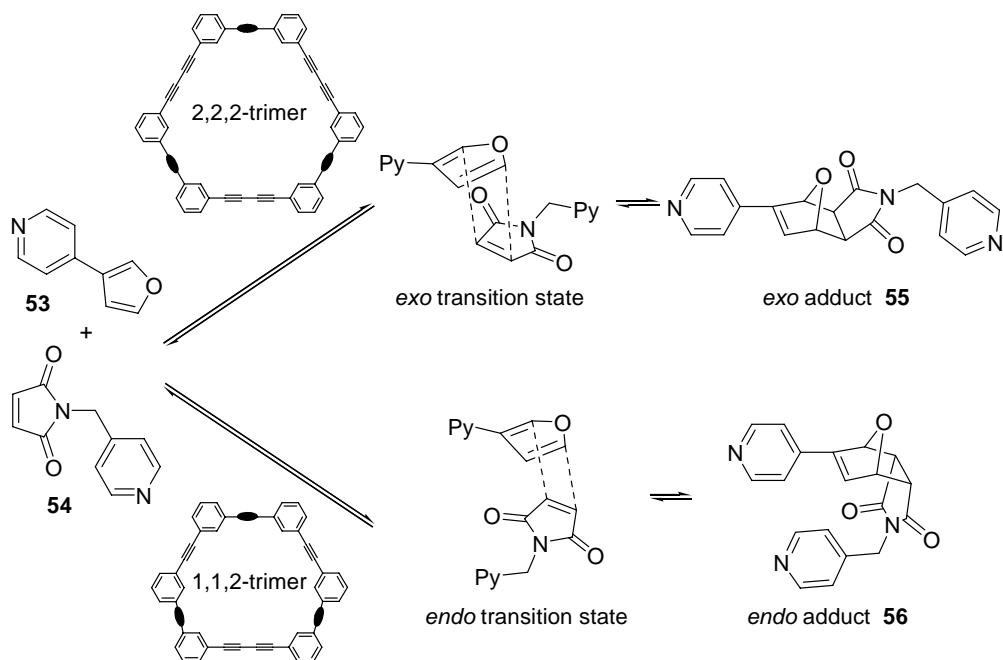


Figure 1.17: Complexation of the two Diels-Alder substrates within the Zn porphyrin.

The Diels-Alder reaction between a functionalised maleimide dienophile **54** and a furan-based diene **53** was studied for this purpose. It was found that subtle changes in the structure of the porphyrin trimer led to drastic changes in the stereochemical outcome of the Diels-Alder reaction (**Scheme 1.18**).⁷⁵



Scheme 1.18: Redirection of the Diels-Alder reaction using geometrical constraints of a host cavity.

At 30 °C, in the absence of hosts, *exo* and *endo* adducts were produced in 2:1 ratio with the *exo* adduct **55** being the thermodynamic product in this reversible Diels-Alder reaction. However when the 2,2,2-trimer was present in the reaction, only the *exo* adduct **55** was obtained, with an acceleration of more than 1000-fold compared to the control reaction, while the 1,1,2-trimer led exclusively to the *endo* adduct **56**, with a 500-fold acceleration.

The reversal of selectivity between the two cyclic trimers was thought to be a result of the greater flexibility of the larger 2,2,2-system. At 30 °C, the larger trimer was able to respond to the geometric demands of the *exo* pathway. This was further supported by a reaction carried out at 60 °C which led to the loss of stereoselectivity within the smaller trimer as well, due again to the increased flexibility. This example demonstrates the importance of the response of host geometry to the spacial demands of the transition state.

1.5.2 Transition State Analogue Selection Approach

Although the design approach has furnished some impressive enzyme mimics, the process from original conception to experimental studies of the artificial enzymes tends to be a laborious task. In order to avoid this linear approach, more recent techniques have concentrated on strategies using the selection approach.

The earliest examples of the selection approach involved generating a library of hosts in the presence of a transition state analogue (TSA) where the hosts which exhibited the highest binding affinity were selected for study. It was thought that if a macromolecule exhibited strong binding to a molecule resembling that of the transition state, it should also bind and stabilise the real transition state. As stabilisation of the transition state lies at the core of enzyme catalysis, the hosts thus selected should act as enzyme mimics for a chosen reaction.

However more recently, it has been recognised that binding to the TSA alone is not enough to obtain rate accelerations that match those of naturally occurring enzymes. Therefore the design of host molecules often incorporates catalytic functional groups in combination with the selection process. It is these examples that will be discussed in the following section.

1.5.2.1 Catalytic Antibodies as Class I Aldolase Mimics

Antibodies are a natural library of hosts which are produced by the immune system in response to a foreign molecule called an antigen, as part of a molecular defence mechanism against pathogens such as viruses and bacteria. Since they are able to bind to antigens particularly strongly and selectively, this led Jencks in 1969 to propose that antibodies generated should function as enzymes.⁷⁶

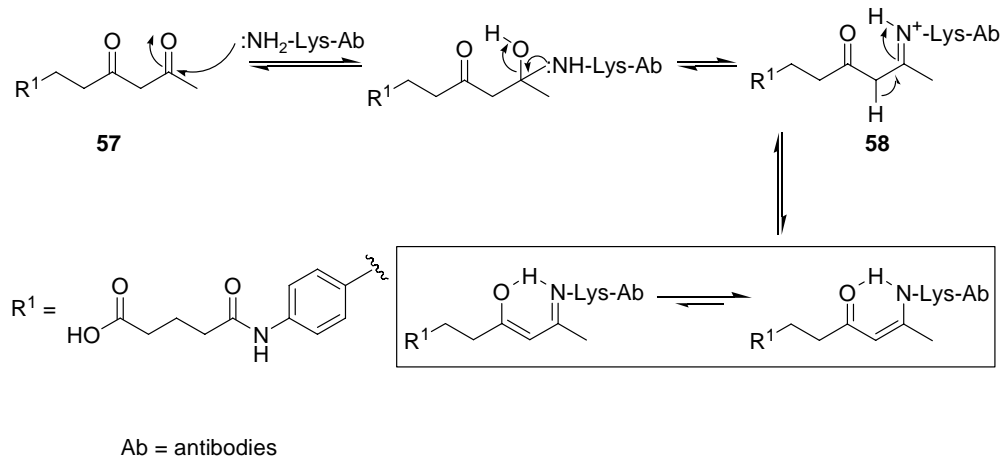
In order to utilise this effect, the field of catalytic antibodies using the transition state analogue (TSA) selection approach was established by Lerner⁷⁷ and Schultz⁷⁸ in 1986. In this method, a TSA was used as a hapten (small molecule

attached to a carrier protein) to stimulate an immune response. The desired monoclonal antibody was then selected on the basis of binding affinity to the TSA. Since the selection was based on binding to the TSA and not on the catalytic activity, rate accelerations never matched up to their enzyme catalysed equivalents. This was to be expected since the transition state is not a discrete molecular entity and thus its exact charge distribution and therefore binding interactions cannot be calculated.

Revolutionary advances in catalytic antibodies came with the introduction of the ‘reactive immunisation’ method by Barbas⁷⁹ in 1995, which based its selection criterion on chemical reactivity and not just binding, evoking the enamine mechanism of natural Class I aldolases.

With this in mind, the 1,3-diketone hapten **57** (**Scheme 1.19**) was designed to stimulate the production of antibodies containing a nucleophilic lysine in their antigen binding site. It was proposed that this would be capable of forming Schiff bases with suitable carbonyl compounds and these could then undergo aldol and retro-aldol reactions in a manner analogous to the mechanism of action of natural Class I aldolases. The chiral environment of the antigen-binding pocket should also provide the stereoselectivity in the binding pocket. This approach led to the generation of two efficient antibody catalysts 33F12 and 38C2.⁹

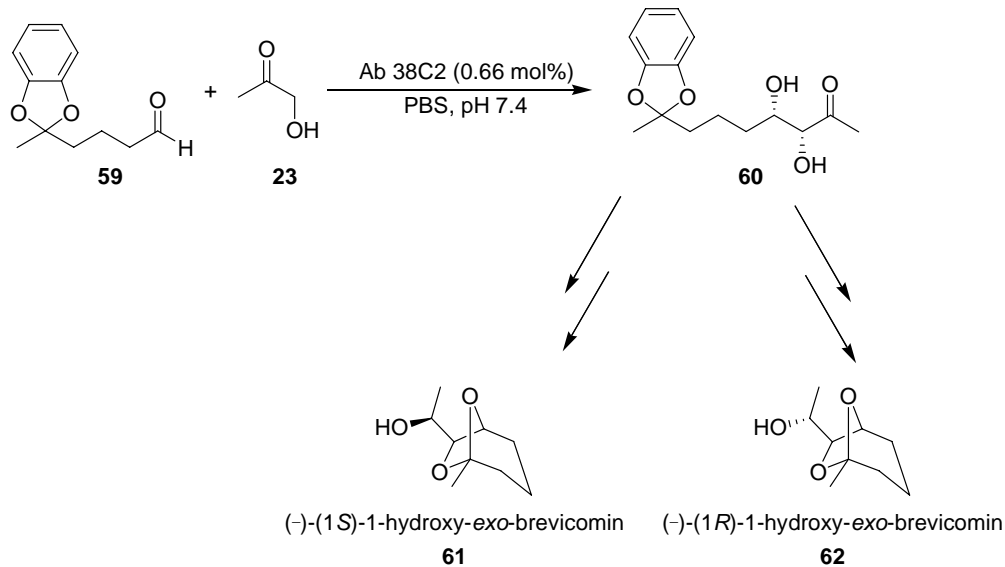
These were isolated by their ability to generate the vinylogous amide **58** of the 1,3-diketone which has a strong UV absorption at 316 nm and is therefore outside the range of the protein (**Scheme 1.19**). The rationale was to generate a library of antibodies against **57** and to select successful candidates on the basis of their ability to absorb in this region.



Scheme 1.19: The mechanism of ‘reactive immunisation’ method used to isolate antibodies 38C2 and 33F12.

The catalytic antibodies isolated in this manner, 38C2 and 33F12 were broad in scope, catalysing over two hundred different aldol reactions involving aldehyde-aldehyde, ketone-aldehyde and ketone-ketone transformations. These catalytic antibodies were found not only to accept a wider range of substrates than their natural enzyme counterparts but also achieve catalytic turnover within ten times that of the natural enzyme. The mechanism of action was shown to be the same as for the natural aldolase in which catalytic activity was derived from a greatly perturbed lysine residue in the hydrophobic binding pocket.⁹

The key aldol reaction used in the highly enantioselective total syntheses of hydroxybrevicomins **61** and **62** was catalysed by aldolase antibody 38C2. Using hydroxyacetone **23** as the donor, the aldol reaction with aldehyde **59** led to the formation of diol **60** with 55% yield and 98% *ee* (**Scheme 1.20**).⁸⁰



Scheme 1.20: The key aldol reaction catalysed by 38C2 used in the total synthesis of hydroxybrevicomins.

In order to shed light on the origin of this remarkable enantioselectivity exhibited by these antibodies, analyses were carried out on two separate groups of aldolase antibodies that catalyse the same aldol reactions with opposite enantioselectivities. One group consists of 38C2, 33F12, 40F12 and 42F1 which catalyse the aldol reaction to afford the (*S*)-enantiomer, as in the example above, and the other includes 84G3 and 93F3, which produce the (*R*)-enantiomer for the same reaction. These were generated using the haptens **63** and **64**: (Figure 1.18).⁸¹

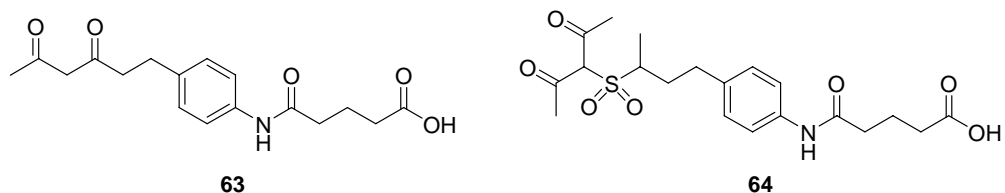


Figure 1.18: The haptens used to generate the two sets of antibodies possessing antipodal selectivity.

Antibodies 38C2, 33F12, 40F12 and 42F1 were generated using hapten **63** and 84G3 and 93F3 were generated using hapten **64**. Looking at the differences in the structure of the two haptens does not however elucidate why these two sets of

antibodies should possess opposite enantioselectivity. Therefore crystal structures of antibodies 33F12 and 93F2 were obtained for structural comparison. Furthermore analyses of amino acid sequences, site-directed mutagenesis and computational docking methods were used to determine the origin of the enantioselectivity of these two antibody families.

The amino acid sequences revealed that 38C2, 33F12, 40F12 and 42F1 which possess the same enantioselectivity share high amino acid sequence identity and have a reactive lysine residue at H93.⁸² The crystal structure analysis of 33F12 and homology model of 40F12 also indicated a similar hydrophobic active site. In an analogous manner, 84G3 and 93F3 contained the same number of lysine residues at the same positions in their variable domains. However their essential lysine residue was found to be L89 within these antibodies compared to H93 in the other family of antibodies. Their complementary enantioselectivity could therefore be attributed to the selection of completely different amino acid sequences from the antibody repertoire.

In order to understand the nucleophilic character of the reactive lysine residues within the two families, the X-ray crystal structures of 33F12 and 93F2 were compared. Both showed a similar arrangement of key lysine residues in their active sites, one which was directly involved in the formation of the Schiff base and the other which perturbed the pK_a of the reactive lysine to enhance the efficiency of the aldolase-catalysed reaction. These lysine residues were also surrounded mostly by hydrophobic residues.

Having identified the key lysine residue responsible for the catalytic activity in the antibody 93F3, it was envisaged that mutation of this essential L89 residue would lead to the loss of catalytic activity. Site-directed mutagenesis of this key amino acid residue indeed did result in the loss of activity within antibody 93F3. Furthermore automated docking analyses revealed that the hydroxyl group of SerL91 played a key role in the catalytic reaction by forming hydrogen bonds with the carbonyl oxygen of the aldehyde in the transition state. This interaction

not only activated the acceptor aldehyde but also fixed its orientation in the transition state and thus determined its reaction face.

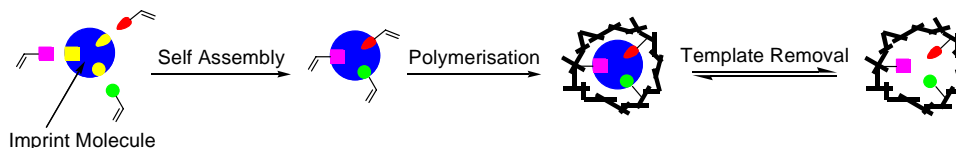
Furthermore when studies were carried out in which the location of the reactive lysine residue in antibody 38C2 was moved from H93 to L89, inversion of the enantioselectivity of the catalysed reaction was observed. In this way, employing careful design and selection processes should, in the future, lead to the creation of even more powerful catalytic antibodies with exceptional activity.

Although catalytic antibodies have provided a vital tool in modern synthetic chemistry, there are a few drawbacks associated with their preparation and use. For example, the method requires the use of mice to generate the antibodies and highly specialised techniques. The effort necessary for the isolation of a monoclonal antibody can be very time consuming. This means that once a truly catalytic antibody is found and separated, it may be a process of many months to years before the structure of the active site is characterised. They also lack thermal stability and chemical robustness which are essential in many chemical reactions. Moreover, they have a short lifetime and are expensive to produce, and so a synthetic analogue would be of much interest.

1.5.2.2 Molecular Imprinted Polymers (MIPs) as Class II Aldolase Mimics

The development of molecular imprinted polymers is more recent than the generation of catalytic antibodies but the underlying principles are very similar. Molecular imprinting is a polymerisation technique which is used to produce ligand selective recognition sites in synthetic polymers to generate substrate selective catalytically active MIPs. If the 'imprint' molecule is a transition state analogue (TSA), then the resulting MIP should behave as an artificial enzyme for the specified reaction.⁸³

The principles of MIP preparation are illustrated in (Scheme 1.21).⁹

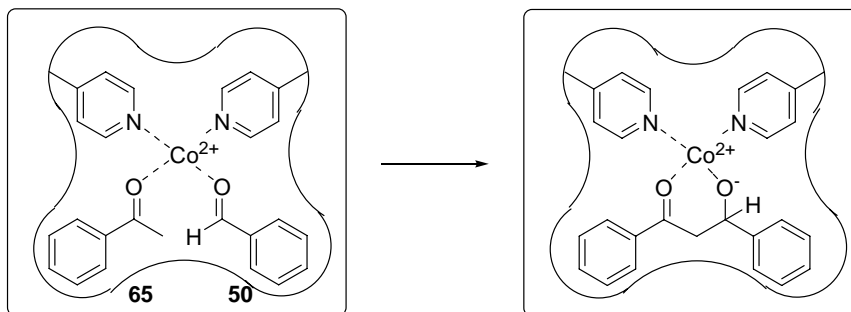


Scheme 1.21: Basic principles of molecular imprinted polymer preparation.

The first step requires pre-organisation or self assembly of the imprint molecule and monomers containing the required functional groups, through covalent or non-covalent interactions. A mixture of the standard monomer and cross-linker is then co-polymerised around the template-monomer complex in a radical polymerisation process. Finally the imprint molecule is extracted to leave a polymer with binding sites ('imprint') complementary to the template, in terms of shape and chemical functionality.

This technique offers potential for developing tailor made catalysts, perhaps with catalytic functionalities not utilised in biology. Despite the inherent heterogeneity of the molecular recognition site produced, the increased stability of MIPs against heat, chemicals and solvents when compared to natural enzymes or other artificial analogues means that the attainment of MIPs remains a highly sought-after aspiration.

Mosbach reported the first true-enzyme-like catalysis of C-C bond formation using MIPs.⁸³ The molecular imprinting technique was used in the development of a 4-vinylpyridine-styrene-divinylbenzene copolymer imprinted with an aldol condensation intermediate analogue, dibenzoylmethane (DBM) and a Co^{2+} ion (Scheme 1.22). The imprinted polymer was able to catalyse the aldol condensation of acetophenone **65** and benzaldehyde **50** in a manner analogous to Class II aldolases.

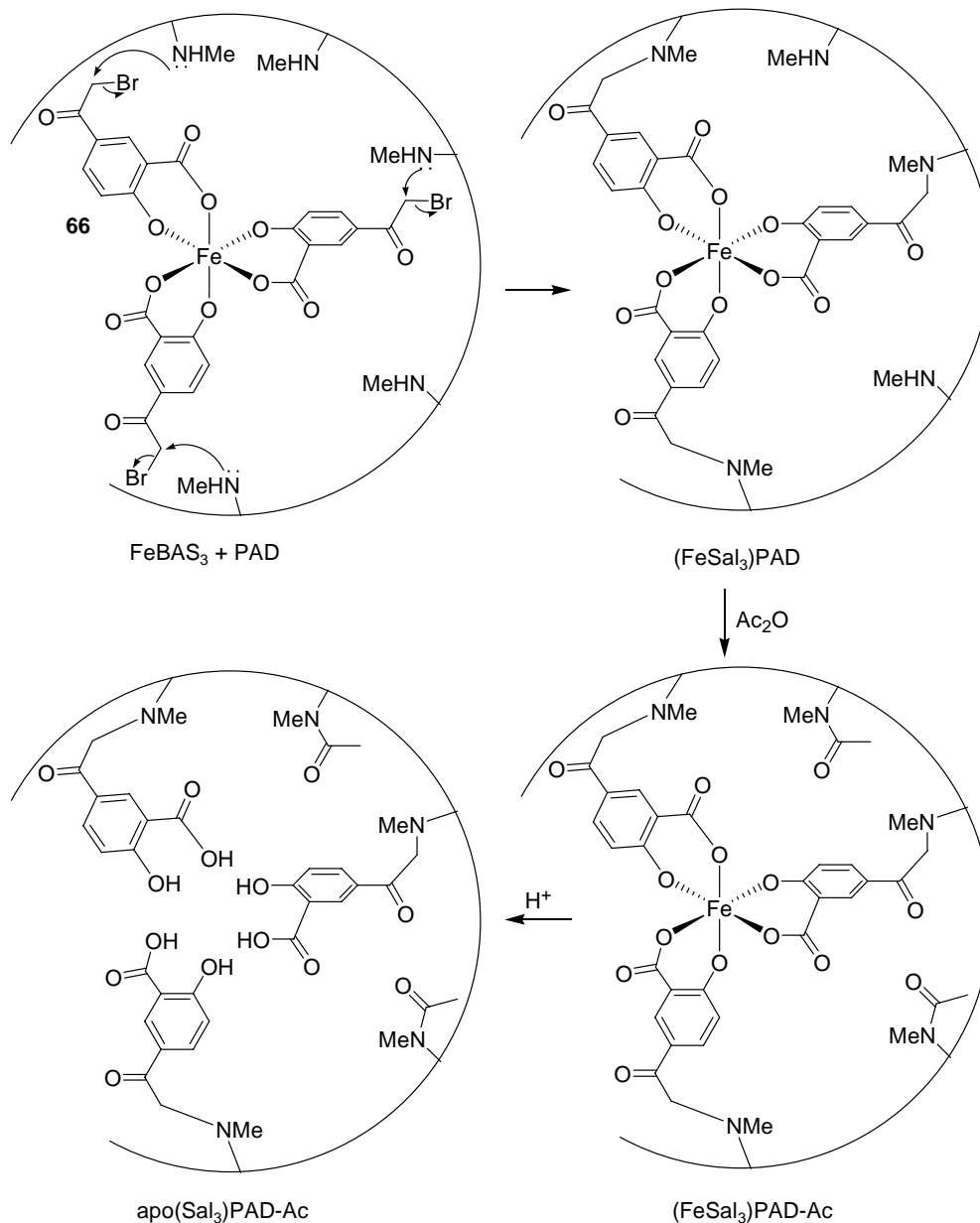


Scheme 1.22: MIP containing Co^{2+} ion used in aldol condensation reaction.

In addition to metal coordination, the pyridinyl residues provided the base necessary for generation of the enolate of acetophenone.

1.5.2.3 Imprinting an Artificial Proteinase

Another technique which utilises the idea of ‘imprinting’ was reported by Suh for the creation of an artificial aspartic proteinase. The two aspartic carboxyl groups found within the natural enzymes are thought to act as key catalytic groups in hydrolysing peptide substrates.⁸⁴ In light of this fact, Suh synthesised an organic artificial protease which contained carboxyl groups in the active site. (**Scheme 1.23**).



Scheme 1.23: Imprinting process for the creation of an artificial aspartic proteinase.

This involved complexation of three molecules of 5-bromoacetylsalicylate **66** to an Fe(III) ion to give the resultant complex (FeBAS_3) which was cross-linked with poly(aminomethylstyrene-co-divinylbenzene) (PAD) to obtain $(\text{FeSal}_3)\text{-PAD}$. These were subsequently capped *via* acetylation to produce $(\text{FeSal}_3)\text{-Ac}$, and the Fe(III) ions removed under acidic conditions to give the active $\text{apo}(\text{Sal}_3)\text{PAD-Ac}$

protease mimics. These were obtained as insoluble catalysts which reproduced the catalytic features of aspartic proteases.

The activity of apo(Sal₃)PAD-Ac was tested in the hydrolysis of bovine serum albumin, in which it was revealed that albumin was cleaved into fragments smaller than 2 k Da. By looking at the pH profile for this reaction, it was found that it manifested optimum activity at pH 3, which is in agreement with conditions found within natural enzymes. Since the active site of apo(Sal₃)PAD-Ac contained both carboxyl and phenol groups, at pH 3, phenol was thought to be acting as a general acid since its activity is likely to be lower than that of the carboxyl groups. Therefore the activity of apo(Sal₃)PAD-Ac at pH 3 is attributable to cooperation of two or more carboxyl groups by a mechanism analogous to that found in natural enzymes. Moreover it has a k_{cat} of over 0.17 h⁻¹ at pH 3, indicating that it has a reasonably high catalytic activity.

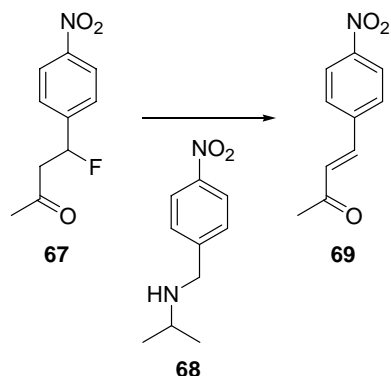
The idea of ‘imprinting’ has also been extended to include biomolecules, mainly proteins, for use as efficient artificial enzymes.

1.5.2.4 Bioimprinting

Biomolecular imprinting or bioimprinting refers to the induction of catalytic activity in proteins by lyophilisation (freeze drying) in the presence of a transition state analogue.⁸⁵ Slade has demonstrated that bioimprinting proteins in the presence of a TSA leads to a conformational change which either manifests itself in the form of a new catalytic site or as improvements of the pre-existing ones, which were then able to carry out catalysis.

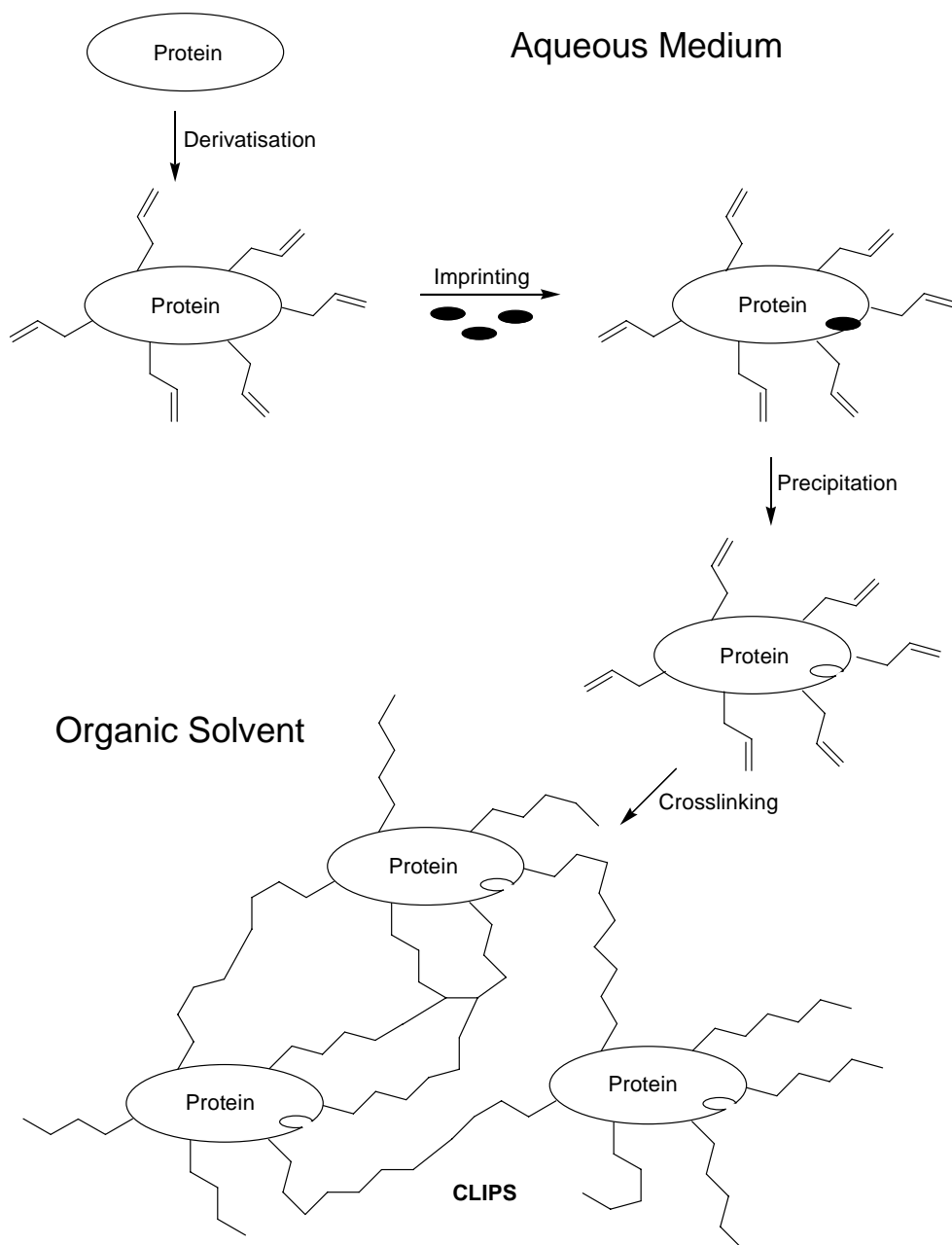
This process was illustrated by bioimprinting β -lactoglobulin in the presence of TSA **68** (Scheme 1.24). β -elimination of substrate **67** was studied using this novel bioimprinted protein and compared with the results of the non-imprinted control. The imprinted β -lactoglobulin showed catalytic activity three times that of the control reaction and almost four orders of magnitude higher than spontaneous β -

elimination. Although this result may seem modest when compared to rate accelerations obtained using catalytic antibodies, it was found that the rate acceleration was almost identical to that observed for molecularly imprinted polymers.



Scheme 1.24: β -elimination of 4-fluoro-4-(*p*-nitrophenyl) butan-2-one and the structure of TSA used for protein imprinting.

A major drawback of this method of imprinting is that the enhanced properties of these proteins can only be sustained in nearly anhydrous environments, since hydration of these proteins causes re-naturation and therefore consequent loss of the imprinted binding sites. This problem however was solved to some degree by Peiffker and Fischer by combining the imprinting step with a subsequent immobilisation method, resulting in the retention of the imprint by the enzymes, allowing their structure to be maintained in aqueous media (Scheme 1.25).⁸⁶

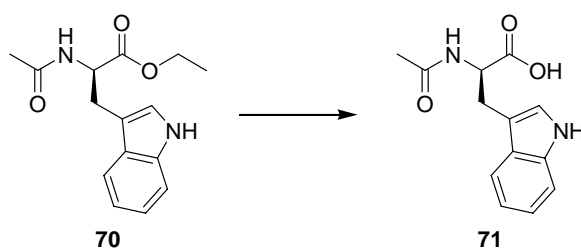


Scheme 1.25: Broadening the substrate selectivity using a combination of bioimprinting and subsequent covalent immobilisation technique.

This technique was used to stabilise the ligand induced acceptance for D-configured substrates by α -chymotrypsin or subtilisin Carlsberg. This involved the vinylation of the proteases by acylation with itaconic anhydride. Subsequent enzyme imprinting and crosslinking furnished the desired crosslinked imprinted

proteins (CLIPs).

These were tested in a hydrolysis of *N*-acetyl-D-tryptophan ethyl ester **70** in phosphate buffer (**Scheme 1.26**). The CLIPs showed no loss of activity with repeated use and displayed rate acceleration for this reaction of magnitude of around $10^4 - 10^5 \text{ mM}^{-1}$. This result suggested that the enzymes tailored by imprinting technique retained their ‘new’ property in the presence of water, when the vinylation/crosslinking method was induced.



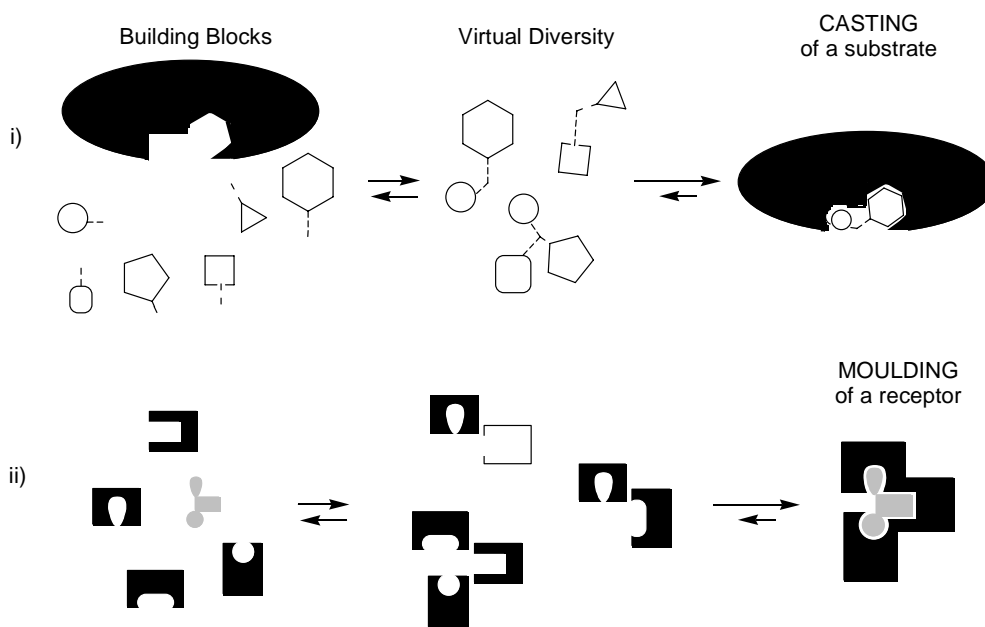
Scheme 1.26: Ester hydrolysis of *N*-acetyl-D-tryptophan ethyl ester using CLIPs.

Other examples of the use of bioimprinting include Luo’s glutathione peroxidase (GPX) mimic⁸⁷ and those based on imprinting of myoglobin in the epoxidation of styrene.⁸⁸

1.5.2.5 Dynamic Combinatorial Libraries

Another method which utilises the selection approach comes in the form of dynamic combinatorial libraries also known as virtual combinatorial chemistry. This exploits the tools of supramolecular chemistry and relies upon reversible interactions formed between a set of building blocks. This multi-component self-assembly process can thus lead to the creation of a virtual combinatorial library (VCL), which contains all possible combinations in number and nature of the available components, taking into account their structural and interactional features. From this VCL, the entity which possesses properties most suitable for the formation of the optimal supramolecular species with the target site can be selected.

In contrast to combinatorial libraries where the compounds are synthesised in the conventional fashion, through covalent non-reversible connections, VCLs are supramolecular in nature and the entity giving the strongest binding or the most thermodynamically stable species is expressed. Reversibility is the essential feature of VCLs since they are allowed to equilibrate in the presence of a receptor or ligand to which binding is desired. This allows for the technique to be applied to either the discovery of a new substrate for a given receptor or to the construction of a receptor for a new substrate. Thus in the framework of VCLs two processes, ‘casting’ and ‘moulding’ may be considered depending on whether a receptor or a substrate acts as template for the assembly of the other partner. In the casting process the cavity of an enzyme, protein or other macromolecule induces the assembly of a substrate that fits the cavity. Moulding involves the assembly of a macromolecular structure around a template molecule. (**Scheme 1.27**)



Scheme 1.27: i) Representation of the casting process. ii) Representation of the moulding process.

Both processes require a set of building blocks, and involve their reversible combination for spontaneous diversity generation. Their selection is directed by

recognition of one partner by the other. Since the system is dynamic, it allows for the evolution of spontaneous recombinations under changes in the partner or in the environmental conditions.

By way of illustration, Lehn implemented the concept of VCL involving a casting process based on the recognition directed assembly of carbonic anhydrase II inhibitors (CAII). CAII is a Zn(II) metalloenzyme whose inhibition particularly by *p*-substituted sulfonamides has been extensively studied.

They utilised the fast and reversible condensation of amines and aldehydes to form imines since this allowed the system to equilibrate in the presence of the receptor. In addition, the imines formed could subsequently be irreversibly reduced by NaBH₃CN. To generate the library, a set of aldehydes and amines was selected based on comparative reactivities and structural variability. Subsequent analysis of the library revealed that the proportion of *p*-sulfonamide **72** was amplified relative to the library formed in the absence of the receptor. (**Figure 1.19**).

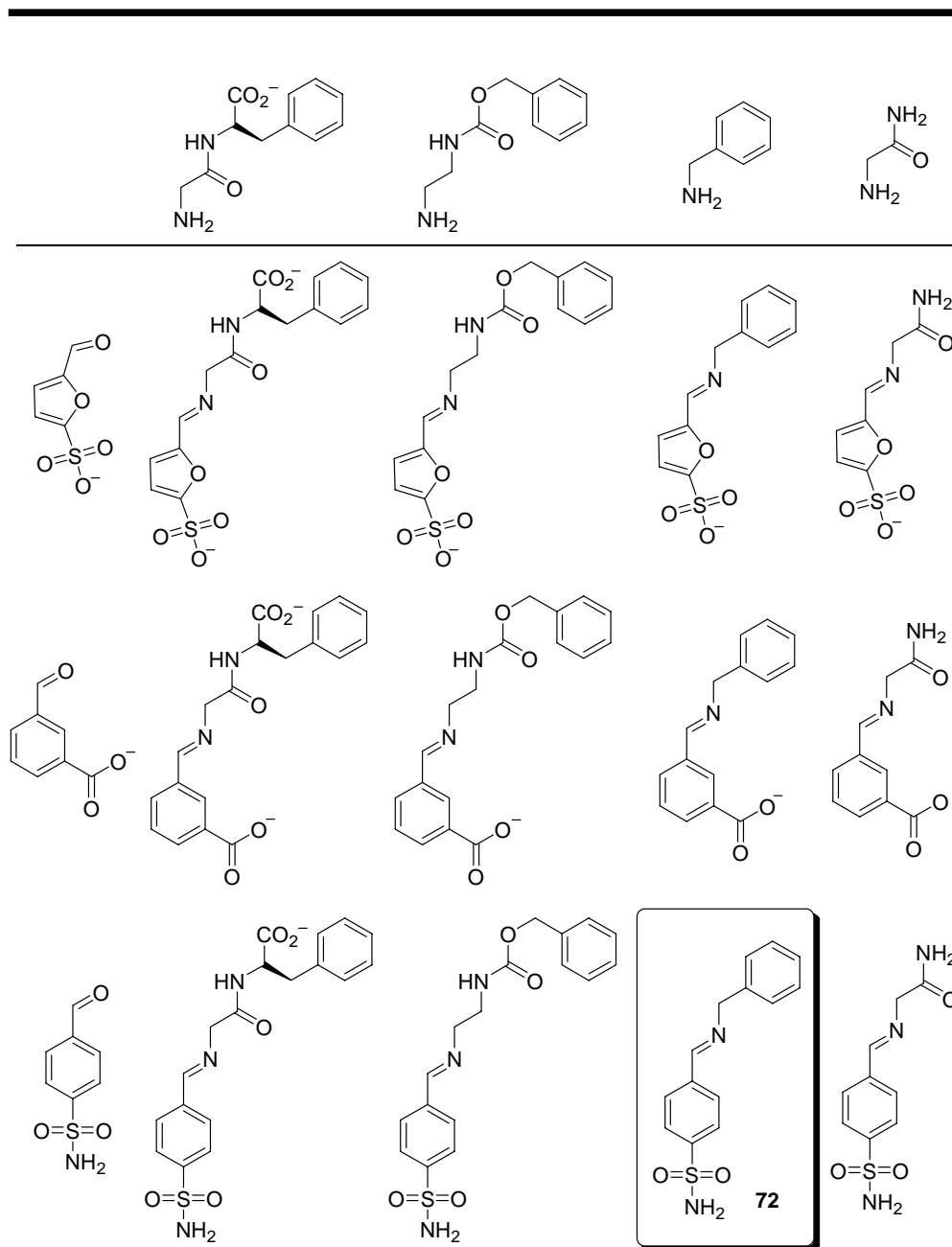
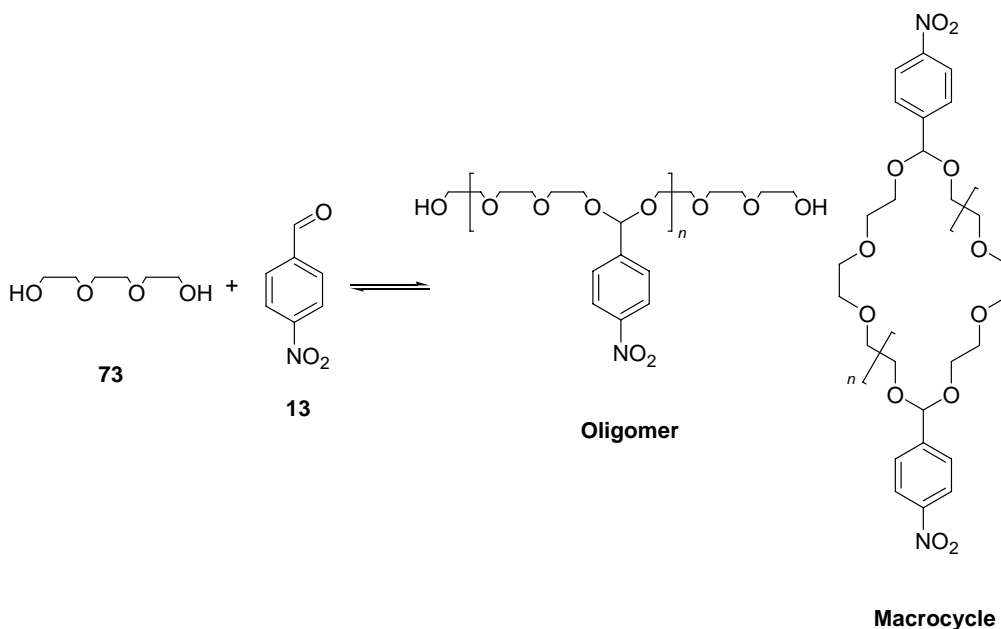


Figure 1.19: Precursor amines and aldehydes and resulting components of the combinatorial library.

Lemcoff recently reported the use of dynamic combinatorial chemistry to study the acid-catalysed reaction between carbonyls and alcohols to give acetals.⁸⁹ The rapid equilibrium and well known methodologies found in these reactions as well as the use of inexpensive reagents made this investigation an ideal candidate for creating DCLs. Furthermore, ‘freezing’ a dynamic library of acetals is readily

achieved by the addition of base and neutralisation of the catalyst.

A combination of 4-nitrobenzaldehyde **13** and triethylene glycol **73** were used to generate an acetal dynamic library which could give both oligomers and macrocycles. Electron-poor aromatic aldehydes were employed to stabilise the inherent acetals formed.⁹⁰⁻⁹³ Triethylene glycol was chosen for the alcohol counterpart due to its ability to mimic crown ethers when macrocycles of this nature are formed. With these two components at hand, a DCL of complex mixtures of both cyclic and acyclic forms was generated and separated by preparative HPLC. 15 library members were isolated and fully characterised in this manner (**Scheme 1.28**).



Scheme 1.28: A DCL built by acetalation of 4-nitrobenzaldehyde using triethylene glycol.

Other examples include the development of a library of thioesters,⁹⁴ acyl hydrazones⁹⁵⁻⁹⁷ and disulphides.⁹⁸⁻¹⁰¹ Molecular amplification in dynamic combinatorial libraries has also been observed by Sanders,¹⁰² Eliseev¹⁰³ Timmerman and Reinhoudt.^{104;105}

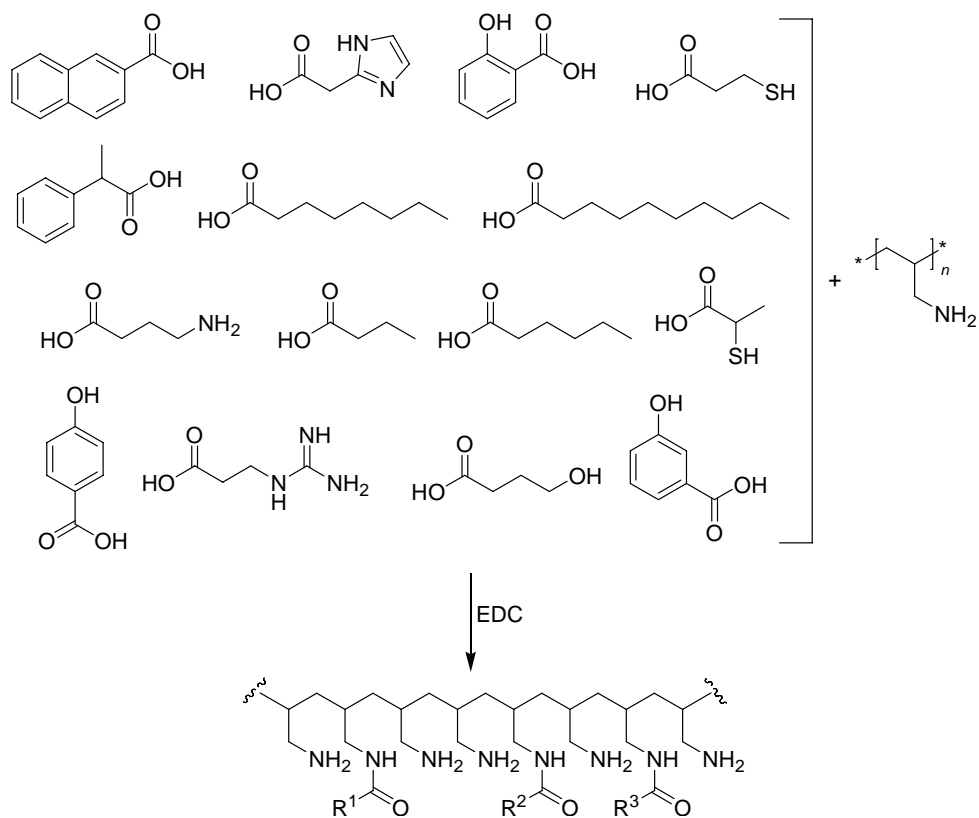
This far however, in spite of the elegance of the conceptions, the limited number of fast and reversible reactions, together with the necessary incorporation of catalytically active groups, has limited the full potential of this approach for artificial enzymes through self assembly of a receptor site.

1.5.3 The Catalytic Activity Selection Approach

This utilises the advances in combinatorial chemistry wherein a library of possible catalysts is generated and directly screened for enzyme-like activity. This not only provides a tool for synthesising a large number of diverse compounds in a short amount of time but also allows for the discovery of effective catalysts which exhibit potential activity when subjected to the relevant screening method.

1.5.3.1 Combinatorial Polymers as Enzyme Mimics

In the mid nineties, Menger introduced a highly original approach towards the creation of novel artificial enzymes. This involved the use of combinatorial chemistry to attach various combinations of three or four carboxylic acids onto poly(allylamine) (PAA) or poly(ethylenimine) (PEI) (**Scheme 1.29**).^{106;107} The figure below gives a general schematic for the synthesis of a functionalised polymeric library using poly(allylamine).



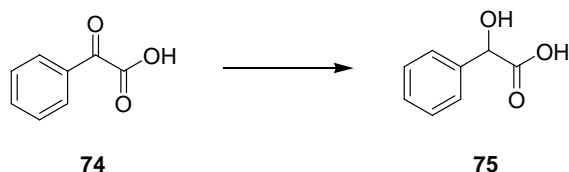
Scheme 1.29: Synthesis of functionalised polyallylamine using combinatorial chemistry.

In addition, the resultant polymers were complexed with either Mg^{2+} , Zn^{2+} or Fe^{2+} . This method allowed the synthesis of hundreds of potential polymeric catalysts, each with a unique set of functional groups.

Although no control was exercised over the attachment of the substituents, they were not necessarily randomly attached throughout the polymer. For example, a polymer with an octanoyl group at one site may be prone to receive another octanoyl group adjacent to it owing to hydrophobic interactions between the two functionalities.

The library of polymers synthesised in this manner were screened for activity, focusing on the reduction of ketones to alcohols. In order to increase the reducing capabilities of the polymers, these were incorporated with a 5 or 10% content of a

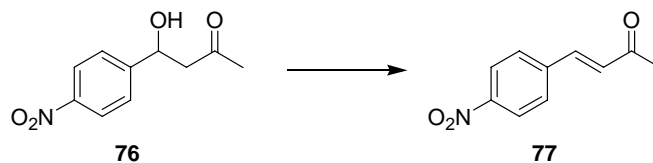
dihydropyridine (DHP), since these are well documented as reducing agents in nicotineamide adenine dinucleotide (NADH) models.¹⁰⁷ These polymers were screened for their ability to reduce benzoylformic acid **74** to mandelic acid **75** (Scheme 1.30):



Scheme 1.30: Reduction of benzoylformic acid to mandelic acid using a combinatorial polymer.

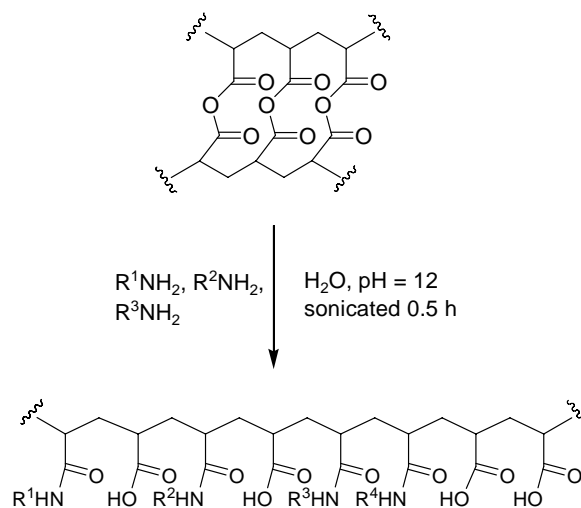
Out of the 8198 polymers which were tested for activity, 92% of these yielded less than 10% of product and therefore were considered to be inactive. 0.3% of the polymers did however give yields over 40%. From these results, several conclusions were drawn about the requirements of the polymers to exhibit activity. A metal ion was found to be necessary for catalytic activity, and the polymers required at least one hydrocarbon side chain as well as an imidazole or guanidine moiety. Polymer activity ceased in the presence of oxalic or malonic acid and a thiol or hydroxy group was found to assist the reduction process. The half-life for these processes was found to be around 2 h which was faster relative to other NADH models.¹⁰⁸

The idea of combinatorial polymers as catalysts was then extended in the study of an elimination reaction where the resultant polymers, were screened for their capability of catalysing the dehydration of the β -hydroxyketone **76** to **77**. (Scheme 1.31).



Scheme 1.31: Dehydration of the β -hydroxyketone using a combinatorial polymer.

Since the corresponding natural enzymes contained both acidic and basic groups for the departure of the hydroxyl group and of the proton respectively, polymers containing these functionalities were thought to mimic these enzymes. These were synthesised in an analogous fashion to the previous example but a poly(acrylic anhydride) was used as the polymer backbone and a collection of amines were used for attachment rather than carboxylic acids. (**Scheme 1.32**).



Scheme 1.32: Combinatorial synthesis of a library of poly(acrylic anhydride) functionalised with amines.

A total of 1344 polymers were synthesised in this fashion and screened for activity. The best polymer displayed a rate acceleration of 920 times above the background reaction.

Although this combinatorial approach has yielded some impressive results, the major drawback is that each combinatorial polymer is a complex system, consisting of numerous polymeric variations. This not only makes the isolation of a pure component near impossible for sequencing and structural characterisation but also provides very little detail to draw any significant mechanistic conclusions.

1.5.3.2 Dendrimers Containing L-Proline as Aldolase Mimics

The combinatorial approach has also been employed in the synthesis of

sophisticated dendrimers as potential artificial enzymes. Dendrimers are tree-like macromolecules that have received interest for its uses in technology and medicine. Reymond¹⁰⁹ used the peptide dendrimer as a framework for the synthesis of a novel aldolase mimic. The one shown below was obtained by functional selection from dendrimer combinatorial libraries using probes specific for aldolase active residues. **L2D1** displays multiple *N*-terminal prolines or primary amines as catalytic groups (**Figure 1.20**).

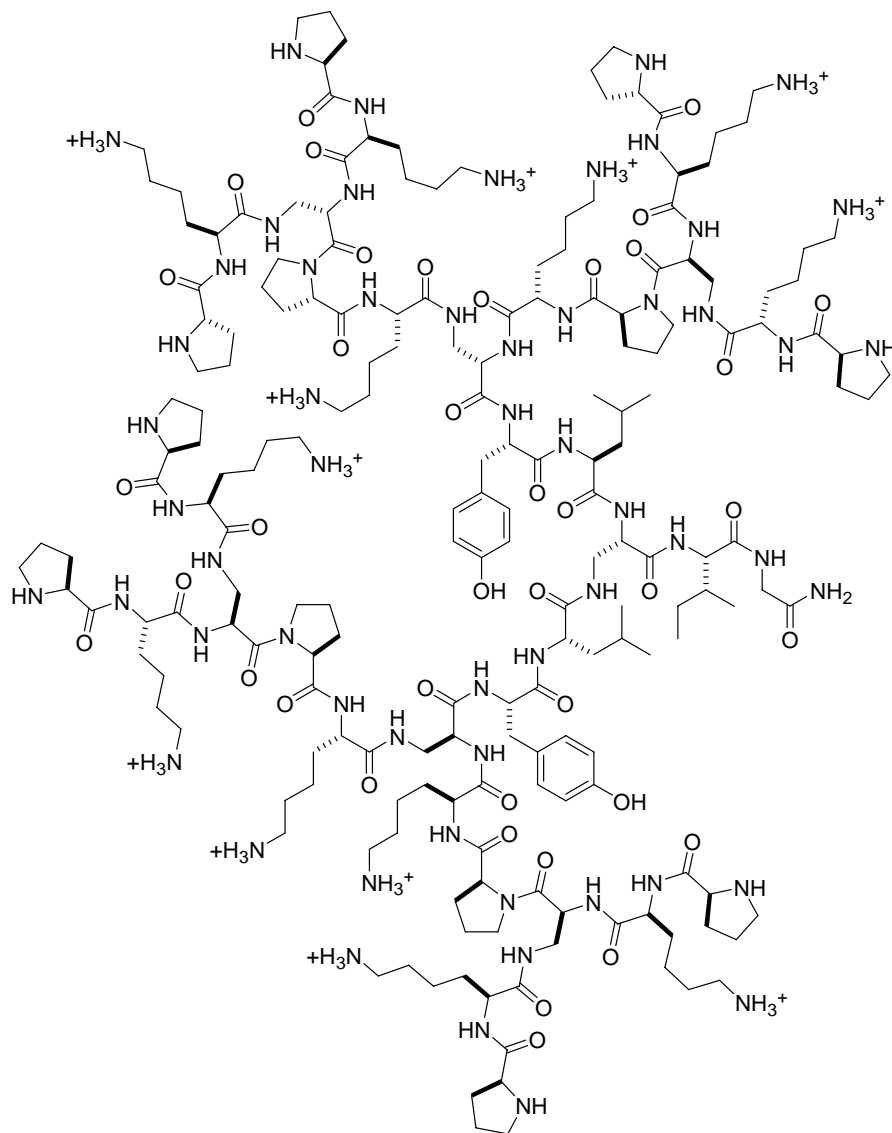
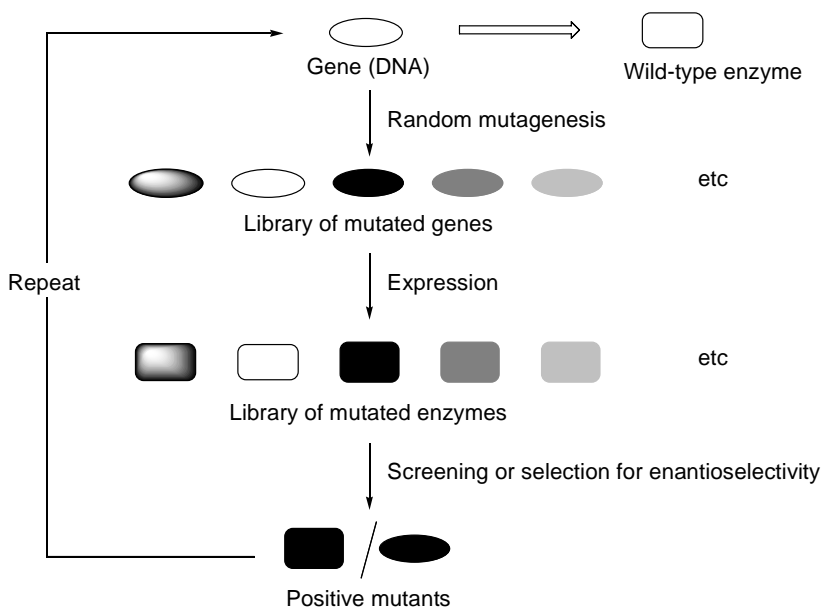


Figure 1.20: L2D1 Peptide dendrimer used to catalyse the aldol reaction.

L2D1 was able to catalyse the aldol reaction of 4-nitrobenzaldehyde with both acetone and cyclohexanone, under organic or aqueous conditions, using 1 mol% of the catalyst and with products showing an enantiometric excess of around 61 – 65%.

1.5.4 Directed Evolution of Enzymes

In quite a different manner to the previous catalytic selection approaches mentioned earlier, in 1995, Reetz began developing a high-throughput screening method for assaying the enantioselectivity of thousands of biocatalysts.¹¹⁰ This involved exploitation of the tools of directed evolution in the creation of enantioselective enzymes for use in organic synthesis (**Scheme 1.33**).



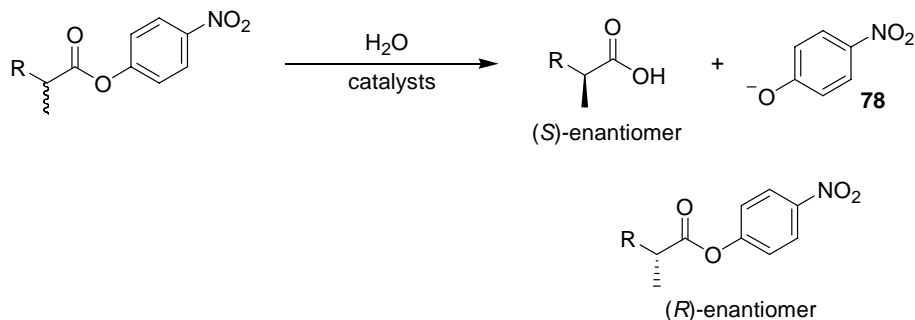
Scheme 1.33: Directed evolution of an enantioselective enzyme.

In order to evolve an enantioselective catalyst for a given reaction, a wild-type enzyme *i.e.* one that occurs in nature which catalyses the chemical transformation with poor level of enantioselectivity was first required. The gene that encodes the enzyme was then subjected to random mutagenesis using the error-prone polymerase chain reaction (epPCR),^{111;112} saturation mutagenesis¹¹³ and/or by DNA shuffling.¹¹⁴ These were then expressed in a suitable bacterial host, to

produce thousands of mutant enzymes which were then screened for enantioselectivity in the reaction of interest using interesting techniques such as infrared thermography. This process could be repeated as many times as required, to create a more superior enzyme with each cycle in a ‘Darwinistic’ manner. This goes beyond conventional combinatorial methods since in principle, the structure or mechanism of the enzymes does not have to be known.

In order to demonstrate this approach, Reetz selected the lipase from *Pseudomonas aeruginosa* which catalyses the hydrolysis of 2-methyl decanoate but with only 2 – 8% enantioselectivity at 40 – 50% conversion, showing a slight preference for the (*S*)-acid to investigate the kinetic resolution of esters.¹¹⁵

The *p*-nitrophenol rather than the methyl ester was used for study in this case since the appearance of the yellow-coloured *p*-nitrophenolate ion could easily be monitored by measuring the absorbance at 410 nm as a function of time (**Scheme 1.34**).



Scheme 1.34: Kinetic resolution of ester catalysed by mutant lipases produced using directed evolution.

The first library of approximately 1500 lipase mutants were isolated and screened for enantioselectivity based on the released *p*-nitrophenolate ion **78**. The candidates which favoured hydrolysis of the (*S*)-enantiomer of the ester were then isolated and exposed to further mutagenesis. After four generations, a mutant lipase displaying an enantioselectivity of 81% at 30% conversion in favour of the (*S*)-enantiomer was identified.

This process of directed evolution identifies sensitive areas or ‘hot spots’ within the enzyme which are responsible for the improved enantioselectivity. Since Dijkstra¹¹⁶ had determined the X-ray crystal structure of *P. aeruginosa*, the locations of the ‘hot spots’ of the most active mutant lipases could be compared relative to the active site of the natural enzyme. Surprisingly it was found that the ‘hot spots’ were not really located close to the active site, and thus contradicted previous studies that attempted to improve enantioselectivity by site-directed mutagenesis. However this picture only depicted a static view and did not reflect the true structures of these enzymes. By carrying out mutagenesis, it is more than likely that these ‘hot spots’ found at remote positions of the enzyme induced the enzyme to take on a slightly different three-dimensional conformation, leading to higher enantioselectivity.¹¹⁵

Another example of the use of directed evolution involved applying this method in the selections of RNA enzymes or ribozymes which catalyse the Diels-Alder cycloadditions between anthracene (diene) and maleimide (dienophile). After subjecting the ribozymes through eleven rounds of mutagenesis, most of the isolated mutants shared the same secondary structure consisting of three helices, an asymmetric internal loop and a single-stranded end, which through intermolecular bonding created a binding pocket. The ribozymes generated in this manner were able to carry out this transformation exhibiting multiple turnover.¹¹⁷

Other examples in this field include artificial esterases¹¹⁸ and artificial cytochrome P450 monooxygenases.^{119;120}

Although there is no disputing the power of directed evolution as a tool for the creation of superior enzymes, the whole strategy can be extremely time-consuming, requiring vast numbers ($10^3 - 10^6$) of mutant enzymes to be screened for activity. In light of this, improved mutagenesis methods have been developed to increase the efficiency of the process.

Previously, the most commonly used methods for mutagenesis involved the use of

It was found that after five sets of mutations carried out using the ISM method, requiring the screening of 20 000 transformants, a selectivity factor of $E = 115$ was achieved compared to a value of $E = 11$ based on the employment of the epPCR technique. This illustrates the strength of this method compared to the previous ones in terms of the sheer number of active transformants containing superior properties.

This method has also been used in the study of *Pseudomonas aeruginosa* lipase (PAL) for the hydrolysis of esters¹²⁴ and kinetic resolution of a racemic allene,¹²⁵ as well as cyclopentanone monooxygenase (CPMO) in the Baeyer-Villiger oxidation.¹²⁶

Similarly the use of B-FIT has been employed to improve the thermostability of *Bacillus subtilis* lipase A by carrying out mutations within areas of the active site exhibiting high degrees of flexibility.¹²⁷

As illustrated above, since the dawn of the use of directed evolution just over a decade ago, the field has flourished, allowing far superior mutants to be synthesised through more advanced mutagenesis methods. However further developments for improved screening processes have yet to receive the same amount of success. Nonetheless, it provides a powerful tool in modern synthetic chemistry.

1.6 Conclusion

In conclusion, the numerous approaches used in the development of artificial enzymes are continually evolving. At the birth of this field of chemistry, studies concentrated on the traditional approach, of rational design of a molecule, based on prior knowledge about catalytic groups found within natural enzymes. Although some impressive results were obtained using this method, the design often focused on just one aspect of the mode of activity of enzymes whether it be

mimicking the binding, catalytic activity or microenvironment of the active site. Furthermore, this process often involved the synthesis of highly complex macromolecular structures which were not only laborious and time consuming to synthesis but the smallest flaw within the design led, in some cases, to the loss of catalytic activity altogether.

As the study of artificial enzymes began to gain momentum, and advances were seen in the fields of molecular biology, biochemistry and combinatorial and polymer chemistry, methods adopting the selection approach, combining the knowledge from all these areas, increased in popularity. Earlier work concentrated on the transition state analogue (TSA) selection approach where a library of hosts were synthesised and those that exhibited highest binding affinity for the TSA were selected for study. However it was soon recognised that binding to the TSA alone was not enough to obtain rate accelerations that matched those of naturally occurring enzymes. Therefore effort was made to incorporate catalytic functional groups in combination with the selection process. This led to some pioneering work most evidently exemplified by the evolution of the reactive immunisation process in catalytic antibodies and the use of dynamic combinatorial libraries.

More recently the use of the catalytic activity selection approach wherein a library of possible catalysts is generated and directly screened for enzyme-like activity has yielded some promising results. This provided a tool for synthesising a large library of diverse compounds in a short amount of time and allowed for the discovery of effective catalysts using the relevant screening method. The combinatorial polymers developed by Menger provide some prime examples of this.

As we have also shown in the brief overview of the workings of natural aldolases, recent investigations undertaken using L-proline and its derivatives highlight the diversity of aldol reactions which are now able to be undertaken.

Despite the fact that significant advances have been made in the area of artificial enzymes, there are still only a handful of artificial enzymes that rival the precision and efficiency of natural enzymes. Clearly many factors govern the processes involved in enzyme catalysis and combining this knowledge and incorporating them into the creation of novel artificial enzymes is not a trivial task. As the technological advances become evermore sophisticated and our understanding of natural enzymes becomes more apparent, perhaps this will one day allow us to create more efficient and superior artificial enzymes.

Chapter 2: Results and Discussion

2.1 Previous Research Within our Group

A novel approach towards the construction of artificial enzymes was first studied within our research group by Atkinson in the form of ‘millipede’ artificial esterases. Here, enzymes were considered at their most simplistic level, as molecules which could ‘hold’, ‘bite’ and possess the flexibility to achieve the operation of bringing the ‘hands’ (binding groups) and the ‘teeth’ (catalytically active groups) together (**Figure 2.1**).¹²⁸

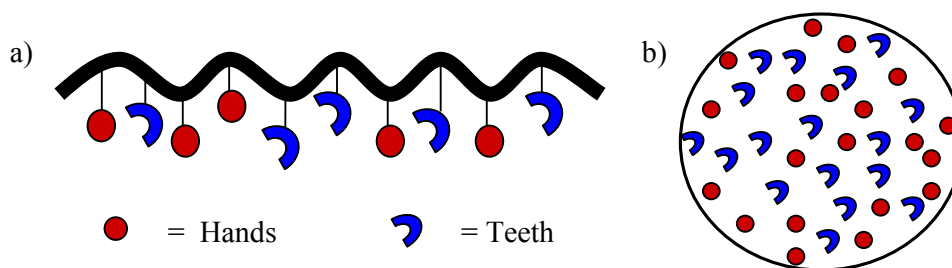
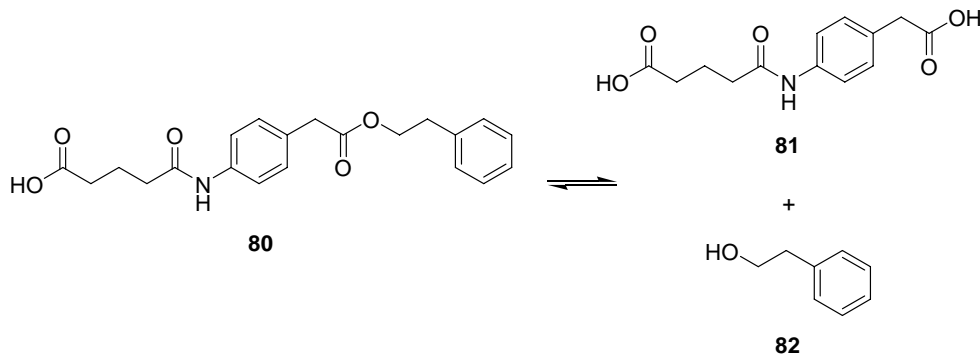


Figure 2.1: a) Representation of an artificial ‘millipede’ enzyme. b) Aerial view.

These systems consisted of a polymeric backbone, to which threads containing ‘hands’ and ‘teeth’ were attached. The backbone provided not only functionality for the attachment of these groups, but also permitted the flexibility to adopt the necessary conformation required for attack on the bound substrate within the active site. The ‘hands’ served as a binding region to ensure that the substrate was kept in close proximity to the ‘teeth’ and were also selected to facilitate the stabilisation of the transition state (*vide infra*). Finally the ‘teeth’ provided the catalytically active functional groups to allow the specific chemical transformation to take place.

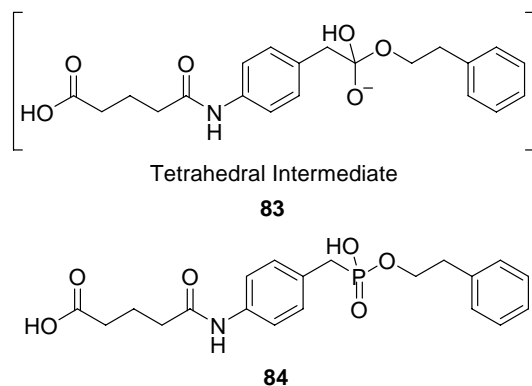
This concept was illustrated by studying the hydrolysis of ester **80** to give **81** and **82** (**Scheme 2.1**).¹²⁹ This substrate was chosen due to the presence of the additional carboxylic acid and amide groups which served as binding regions for

the 'hands'. The changes in the concentration of both the ester substrate **80** and the acid product **81** were monitored by HPLC.



Scheme 2.1: Test ester hydrolysis.

The next step involved the well known practice of choosing an appropriate transition state analogue (TSA) for the binding unit. Since the substrate is known to pass through a tetrahedral intermediate **83** during ester hydrolysis, the corresponding phosphonate ester **84** was selected based on similarities in geometry and charge distribution (**Scheme 2.2**).



Scheme 2.2: Tetrahedral intermediate and corresponding TSA.

A suitable unit that could bind the TSA and also therefore encourage the substrate towards products was then selected through the application of a novel NMR protocol. Thus, dipeptides were chosen due to their rich acidic, basic and hydrogen bond donor/acceptor functionalities in the form of carboxylic acids and amines. Nine dipeptides were studied in binding affinity experiments using Pulsed Field Gradient (PFG) NMR technique.¹³⁰⁻¹³² When a complex was formed

between two molecules, an increase in the molecular mass and therefore decrease in diffusion was observed. This resulted in a decrease in the translational diffusion coefficient (D). The dipeptides, with the lowest D and thus the highest binding affinity for the TSA were identified by PFG. The experiments were carried out in D_2O at pD 7 and dipeptide, H-Arg-Arg-OH displayed the best binding potential towards the TSA, possibly as a consequence either of phosphate recognition or of the well documented interaction between the guanidine of arginine and the carboxylic acid of the TSA, which has also been confirmed by molecular modelling studies (**Figure 2.2**).

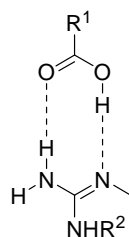


Figure 2.2: Interaction between guanidine and carboxylic acid.

Having chosen a suitable binding unit or ‘hands’, which would also encourage formation of the tetrahedral transition state, an appropriate catalytic group or ‘teeth’ was investigated. Amino acid residues are renowned for their participation in ester hydrolysis in natural enzymes. Cysteine, histidine and serine all had the potential to act as ‘teeth’ since they all feature as key catalytic residues in natural esterases. However histidine was considered to be the most suitable since it could function as a general acid/base pair as observed in ribonucleases.¹³³

With the ‘hands’ and ‘teeth’ at hand, the first generation of ‘millipede’ artificial esterases were synthesised (**Figure 2.3**). Poly(allylamine) was chosen for the polymer backbone due to its flexibility and the presence of free amino groups which provided solubility and facile incorporation of the ‘hands’ and ‘teeth’. In addition, a linker in the form of 6-aminohexanoic acid was added between the polymer and the dipeptide, to ensure conformational freedom of the binding group so that it was not restricted by proximity to the backbone. Finally all of the unfunctionalised amino groups on the polymer were capped by lysine residues

which could be viewed as hydrophilic groups to further assist the solubility of the polymer.

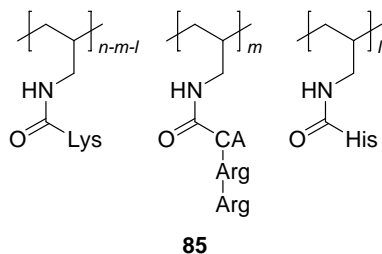
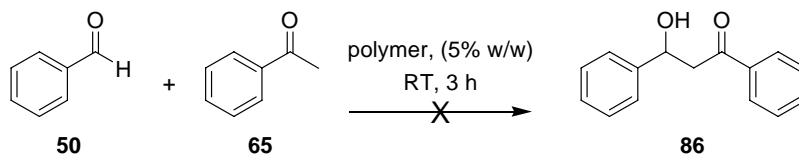


Figure 2.3: First generation of ‘millipede’ artificial enzyme.

In addition to polymer **85**, control polymers were also synthesised to identify the significance of each component and hence examine cooperativity effects in catalysis. The polymers were then screened for their efficiency in ester hydrolysis. Whilst no hydrolysis occurred when the blank polymer was used, hydrolysis was observed when just ‘teeth’ or even more interestingly just ‘hands’ were present. However the rate of ester hydrolysis was extremely high when both ‘hands’ and ‘teeth’ were attached, showing the importance of cooperativity effects. Moreover, exposure of a 1:1 mixture of ester substrate and phosphonate TSA led to inhibition.

Having established a good basis, Smiljanic then utilised a simpler variant of this to extend our research into artificial aldolases.¹³⁴ The following aldol reaction between benzaldehyde **50** and acetophenone **65** to give **86** was studied for this purpose (**Scheme 2.3**).



Scheme 2.3: Test aldol reaction between benzaldehyde and acetophenone.

Initially, a polymer backbone with both a lysine residue and a carboxylic acid group was chosen to mimic the essential characteristics of the natural enzyme. A nucleophilic enamine is formed from the lysine residue with the carboxylic acid

functioning as a proton source to enhance the electrophilicity of the aldehydic carbonyl group (**Figure 2.4**):

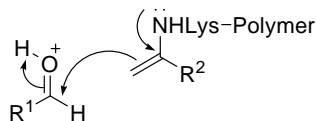


Figure 2.4: Enamine attack on an aldehyde during an aldol reaction.

Poly(lysine) was initially investigated for this purpose since the necessary amino groups were already present in the polymer. Incorporation of carboxylic acid groups was then the only requirement to furnish the artificial aldolase **87** (**Figure 2.5**).

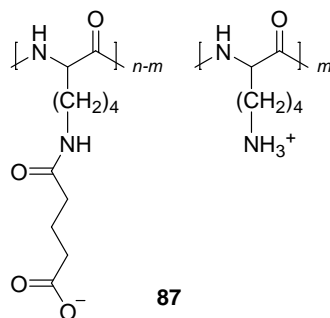


Figure 2.5: Synthesis of the first aldolase mimic by Smiljanic.

Despite modification of reaction conditions, product formation could not be detected. As a result, the morphology of the polymer was questioned. With concerns that the lysine residues may have been hindered by the three dimensional structure of the polymer, alternative aldolase mimics using poly(allylamine) and tentagel resin as the backbone were synthesised. Again, the resultant polymers showed no reactivity.

In light of these findings, the ability of the lysine residue to form the enamine was next investigated. As previously discussed (section 1.3.3), the lysine residues in natural aldolases exist in protonated form at physiological pH and are also in highly perturbed conditions, surrounded by amino acids which assist through hydrogen bond formation and hydrophobic interactions. It was likely that the microenvironment provided by the polymers synthesised was not sufficient to

replicate those found within their natural counterparts. As a result, proline was next employed to act as the activating group to replace the lysine residues previously utilised. The ability of proline to form the enamine species and thus act as an excellent catalyst in the aldol reaction has already been discussed in the introduction (section 1.4). The polymers synthesised thus, in contrast to those containing lysine gave some promising positive results. The most successful polymer **88** involved incorporating a catalytic proline group and a pentadioic acid moiety onto a tentagel resin (**Figure 2.6**). By attaching a mixture of FmocGlyOH and BocGlyOH onto the tentagel resin, a slightly more controlled synthesis compared to those synthesised by Atkinson was achieved, resulting in an approximate 2:3 ratio of proline to acid.

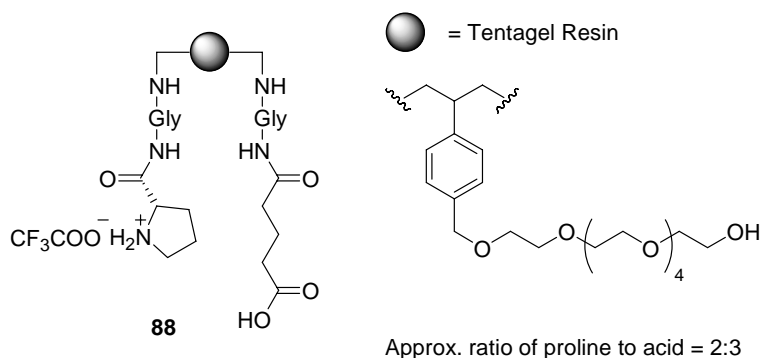


Figure 2.6: Tentagel-based aldolase mimic.

Even with the employment of this more controlled synthetic method, the resultant polymers still exhibited varying degrees of irreproducibility from batch to batch, even though in theory, all polymers could have displayed the same reactivity towards their substrates. This was because this method only allowed for the attachment of functional groups in a specific ratio, not at targeted locations. As a result, even those polymers which contained for example an approximate 2:3 ratio of proline to acid, could differ with a slight variation in experimental technique since the functional groups were attached ‘randomly’ throughout the polymer. Two supposedly identical catalysts could therefore differ dramatically in their points of attachment within the backbone and subsequently in their three dimensional structures. As a result of this, the polymers which should have displayed the same reactivity towards the reaction under study often varied

considerably in their efficiency to act as catalysts. Nonetheless when test reactions were carried out with this polymer it was able to catalyse the aldol reaction between numerous aromatic aldehydes containing electron withdrawing groups and acetone. Using the most active batch of catalysts, a yield of 30% with an enantioselectivity of 48% was obtained for the aldol product of acetone with 4-nitrobenzaldehyde. Unfortunately the polymer catalyst was never able to catalyse the test reaction shown in **Scheme 2.3**. Also the isolated yields for the aldol products using these polymers were often low, which was believed to be due to the product remaining on the polymer after the reaction.

2.2 Objectives of the Current Research Programme

In contemplating an extension to the previous work carried out within the group on the idea of using modified polymeric systems as novel artificial enzymes, it was therefore clear that one of the major challenges encountered in earlier studies involved the attachment of functionalities at specific locations within the polymeric backbone, and this issue clearly had to be solved.

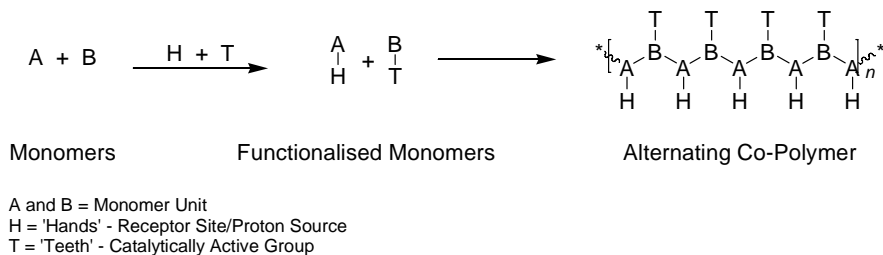
Although Smiljanic was able to exercise some control over the attachment of the proline and carboxylic acid groups to the polymeric backbone in a specific ratio, by using complementary protecting groups for the incorporation of these functionalities, the resultant polymers exhibited unpredictable reactivities in test aldol reactions. This irreproducibility of results also clearly had to be resolved.

Finally, the problems of low isolated yields for the aldol products using these polymers was again an issue which needed to be dealt with by careful choice and consideration of the polymeric systems, which would be used in this investigation.

The primary objective of our work was therefore to synthesise more structurally defined aldolase polymers containing a catalytic group and a binding group or proton donor. As a potential solution to the difficulties outlined above, attention

was initially turned towards the synthesis of artificial aldolase mimics in the form of alternating co-polymers (**Scheme 2.4**).

The basic idea behind this general concept for all artificial enzymes was to have two monomers A and B which could be functionalised separately so that one was equipped with ‘hands’ and the other with ‘teeth’. By employing a radical polymerisation technique in the presence of an initiator, this should then furnish regiochemically defined co-polymers with alternating ‘hands’ and ‘teeth’. It was hoped that the ‘identical thread’ approach would solve the problems of irreproducibility arising from differences in polymer morphology. Also, by careful choice of monomers required for this purpose, a more soluble polymer could be synthesised to facilitate hydrolytic release of the products into solution once the reaction had taken place. This should solve the low isolated yields observed with the previous systems employed by Smiljanic.



Scheme 2.4: Alternating co-polymers as aldolase mimics.

A complementary strategy was also envisaged in which both the ‘hands’ and ‘teeth’ could be attached to the monomer and then subsequently subjected to polymerisation. Such an approach would guarantee attachment of these two groups in a fixed 1:1 ratio. Not only would such monomers be structurally more concise but they would also have the added advantage of acting as an organocatalyst in their own right. For this purpose, several motifs were considered. These included those based on 7-azabicyclo[2.2.1]hept-2-ene **89**, tropane alkaloid derivatives **90** and **91** and the functionalised norbornene **92** (**Figure 2.7**).

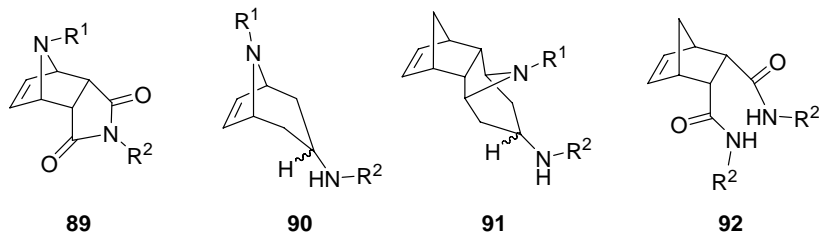
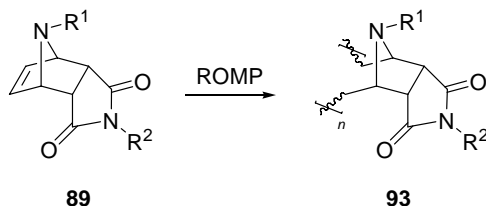


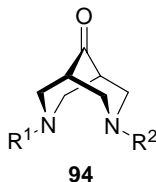
Figure 2.7: Monomers for subsequent polymerisation.

Any one of the functionalised monomers shown in **Figure 2.7** could then be subjected to ring opening metathesis polymerisation (ROMP) to yield the polymeric equivalent. **Scheme 2.5** illustrates the ROMP process for the 7-azabicyclo[2.2.1]hept-2-ene derivative **89** to afford polymer **93**.



Scheme 2.5: ROMP of 7-azabicyclo[2.2.1]hept-2-ene derivatives.

At this planning stage, functionalised bispidinone derivatives **94** were also considered within the above framework (**Figure 2.8**).



Scheme 2.8: Functionalised bispidinone derivatives.

2.3 Alternating Co-polymers as Aldolase Mimics

As discussed above, initial investigations focused on the synthesis of aldolase mimics involving the preparation of complementary monomers whose copolymerisation would result in more structurally defined alternating co-polymers. This approach was particularly appealing because of the inherent potential for

further rapid variation of both monomers in exploring functional group cooperativity in artificial enzyme behaviour, thus allowing for optimisation of active catalysts.

Maleimide and styrene units were chosen as building blocks for the synthesis of the two monomer species, due to their well established preference for formation of alternating co-polymers, due to the difference in their electronic properties. Maleimide is a good electron-deficient monomer. Therefore in the presence of a strongly electron rich co-monomer such as styrene, this should increase their tendency towards alternation during co-polymerisation as a consequence of the preference for the styryl radical to react 10^3 faster with the electron poor maleimide.¹³⁵ The resultant polymers should also be more soluble in organic solvents due to the presence of increased hydrocarbon functionalities, which would allow the aldol products to be released into solution instead of remaining within the polymeric mass. With this information at hand, various functionalised maleimide and styrene monomers were synthesised.

2.3.1 Synthesis of Functionalised Maleimide Monomer with Proline

In order for the alternating co-polymer to act as an efficient aldolase mimic, suitable functionality had to be selected for the maleimide moiety. Proline, for reasons previously mentioned (*vide infra* section 1.4) was chosen as the catalytic group of choice. Also in order to add some flexibility within these structures, a hydrocarbon linker was included (**Figure 2.9**).

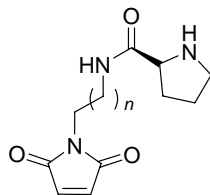
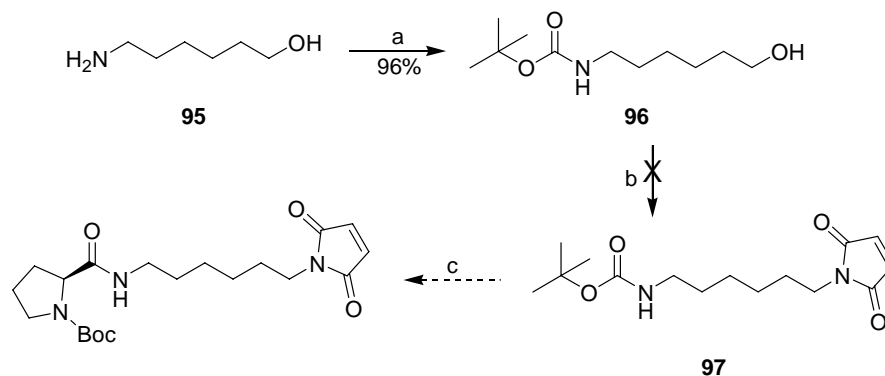


Figure 2.9: Functionalised maleimide monomer.

The initial approach towards the synthesis of a functionalised maleimide monomer is outlined below (**Scheme 2.6**). This approach was chosen since it

would furnish the desired maleimide monomer in three synthetic steps.

The Boc protection of 6-aminohexanol **95** to yield **96** proceeded smoothly and in good yield. However mostly starting material was recovered when the key Mitsunobu reaction¹³⁶ was attempted. Although various reaction conditions were undertaken, including the use of DIAD¹³⁷ instead of DEAD, the desired product could not be isolated. In this case, maleimide was not sufficiently nucleophilic to yield the desired product **97** and this route therefore was not taken further.

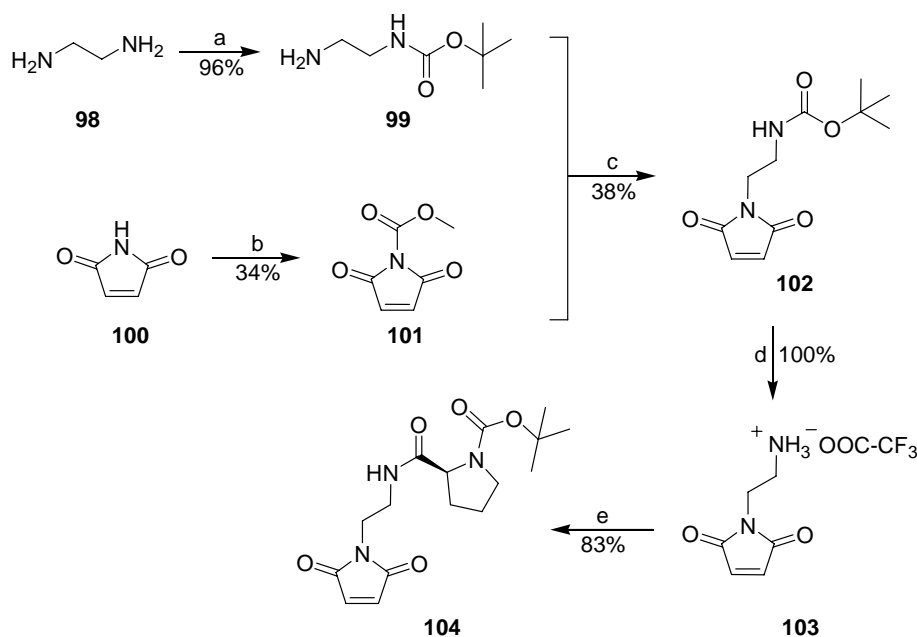


Scheme 2.6: a) Boc_2O , DCM , 21 h,¹³⁸ b) maleimide, PPh_3 , DEAD, -78°C , THF, 48 h.¹³⁶

An alternative route to a maleimide monomer was therefore devised (**Scheme 2.7**), in which the first step required mono-Boc protection of the linker in order to differentiate two amino groups. Butane-1,4-diamine was initially chosen for this purpose, since it would provide ample flexibility to the resultant monomer, and act as an efficient linker. In the event however, this turned out to be a problematic process, often resulting in a viscous mixture of both mono- and di-Boc protected products which were difficult to work up and purify by means of distillation. As a result, the yield for this process was low, around 20%. Since this was the first step of a sequential synthetic route, this reaction was not efficient enough for our purposes and butane-1,4-diamine was therefore replaced with ethane-1,2-diamine **98**. Although this linker would not allow as much flexibility, it was thought to be adequate in this instance since our intention was to synthesise polymers which would have functional groups in close proximity to one another. Therefore the

shorter linker would still serve its function of bringing the required functionalities together.

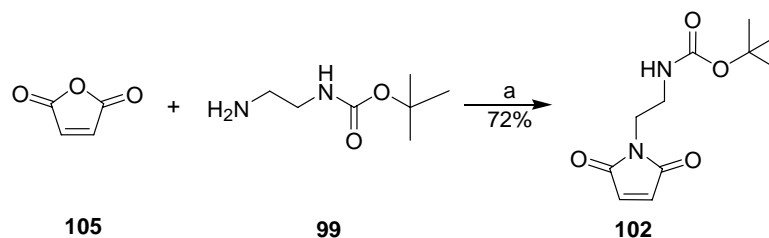
In contrast to butane-1,4-diamine, ethane-1,2-diamine was mono-Boc protected with great efficiency to yield *N*-*tert*-Butoxy(2-aminoethyl)carbamate **99**. Initially this amine was then reacted with maleimide **100**, but this did not yield the desired product **102**. Therefore maleimide was transformed into the carbamate **101**, which acted as a better leaving group in terms of facilitating the reaction to give **102**, in moderate yield. Deprotection of the Boc group with TFA gave the salt **103** which was then coupled to proline to generate the functionalised maleimide monomer **104**.



Scheme 2.7: a) Boc₂O, DCM, 24 h;¹³⁹ b) Et₃N, DMAP (10 mol%), methyl chloroformate, EtOAc, 2 h; c) sat. NaHCO₃, 24 h;¹⁴⁰ d) TFA, DCM, 24 h;¹³⁶ e) *N*-Boc-L-proline, NMM, ethyl chloroformate, DCM, 18 h.

Although this method provided the desired maleimide monomer, the yields for two of the steps (b and c) were not satisfactory and the overall yield using this synthetic route was just over 10%, thus requiring large amounts of starting material to furnish enough monomer species to be utilised in the polymerisation

step in latter stages. The synthetic method therefore required modification. While searching for an alternative route to functionalised maleimide derivatives, a reaction involving the use of maleic anhydride and an amine to directly give related species was investigated.¹⁴¹ This would not require the use of maleimide as a starting material, which was not only much more expensive, but also inherently more difficult to functionalise. This reaction was far more concise than the previous method employed, requiring fewer synthetic steps and giving much higher yields (**Scheme 2.8**). This new method allowed the key maleimide species **102** to be synthesised in 72% yield. Employing the same deprotection and proline coupling steps previously discussed in the earlier synthetic route (**Scheme 2.7**) furnished the monomer in four steps, with an overall yield of 57%, almost six times greater than the previous method.



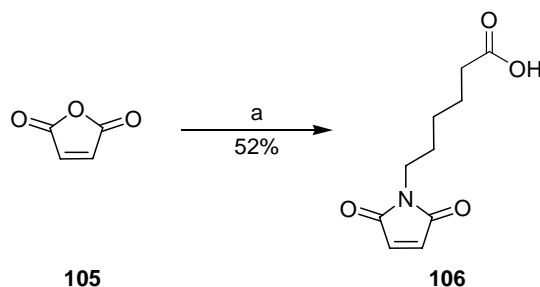
Scheme 2.8: a) DMF, *N*-hydroxysuccinimide, DCC, 18 h.¹⁴¹

2.3.2 Synthesis of Functionalised Maleimide Monomer with Flexible Carboxylic Acid Group

A maleimide monomer with a proton donor instead of a catalytic proline group was also synthesised in order to investigate whether this exchange of functionalities would have an effect on the reactivity of the resultant polymers. In theory, it should not make a difference whether the proline residue was attached to the maleimide or to the styrene monomer and *vice versa* for the proton donor. However carrying out this comparison would either prove or disprove this hypothesis.

Utilising the method developed for the previous monomer, the requisite maleimide monomer **106** was prepared in one step from maleic anhydride **105** and

6-aminocaproic acid to yield the desired product **106** in 52% yield (**Scheme 2.9**).



Scheme 2.9: a) 6-aminocaproic acid, AcOH, sodium acetate, 90 °C, 2 h.

2.3.3 Functionalised Styrene Monomers

Four monomers based on styrene were also synthesised to allow the incorporation of a proton donor, a binding group, or an activating proline unit (**Figure 2.10**). The presence of a proton donor in the form of a carboxylic acid group within the polymeric system was envisaged to assist in several of the key steps of the aldol reaction requiring proton transfer processes (*vide infra* section 1.4). The incorporation of a binding group in the form of a thiourea on the other hand was considered to act as a means of ‘holding’ the substrate through hydrogen bonding to allow the activating catalytic proline group to carry out the aldol reaction.

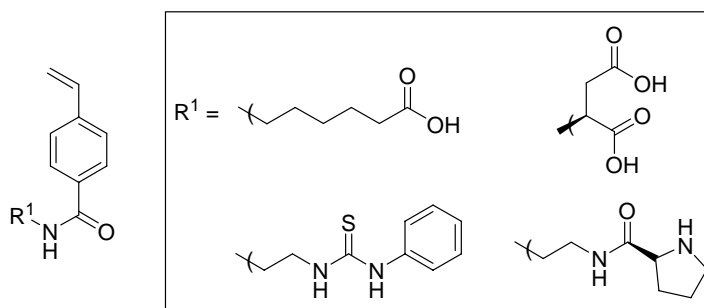


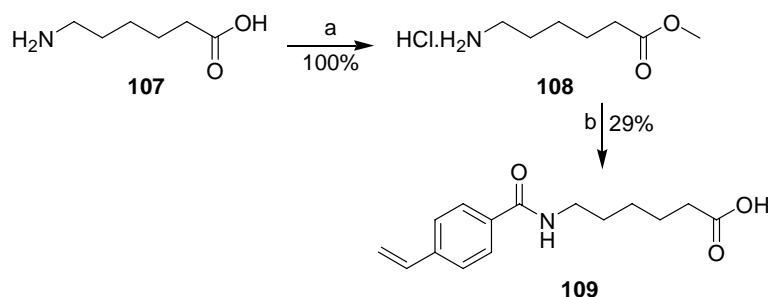
Figure 2.10: Functionalised styrene monomers.

As well as the functionalised styrene monomers shown above, commercially available 3- and 4-vinylbenzoic acids were also employed as monomers in the synthesis of the alternating co-polymers, since they already possessed the carboxylic acid functionality required to act as an efficient proton donor. Also the

effect of altering the carboxylic acid regiochemistry could then be studied to determine whether this displayed any significant difference in their reactivity. These monomers lacked the presence of a flexible hydrocarbon linker, and therefore they could also be compared to those that contain a linker in order to establish the importance or otherwise of its presence.

2.3.3.1 Synthesis of Functionalised Styrene Monomer with Flexible Carboxylic Acid Group

As previously mentioned, the enamine mechanism (**Scheme 1.7**) involves many proton transfer processes, and therefore it was proposed that the presence of a flexible carboxylic acid group would enhance the aldol reaction catalysed by proline. Starting from 4-vinylbenzoic acid, a flexible hydrocarbon chain with a terminal carboxylic acid group was attached to yield the desired monomer (**Scheme 2.10**). In order to avoid any intramolecular cyclisation, 6-aminohexanoic acid **107** was first transformed into the methyl ester **108** in good yield, prior to coupling with 4-vinylbenzoic acid to yield **109**. Various coupling methods involving the use of DCC, DIC, EDC or HATU were attempted for step b but these afforded either the recovery of starting materials or an intractable mixture of products. However the desired product was successfully produced, albeit in low yield through the use of NMM with ethyl chloroformate.

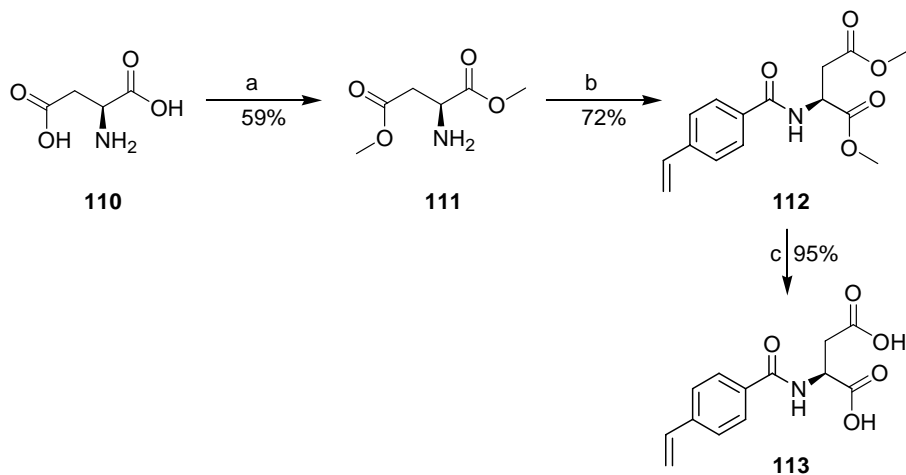


Scheme 2.10: a) SOCl_2 , MeOH, RT, 18 h;¹⁴² b) i) 4-vinyl-benzoic acid, NMM, ethyl chloroformate, DCM, 18 h, ii) NaOH, THF, 12 h.

2.3.3.2 Functionalised Styrene Monomer with Chiral Dicarboxylic Acid Group (L-Aspartic Acid)

The chiral dicarboxylic acid, aspartic acid, was then selected for incorporation with the idea that it would not only facilitate the aldol reaction by having twice as many proton donors, but also provide a chiral environment with the resultant possibility for enantioselective aldol reactions to take place. In light of this fact, the following monomer was synthesised (**Scheme 2.11**).

The carboxylic acid groups of aspartic acid **110** were first methylated to give **111** to prevent any homo coupling reactions from taking place. 4-vinylbenzoic acid which was activated in the form of the mixed anhydride derived from ethyl chloroformate was then coupled with **111** to yield **112**. Deprotection of the two ester groups then furnished the product **113** in good yield.



Scheme 2.11: a) AcCl, MeOH, 10 h; b) 4-vinylbenzoic acid, NMM, ethyl chloroformate, DCM, 2 h; c) 2 M NaOH, MeOH, 1 h.

2.3.3.3 Synthesis of Functionalised Styrene Monomer with Thiourea Binding Group

Having successfully synthesised the styrene monomers containing various proton donors by incorporation of a carboxylic acid group, attention was then focused on

the synthesis of a monomer containing a binding group.

Natural aldolases contain various binding groups in the active site to increase their reactivity. Although ‘unnatural’, the thiourea moiety is well known to act as a binding unit for the carbonyl group through hydrogen bonding.

A beautiful illustration of the use of a thiourea can be seen in the work of Takemoto *et al.* who introduced a chiral, bifunctional thiourea, in order to accelerate a variety of enantioselective reactions, through dual activation of the electrophile and the nucleophile (**Figure 2.11**).¹⁴³ This involved the use of a thiourea moiety bearing a chiral scaffold and a basic functionality, to promote nucleophilic addition reactions.

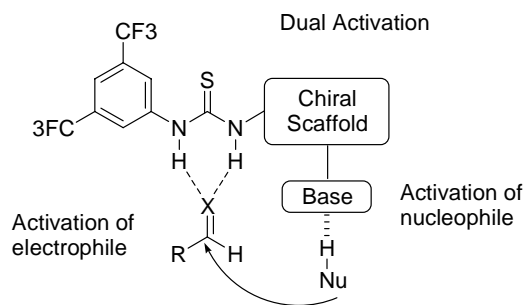
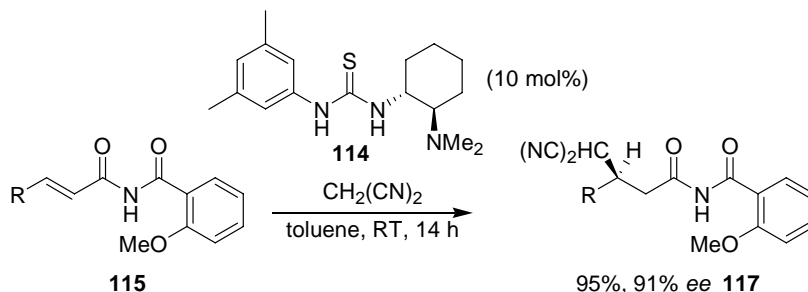


Figure 2.11: Design of bifunctional thioureas having a chiral amino moiety.

The chiral thiourea **114**, was able to catalyse the enantioselective Michael addition of malononitrile **116** and *N*-acyl-2-methoxybenzamide **115**. The desired product **117** was obtained in 95% yield and 91% *ee*. In this instance, both the rigidity of the chiral diamine scaffold and cooperative function of the two N-H bonds and the tertiary amino group in the catalyst, were thought to be crucial for this enantioselective Michael reaction (**Scheme 2.12**).



Scheme 2.12: Michael addition of malononitrile and *N*-acyl-2-methoxybenzamide.

An X-ray crystallographic structure of **114** revealed that both the dimethylamino group and the thiourea group were located in equatorial positions on a chair-formed cyclohexane group, which were in an ideal conformation for dual activation (**Figure 2.12**).

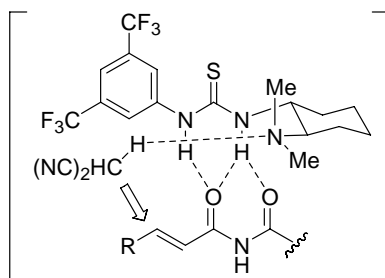


Figure 2.12: Transition state of Michael addition of malononitrile and *N*-acyl-2-methoxybenzamide.

It was hoped that the presence of a thiourea group for our purposes could also allow the substrate to be activated through a hydrogen bonding network so that when held in close proximity to the catalytic proline site, this would facilitate the aldol reaction.¹⁴⁴ The target molecule is shown in **Figure 2.13**, which contains the key thiourea moiety, a styrene portion for polymerisation, and an ethylenediamine linker.

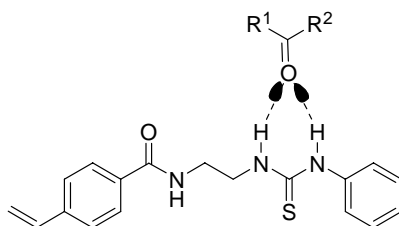
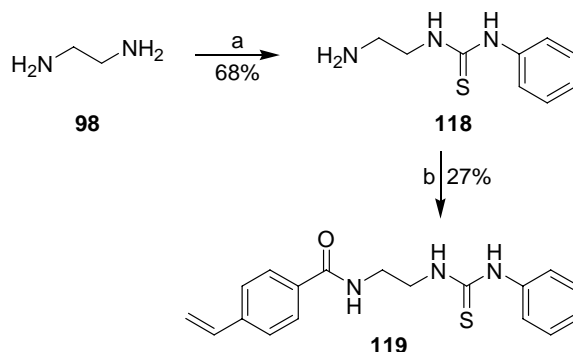


Figure 2.13: Binding interaction between thiourea and carbonyl compounds.

In order to incorporate this thiourea moiety within the styrene monomer, ethane-1,2-diamine **98** was first reacted with phenylisothiocyanate to yield **118** in good

yield. The rest of the synthesis was carried out in an analogous manner to the previous styrene monomers by coupling to 4-vinylbenzoic acid to give the desired monomer **119** (**Scheme 2.13**).

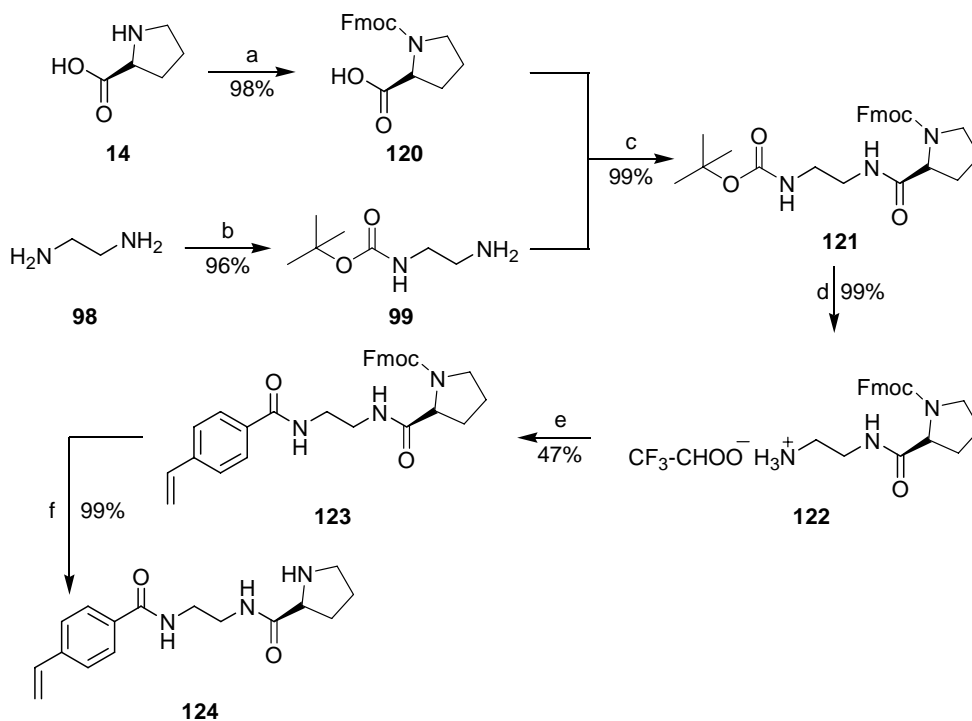


Scheme 2.13: a) phenylisothiocyanate, benzene 2 h;¹⁴⁵ b) 4-vinylbenzoic acid, NMM, ethyl chloroformate, DCM, 18 h.

2.3.3.4 Functionalised Styrene Monomer with L-Proline

A functionalised styrene monomer with a proline moiety was then prepared as complementary alternative to the corresponding maleimide monomer **106**. As previously mentioned (section 2.3.2) this would allow the effect of exchanging the location of the two functionalities relative to the polymer backbone to be studied.

The target monomer **123** was thus prepared by following the synthetic route outlined in **Scheme 2.14**. Proline was first protected with an Fmoc instead of a Boc group to allow the Boc group to be deprotected selectively in the final step of the synthesis. Without this orthogonal protection, the proline group could compete as a nucleophile and yield unwanted side products. The protection of proline **14** proceeded smoothly to give Fmoc proline **120** in excellent yield. This was then coupled to *N*-*tert*-butoxy(2-aminoethyl)carbamate **99** used previously, to give compound **121** in good yield. Selective deprotection of the Boc group gave the TFA salt of the desired species **122** which was again coupled to 4-vinylbenzoic acid to give **123**. Final deprotection of the Fmoc group using a mild base furnished the functionalised styrene product **124** in moderate yield.



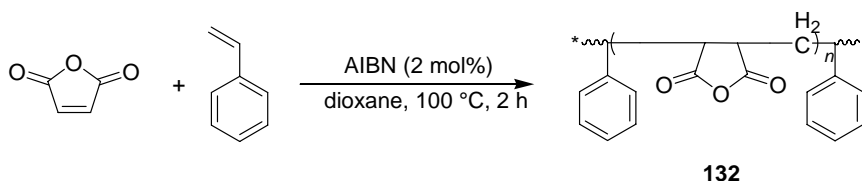
Scheme 2.14: a) Fmoc-Cl, 10% Na₂CO₃, dioxane, 12 h; b) Boc₂O, DCM, 24 h; c) NMM, ethyl chloroformate, DCM, 3 h; d) TFA, DCM; e) 4-vinylbenzoic acid, NMM, ethyl chloroformate, DCM, 2 h; e) 5% diethylamine, MeCN, 2 h.

2.3.4 Polymerisation of Functionalised Maleimide and Styrene Monomers

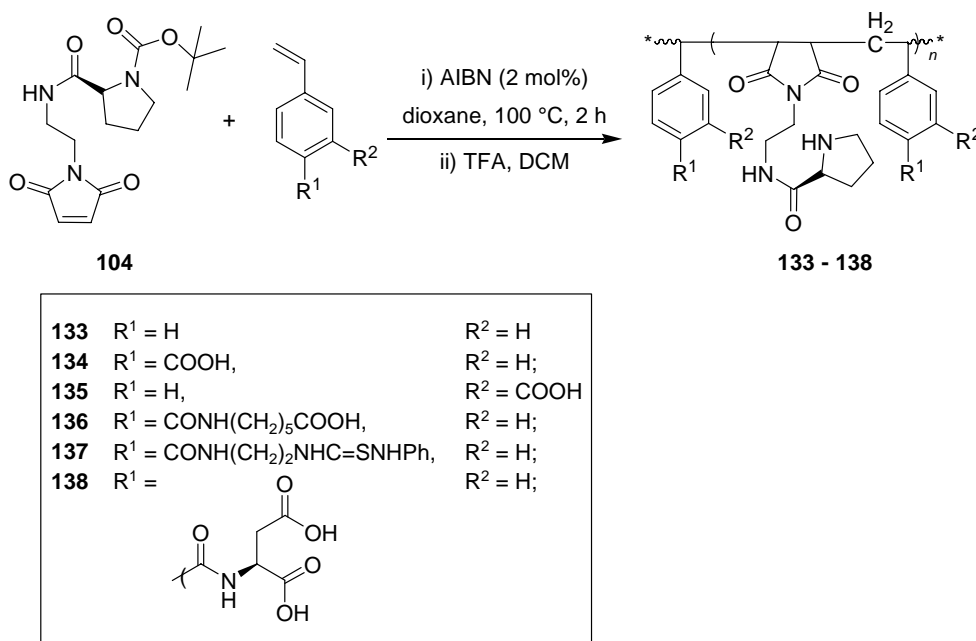
With the functionalised maleimide and styrene monomers to hand, the relevant conditions for the free radical polymerisation process required for the synthesis of various alternating co-polymers were then investigated.

2,2'-azobisisobutyronitrile (AIBN) was selected as a suitable radical initiator since it is often used in related systems. The mechanism for this polymerisation reaction is illustrated below (**Scheme 2.15**). The AIBN **125** acts as an initiator and first undergoes homolysis to generate the active radical. Addition of this radical to the styrene monomer **126** then occurs to give the lower energy benzylic radical **127**, which because of its nucleophilic character, prefers to add to the electron deficient maleimide co-monomer **128** to give radical **129**. In terms of relative rates, addition of **127** to the maleimide is preferred over the addition to

proceeded to give the known polymer in 70% yield.

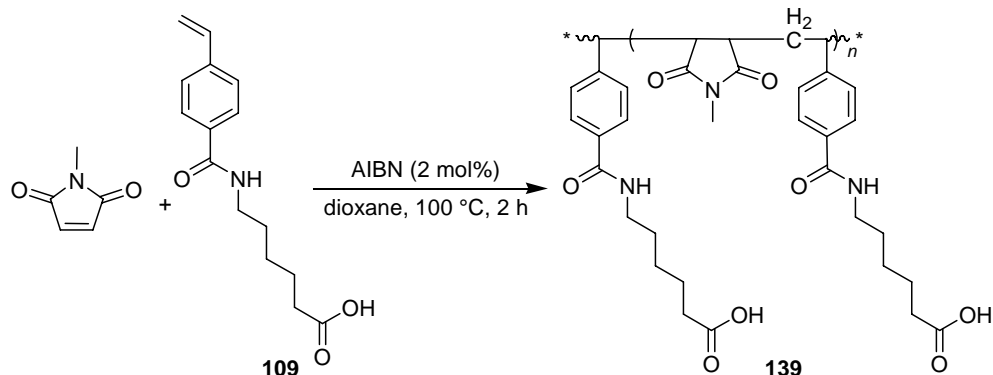


Scheme 2.16: Alternating co-polymerisation of maleic anhydride and styrene. Since the co-polymerisation of styrene and maleic anhydride gave the desired polymer, the same method was then employed using the functionalised maleimide monomer **104** and the styrene monomers (**Scheme 2.17**).¹⁴⁶ After the additional deprotection step of the Boc group was carried out, polymers **133** – **138** were successfully synthesised with yields ranging from 40 – 70%.



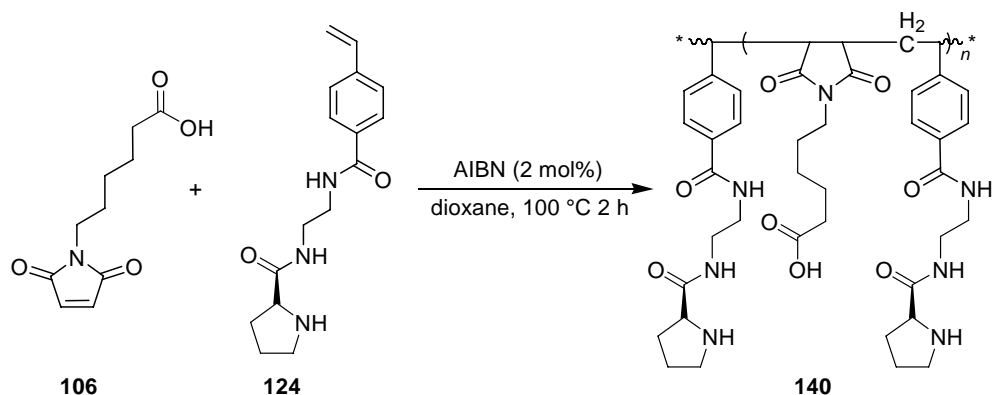
Scheme 2.17: Alternating co-polymers.

In order to investigate the effectiveness of the carboxylic acid group alone in catalysing the aldol reaction *i.e.* without the presence of the proline group, another polymer was synthesised using *N*-methyl maleimide and a styrene monomer **109** with a flexible carboxylic acid chain (**Scheme 2.18**). The same method previously employed was used to yield the corresponding polymer **139** in 83% yield.



Scheme 1.18: Co-polymer without catalytic proline.

Finally, as previously discussed in section 2.3.2, the complementary alternating co-polymer wherein the proline residue was attached to the styrene monomer and the carboxylic acid group was attached to the maleimide monomer was prepared, in order to investigate whether alteration of the polymeric backbone would have an effect on catalyst activity. The desired polymer was synthesised by taking monomers **106** and **124** to give the desired polymer **140** in 92% yield.

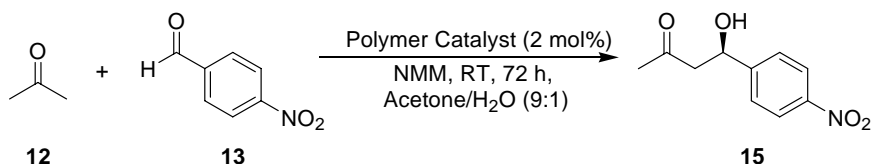


Scheme 2.19: Co-polymer with functionalities on opposite monomer.

2.3.5 The Aldol Reaction using 4-Nitrobenzaldehyde and Acetone

In order to assess the efficiency of these alternating co-polymer catalysts, the reaction between acetone **12** and 4-nitrobenzaldehyde **13** was investigated with each of the polymers (**Scheme 2.20**). Various solvent systems, reaction times and

temperatures were explored in order to find the optimum conditions for this reaction. However it was found that those selected by Smiljanic displayed the greatest reactivity.¹³⁴ Therefore these conditions were employed in all subsequent aldol reactions. A control reaction was also set up, where the polymer catalyst was omitted.



Scheme 2.20: Aldol reaction using polymer catalysts.

All eight polymer catalysts **133** – **140** afforded the desired aldol product **15**, although considerable variations in yields were observed (**Table 2.1**). The enantiomeric excess, which measures the extent to which a particular enantiomer dominates the mixture, was also calculated using the following equation:

$$ee = ((R - S) / (R + S)) \times 100$$

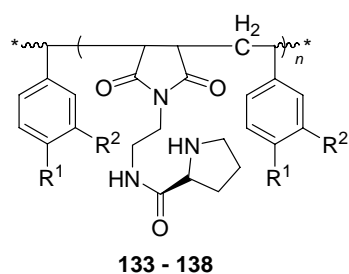
where R and S are the respective fractions of enantiomers in a mixture such that

$$R + S = 1$$

In each case, the *R* enantiomer was favoured over the *S* enantiomer.

Catalyst	Yield of 15 / %	Enantiomeric Excess / % ^a
Control	Trace	-
L-proline	68	67
133	41	39
134	64	38
135	65	35
136	78	40
137	19	37
138	75	29
139	10	-
140	24	38

^a Chiral HPLC (OB, 70:30 hexane/isopropanol, 0.50 ml/min).



- | | | |
|------------|---|-----------------------|
| 133 | R ¹ = H | R ² = H |
| 134 | R ¹ = COOH, | R ² = H; |
| 135 | R ¹ = H, | R ² = COOH |
| 136 | R ¹ = CONH(CH ₂) ₅ COOH, | R ² = H; |
| 137 | R ¹ = CONH(CH ₂) ₂ NHC=SNHPh, | R ² = H; |
| 138 | R ¹ = | R ² = H; |

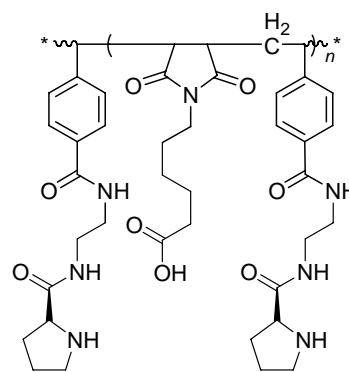
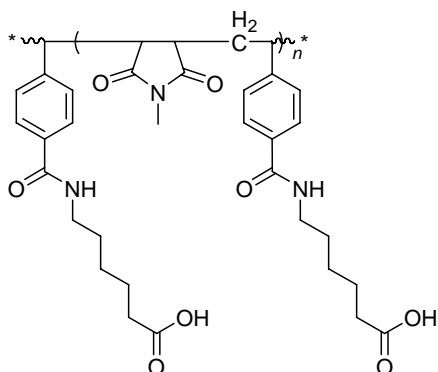
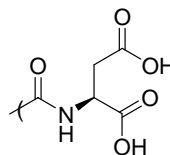


Table 2.1: Summary of results using polymer catalysts.

As expected, the control reaction did not yield significant amounts of the aldol product, nor did polymer **139** where only the carboxylic acid group was present without the benefit of the catalytic proline moiety. The presence of the carboxylic acid group with proline (polymers **134** and **135**) seemed to enhance the reaction, when compared to the corresponding yield with polymer **133** in which styrene was used instead of 3- (**135**) or 4-vinylbenzoic acid (polymer **134**). However the relative lack of flexibility in the polymer backbone is likely to be the reason for the catalytic activity of these three proline-containing polymers producing lower yields than when proline itself was used. The most promising catalyst was found to be **136** which contained a more flexible carboxylic acid as the proton donor. The presence of this functionality alongside the proline group seemed to show a cooperative effect, increasing the catalytic activity of the reaction.

One initially surprising result was the dramatic reduction in yield to 19% when a

carbonyl binding group in the form of a thiourea was present (polymer **137**). There are a number of possible reasons for this outcome. Firstly due to the large excess of acetone which is present in the reaction mixture, it is possible that this binding site was already occupied by the ketone and therefore unable to bind to the aldehyde, and this in turn, would have hindered the aldol reaction from taking place. It is also possible that the binding group was organised in such a way that it had an antagonistic effect with the proline catalyst, with the substrate being bound to the thiourea group without ever coming into contact with proline and as a result, remaining unchanged.

Another initially surprising outcome was seen for polymer **140** where the catalytic proline group and the proton donor were attached to the opposite monomer. Since the two groups being attached were the same as those used previously, it was expected that this polymer would be as active as polymer **136**. However this clearly was not the case since the yield was dramatically reduced from 78% (polymer **136**) to 24% (polymer **140**), although the enantiometric excess remained similar for both polymers [40%, (polymer **136**) and 38%, (polymer **140**)].

One explanation for this is that polymer **140** lacked favourable internal hydrogen bonding between the two monomers. This can be illustrated by considering the possible structures of the two polymers **136** and **140** in more depth (**Figure 2.14**).

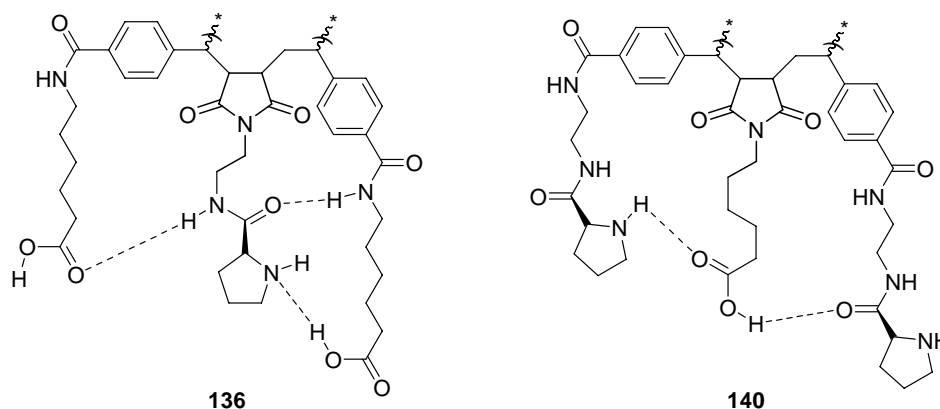


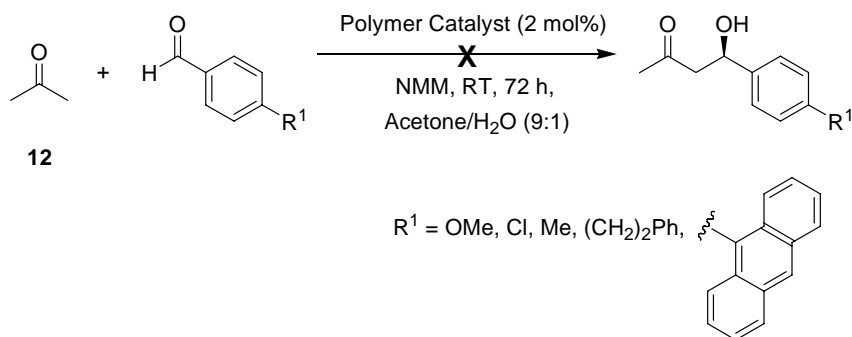
Figure 2.14: Illustrative hydrogen bonding patterns for polymers **136** and **140**.

Although the two polymers are similar in terms of their backbone structure as illustrated in **Figure 2.14**, it is likely that they possess entirely different hydrogen bonding patterns between the different functional groups. Casual inspection of the two structures suggests that the relatively rigid nature of the *para*-benzamide unit in particular may well preclude effective cooperativity between the functional groups unless there is sufficient conformational mobility in the attached chain. Thus, as implied in structure **136**, a greater number of possibilities for salt formation and hydrogen bonding appear to exist than for polymer **140** where the proline residue and the carboxylic acid are operating as two ‘separate’ units. The poorer yield of aldol product using polymer **140** can possibly be explained in this way, and, in future studies, modelling of units such as **136** and **140** could prove to be very informative.

Finally polymer **138** which contained a dicarboxylic acid unit with additional chirality in the form of aspartic acid, did not improve either the yield or enantioselectivity. Although the yield was very high, almost matching polymer **136**, the catalyst displayed the lowest enantiomeric excess of 29% compared to 35 – 40% for all the other polymers. The idea of ‘match’ and ‘mismatch’ is of course a very well established phenomenon in catalytic reactions, which feature two different chiral entities, and in this instance the chirality imposed by the aspartic acid residue clearly opposed rather than enhanced the dominant trend deriving from the proline group. It would therefore be of interest to examine other dicarboxylic acids and related congeners which possess the opposite absolute configuration at this site.

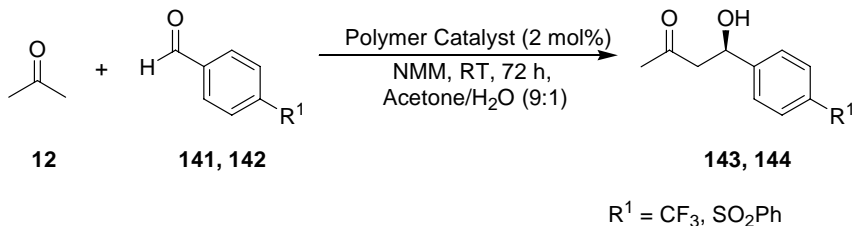
Although all polymers displayed reasonable enantioselectivities ranging from 35 – 40% except polymer **138** (29%), none matched up to when proline itself was used in the reaction (67%). The carboxylic acid groups found within the polymers are not located at a specific site as is found within proline and it is therefore almost impossible to mimic the exquisite geometry adopted by proline, especially in the cases where flexible chains are present (polymer **136**).

Having established that polymer catalysts **133** – **140** catalysed the aldol reaction of acetone with 4-nitrobenzaldehyde, several other aldehyde substrates were then tested. These included 4-methoxybenzaldehyde, 4-chlorobenzaldehyde, 4-tolualdehyde, hydrocinnamaldehyde and 9-anthraldehyde (**Scheme 2.21**).



Scheme 2.21: Attempted aldol reactions.

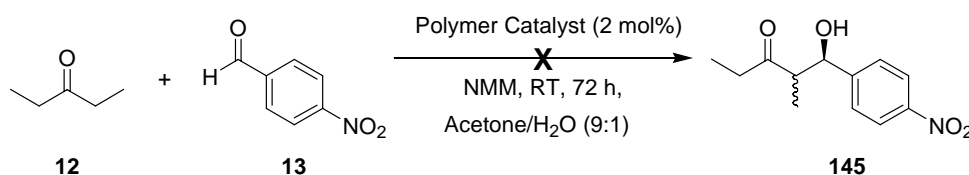
Unfortunately the aldol product could not be detected in any of these reactions, and starting material was recovered in each case. It was believed that the polymers required electron deficient aldehydes containing highly electron withdrawing groups at the 4- position. Two other substrates, 4-(trifluoromethyl)benzaldehyde and 4-(benzenesulfonyl)benzaldehyde were therefore tested against the most active polymer **136**, and as expected the corresponding aldol products for both aldehydes were obtained in 61% yield, 29% *ee* and 55% yield, 32% *ee* respectively (**Scheme 2.22**).



Scheme 2.22: Aldol reaction using polymer catalysts.

Having examined the scope of the aldehyde component of the reaction, the aldol reaction was next tested by changing the ketone component (**Scheme 2.23**). 4-

Nitrobenzaldehyde gave the corresponding aldol product in good yields with acetone and was therefore chosen as the aldehyde. 3-pentanone was selected as a suitable ketone since this reaction would not only reveal the reactivity of the polymers against other ketones but also test further aspects of stereoselectivity of the polymer catalysts. Unfortunately this reaction did not yield any aldol products, and only the two starting materials were recovered, and thus this concept could not be investigated further.



Scheme 2.23: Aldol reaction to determine the regioselectivity.

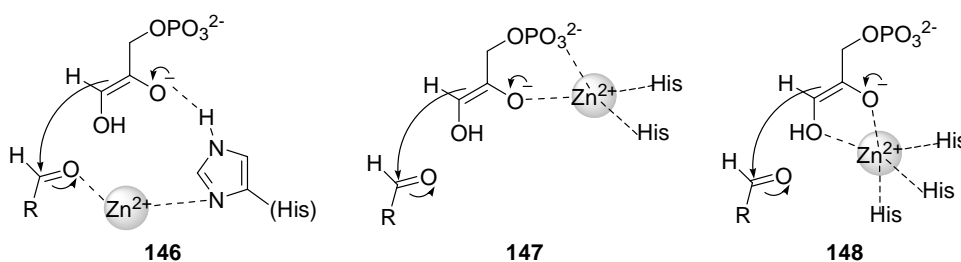
Comparing the alternating co-polymers to the tentagel aldolase mimic by Smiljanic, the isolated yields were generally a lot higher with these co-polymers. The isolated yield for **15** using the tentagel polymer mentioned previously was 30% (**Figure 2.6**), therefore these alternating co-polymers already showed more promise as catalysts. The presence of the carboxylic acid group in the tentagel aldolase mimic had no effect on the reactivity of the aldol reaction, whereas here, the polymers containing the acid group showed an increase in yield. It is likely that ensuring that the functional groups were alternating and therefore in closer proximity had a beneficial effect. The only disappointing aspect of the polymer catalysts at this stage was their lack of reactivity towards other substrates, thus being able to only catalyse the aldol reaction between aldehyde substrates containing highly electron withdrawing groups with acetone.

2.3.6 Type II Aldolase Mimics

As outlined earlier (section 1.3.3), there are two types of natural aldolases, type I and type II. The alternating co-polymers synthesised in the previous section fall into the category of type I aldolase mimics since no metal counterion was present

in the catalytic aldol reaction. In nature, zinc is the most commonly found metal in type II aldolases. These Zn^{2+} cations are thought to act as essential Lewis acid cofactors in type II aldolases, to facilitate deprotonation.

Numerous studies of type II aldolases, namely D-fructose 1,6-bisphosphate aldolase (FruA) and L-fuculose-1-phosphate aldolase (FucA) have been carried out in order to elucidate the possible mechanism by which these aldolases are likely to operate (**Scheme 2.24**).¹⁴⁷

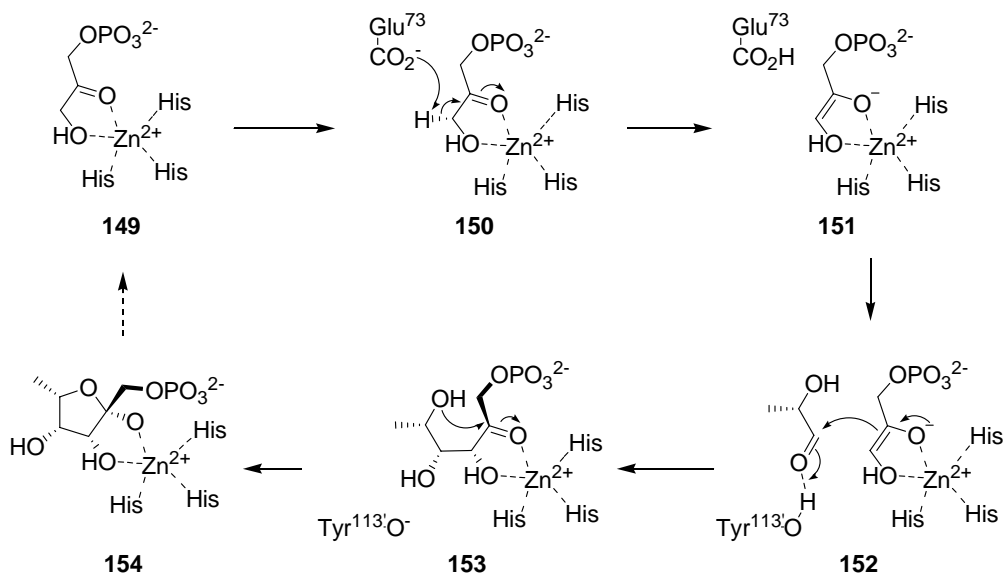


Scheme 2.24: Proposed mechanisms for type II aldolases.

According to ESR and NMR studies, it was thought that the carbonyl group of DHAP was polarised by the Zn^{2+} cation, through an intervening imidazole ring, and the aldehyde was also coordinated to the Zn^{2+} cation **146**. Subsequent FT-IR and deuterium exchange studies led to the conclusion that aldehyde activation occurred by coordination of both carbonyl and phosphate group of DHAP to the Zn^{2+} cation **147**. The X-ray structure for FucA, the first of a type II aldolase, however revealed that the active site contained catalytically active Zn^{2+} tightly coordinated by three histidine residues (His92, His94 and His155) **148**.¹⁴⁸ In light of this, hypotheses **146** and **147** must be rejected since the steric restraints imposed on the Zn^{2+} ion precludes coordination of more than a single substrate, and on its histidine ligands, which cannot act as a proton relay between bound substrate.¹⁴⁷

Based on this data from X-ray structure analysis and through studies of enzyme-substrate interactions, Fessner *et al.* proposed the following mechanism by which the type II aldolases could catalyse the aldol reaction (**Scheme 2.25**).

In the first instance, DHAP coordinates through both hydroxyl and carbonyl oxygen atoms to the Zn^{2+} cation **149**. Polarisation of the carbonyl bond increases the acidity of the hydroxymethylene hydrogen atoms and facilitates abstraction of the *pro-R* proton by a general base, most likely to be Glu73 as shown in **150**, to give **151**. Next, the nucleophilic *cis*-enediolate attacks the *Si* face of an incoming lactaldehyde carbonyl, assisted by Tyr113', which is able to donate a proton to stabilise the developing charge **152**. The ring closure from attack of the hydroxyl group **153** yields the product **154** (DHAP), which is then liberated to regenerate the catalyst.¹⁴⁷

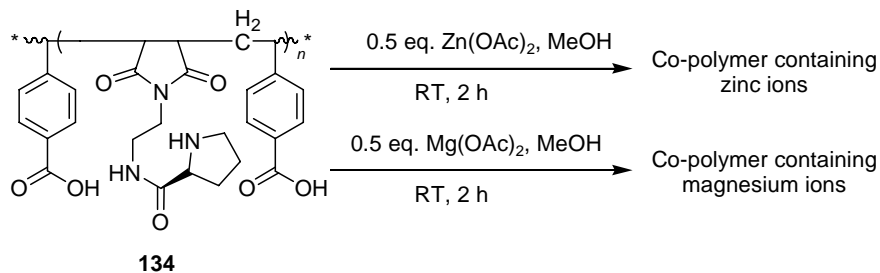


Scheme 2.25: Catalytic cycle for type II aldolases.

It was therefore envisaged that the incorporation of Zn^{2+} cation might encourage some of the polymers already synthesised to act as type II aldolases. Unnatural polymers containing a Mg^{2+} cation as a Lewis acid were also considered.

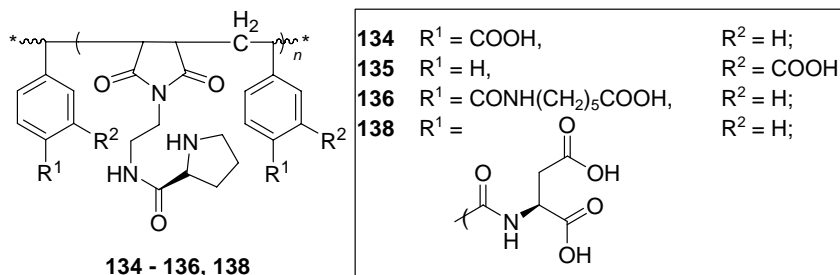
It was decided to test this simple idea through addition of a metal salt to the polymer to yield the corresponding carboxylate complexes. Thus, all polymers synthesised previously which contained a carboxylic acid moiety were transformed into 'type II aldolase mimics'. **Scheme 2.26** illustrates the

modification method used, exemplified by polymer **134**.



Scheme 2.26: Modification of type I aldolase mimics.

Each polymer containing a carboxylic acid group (**Scheme 2.27**) was modified to give the corresponding oxo-metal complex by dissolving the polymer in methanol with 0.5 equivalents of either magnesium or zinc acetate, in all cases except when aspartic acid was present. In this case one equivalent of the metal salt was used due to the presence of two carboxylic acid groups, to give the modified type II aldolase mimics.



Scheme 2.27: Polymers used in the construction of Type II aldolase mimics

In this manner, each Zn²⁺ cation was thought to coordinate to two carboxyl groups, although the exact coordination sphere could not be determined for the resultant polymers. It is likely that each polymer strand would coordinate to Zn²⁺ cations in a different way. **Figure 2.15** shows the possible coordination of the Zn²⁺ cation to the polymers.

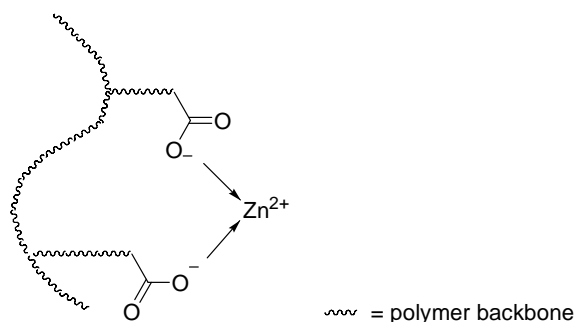


Figure 2.15: Coordination of Zn^{2+} to polymer catalysts.

In the case for aspartic acid, since it contains two carboxyl groups, as well as showing binding as in **Figure 2.15**, it is possible for the Zn^{2+} cation to bind to the two carboxyl groups of the aspartic acid in the following manner (**Figure 2.16**).

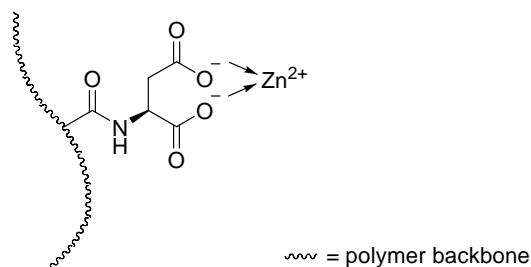
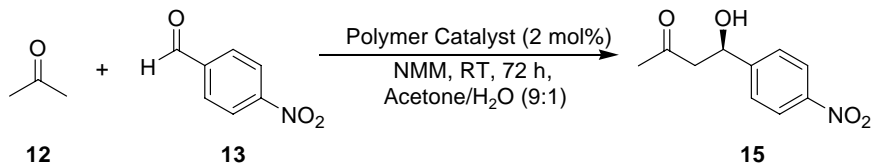


Figure 2.16: Zn^{2+} coordination to aspartic acid.

With these polymers to hand, they were then used without further modification, in the aldol reaction between acetone and 4-nitrobenzaldehyde under the same reaction conditions as the previous non-metallic polymers (**Scheme 2.28**).



Scheme 2.28: Test aldol reaction.

In addition to the four polymers synthesised above, control reactions using only magnesium acetate or zinc acetate were also carried out for comparison. The following table summarises the results obtained (**Table 2.2**)

Catalyst	Yield of 13 / %	Enantiomeric Excess / % ^a
Zn(OAc) ₂	14	-
155 : [Zn(OAc) ₂ + 134]	27	22
156 : [Zn(OAc) ₂ + 135]	33	21
157 : [Zn(OAc) ₂ + 136]	32	27
158 : [Zn(OAc) ₂ + 138]	35	19
Mg(OAc) ₂ (1 mol %)	30	-
Mg(OAc) ₂ (2 mol %)	33	-
159 : [Mg(OAc) ₂ + 134]	32	17
160 : [Mg(OAc) ₂ + 135]	41	10
161 : [Mg(OAc) ₂ + 136]	42	12
162 : [Mg(OAc) ₂ + 138]	54	15

^a Chiral HPLC (OB, 70:30 hexane/isopropanol, 0.50 ml/min).

Table 2.2: Summary of results using type II aldolase mimics.

As expected, the control reactions using only zinc acetate or magnesium acetate as Lewis acids both yielded the aldol product, with magnesium acetate giving twice the conversion of zinc acetate. In general, all of the modified type II aldolase mimics gave lower yields and enantioselectivities when compared to using the polymer alone as type I aldolase mimics. For example, when using **157** as the catalyst a yield of only 32% with an *ee* of 27% was obtained compared to a yield of 78% with an *ee* of 40% for polymer **136**.

Comparing the difference in reactivity of the two metals within the polymers, it is clear that those containing magnesium ions gave higher yields than the zinc equivalent in all cases, but the enantioselectivity was, on the whole, slightly higher for those with zinc ions than magnesium ions. This is perhaps not surprising since the control reaction containing magnesium acetate gave a higher yield than when zinc acetate was present.

It is interesting to note that the yield for all the polymers except polymer **162**

containing a magnesium ion was not substantially higher than the control reaction in which magnesium acetate alone was present in the reaction. At first it could even be argued that the reason why the yield for polymer **162** was almost twice as much as the other three polymers was because it contained twice as much magnesium ions. However the background reaction containing twice the loading of magnesium acetate revealed that doubling the catalyst loading did not double the yield. This result highlighted the complexity of these polymeric systems and how a small change had dramatic consequences in their ability to act as efficient catalysts. In an earlier example when the catalytic and proton donor groups were exchanged on the relevant monomers, the resultant polymers revealed a dramatic reduction in yield for polymer **140** (24%) and the highest of all the yields for polymer **136** (78%). Here a similar anomaly is found where the yield is not expected to be high, based on the background reactions using 1 and 2 mol% magnesium acetate and yet, the results demonstrate a cooperativity effect between the polymer catalyst **162** and the magnesium ions. In this case, the combination of the presence of the aspartic acid functionality, coordinated to the magnesium ions displayed an enhanced catalytic activity. It is likely that the proximity of the two Lewis acidic magnesium ions with the catalytic proline group provided an optimal binding site for the aldol reaction to take place.

It is unfortunate that the polymers containing magnesium ions all displayed low enantioselectivities (10 – 17%). This perhaps meant that in order for the magnesium ion to exhibit greater enantioselectivity, a more flexible linker was required and that the other three polymers were just too rigid in structure to allow the magnesium ion to work in conjunction with the catalytic group.

In high contrast to the polymers containing magnesium ions, the polymers with zinc ions showed much more interesting results. By comparing the yield for the control reaction with zinc acetate, in all cases, the yield was higher when the zinc ions were coordinated to the polymers. For polymers **156 – 158**, yields of between 33 – 35%, were obtained which is over twice when compared to zinc acetate (14%). This pointed to the idea that the zinc ion and the proline groups

seemed to be exhibiting some cooperativity effects. This hypothesis was further supported by the higher enantioselectivity exhibited, compared to when the magnesium ion was present. It looked as though by having the zinc metal ions in close proximity to a chiral environment enhanced the enantioselectivity. This conclusion however can only be made within the analysis of the type II polymers alone. If the reactivity between the type I and type II polymers were to be compared, it can clearly be seen that the type I polymers on their own exhibited higher enantioselectivity and yield. This therefore raises doubts as to what extent the metal cations were actually bound to the polymers and whether there any cooperativity effect existed within the type II polymers.

2.3.7 Summary

In summary, various alternating co-polymers using functionalised maleimide and styrene monomers were successfully synthesised. These polymers were first studied in the form of type I aldolase mimics and their ability to act as catalysts was investigated in test aldol reactions between acetone and 4-nitrobenzaldehyde. It was established, by using a polymer containing only a carboxylic acid group that a catalytic proline group was essential for the polymer to act as an efficient catalyst. It was found however that the presence of a carboxylic acid group was beneficial in terms of obtaining high yields, increasing the yield from 41% (polymer **133**) to 64 – 78% (polymers **134** – **136**). The best results were obtained using polymer **136**, which contained a flexible carboxylic acid chain (78% yield, *ee* 40%), thus highlighting the importance of access to the free carboxylic acid group. The relative inefficiency of polymers **134** and **135** where the carboxylic acid groups are rigidly sited and close to the polymeric backbone provides further confirmation of the necessity for proton availability.

The presence of the thiourea binding group within the polymer **137** led to a dramatic decrease in the yield (19%), possibly as a consequence of either to the substrate being bound too strongly to the thiourea moiety, thus preventing the aldol reaction from taking place, or the product not being released after reaction.

The addition of the aspartic acid group, rather than enhancing enantioselectivity, displayed the opposite effect, giving an *ee* of only 29% compared to 35 – 40% shown for all other polymers. Nevertheless, this negative observation would suggest that incorporation of other chiral acids might well have a beneficial cooperative effect. Clearly, the idea that the overall chiral environment requires both the proline and the carboxylic acid residues is substantiated, as is the concept that preparation of an alternating co-polymer can encourage such enforced propinquity. Having two carboxylic acid groups did not dramatically increase the yield (75%) either, showing results similar to polymer **136** (78%).

Finally, comparison of the two polymers **136** and **140** which differed only in attachment of their proline and carboxylic acid residues to the alternative monomer provided some very valuable insights for further work. As we have seen, polymer **136** gave the best yield of 78% with an *ee* of 40% whereas polymer **140** furnished only 29% with a comparable *ee* of 38%. These results emphasised that, although the essential polymer backbone is the same in both **136** and **140**, the selection of styrene and maleimide as monomers can certainly influence the final three dimensional arrangements of the active catalytic groups. In particular, it would seem that a *para*-disposed styrene unit requires a conformationally mobile spacer unit in order for the attached catalytically active functional group to be actively engaged with the second. In general terms, it would therefore seem that there is an optimal length of spacer to be incorporated into both monomer units such that any influence of the polymer backbone is negated.

All of the type I aldolases, save for that incorporating aspartic acid, gave similar *ees* ranging from 35 – 40%, implying that the proline residue is the dominant influence. Also when the polymers were tested for their scope of substrates, it was found that only reactions between aromatic aldehydes containing highly electron withdrawing groups with acetone successfully furnished the aldol product.

In the second part of the investigation of alternating co-polymers, the type I

aldolase mimics containing a carboxylic acid moiety were modified to type II aldolase mimics by addition of Zn^{2+} and Mg^{2+} ions.

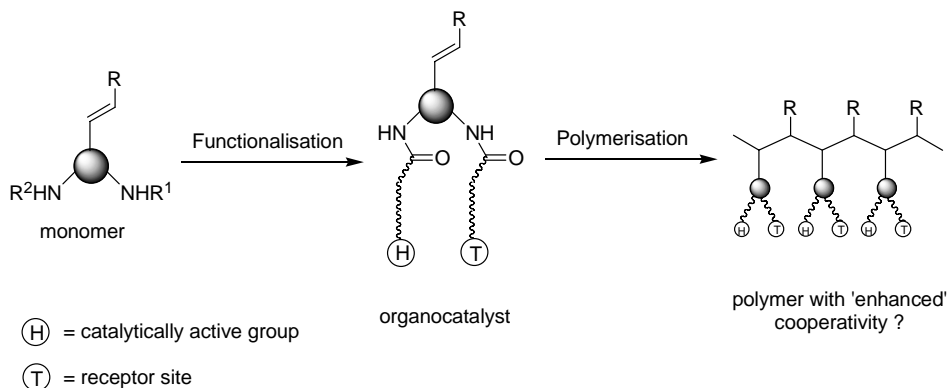
In general, all of these polymers gave lower yields and enantioselectivities when compared to using the polymer alone as type I aldolase mimics. Comparing the difference in reactivity of the two metals, those containing magnesium ions gave higher yields (32 – 54%) than those with zinc ions present (27 – 35%). In terms of the enantioselectivity, those containing zinc ions displayed better *ees* (19 – 27%) than those with magnesium ions (10 – 17%).

Once again, these type II aldolase mimics were only able to catalyse the aldol reaction between acetone and aromatic aldehydes containing highly electron withdrawing groups.

2.4 A Complementary Approach to the Synthesis of Regiochemically Defined Polymers: - The Organocatalytic Route

The results presented in the above section are clearly very encouraging in terms of providing proof of concept for the alternating co-polymer approach, and can certainly be developed further in terms of the lessons which have been learnt in the course of this preliminary study. It is important to recognise however, that whilst this work was ongoing throughout the thesis, contemporaneous efforts were also being directed towards an alternative strategy for the construction of regiochemically defined polymers which would also ensure cooperativity between the ‘hands’ and the ‘teeth’ of an artificial enzyme. The essence of this complementary approach is outlined in **Scheme 2.29** and differs substantially from the idea of preparing a designed co-polymer. In this instance, the key building block is a single monomer which contains two differentiated amino groups, one of which can be used for the addition of the catalytically active group(s), whilst the other can be used for elaboration of the receptor site. The monomer is therefore an organocatalyst in its own right, but with the added bonus

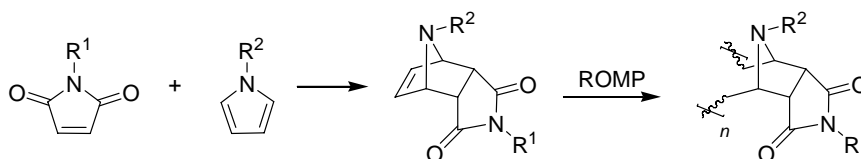
that, on polymerisation, the resulting polymer strand can adopt a host of three dimensional conformations which might be even more effective than the monomer itself.



Scheme 2.29: Organocatalytic approach.

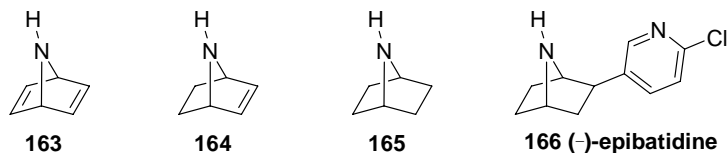
2.4.1 Systems Based on a 7-Azabicyclo[2.2.1]hept-2-ene Core

Initial investigations centred around an examination of systems based on a 7-azabicyclo[2.2.1]hept-2-ene core which can be obtained through a [4+2] cycloaddition reaction (**Scheme 2.30**). As required, these species possess two points of functional group attachments for the 'hands' and 'teeth', and the cycloadduct can act not only as an organocatalyst in its own right but also the monomer for the ubiquitous ring opening metathesis polymerisation (ROMP) step at a later stage. As well as this, these systems had an advantage over other systems which contained the same features since these compounds could be accessed *via* use of the same functionalised maleimide monomer utilised earlier for the synthesis of the alternating co-polymers **104**. This meant that only the preparation of the functionalised pyrrole moieties was required in order to obtain the target molecules.



Scheme 2.30: 7-azabicyclo[2.2.1]hept-2-ene systems.

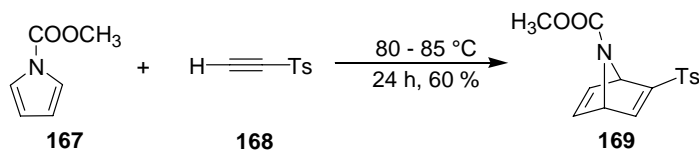
The synthesis of 7-azabicyclo[2.2.1]hepta-2,5-diene **163**, 7-azabicyclo[2.2.1]hept-2-ene **164** and 7-azabicyclo[2.2.1]heptane **165** systems, the latter of which can be found in the natural product (-)-epibatidine **166** are commonly obtained, as previously mentioned, through [4+2] cycloaddition reactions (**Scheme 2.31**).¹⁴⁹



Scheme 2.31: (-)-epibatidine and other azabicyclic systems.

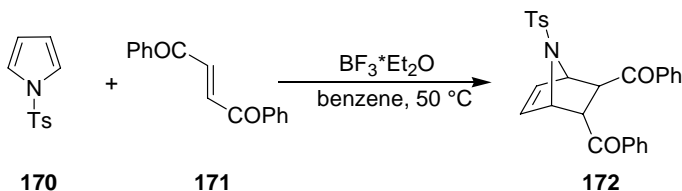
The essential problem in such Diels-Alder reactions is of course that pyrrole and its *N*-alkyl derivatives are, unlike furan, essentially aromatic in character and it is therefore necessary to enhance their reactivity as dienes through introduction of an electron withdrawing group on the nitrogen atom.

Thus, Altenbach first described the synthesis of a 7-azabicyclo[2.2.1]hepta-2,5-diene derivative **169** by the [4+2] cycloaddition reaction of *N*-methoxycarbonylpyrrole **167** with ethynyl-*p*-tolyl sulfone **168** (**Scheme 2.32**).¹⁵⁰



Scheme 2.32: 7-azabicyclo[2.2.1]hepta-2,5-diene derivative.

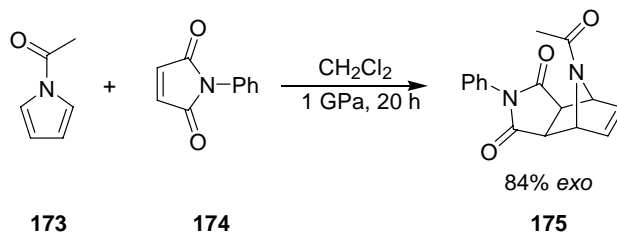
Since then, there have been numerous examples of this approach. Rajakumar has shown that boron trifluoride etherate catalysed the [4+2] cycloaddition between *N*-*p*-toluenesulphonylpyrrole **170** and *trans*-1,4-diphenyl-2-butene-1,4-dione **171** to give the cycloaddition adduct **172** in 80% yield (**Scheme 2.33**).¹⁵¹



Scheme 2.33: 7-azabicyclo[2.2.1]hept-2-ene derivative.

It is believed that the Lewis acid does not simply lower the energy differential between the HOMO and LUMO of the dienophile and pyrrole, but forms a stabilised complex with pyrrole, deactivating it towards electrophiles while enhancing its reactivity as a diene by diminishing the aromaticity.

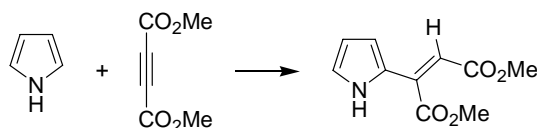
A high-pressure approach has also been employed for the synthesis of 7-azabicyclo[2.2.1]hept-2-ene derivatives between *N*-acylpyrroles **173** with *N*-substituted maleimides **174** (Scheme 2.34).¹⁵² Employing similar methods, it was hoped that the target 7-azabicyclo[2.2.1]hept-2-ene derivatives could thus be synthesised.



Scheme 2.34: Using high pressure to obtain 7-azabicyclo[2.2.1]hept-2-ene derivatives.

2.4.2 Synthesis of [4+2] Cycloaddition Adducts

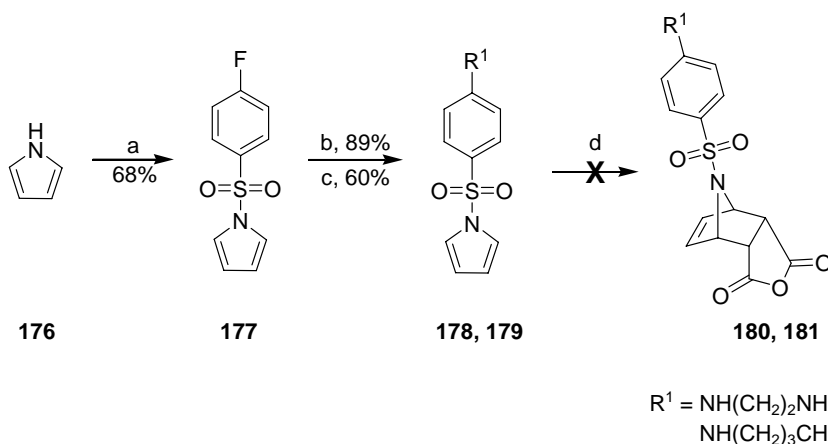
The [4+2] cycloaddition between pyrroles and dienophiles has inherent problems since pyrrole is a poor diene for this process and usually reacts for example, with alkenyl and acetylenic dicarboxylic acid derivatives *via* Michael addition (Scheme 2.35).¹⁵³



Scheme 2.35: Michael addition reaction of pyrrole and acetylene.

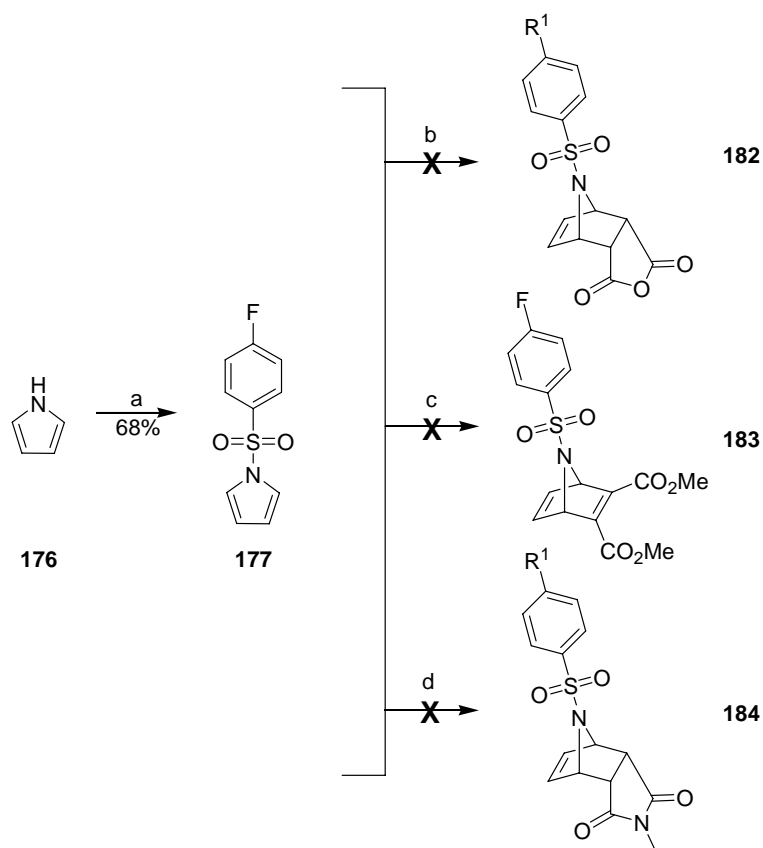
Taking this point into account, the following method was devised to obtain 7-azabicyclo[2.2.1]hept-2-ene derivatives (Scheme 2.36). In order to try and

minimise the undesired Michael addition reaction, a sulphonyl group was attached to pyrrole **176** to give **177** in order to enhance its reactivity towards [4+2] cycloadditions and reduce its nucleophilicity. It was hoped that this increased reactivity would be sufficient to obtain the adducts (**180** and **181**) with various Lewis acids without the requirement of high pressure. The functionalised pyrrole derivative **177** was then modified by exchanging the fluorine atom for either a butylamine or ethylene diamine moiety to give **178** and **179** respectively. Unfortunately however, when the reaction between these two species and maleic anhydride was carried out with various Lewis acids, no cycloadducts were obtained.



Scheme 2.36: a) NaH (60% in oil), 4-fluorobenzenesulphonyl chloride, THF, 30 min; b) ethane 1,2-diamine, reflux, 2 h; c) butylamine, reflux, 2 h; d) i) maleic anhydride, $\text{BF}_3 \cdot \text{Et}_2\text{O}$, benzene, 50 °C, 24 h, ii) maleic anhydride, neat, 85 °C,¹⁵⁴ 24 h, iii) maleic anhydride, AlCl_3 , DCM, RT, 24 h.

Since the functionalised pyrrole derivatives used in **Scheme 2.36** did not yield the desired cycloadducts, it was thought that perhaps the substituents on the benzene ring should be more electron withdrawing. Therefore it was decided to test the reaction with 1-(4-fluoro-benzenesulfonyl)-1*H*-pyrrole **177** instead (**Scheme 2.37**).



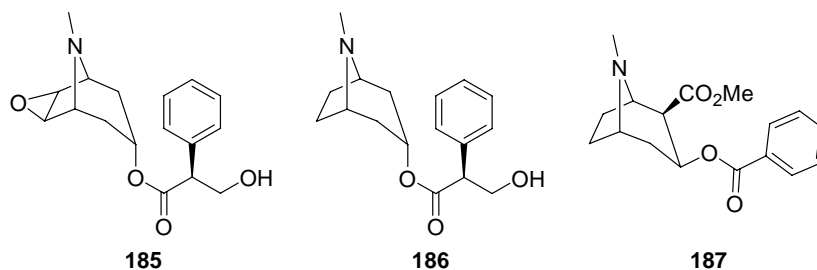
Scheme 2.37: a) NaH (60%), 4-fluorobenzenesulphonyl chloride, THF, 30 mins; b) i) maleic anhydride, $\text{BF}_3 \cdot \text{Et}_2\text{O}$, benzene, 50 °C, 24 h, ii) maleic anhydride, neat, 85 °C,¹⁵⁴ 24 h, iii) maleic anhydride, AlCl_3 , DCM, RT, 24 h; c) i) dimethyl acetylene dicarboxylate, $\text{BF}_3 \cdot \text{Et}_2\text{O}$, toluene, 100 °C, 24 h, ii) dimethyl acetylene dicarboxylate, $\text{BF}_3 \cdot \text{Et}_2\text{O}$, THF, 50 °C, 24 h, iii) dimethyl acetylene dicarboxylate, LiClO_4 , Et_2O , RT, 24 h; d) *N*-methylmaleimide, $\text{BF}_3 \cdot \text{Et}_2\text{O}$, toluene, 100 °C, 24 h.

Unfortunately, the use of $\text{BF}_3 \cdot \text{Et}_2\text{O}$, AlCl_3 or LiClO_4 did not yield any of the desired adducts with the three dienophiles. This is likely to be due to the high activation energy barriers of intermolecular [4+2] cycloaddition reactions which often require very high temperatures or pressures. This however coupled with the tendency for these compounds to decompose made them difficult targets for synthesis, and, in spite of literature precedent, this avenue was not further pursued.¹⁵⁵

2.4.3 Systems Based Around the Tropane Alkaloid Core

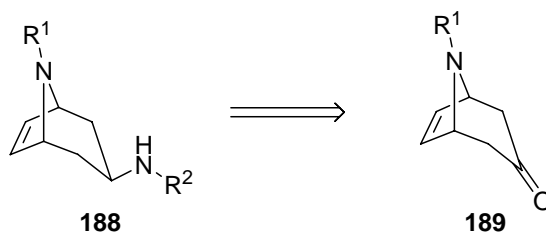
Since efforts to prepare systems based on the 7-azabicyclo[2.2.1]hept-2-ene motif were unsuccessful, our attention turned to other bicyclic systems which would fulfil the same requirements of versatility for functional group attachment, whilst, at the same time, acting as a monomer for the ROMP processes. The tropane alkaloid skeleton seemed to fit this profile well and therefore this system was selected for study.

Tropane alkaloids are a class of naturally occurring compounds that display a diverse range of biological and medicinal activities and are now also finding applications as novel imaging agents. Representative examples of this class of compounds include scopolamine **185**, atropine **186**, and cocaine **187** (Scheme 2.38).¹⁵⁶



Scheme 2.38: Examples of tropane alkaloids.

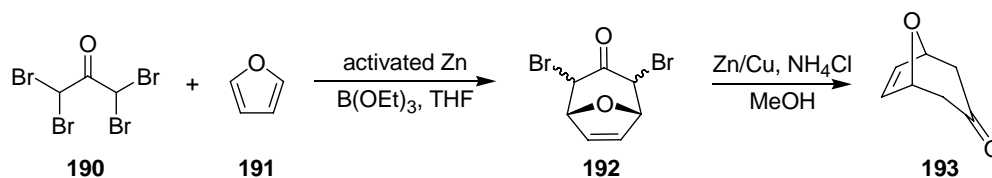
For our purposes, we therefore wished to prepare derivatives of the general type **188** shown in Scheme 2.39. It was envisaged that these, in turn, would be accessible from ketones **189**, either through a reductive amination sequence or stereocontrolled displacement reactions of the derived alcohols.



Scheme 2.39: Tropane derivatives.

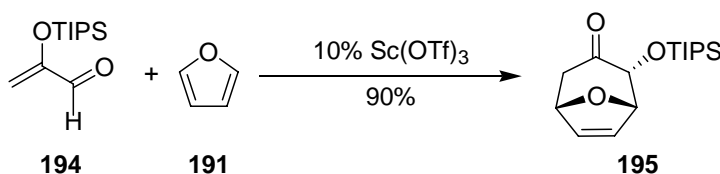
As a consequence of their biological activity, there has of course been intense synthetic interest in the synthesis of tropane derivatives and a wide variety of strategies are available for their construction.

Hoffmann *et al.*¹⁵⁷ reported the synthesis of 8-oxabicyclo[3.2.1]oct-6-en-3-one, **193** using tetrabromoacetone **190** and furan **191** (Scheme 2.40).



Scheme 2.40: Synthesis of 8-oxabicyclo[3.2.1]oct-6-en-3-one.

Likewise Harmata *et al.* constructed a similar cycloadduct starting from the aldehyde **194** and furan **191** (Scheme 2.41).¹⁵⁸

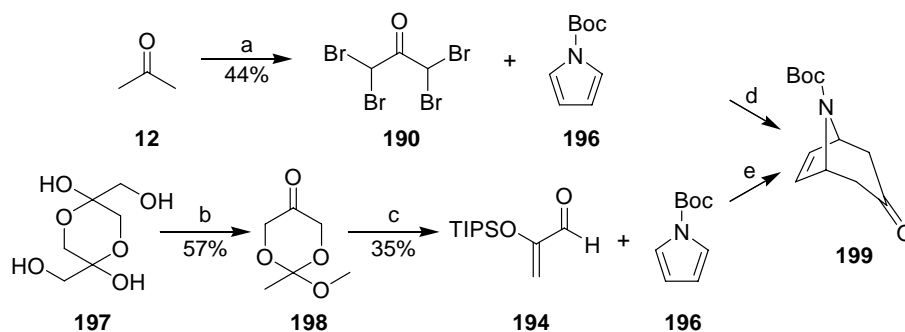


Scheme 2.41: Synthesis of cycloadduct **195**.

In both cases, the key reaction involved a [4+3] cycloaddition reaction between an allylic cation with a diene.

For our purposes, we decided to modify these synthetic methods by replacing furan with *N*-Boc pyrrole **196** as the key component of a [4+3] cycloaddition reaction. This seemed to be a particularly attractive prospect since this would lead to direct installation of the carbon-carbon double bond for ROMP (Scheme 2.42). Unfortunately the [4+3] cycloaddition reaction between *N*-Boc-pyrrole **196** and tetrabromoacetone **190** to give an *N*-protected tropinone derivative **199** was unsuccessful.¹⁵⁴ Similarly the method using 2,5-bis-hydroxymethyl-[1,4]dioxane-2,5-diol **197** as the starting material failed at the cycloaddition step using Sc(OTf)₃ to give **199**.¹⁵⁶ In both cases a black intractable mixture was obtained,

resulting from both unreacted starting materials as well as decomposition of either products or intermediate species. The crude $^1\text{H-NMR}$ and $^{13}\text{C-NMR}$ spectra did not indicate any promising peaks corresponding to the tropane alkaloid skeleton. As a result, these two routes were abandoned in search for alternative starting materials which were more stable to the conditions required for the synthesis of the core tropane alkaloid moiety.

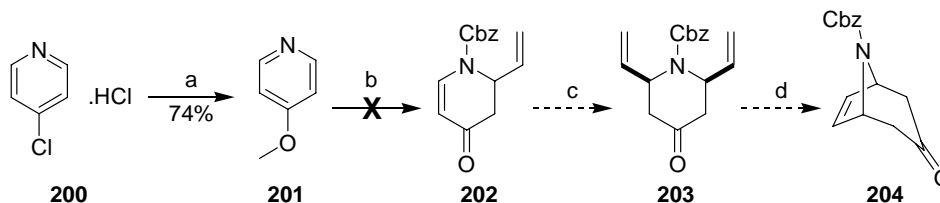


Scheme 2.42: a) HBr (48% aq. soln), Br_2 , RT, 10 days;¹⁵⁷ b) CSA (10 mol%), trimethyl orthoacetate, dioxane, $60\text{ }^\circ\text{C}$, 12 h;¹⁵⁹ c) Et_3N , TIPSOTf, benzene, $50\text{ }^\circ\text{C}$, 12 h;¹⁵⁸ d) activated zinc dust, trimethylborate, Br_2 , THF, $-15\text{ }^\circ\text{C} \rightarrow \text{RT}$, 20 mins;¹⁵⁷ e) $\text{Sc}(\text{OTf})_3$, DCM, $0\text{ }^\circ\text{C} \rightarrow \text{RT}$, 2 h;¹⁵⁹ e) NH_2R , 10% Pd/C, MeOH/ H_2O , RT, 24 h.¹⁶⁰

In particular, we were attracted to a literature report by Martin *et al.*¹⁶¹ who described the use of ring closing metathesis (RCM) for the formation of bridged azabicyclic structures. Until recently little literature on the use of RCM to obtain these species with a nitrogen atom in the one-atom bridge had been reported. It was hoped that by repeating this method, it would lead to the desired motif required for our purposes as outlined below (**Scheme 2.43**).

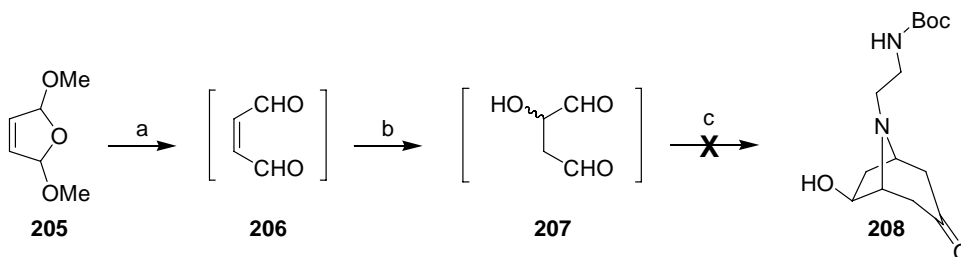
The first step involving the synthesis of 4-methoxypyridine **201** from 4-chloropyridine hydrochloride **200** proceeded in good yield. However the addition of the first vinylic group with the use of vinyl magnesium bromide in the presence of CBz-Cl was unsuccessful. Therefore the subsequent addition of the second vinylic group and the hydrolysis of the intermediate methoxydiene could not be carried out. Again an intractable mixture was obtained, mostly consisting of

unreacted starting material. There was no indication in the $^1\text{H-NMR}$ or IR spectra to suggest that the CBz protection had taken place successfully, nor the addition of the vinyl magnesium bromide. Therefore this literature synthetic route could not be repeated and the RCM to yield **204** could not be carried out.



Scheme 2.43: a) MeOH; b) Cbz-Cl, vinyl magnesium bromide, THF, $-78\text{ }^\circ\text{C}$, 1 h; c) vinyl magnesium bromide, MeLi, CuCN, THF, $-78\text{ }^\circ\text{C}$, 1 h; d) Grubbs II catalyst.

Whilst searching for an alternative approach to the tropane derivative, we turned our attention to reports by Kozikowski *et al.* involving a Robinson-Schöpf synthesis, starting from dimethoxy-2,5-dihydrofuran **205**.¹⁶² This method was therefore modified for our purposes (**Scheme 2.44**). 2 Dimethoxy-2,5-dihydrofuran **205** was transformed into the desired succinaldehyde derivative **207** through direct acid hydrolysis followed by neutralisation. The mixture was then added to a solution of acetone dicarboxylic acid, *N-tert*-butoxy(2-aminoethyl)carbamate and sodium acetate in water in the hope of obtaining **208**. However the 6-hydroxy tropinone **208** could not be obtained. Therefore subsequent modification steps could not be carried out. It was thought that perhaps 2,5-dimethoxyfuran was too unstable to the reaction conditions which were being used and therefore this was the reason for the desired product not being obtained.



Scheme 2.44: a) 3 M HCl, RT, 12 h;¹⁶² b) neutralisation with 6 M NaOH;¹⁶² c)

NaOAc, *N*-Boc-ethylene diamine, RT, 3 d.

At this stage, whilst searching for further literature precedent on the use of the 2,5-dimethoxyfuran motif as a latent 1,4-dicarbonyl unit in the Robinson-Schöpf reaction, we were intrigued to discover a paper by Alder¹⁶³ which described a synthetic route to the tetracyclic congener **212**, and also features the apparently unlikely use of 2,5-dimethoxyfuran as a dienophile in a Diels-Alder reaction with cyclopentadiene **209** (Scheme 2.45).



Scheme 2.45: a) Conc. HCl, H₂O, 0 °C, 10 h; b) acetone dicarboxylic acid, methylamine, conc. HCl, H₂O, 80 °C, 24 h.

Interestingly, closer inspection of the highly acidic reaction conditions suggests that the derived oxocarbenium ion may well be the reactive dienophile. The tetracyclic amino ketone **212**, although not a tropane derivative, embodies all of the necessary framework features and ROMP monomer.

Accordingly, since no spectral data were reported in the original paper, the synthesis of the adduct **212**, reported in the paper was carried out in order to confirm its structure.¹⁶³ Thus, **212** was synthesised in moderate yield and the spectral data supported the proposed structure. Further data were obtained in order to investigate whether the product existed in the *endo* or *exo* form. A NOESY-NMR experiment was carried out to look at the interactions between the key hydrogen atoms shown below for the *exo* and *endo* adducts (**Figure 2.17**):

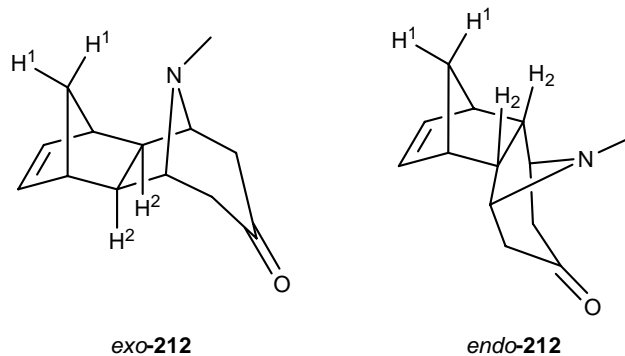


Figure 2.17: *Endo* adduct of tropane alkaloid derivative.

The following 3D structures of the *exo* and *endo* forms of the molecule **212** respectively reveal the different interactions which exist within the two structures (**Figure 2.18**). The dashed lines show the interaction between the H¹ and H² atoms for both *exo* and *endo* forms. It can be seen that for the *exo* isomer, the interactions between H¹ and H² are arranged *anti* to one another and therefore little interaction would be expected on examination of the NOESY-NMR spectrum. The opposite effect would be anticipated for the *endo* isomer which would show a significant interaction between the H¹ and H² atoms involved. Inspection of the NOESY-NMR spectrum did reveal a strong interaction between the atoms under study and it was therefore concluded that the *endo* isomer was obtained as expected.

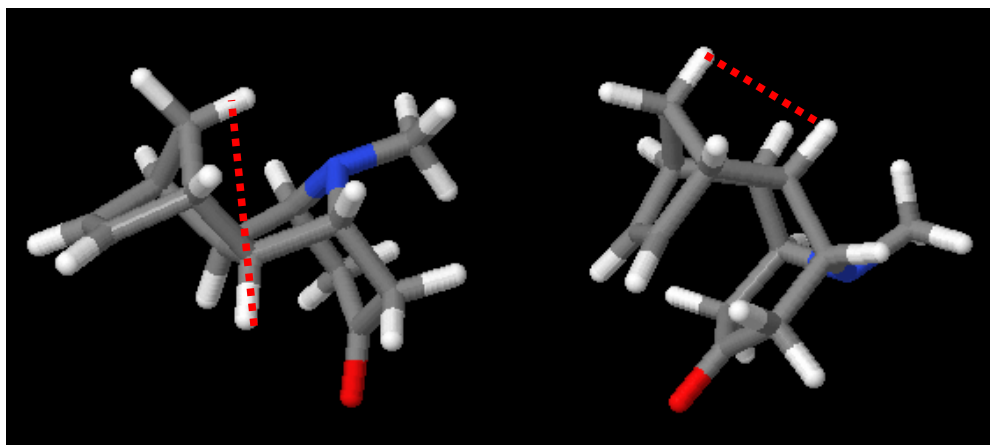
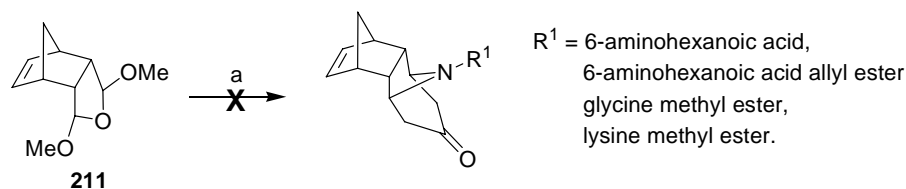


Figure 2.18: 3D Structure of the *exo* and *endo* forms of the tropane alkaloid derivative.

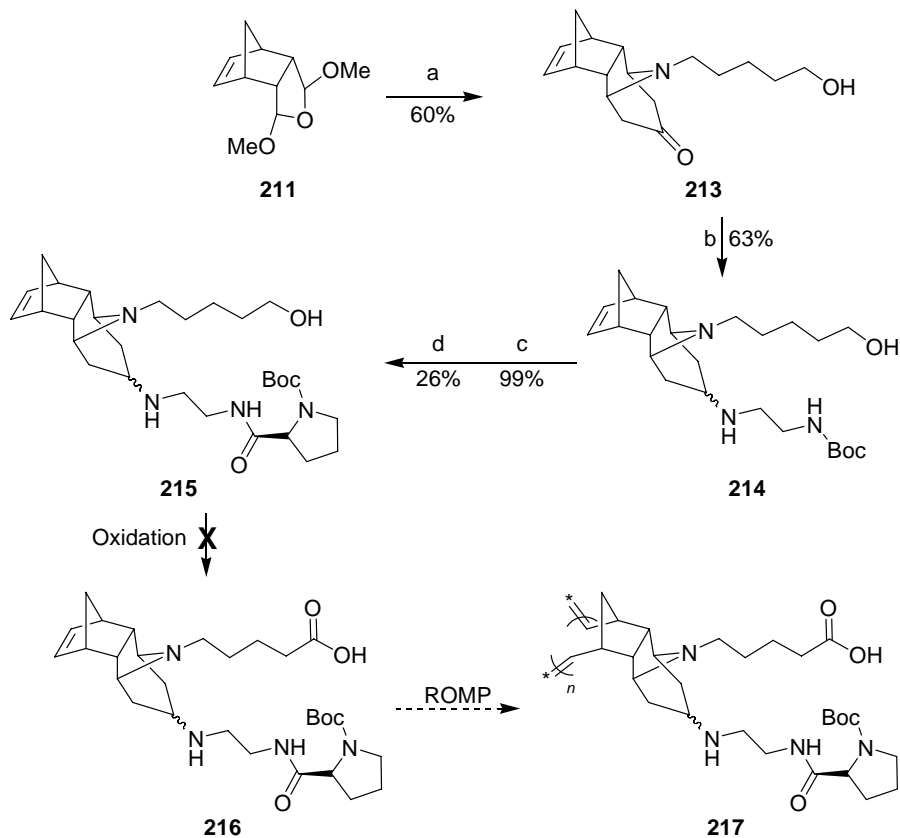
Encouraged by this route, it was decided to modify this synthesis using a more useful substrate. By selecting other amines to replace methylamine, it was hoped that the core structure would then contain functionalities which were more amenable to further manipulation.

Various amines were utilised in the place of methylamine, including 6-aminohexanoic acid methyl ester, glycine methyl ester and lysine methyl ester (**Scheme 2.46**). Unfortunately none of the substrates yielded the desired product. It was thought that perhaps the strong acidic environment in which the reaction was taking place was forming the free carboxylic acid of the methyl ester which was then interfering with the reaction by self condensation reactions or degradation. The reaction was also tried using 6-aminohexanoic acid allyl ester which is stable to these conditions; however the desired derivative was not obtained.



Scheme 2.46: a) acetone dicarboxylic acid, NH₂R¹, conc. HCl, H₂O, 24 h.

Success however was found with the use of 5-aminopentanol which gave the desired compound **213** in good yield (**Scheme 2.47**). It should be noted that 6-aminohexanol was also used in the place of 5-aminopentanol but the yield was significantly lower and therefore the use of 5-aminopentanol was continued as the amine counterpart.



Scheme 2.47: a) acetone dicarboxylic acid, 5-aminopentanol, conc. HCl, H₂O, 24 h; b) *N*-*tert*-butoxy(2-aminoethyl)carbamate, NaBH(OAc)₃, AcOH, THF, 12 h; c) AcCl, MeOH, 2 h; d) *N*-Boc-L-proline, NMM, ethyl chloroformate, DCM, 18 h.

Reductive amination of **213** was carried out with *N*-*tert*-butoxy(2-aminoethyl)carbamate to give **214** as a mixture of two diastereoisomers in good yield. At this stage, it was not of great concern that the product was not obtained in a more stereocontrolled manner since it was envisaged that both linker groups would provide ample flexibility for the catalyst to act efficiently.

The deprotection of the Boc group proceeded smoothly to yield the free amine, but the subsequent coupling step with *N*-Boc-proline to give **215** was unsuccessful. Various coupling reagents were employed to increase the yield for this step such as DCC, EDC and HATU in various solvent systems (DMF, DCM, MeOH, DMSO) but none of the reactions were successful. Employing the formation of

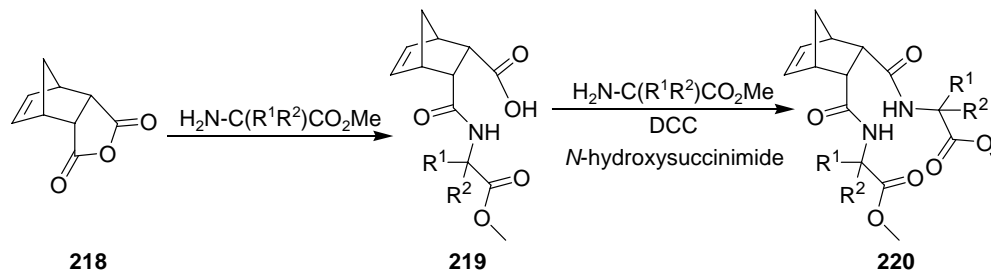
the mixed anhydride of *N*-Boc-proline using ethyl chloroformate prior to the addition of the deprotected compound **214**, did however give the desired product **215**, albeit in moderate yield.

Unfortunately however, the final oxidation of the alcohol to the corresponding carboxylic acid **216** was unsuccessful. Various conditions were attempted including Jones' reagent¹⁶⁴, PDC in DMF,¹⁶⁵ KMnO₄,¹⁶⁶ and Swern Oxidation,¹⁶⁷ followed by oxidation using sodium chlorite-hydrogen peroxide.¹⁶⁸ Both incomplete reactions and purification problems also contributed. By this stage, normal phase flash column chromatography could not be used to purify the compound due to the inherent polarity of the molecule and it was too unstable for purification by distillation. Reverse phase flash column chromatography could not be used either due to the presence of the starting materials which had similar polarities to the product. Acid base extraction did not give the compound in an acceptable form. Therefore it could not be confirmed whether this step was successful or not. As a consequence, the polymerisation step was not attempted.

2.4.4 Aldolase Mimics Based on Norbornene Derivatives

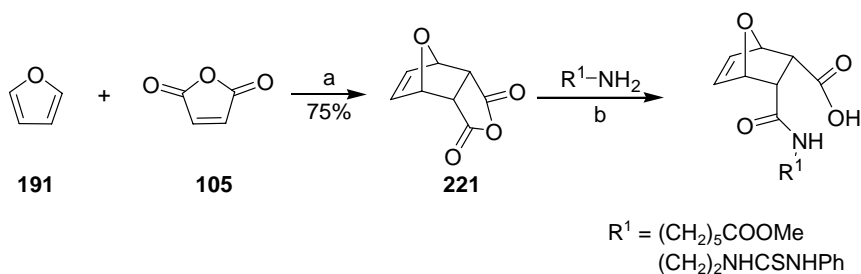
In view of the complications outline above, which were encountered during the synthesis of the 'extended' tropane alkaloid derivative, attention then focused on simpler functionalised norbornene derivatives as an alternative. It was considered that these species would not only be easier to functionalise but also that, since the ROMP of these compounds are well documented, this step should also prove less problematic.

In this respect, we were encouraged by a literature report by Ranganathan *et al.* who demonstrated a facile synthesis of norborneno peptide analogues **220** (Scheme 2.48).¹⁶⁹ It was therefore hoped that a similar method to that used by Ranganathan could be used for the synthesis of the desired organocatalytic monomer.



Scheme 2.48: Norborneno peptide analogues.

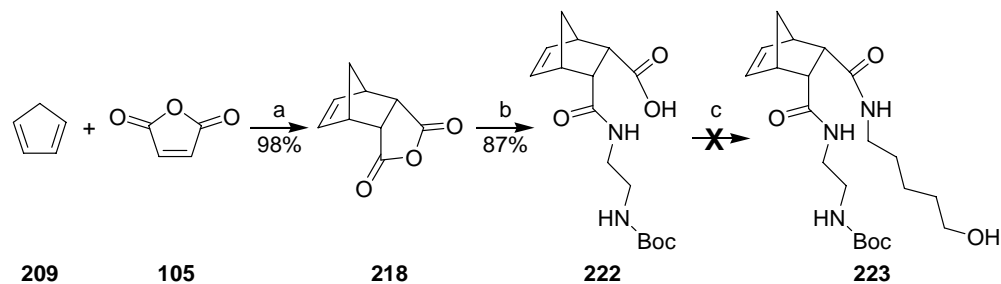
Before embarking on the substrate, a test reaction was carried out using furan **191** and maleic anhydride **105** to give the corresponding *endo* cycloaddition adduct **221** (**Scheme 2.49**). Having successfully formed the adduct, attempts were then made to open up the anhydride with an amine.



Scheme 2.49: a) diethyl ether, 48 h, RT; b) quinine, toluene, Et₃N.

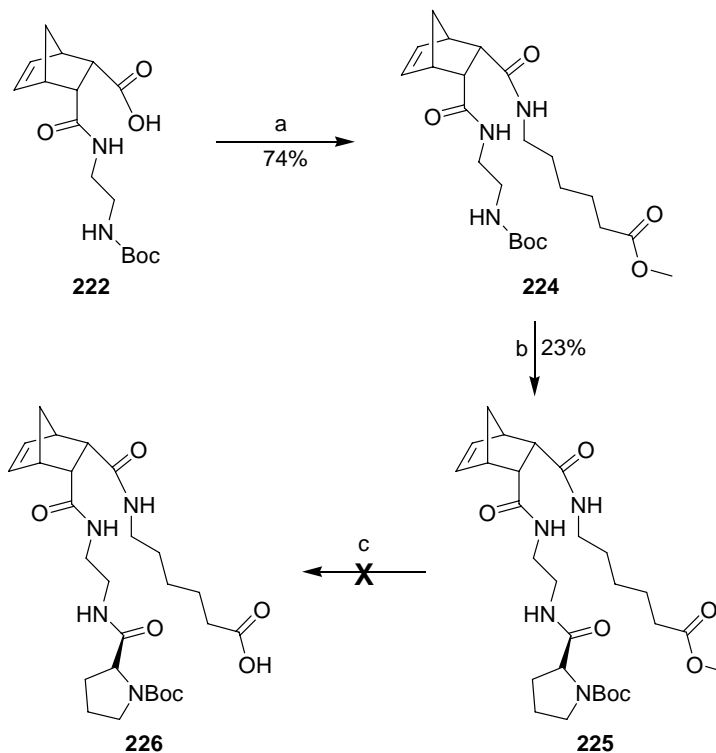
Unfortunately the desired product could not be isolated due to purification complications. Acid base extractions gave mixtures of compounds which were not of acceptable purity to be used in subsequent steps and purification by normal and reverse phase flash column chromatography was unsuccessful due to the polarity of the molecule. As a result furan was replaced by the much more reactive cyclopentadiene unit (**Scheme 2.50**). The classical *endo* adduct **218** was prepared in good yield. The anhydride was opened successfully using *N*-*tert*-butoxy(2-aminoethyl)carbamate, with the product **222** precipitating as a white solid over the course of the reaction. Unfortunately the next coupling step to 5-aminopentanol was unsuccessful, resulting in the recovery of starting materials. Since this should have been a fairly standard reaction, it is difficult to analyse why the reaction did not yield the desired product. The solvent system was first investigated since the norbornene moiety showed little solubility in DCM. The

reaction was tried in DMF, THF, methanol and Et₂O but again the product could not be obtained, resulting in the recovery of starting materials. Alternative coupling agents were also tested, including DIC, HATU and EDC but again the reaction did not yield the required species.



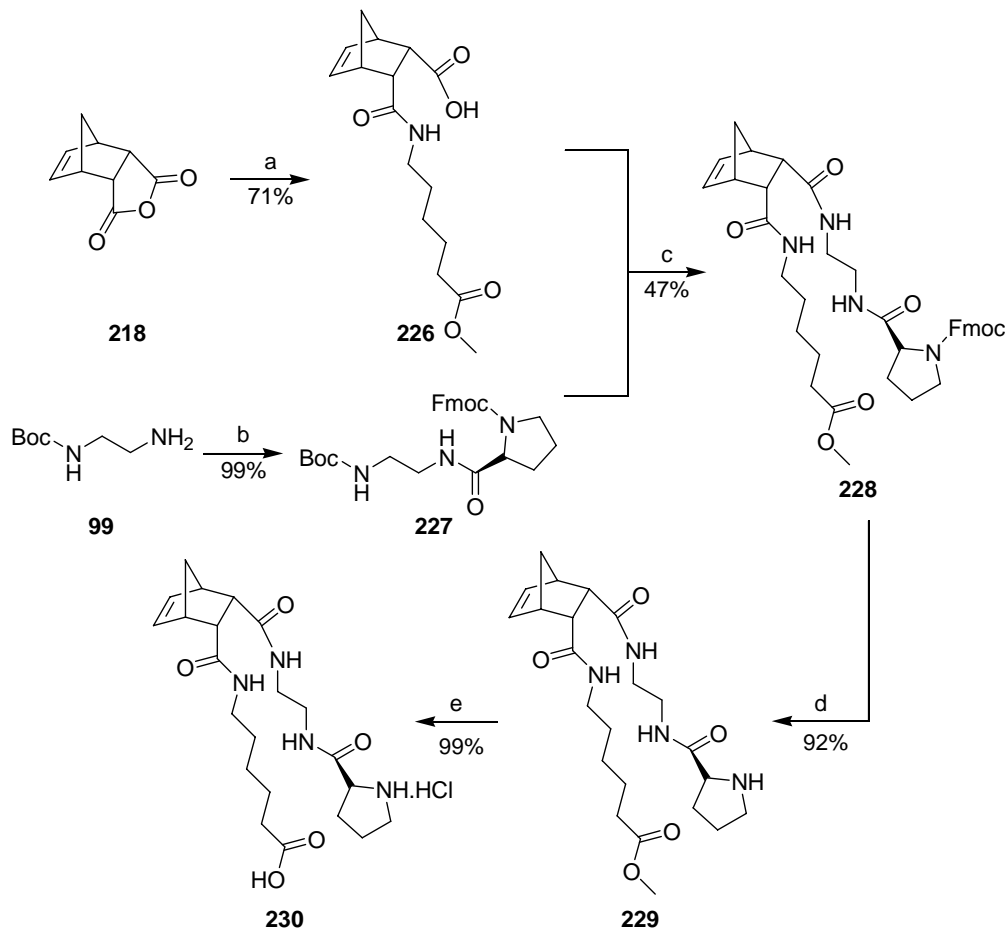
Scheme 2.50: a) benzene, 10 h, RT; b) *N*-*tert*-butoxy(2-aminoethyl)carbamate, DCM, 12 h, RT; c) 5-aminopentanol, DCC, DCM, 2 h, RT.

It was therefore decided that an alternative amine might provide more fruitful results. The obvious choice of amine in this case was 6-aminocaproic acid methyl ester which would provide the flexible carboxylic acid chain once subjected to ester hydrolysis in the latter stages of the synthesis. The synthetic route was therefore repeated using this alternative amine (**Scheme 2.51**). The coupling reaction between **222** worked when using 6-aminohexanoic acid methyl ester as the amine to give **224**. Although the yield was not high, the coupling of the *N*-Boc-proline also proceeded smoothly to give **225**. Unfortunately complications were encountered during the ester hydrolysis step when using either mild acidic or basic conditions. Once again, on attempted purification, these species were too polar to be subjected to normal phase flash column chromatography and again their similarity in polarity to starting materials prevented purification by reverse phase flash column chromatography. Acid base extractions did not yield the compound in an acceptable form. Further complications due to the instability of the Boc group when subjected to acidic conditions may have also been a factor.



Scheme 2.51: a) 6-aminocaproic acid methyl ester, DCC, DCM, 3 h, RT; b) i) TFA, DCM, ii) *N*-Boc-L-Proline, NMM, ethyl chloroformate, DCM, 2 h, RT; c) 2N NaOH, 2 h, RT.

The whole synthetic route was repeated using 6-aminohexanoic acid allyl ester instead of 6-aminohexanoic acid methyl ester in hopes that the deprotection could be achieved using milder conditions of $\text{Pd}(\text{PPh}_3)_4$ and $\text{Bu}_3\text{SnH}^{170}$ or $\text{Me}_2\text{CuLi}^{171}$. The allyl group should also be stable to the ester hydrolysis conditions employed previously. Unfortunately the free carboxylic acid group could not be obtained since the allyl group could not be deprotected under milder conditions and degradation of the product occurred when harsher conditions were used. The key step of coupling the catalytic group was also too low yielding to be efficient and therefore a new synthetic route was proposed for its synthesis (**Scheme 2.52**).



Scheme 2.52: a) DCM, 12 h, RT, 6-aminohexanoic acid methyl ester; b) *N*-Fmoc-L-Proline, NMM, ethyl chloroformate, DCM, 3 h, RT; c) i) TFA, DCM, 2 h, RT, ii) DCC, DCM, 5 h, RT; d) 5% diethylamine, MeCN, 2 h, RT; e) 2 M HCl, 1 h, RT.

This alternative synthetic route involved altering the order of addition of the side chains by using 6-aminohexanoic acid methyl ester as the nucleophile instead of *N*-*tert*-butoxy(2-aminoethyl)carbamate to open up the anhydride to give the corresponding adduct **226**. Having already discovered the low yielding step to be the coupling of the proline unit to the molecule, it was also decided that this should be attached to *N*-*tert*-butoxy(2-aminoethyl)carbamate **99** prior to coupling with the norbornene derivative. An orthogonal protecting group in the form of Fmoc was also employed to protect the pyrrolidine unit on the proline to allow

deprotection of the Boc group selectively on *N*-*tert*-butoxy(2-aminoethyl)carbamate once the coupling was carried out. This reaction gave **227** in 99% yield. The Boc group was then deprotected to give the TFA salt of **227** which was finally coupled to the norbornene **226** to yield the desired adduct **230** in 47% yield. Both the deprotection of the Fmoc group under mild basic conditions and ester hydrolysis using weak acidic conditions furnished the desired product as the HCl salt. This synthetic pathway gave a much better overall yield of 30% in the fully deprotected form rather than an overall yield of 14% for the protected form obtained using the previous method.

It should be noted that although the norbornene derivative **230** was obtained as a mixture of two diastereoisomers in this preliminary work, it was thought that since there were so many degrees of conformational freedom within the molecule in terms of the flexible carboxylic acid tether and the 1,2-diamine linker, it was unnecessary to synthesise the compound as a single enantiomer. Moreover, it was anticipated that when used, either in polymeric form or as an organocatalyst, the enantioselectivity would be directed from the catalytic proline unit and not substantially influenced by the polymeric backbone.

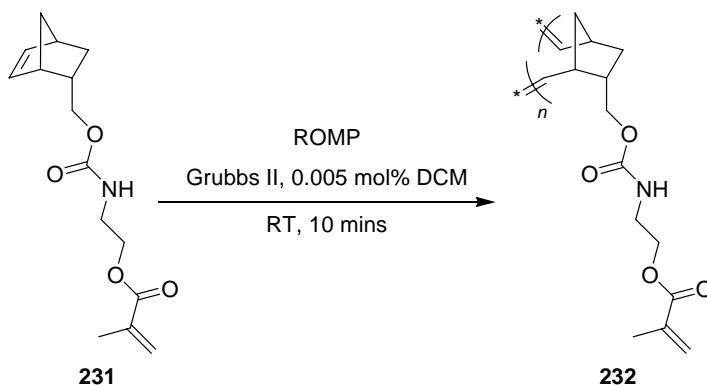
2.4.4.1 Ring Opening Metathesis Polymerisation (ROMP) of Norbornene Derivative

With the desired monomer at hand, the next step in the sequence required carrying out the ROMP of the norbornene derivative to obtain the corresponding polymer.

ROMP of norbornene derivatives have been the subject of intense research activity for the past few decades.¹⁷² In particular, the discovery of the Grubbs family of catalysts from the mid 1990s has led to an explosion of interest and shown the importance of olefin-metathesis reactions because of their high catalytic activity and excellent tolerance towards polar functional groups.¹⁷³⁻¹⁷⁵

Since then various norbornene derivatives have been subjected to ROMP to give

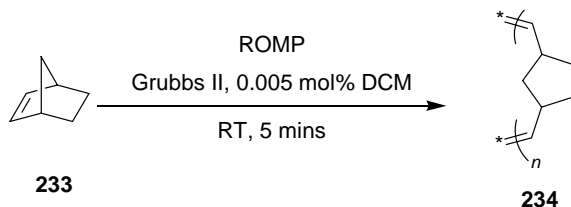
the corresponding polymer. Most of these examples require catalytic amounts of Grubbs catalyst, either first, second or third generation in DCM and are carried out at room temperature. An illustrative example is that reported by D-J. Liaw *et al.* (Scheme 2.53).¹⁷⁶



Scheme 2.53: ROMP of functionalised norbornene derivative.

Encouraged by the ROMP efficiency of this monomer which contained both amide and ester functionalities which can, under certain circumstances, deactivate the Grubbs II catalyst, it was hoped that the same method could be employed in order to obtain the desired polymer.

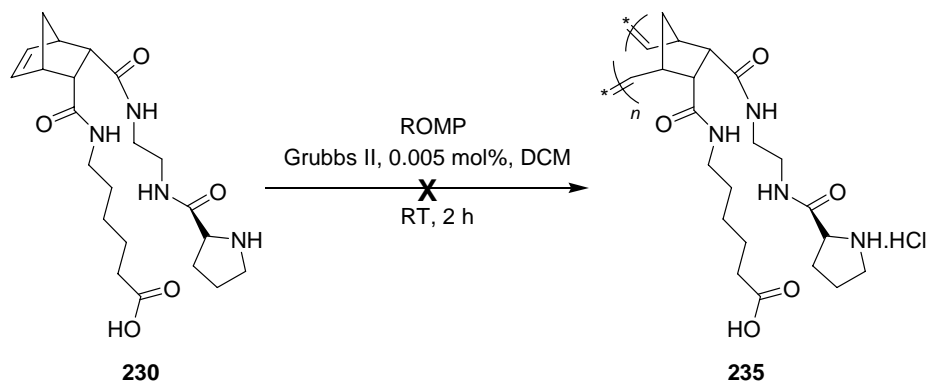
Before undertaking ROMP on the actual substrate a test reaction was carried out using bicyclo[2.2.1]hept-2-ene **233** (Scheme 2.54). This reaction was almost instantaneous and the product **234** was obtained immediately as a viscous gum in 79% yield.



Scheme 2.54: Test ROMP reaction.

Encouraged by this reaction, the same conditions were then applied to the monomer at hand (Scheme 2.55). Although the literature regarding the ring opening metathesis polymerisation reactions of norbornene derivatives is well

documented, none as complex as this have ever been reported. Most tend to contain either ester groups or carboxylic acid functionalities, and none with as many polar amide, acid and amino groups have been reported. Therefore it was not greatly surprising to find that ROMP of norbornene derivative **230** was unsuccessful, and led to extensive decomposition of the monomer species. It was thought that the amino group was perhaps interfering with the catalyst, perhaps deactivating it, and thus rendering it difficult for polymerisation to occur. Despite various solvent systems and reaction conditions attempted, the polymerisation step could not be carried out.



Scheme 2.55: ROMP of norbornene derivative.

Attempts at using intermediates (**228** and **222**) from earlier steps of the monomer synthesis (**Figure 2.19**), in which the functionalities within the substrates were protected were investigated but no polymerisation could be observed.

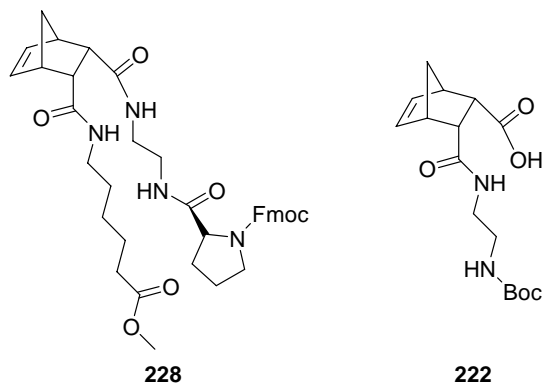
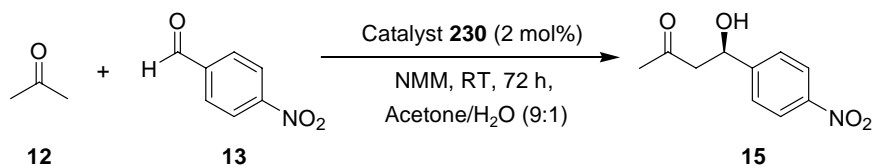


Figure 2.19: Alternative norbornene derivatives for ROMP.

Although this was discouraging, it had nevertheless been originally planned that the monomer itself could still be tested as an organocatalyst in its own right. Therefore, using a similar experimental protocol to that developed for the alternating co-polymers, a test aldol reaction between acetone and 4-nitrobenzaldehyde was carried out (**Scheme 2.56**). This reaction afforded the product **15** in 72% yield and 57% *ee*. This was, in fact, the highest enantioselectivity obtained for any of the aldolase mimics synthesised previously, and therefore was an extremely encouraging result. The reaction was also carried out using 4-(trifluoromethyl)benzaldehyde which also gave the corresponding aldol product in 61% yield and 52% *ee*.



Scheme 2.56: Test aldol reaction.

Once again, this catalyst was screened using different aldehydes, 9-anthraldehyde, hydrocinnamaldehyde, 4-methoxybenzaldehyde, 4-chlorobenzaldehyde and 4-tolualdehyde in order to assess the scope of the aldehyde component. Unfortunately the aldol product could not be obtained for any of the above examples, resulting in the recovery of the starting aldehyde in each case.

2.5 Functionalised Bispidinone Derivatives as Organocatalysts

At the same time as the above studies on norbornene derivatives were in progress, efforts were also being made towards another scaffold which fulfilled the same criteria of being able to function both as an organocatalyst and as a monomer for subsequent polymerisation.

In this instance, our inspiration was derived from (–)-sparteine **236** (**Figure 2.20**) which is a naturally occurring alkaloid extracted from plants such as Scotch Broom and has proven to be a useful chiral ligand for a wide range of asymmetric

reactions.¹⁷⁷ At the core of (-)-sparteine lies a bispidine unit, a bicyclic nitrogen heterocycle, which has been shown to be an excellent ligand for the steric steering of enantioselective metal-catalysed reactions.¹⁷⁸

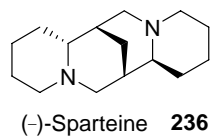
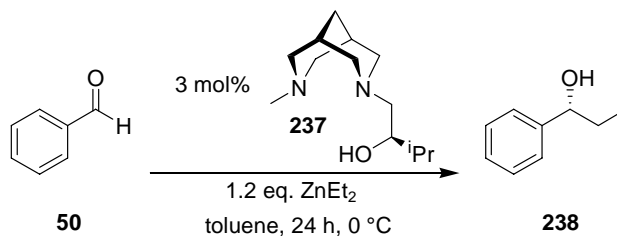


Figure 2.20: (-)-Sparteine.

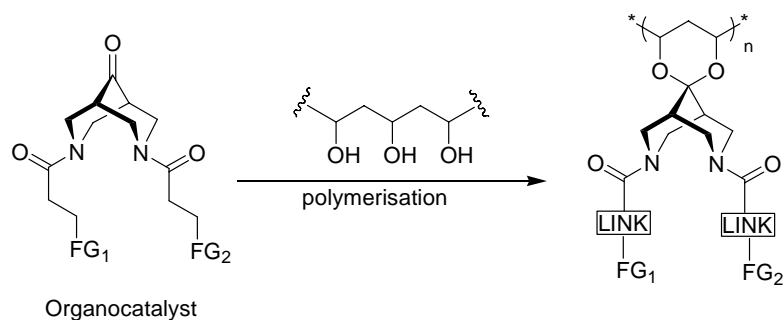
One such example involves the use of a chiral bispidine-derived ligand **237** in the asymmetric addition of diethylzinc to aromatic and aliphatic aldehydes (**Scheme 2.57**). In this example, diethyl zinc was added to benzaldehyde **50** to give the corresponding secondary alcohol **238** in 97% yield and 96% *ee*.



Scheme 2.57: Chiral bispidine as ligand.

In most cases, including the example above, these bispidine derivatives are most commonly employed as ligands to be used in catalysis rather than as catalysts themselves. However it was hoped that by modifying these species with the relevant functionalities, these would serve as excellent organocatalysts and monomers. Not only were they likely to exhibit enantioselectivity due to their inherent structural features but also exhibit great cooperativity effects if the two functionalities attached to the nitrogen atoms were selected in such a way as to bring these groups in close proximity to one another.

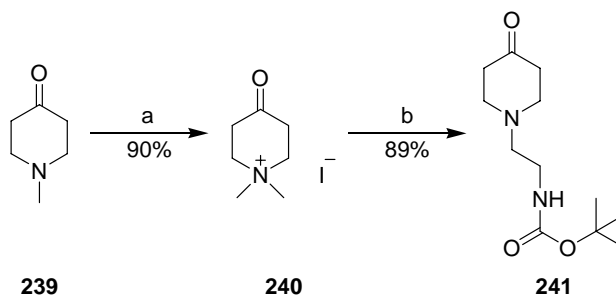
Thus, as shown in **Scheme 2.58**, our intention was to construct suitably functionalised bispidine derivatives for examination of their potential for cooperativity effects in catalysis.



FG = Funcional Group

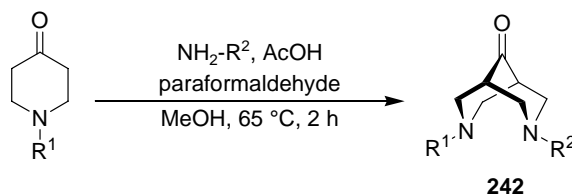
Scheme 2.58: Synthesis of functionalised bispidone derivatives.

In order to achieve this objective, a functionalised piperidone species was first prepared (**Scheme 2.59**). The first step involved reacting *N*-methyl piperidone **239** with iodomethane to give the quarternary iodonium salt **240**. This was subsequently reacted with *N*-*tert*-butoxy(2-aminoethyl)carbamate in a sequential addition/elimination process to give **241** in good yield.



Scheme 2.59: a) iodomethane, diethyl ether, reflux, 8 h; b) *N*-*tert*-butoxy(2-aminoethyl)carbamate, K_2CO_3 , EtOH//H₂O, reflux, 10 h.

Armed with this piperidone species, the commercially available benzyl piperidone and the Boc piperidone, reactions to obtain the bispidinone species **242** *via* the classical double Mannich reaction were attempted (**Scheme 2.60**):¹⁷⁹



Scheme 2.60: Synthesis of bispidinone derivatives.

The following table shows the various combinations of piperidone and amine attempted (Table 2.3).

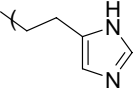
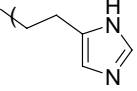
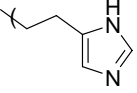
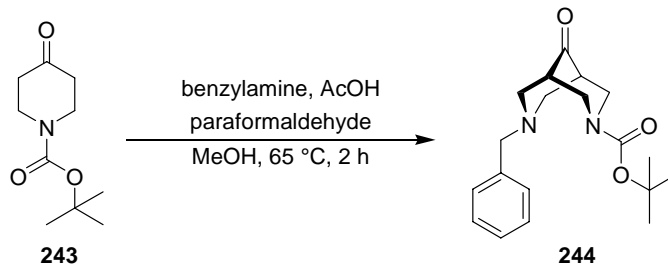
R ₁	R ₂	Result
(CH ₂) ₂ NHBoc	(CH ₂) ₅ OH	Decomposition
(CH ₂) ₂ NHBoc	(CH ₂) ₅ COOMe	Decomposition
(CH ₂) ₂ NHBoc	(CH ₂) ₂ COOMe	Decomposition
(CH ₂) ₂ NHBoc	(CH ₂) ₂ NHBoc	Decomposition
(CH ₂) ₂ NHBoc		Recovery of starting materials
(CH ₂) ₂ NHBoc	CH ₂ Ph	Decomposition
CH ₂ Ph	(CH ₂) ₅ OH	Recovery of starting materials
CH ₂ Ph	(CH ₂) ₅ COOMe	Decomposition
CH ₂ Ph	(CH ₂) ₂ COOMe	Decomposition
CH ₂ Ph	(CH ₂) ₂ NHBoc	Decomposition
CH ₂ Ph		Recovery of starting materials
CH ₂ Ph	(CH ₂) ₅ OH	Recovery of starting materials
CH ₂ Ph	CH ₂ Ph	Recovery of starting materials
Boc	(CH ₂) ₅ COOMe	Decomposition
Boc	(CH ₂) ₂ COOMe	Decomposition
Boc	(CH ₂) ₂ NHBoc	Decomposition
Boc		Recovery of starting materials
Boc	CH₂Ph	Obtained as orange oil

Table 2.3: Bispidinone synthesis.

Unfortunately none of the combinations yielded any isolable products except when using Boc-piperidine **243** and benzylamine to give **244** which was however obtained in 75% yield (Scheme 2.61).



Scheme 2.61: Bispidinone derivative.

Although this was an encouraging result, more complex bispidinone derivatives could not be obtained and subsequent manipulations of these species were unsuccessful possibly as a result of relatively facile retro-Mannich reactions. Due to time constraints, however, these target organocatalytic species were not further developed.

2.6 Conclusions and Perspectives

The primary objective of the present thesis was to demonstrate and validate the idea that a simple protocol for examination of functional group cooperativity in artificial enzymes could be based in the construction of an alternating co-polymer, with each of the two monomers possessing one (or more) catalytically active groups.

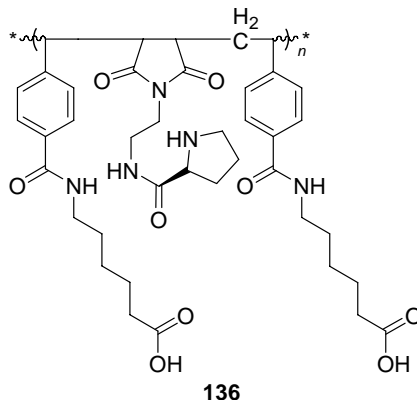
The reaction selected for study was the aldol reaction and consideration of type I aldolase systems in nature suggested that, at the most simplistic level, the two catalytically active groups should be an amine for enamine formation, and a carboxylic acid to enhance the electrophilicity of the carbonyl group acceptor. Styrene and maleimide monomers were then selected for their known ability in alternating co-polymer formation.

Based on these thoughts, a number of alternating co-polymers were then successfully synthesised, first in the form of novel type I aldolase mimics and then

later as type II aldolase mimics through incorporation of either zinc or magnesium acetate. All of these were found to be efficient catalysts for the aldol reaction between aldehydes containing an electron withdrawing group and acetone, with yields varying from 19 – 78% and with moderate *ees* ranging from 29 – 42%, thus providing proof of concept for such an approach.

Even although the polymers prepared do not rival the simple and exquisite organocatalyst proline, many valuable lessons have been learnt in this preliminary study. The first of these is that the use of the rigid *para*-substituted moiety of the styrene monomer then requires that a relatively flexible chain is then incorporated to favour functional group cooperativity. In future work, attention could also be given to tailoring these flexible groups on each monomer such that usefully networked complementary hydrogen bonding patterns were formed. The experiment in which selection of a chiral dicarboxylic acid as the proton donor led to a lower enantiomeric excess was indicative of a ‘mismatched pair’ but also suggests that selection of other chiral carboxylic acids of opposite absolute configuration could lead to a ‘matched pair’ and enhanced enantioselectivity.

In specific terms of the aldol reaction itself, the present study clearly demonstrated the necessity for a carboxylic acid as a proton donor, but even with incorporation, aldol reactions were limited to highly electron deficient aldehydes as the partner for acetone. Efforts to facilitate binding and proton transfer through selection of a thiourea unit were unfortunately to no avail and no definitive conclusion could be reached as to whether protonation was more difficult or whether product inhibition was responsible. In summary, for an aldolase type I system, the most efficient polymer thus far developed is **136**, shown below, which was able to catalyse the reaction between acetone and 4-nitrobenzaldehyde in 78% yield and with an enantiomeric excess of 40%.

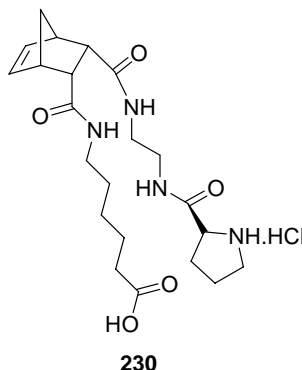


As a consequence of the apparent limitations of the type I aldolase polymeric catalysts, a very preliminary study was also made of type II catalysis through incorporation of both ‘natural’ Zn^{2+} cations and ‘unnatural’ Mg^{2+} cations.

With these type II aldolases, the polymers containing magnesium ions all gave higher yields than those containing the zinc ions but gave lower enantioselectivities. This led to the conclusion that magnesium ions were not working synergistically with the catalytic proline group. In contrast, the raised yields of the polymer containing zinc ions in comparison to when only zinc acetate was present led to the conclusion that in this case, the zinc ions were involved and exhibiting cooperativity effects with proline. This was also supported by the higher enantioselectivities. Further work using more tailored zinc binding sites would certainly be of interest.

Whilst the above work was ongoing, an alternative approach involving construction of a monomeric organocatalyst which could then be subjected to either ROMP or attachment to a polymer was also under active investigation. Amongst these, whilst systems based on 7-azabicyclo[2.2.1]hept-2-ene, or unnatural tropane-like derivatives led to synthetic complication in the latter stages, an efficient monomeric organocatalyst was obtained in the form of the norbornene derivative **230** which exhibited high yield (72%) and the highest enantioselectivity (57%) for the aldol reaction of all the polymer catalysts synthesised. Unfortunately it was unstable to ROMP conditions and therefore the polymeric

equivalent could not be tested as a catalyst.



Attempts were also made to synthesise bispidinone derivatives as potential novel organocatalysts but once again, these species could not be obtained or modified to a useful degree.

One of the fundamental principles behind the design of both the alternating co-polymers and the various multi-cyclic compounds is that these systems can be easily adapted to study any desired reaction. Although this research programme has focused on the aldol reaction to test the concept, by altering the functional groups attached to the core structure, which can easily be carried out by modification of a few steps, a catalyst can, in theory, be designed for any required reaction.

In general terms, more work could be done to study the aldol reaction using either the alternating co-polymer systems or by those based on norbornene derivatives. Since the catalysts only performed the aldol reaction using aldehydes containing highly electron withdrawing groups with acetone, it would be beneficial if modifications could be applied to the catalysts so that a wider spectrum of both aldehydes and ketones could be subjected to the aldol reaction. Since the very nature of these systems was designed for easy manipulations of the catalytic and binding groups, it should not be too difficult to alter these groups to synthesise a small library of these compounds which are more active. Initial investigation should focus on other proline derivatives of which there are numerous examples which tolerate a wider range of substrates, as well as designer binding sites for

zinc ions.

Since the concept of ‘hands’ and ‘teeth’ could not be fully studied within this project, it would be of great interest to find actual binding groups which could act as potential ‘hands’ for the aldol reaction using NMR studies on an appropriate transition state analogue such as a chiral β -keto sulfoxide for this reaction. Small peptide units should be ideal for this purpose. Also since the natural aldolases contain a lysine residue in the active site, it would truly be an aldolase mimic if lysine could be used as the ‘teeth’ instead of proline. This perhaps is a much more difficult task since the pathway by which this lysine residue is activated in nature is still unknown. Perhaps the ‘hands’ could be designed in such a way that it not only acts as a binding group for the substrate but also perturb the lysine residue in the process.

Since the ‘millipede’ artificial enzymes synthesised by Atkinson showed great promise as artificial esterases, the same ‘hands’ and ‘teeth’ used in that study could be applied to the alternating polymeric systems here. It would be interesting to compare the catalytic activities of the two different systems. It would also be of great interest to broaden the scope of these polymer catalysts by manipulating these species to explore Mannich-type reactions, nitro-Michael additions and many others currently under study using organocatalysts.

Chapter 3: Experimental

All chemicals were purchased from Sigma Aldrich, Alfa Aesar, BDH, Nova Biochem or Bachem and unless otherwise stated, were used without further purification.

^1H NMR spectra were recorded at 300 MHz on a Bruker AMX300 spectrometer, 400 MHz on a Bruker AMX400 spectrometer, 500 MHz on a Bruker Avance DRX500 spectrometer or 600 MHz on a Bruker Avance DRX600 spectrometer in the stated solvent using residual protic solvent CHCl_3 ($\delta = 7.26$ ppm, s), DMSO ($\delta = 2.56$ ppm, qn) or D_2O ($\delta = 4.79$, s) as the internal standard. The chemical shift (δ) of each peak is given relative to tetramethylsilane (TMS), where $\delta_{\text{TMS}} = 0$ ppm. Chemical shifts are quoted using the following abbreviations: s, singlet; d, doublet; t, triplet; m, multiplet; br, broad or a combination of these. NMR data are reported as follows: number of protons, multiplicity, coupling constants (J values) recorded in Hertz.

^{13}C NMR spectra were recorded at 75 MHz on a Bruker AMX300 spectrometer, 125 MHz on a Bruker Avance DRX500 or 150 MHz on a Bruker Avance DRX600 in the stated solvent using the central reference of CHCl_3 ($\delta = 77.0$ ppm, t), DMSO ($\delta = 39.52$ ppm, septet) as the internal standard. The chemical shift (δ) of each peak is given relative to the residual solvent peak and are reported to the nearest 0.1 ppm. Solid state ^{13}C NMR spectra were recorded at 75 MHz on a Bruker MSL300 spectrometer.

Infrared (IR) spectra were obtained from a Perkin Elmer Spectrum 100 FT-IR spectrometer, and were recorded as thin films of pure sample. Absorption maxima are reported in wavenumbers (cm^{-1}), using the following abbreviations: w, weak; m, medium; s, strong; br, broad. Only selected absorbencies are reported.

Mass spectra were obtained using VG ZAB SE instrument at the University College London Chemistry Department either by Electron Impact (EI), Chemical Ionisation (CI), Electrospray Ionisation (ESI) or Fast Atom Bombardment (FAB).

Melting Points were measured on a Reichert Hotstage apparatus for all solids where possible and are quoted to the nearest °C and are uncorrected.

Optical rotation was measured in a Perkin Elmer Model 343 Polarimeter (using the sodium D-line, 529 nm) and $[\alpha]_D^T$ values are given in 10^{-1} deg cm² g⁻¹, concentration (*c*) in g per 100 ml.

Enantiometric excess determination was carried out with normal phase high-performance liquid chromatography (HPLC) and was measured using UV detector type prostar/dynamic system24 (2 Volts) absorbance 254 nm. The analytes were separated and determined by using a Chiralcel OB column. The polar stationary phase (isopropanol) and the non-polar mobile phase (hexane) was used as indicated.

Molecular weight average and polydispersity of the polymers were obtained using gel permeation chromatography at the Polymer laboratories Ltd, Shropshire.

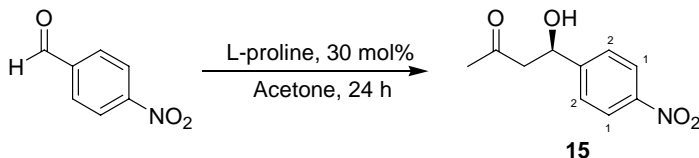
Analytical thin layer chromatography (t.l.c.) was carried out on pre-coated, aluminium backed (Merck 60 F₂₅₄ silica) plates. T.l.c. visualising systems used were ultraviolet light (254 nm), potassium permanganate solution, acidic vanillin or acidic anisaldehyde solution.

Tetrahydrofuran and dichloromethane were used following purification from anhydrous engineering zeolite drying apparatus. Anhydrous methanol was distilled from a solution of methanol, magnesium turnings and iodine.

Brine refers to a saturated aqueous sodium chloride solution.

For all air and moisture sensitive reactions, glassware was dried at 120 °C and cooled under a flow of nitrogen.

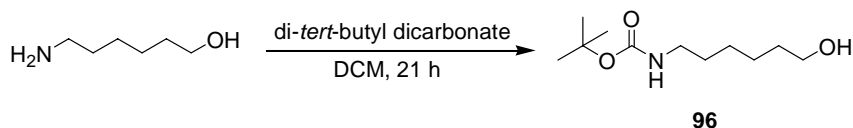
3.1 (*R*)-4-Hydroxy-4-(4-nitrophenyl)butan-2-one (**15**)¹⁹



A suspension of 4-nitrobenzaldehyde (0.76 g, 5.0 mmol) and L-proline (0.17 g, 30 mol%) was stirred in acetone (20 ml) at room temperature for 24 h. Solvent was removed under reduced pressure and the residue purified by flash column chromatography (SiO₂; EtOAc/petroleum spirit (40 – 60 °C); 1:1) to yield the product as a pale yellow solid (0.71 g, 68%).

m.p. 58 – 61 °C [lit. 59 – 61 °C];⁴³ **R_f** = 0.33 (SiO₂; EtOAc/petroleum spirit (40 – 60 °C); 1:1); **¹H NMR** (300 MHz, CDCl₃) 8.18 (2H, d, ³J = 8.5 Hz, *o*-Ar), 7.51 (2H, d, ³J = 8.5 Hz, *m*-Ar), 5.26 (1H, m, CH), 3.70 (1H, br s, OH), 2.82 (2H, m, CH₂), 2.20 (3H, s, CH₃); **¹³C NMR** (125 MHz, CDCl₃) 208.6 (C=O), 150.4 (C-NO₂), 147.2 (C-CHOH), 126.3 (C₁), 123.7 (C₂), 68.9 (CHOH), 51.6 (CH₂), 30.8 (CH₃); **ν_{max}** (neat/cm⁻¹) 3412.5 (br, O-H), 2671.2 (m, Ar-H), 1706.6 (s, C=O), 1600.1 (s, Ar-NO₂), 1514.2, 1342.1 (w, NO₂), 1258.0, 1162.6 (s, C-O); **m/z** (Positive CI-Methane) 210 ([M + H]⁺, 69%), 192 (78), 174 (57), 162 (72), 150 (70), 135 (44), 122 (100), 101 (28); **HRMS** found [M + H]⁺, 210.07607; C₁₀H₁₂NO₄ requires 210.07663.

3.2 *N*-*tert*-Butoxy(6-hydroxyhexyl)carbamate (**96**)¹³⁸

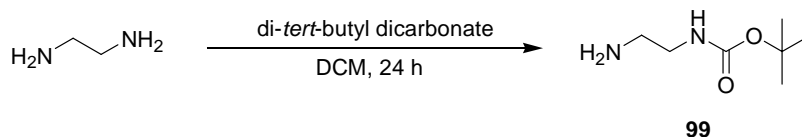


A solution of di-*tert*-butyl dicarbonate (20.00 g, 85.3 mmol) in dichloromethane (DCM) (50 ml) was added dropwise to a solution of 6-amino-hexan-1-ol (10.00 g, 85.3 mmol) in DCM (50 ml) and the resulting mixture was allowed to stir for 21 h

at room temperature. The reaction was washed with distilled water (100 ml), brine (100 ml) and sat. NaHCO₃ (100 ml), dried (MgSO₄) and filtered. Solvent was removed under reduced pressure to yield a pale yellow oil. Purification by flash column chromatography (SiO₂; EtOAc/petroleum spirit (40 – 60 °C); 1:1) yielded the product as a colourless solid (17.77 g, 96%).

m.p. 38 – 40 °C [lit. 35 – 37 °C]; ¹⁸⁰ **R_f** = 0.35 (SiO₂; EtOAc/petroleum spirit (40 – 60 °C); 1:1); **¹H NMR** (300 MHz, CDCl₃) 4.66 (1H, br s, NH), 3.56 (2H, m, CH₂OH), 3.05 (2H, m, NHCH₂), 1.61 – 1.21 (8H, m, (CH₂)₄CH₂OH), 1.47 (9H, s, ^tBu); **¹³C NMR** (75 MHz, CDCl₃) 156.1 (C=O), 79.1 (C(CH₃)₃), 62.5 (NHCH₂), 40.5 (CH₂OH), 32.6, 30.0, 26.4, 25.3 ((CH₂)₄CH₂OH), 28.4 (C(CH₃)₃); **ν_{max}** (neat/cm⁻¹) 3416.8 (br, O-H), 3365.9 (br, N-H), 2932.1, 2856.4 (m, C-H), 1684.5 (s, C=O), 1517.8, 1464.2, 1362.7 (m, C-H bend), 1246.3 (m, C-O); **m/z** (Positive Cl-Methane) 218 ([M + H]⁺, 98%), 162 (100); **HRMS** found [M + H]⁺, 218.17624; C₁₁H₂₄NO₃ requires 218.17507.

3.3 *N-tert*-Butoxy(2-aminoethyl)carbamate (**99**)¹³⁹

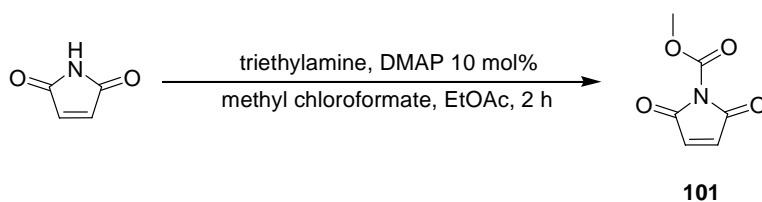


A solution of di-*tert*-butyl dicarbonate (16.35 g, 74.9 mmol) in DCM (150 ml) was added over a period of 3 h to a solution of ethane-1,2-diamine (14.08 g, 15.64 ml, 234.0 mmol) in DCM (150 ml). The mixture was allowed to stir for 24 h at room temperature, after which the reaction mixture was filtered, the solid cake washed with DCM (3 × 50 ml) and the combined organic layers concentrated. Excess ethane-1,2-diamine was removed under reduced pressure from the crude mixture to yield the product as a yellow oil (11.48 g, 96%).

¹H NMR (300 MHz, CDCl₃) 4.93 (1H, br s, NH), 3.15 (2H, m, NHCH₂), 2.77

(2H, t, $^3J = 5.9$ Hz, NH_2CH_2), 1.42 (9H, s, ^tBu), 1.37 (2H, br s, NH_2); ^{13}C NMR (75 MHz, CDCl_3) 156.2 (C=O), 79.2 ($\text{C}(\text{CH}_3)_3$), 43.3 (NHCH_2), 41.8 (NH_2CH_2), 28.4 ($\text{C}(\text{CH}_3)_3$); ν_{max} (neat/ cm^{-1}) 3354.1 (s, N-H), 2975.5, 2931.4 (s, C-H), 1686.2 (s, C=O), 1517.5 (s, N-H bend), 1453.0, 1391.2, 1364.7 (m, C-H bend), 1248.8 (m, C-O); m/z (Positive CI-Methane) 161 ($[\text{M} + \text{H}]^+$, 95%), 105 (100); HRMS found $[\text{M} + \text{H}]^+$, 161.12921; $\text{C}_7\text{H}_{17}\text{N}_2\text{O}_2$ requires 161.12900.

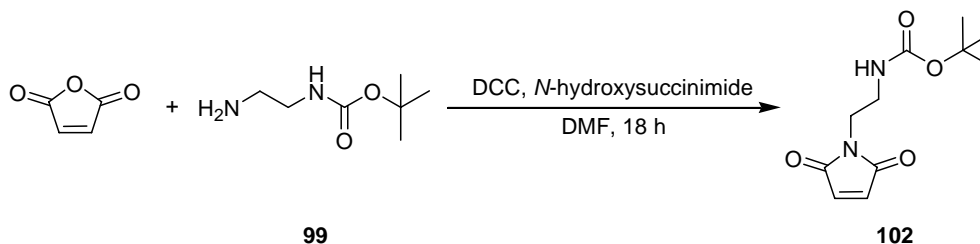
3.4 2,5-Dioxo-2,5-dihydro-pyrrole-1-carboxylic acid methyl ester (101)



A solution of maleimide (1.94 g, 20.0 mmol), triethylamine (3.04 g, 4.10 ml, 30.0 mmol) and 4-dimethylaminopyridine (DMAP) (0.24 g, 10 mol%) in ethyl acetate (EtOAc) (80 ml) were stirred at room temperature for 10 mins. Methyl chloroformate (2.27 g, 1.85 ml, 24.0 mmol) was added dropwise and the reaction stirred for a further 2 h. The reaction mixture was washed with distilled water (50 ml), 0.5 M HCl (2×50 ml), dried (MgSO_4) and filtered. Solvent was removed under reduced pressure to yield the product as a dark brown oil, which crystallised on standing (1.07 g, 34%).

m.p. 68 – 70 °C (EtOAc) [lit. 61 – 63 °C]; ^{181}H NMR (300 MHz, CDCl_3) 6.84 (2H, s, $\text{CH}=\text{CH}$), 3.98 (3H, s, CH_3); ^{13}C NMR (75 MHz, CDCl_3) 165.6 ($\text{CH}=\text{CHC}=\text{O}$), 148.1 ($\text{CH}_3\text{OC}=\text{O}$), 135.3 ($\text{CH}=\text{CH}$), 54.3 (CH_3); ν_{max} (neat/ cm^{-1}) 2698.0 (w, C-H), 1752.2 (s, C=O, carbamate), 1687.3 (m, C=O, amide), 1650.7 (w, C=C), 1503.6, 1430.8 (s, C-H bend); m/z (Positive CI-Methane) 156 ($[\text{M} + \text{H}]^+$, 100%), 124 (76), 99 (26); HRMS found $[\text{M} + \text{H}]^+$, 156.02929; $\text{C}_6\text{H}_6\text{NO}_4$ requires 156.02968.

3.5 *N*-*tert*-Butoxy[2-(2,5-dioxo-2,5-dihydro-pyrrol-1-yl)ethyl]carbamate
(102)

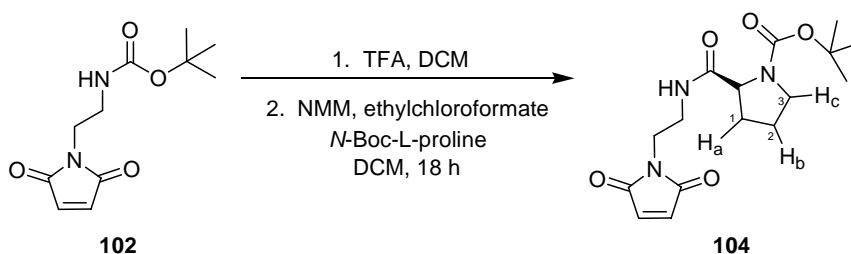


Maleic anhydride (1.96 g, 20.0 mmol) and *N*-*tert*-butoxy(2-aminoethyl)carbamate (3.20 g, 20.0 mmol) were stirred in dimethyl formamide (DMF) (25 ml) at room temperature for 1 h. The reaction mixture was cooled to 0 °C after which *N*-hydroxysuccinimide (2.88 g, 25.0 mmol) and 1,3-dicyclohexylcarbodiimide (DCC) (8.25 g, 40.0 mmol) were added. It was then allowed to warm to room temperature and stirred for a further 18 h. The colourless precipitate was filtered and the solid cake was washed with distilled water (100 ml) and DCM (100 ml). The DCM layer was separated, washed with sat. NaHCO₃ (60 ml), brine (60 ml), dried (MgSO₄) and filtered. Solvent was removed under reduced pressure to yield the crude product which was purified by flash column chromatography (SiO₂; EtOAc/petroleum spirit (40 – 60 °C); 3:2) to give the product as a colourless solid (3.48 g, 72%).

m.p. 118 – 120 °C [lit. 116 °C];¹³⁶ **R_f** = 0.64 (SiO₂; EtOAc/petroleum spirit (40 – 60 °C); 2:1); **¹H NMR** (300 MHz, CDCl₃) 6.69 (2H, s, CH=CH), 4.71 (1H, br s, NH), 3.66 (2H, m, CH₂CH₂NH), 3.33 (2H, m, CH₂CH₂NH), 1.40 (9H, s, CH₃); **¹³C NMR** (75 MHz, CDCl₃) 172.1 (CH=CHC=O), 147.1 (NHC=O), 134.2 (CH=CH), 72.2 (C(CH₃)₃), 54.2 (CH₂CH₂NH), 38.0 (CH₂CH₂NH), 28.3 (C(CH₃)₃); **ν_{max}** (neat/cm⁻¹) 3348.0 (s, N-H), 2979.5 (s, C-H), 1701.5 (s, C=O, amide), 1679.1 (s, C=O, carbamate), 1516.8 (m, N-H bend), 1434.2, 1361.6 (m, C-H bend), 1251.9 (m, C-O); **m/z** (Positive CI-Methane) 241 ([M + H]⁺, 38%), 225 (12), 186 (10), 185 (100), 141 (71); **HRMS** found [M + H]⁺, 241.11931;

C₁₁H₁₇N₂O₄ requires 241.11828.

3.6 (S)-2-[2-(2,5-Dioxo-2,5-dihydropyrrol-1-yl)ethylcarbamoyl]pyrrolidine-1-carboxylic acid *tert*-butyl ester (104)

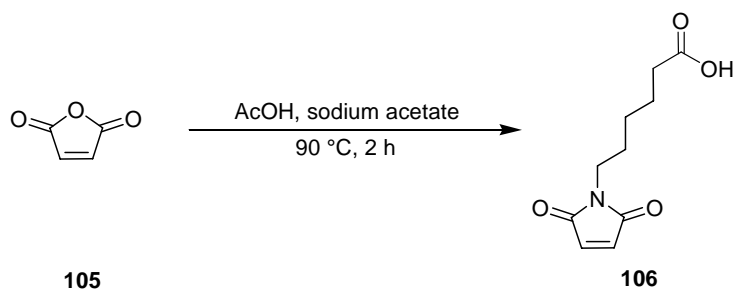


Trifluoroacetic acid (TFA) (10 ml) was added to a cooled solution of [2-(2,5-dioxo-2,5-dihydro-pyrrol-1-yl)ethyl]carbamic acid *tert*-butyl ester (1.20 g, 5.0 mmol) in DCM (24 ml) and stirred for 20 mins. DCM was removed under reduced pressure and the excess TFA by co-evaporation with toluene. The product was used in the next step without further purification.

N-Methyl morpholine (NMM) (0.51 g, 0.55 ml, 5.0 mmol) was added to a stirred solution of *N*-Boc-L-proline (1.08 g, 5.0 mmol) in DCM (40 ml) at $-15\text{ }^{\circ}\text{C}$. Ethyl chloroformate (0.54 g, 0.48 ml, 5.0 mmol) in DCM (10 ml) was added dropwise and stirred at this temperature for 20 mins. A further portion of NMM (1.01 g, 1.10 ml, 10.0 mmol) was added, followed by portionwise addition of the TFA salt of [2-(2,5-dioxo-2,5-dihydro-pyrrol-1-yl)ethyl]carbamic acid *tert*-butyl ester prepared earlier. The reaction mixture was allowed to warm to room temperature and left to stir for a further 18 h. Distilled water (50 ml) was added and the DCM layer separated. The aqueous phase was extracted with DCM (3×40 ml) and the combined organic layers washed with 0.5 M HCl (100 ml), sat. NaHCO₃ (100 ml), brine (100 ml), dried (MgSO₄) and filtered. Solvent was removed under reduced pressure to yield the product as an off-white solid (1.40 g, 83%).

m.p. 124 – 127 °C; $[\alpha]_D^{22} = -11.5$ (*c* 1, CHCl₃); **¹H NMR** (300 MHz, CDCl₃) 6.90 (1H, br s, NH), 6.70 (2H, s, CH=CH), 5.30 (1H, s, CH), 4.19 (2H, m, CH₂CH₂NH), 3.67 (2H, m, CH₂CH₂NH), 3.40 (4H, m, H_a and H_c), 1.84 (2H, m, H_b), 1.45 (9H, s, CH₃); **¹³C NMR** (125 MHz, CDCl₃) 170.8 (CH=CHC=O), 155.8 (NHC=O), 148.9 (^tBuOC=O), 134.2 (CH=CH), 80.5 (C(CH₃)₃), 60.0 (CH), 50.0 (C₃), 38.5 (CH₂CH₂NH), 37.6 (CH₂CH₂NH), 33.4 (C₁), 28.5 (C(CH₃)₃), 24.5 (C₂); **ν_{max}** (neat/cm⁻¹) 3312.4 (m, N-H), 2935.6 (w, C-H), 1703.7 (s, C=O, maleimide), 1697.5 (s, C=O, amide), 1662.5 (s, C=O, carbamate), 1530.4 (m, N-H bend), 1438.1, 1403.3, 1390.2, 1365.6 (m, C-H bend); **m/z** (Positive CI-Methane) 338 ([M + H]⁺, 44%), 360 (100), 282 (8), 238 (22); **HRMS** found [M + H]⁺, 360.15321; C₁₆H₂₄N₃O₅ requires 360.15299.

3.7 6-(2,5-Dioxo-2,5-dihydropyrrol-1-yl)hexanoic acid (106)¹⁸²

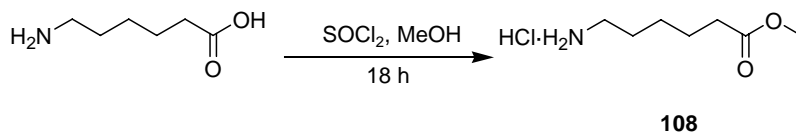


6-Aminocaproic acid (6.72 g, 51.2 mmol) was added to a solution of maleic anhydride (5.02 g, 51.2 mmol) in AcOH (60 ml). A colourless precipitate began to form immediately and the reaction mixture was stirred at room temperature for a further 3 h. The colourless solid was collected by filtration and redissolved in AcOH (45 ml). Sodium acetate (2.24 g, 27.3 mmol) was then added and the reaction mixture was heated at 90 °C for 2 h. Excess solvent was removed under reduced pressure and the crude product was dissolved in EtOAc (100 ml). The organic layer was washed with distilled water (100 ml), brine (100 ml), dried (MgSO₄) and filtered. Solvent was removed under reduced pressure to yield the crude product which was purified by flash column chromatography (SiO₂;

EtOAc/petroleum spirit (40 – 60 °C); 3:2) to give the product as a colourless solid (5.65 g, 52%).

m.p. 85 – 86 °C [lit. 88 – 89 °C];¹⁸² **R_f** = 0.18 (SiO₂; EtOAc/petroleum spirit (40 – 60 °C); 3:2); **¹H NMR** (500 MHz, CDCl₃) 10.83 (1H, br s, OH), 6.68 (2H, s, CH=CH), 3.52 (2H, m, N-CH₂), 2.34 (2H, m, CH₂COOH), 1.68 – 1.60 (4H, m, N-CH₂CH₂CH₂CH₂CH₂COOH), 1.33 (2H, m, N-(CH₂)₂CH₂(CH₂)₂COOH); **¹³C NMR** (125 MHz, CDCl₃) 179.3 (C=O, acid), 169.2 (C=O, maleimide), 134.1 (CH=CH), 37.6 (CH₂-N), 33.8 (CH₂COOH), 28.3 (CH₂CH₂-N), 26.2 (CH₂CH₂COOH), 24.2 (CH₂(CH₂)₂COOH); **ν_{max}** (neat/cm⁻¹) 3451.4 (br, O-H), 2937.5, 2871.8 (m, C-H), 1767.9, (C=O, acid), 1684.2 (C=O, maleimide), 1587.7 (w, C=C), 1469.9, 1408.2, 1368.1, 1308.8 (m, C-H bend), 1258.0, 1208.0 (m, C-N); **m/z** (EI) 211 ([M]⁺, 12%), 193 (17), 165 (12), 130 (13), 110 (100), 98 (17), 82 (11); **HRMS** found [M]⁺, 211.08440; C₁₀H₁₃NO₄ requires 211.08391.

3.8 6-Aminohexanoic acid methyl ester hydrochloride (108)¹⁴²

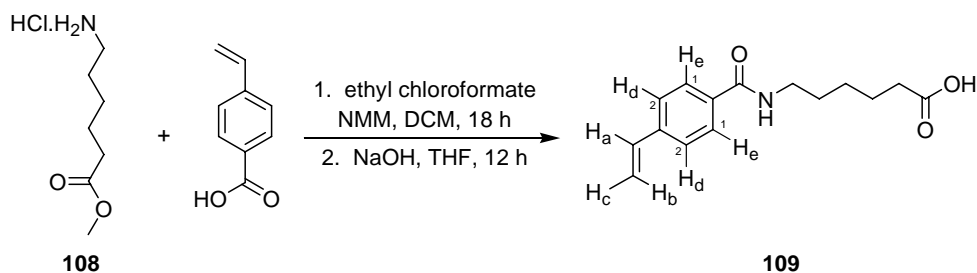


Thionyl chloride (65.25 g, 40.12 ml, 549.0 mmol) was added dropwise to methanol (MeOH) (200 ml) at 0 °C followed by addition of 6-aminohexanoic acid (20.00 g, 152.0 mmol) and the resulting suspension stirred at room temperature for 18 h. The reaction mixture was concentrated and hexane (50 ml) was added. EtOAc (50 ml) was slowly added and the product precipitated out as a colourless solid which was collected by filtration. (27.51 g, 99%).

m.p. 119 – 120 °C [lit. 120 – 121 °C];¹⁴² **¹H NMR** (300 MHz, CDCl₃) 8.19 (2H, br s, NH₂), 3.63 (3H, s, CH₃), 3.00 (2H, m, CH₂C=O), 2.30 (2H, t, ³J = 6.7 Hz, CH₂NH₂), 1.79 – 1.41 (6H, m, (CH₂)₃CH₂COOCH₃); **¹³C NMR** (125 MHz, CDCl₃) 173.2 (C=O), 51.2 (CH₃), 40.0 (CH₂C=O), 33.0 (CH₂NH₂), 26.5, 25.3,

23.9 ((CH₂)₃CH₂COOCH₃); ν_{\max} (neat/cm⁻¹) 2930.8, 2896.4, 2669.8, 2530.3 (m, C-H), 1728.8 (s, C=O), 1621.9, 1516.9, 1458.5 (m, C-H bend), 1581.7 (m, N-H bend), 1313.2, 1250.4, 1177.4 (m, C-O); m/z (Positive CI-Methane) 146 ([M + H]⁺, 100%), 129 (27), 114 (44), 97 (17); **HRMS** found [M + H]⁺, 146.11778; C₇H₁₆NO₂ requires 146.11810.

3.9 6-(4-Vinylbenzoylamino)hexanoic acid (109)

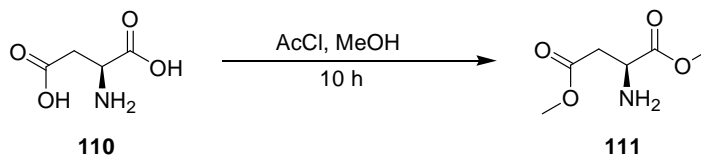


NMM (0.20 g, 0.22 ml, 2.0 mmol) was added to a stirred solution of 4-vinylbenzoic acid (0.30 g, 2.0 mmol) in DCM (5 ml) at -15 °C. Ethyl chloroformate (0.22 g, 0.20 ml, 2.0 mmol) in DCM (5 ml) was added dropwise and the reaction stirred at this temperature for 20 mins. A further portion of NMM (0.20 g, 0.22 ml, 2.0 mmol) was added, followed by portionwise addition of 6-aminohexanoic acid methyl ester hydrochloride (0.36 g, 2.0 mmol). The reaction mixture was allowed to slowly warm to room temperature and left to stir for a further 18 h. Solvent was removed under reduced pressure and the residue partitioned between distilled water (20 ml) and EtOAc (20 ml). The EtOAc layer was separated and the aqueous layer was extracted with EtOAc (3 × 30 ml). The combined organic layers were washed with dilute citric acid (20 ml of a 20% aq. solution), sat. NaHCO₃ (40 ml), brine (40 ml), dried (MgSO₄) and filtered. Solvent was removed under reduced pressure and the crude product purified by flash column chromatography (silica gel, 1:1 EtOAc/petroleum spirit (40 – 60 °C)) to give 6-(4-vinylbenzoylamino)hexanoic acid methyl ester as a colourless solid.

6-(4-Vinylbenzoylamino)hexanoic acid methyl ester thus obtained was then stirred in a mixture of NaOH/THF; 1:6 (10 ml) for 12 h. Solvent was removed under reduced pressure and the residue redissolved in distilled water (20 ml). The solution was acidified with 2 M HCl to pH 5 and extracted with EtOAc (3 × 30 ml). The combined organic layers were dried (MgSO₄), filtered and solvent removed under reduced pressure to give the product as a colourless solid (0.14 g, 29%).

m.p. 114 – 118 °C; **¹H NMR** (300 MHz, DMSO) 12.17 (1H, br s, COOH), 8.43 (1H, s, NH), 7.81 (2H, d, ³J = 8.3 Hz, H_c), 7.53 (2H, d, ³J = 8.3 Hz, H_d), 6.77 (1H, dd, ³J = 17.7 Hz, ³J = 11.0 Hz, H_a), 5.93 (1H, d, ³J = 17.7 Hz, H_b), 5.35 (1H, d, ³J = 11.0 Hz, H_c), 3.26 – 3.19 (2H, m, CH₂NH), 2.22 – 2.17 (2H, m, CH₂COOH), 1.53 – 1.25 (6H, m, (CH₂)₃CH₂COOH); **¹³C NMR** (75 MHz, DMSO) 174.4 (C=OOH), 166.9 (C=ONH), 139.5 (CCH=CH₂), 135.9 (CH=CH₂), 133.8 (C-C=O), 127.4 (C₁), 125.8 (C₂), 116.0 (CH=CH₂), 40.3 (CH₂NH), 33.5 (CH₂COOH), 28.8, 26.0, 24.2 ((CH₂)₃CH₂COOH); **ν_{max}** (neat/cm⁻¹) 3334.6 (br, O-H), 2931.6 (w, Ar-H), 2860.4, 2667.4 (w, CH₂), 1692.9 (s, C=O, acid), 1625.6 (s, C=O, amide), 1607.8 (m, C=C), 1532.9 (m, N-H bend), 1503.6, 1470.2, 1430.9, 1346.8 (m, C-H bend), 1278.4 (s, C-O); **m/z** (Positive CI-Methane) 262 ([M + H]⁺, 100%); **HRMS** found [M + H]⁺, 262.14423; C₁₅H₂₀NO₃ requires 262.14377.

3.10 Aspartic acid dimethyl ester (111)¹⁸³

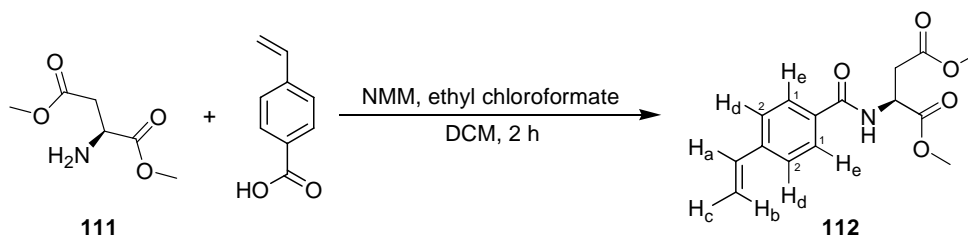


Acetyl chloride (AcCl) (11.04 g, 10.00 ml, 140.6 mmol) was added dropwise to MeOH (100 ml) at 0 °C followed by addition of L-aspartic acid (7.00 g, 52.6 mmol) and the resulting suspension stirred at room temperature for 10 h. Solvent

was removed under reduced pressure and the crude product was dissolved in sat. NaHCO₃ (50 ml). The aqueous layer was extracted with EtOAc (5 × 50 ml), washed with brine (50 ml), distilled water (50 ml), dried (Na₂SO₄) and filtered. Solvent was removed under reduced pressure to give the product as a colourless oil (4.98 g, 59%).

$[\alpha]_D^{24} = -15.6$ (*c* 1, DMSO); ¹H NMR (300 MHz, CDCl₃) 3.80 (1H, m, CH), 3.71, 3.67 (6H, s, CH₃), 2.86 – 2.76 (2H, m, CH₂), 1.87 (2H, br s, NH₂); ¹³C NMR (75 MHz, CDCl₃) 174.5 (CHC=O), 171.6 (CH₂C=O), 52.3 (CH), 51.8, 51.2 (CH₃), 38.7 (CH₂); ν_{\max} (neat/cm⁻¹) 3390.6 (w, N-H), 2955.6 (w, C-H), 1729.0 (s, C=O), 1437.1, 1364.9 (m, C-H bend), 1198.2, 1169.7 (s, C-O); *m/z* (Positive CI-Methane) 162 ([M + H]⁺, 36%), 102 (100), 88 (39), 70 (13); HRMS found [M + H]⁺, 162.07555; C₆H₁₂NO₄ requires 162.07663.

3.11 (S)- 2-(4-Vinyl-benzoylamino)succinic acid dimethyl ester (112)

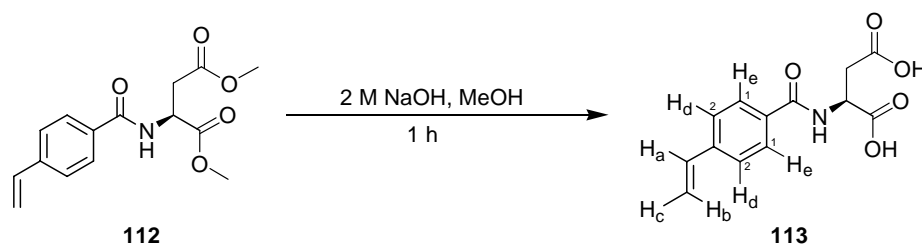


NMM (0.34 g, 0.37 ml, 3.4 mmol) was added to a stirred solution of 4-vinylbenzoic acid (0.50 g, 3.4 mmol) in DCM (10 ml) at -15 °C. Ethyl chloroformate (0.41 g, 0.32 ml, 3.4 mmol) in DCM (5 ml) was added dropwise and the reaction stirred at this temperature for 20 mins. L-Aspartic acid dimethyl ester was then added and the reaction mixture was allowed to slowly warm to room temperature and left to stir for a further 2 h. Solvent was removed under reduced pressure and the residue partitioned between distilled water (20 ml) and EtOAc (20 ml). The EtOAc layer was separated and the aqueous layer was extracted with EtOAc (3 × 30 ml). The combined organic layers were washed with dilute citric

acid (20 ml of a 20% aq. solution), sat. NaHCO₃ (40 ml), brine (40 ml), dried (MgSO₄) and filtered. Solvent was removed under reduced pressure and the crude product purified by flash column chromatography (SiO₂; EtOAc/ petroleum spirit (40 – 60 °C); 2:3) to give product as a colourless solid (1.77 g, %).

m.p. 93 – 95 °C; **R_f** = 0.32 (SiO₂; EtOAc/ petroleum spirit (40 – 60 °C); 2:3); **[α]_D²³** = + 59.3 (*c* 1, CDCl₃); **¹H NMR** (500 MHz, CDCl₃) 7.77 (2H, d, ³*J* = 8.3 Hz, H_e), 7.47 (2H, d, ³*J* = 8.3 Hz, H_d), 7.21 (1H, br s, NH), 6.74 (1H, dd, ³*J* = 17.6 Hz, ³*J* = 10.9 Hz, H_a), 5.84 (1H, d, ³*J* = 17.6 Hz, H_b), 5.36 (1H, d, ³*J* = 10.9 Hz, H_c), 5.05 (1H, m, CH-NH), 3.79 (3H, s, CH₃), 3.71 (3H, s, CH₃), 3.16 – 2.98 (2H, m, CH₂); **¹³C NMR** (125 MHz, CDCl₃) 171.9 (CHC=O), 171.4 (CH₂C=O), 166.6 (C=O, vinyl benzoic acid), 141.1 (CCH=CH₂), 136.0 (CC=O), 132.7 (CH=CH₂), 127.6 (C₁), 126.4 (C₂), 116.3 (CH=CH₂), 53.0 (CHNH), 52.2, 48.9 (CH₃), 36.2 (CH₂); **ν_{max}** (neat/cm⁻¹) 3298.3 (m, N-H), 2950.6, 2989.4 (w, Ar-H), 1731.9, 1632.9 (s, C=O), 1540.7, 1504.4 (s, C=C), 1436.2, 1325.8 (s, C-H bend), 1294.5 (s, N-C), 1169.1, 1116.9 (m, C-O); ***m/z*** (Positive ESI) 314 ([M + Na]⁺, 100%); **HRMS** found [M + Na]⁺, 314.10160; C₁₅H₁₇NO₅Na requires 314.10040.

3.12 (S)- 2-(4-Vinyl-benzoylamino)succinic acid (113)

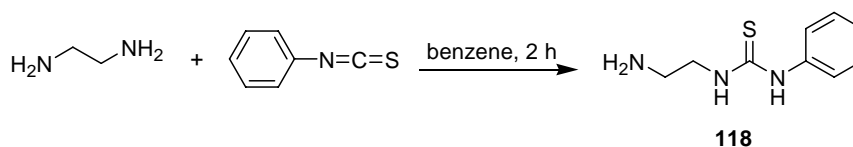


(S)- 2-(4-Vinyl-benzoylamino)succinic acid methyl ester (0.30g, 1.0 mmol) was stirred in a mixture of NaOH/MeOH; 1:3 (10 ml) for 1 h. Solvent was removed under reduced pressure and the residue redissolved in distilled water (20 ml). The solution was acidified with 2 M HCl to pH 5 and extracted with EtOAc (3 × 30 ml). The combined organic layers were dried (MgSO₄), filtered and solvent

removed under reduced pressure to give the product as a colourless solid (0.25 g, 95%).

m.p. 168 – 170 °C; $[\alpha]_D^{23} = -21.1$ (c 1, DMSO); **$^1\text{H NMR}$** (500 MHz, DMSO) 12.55 (2H, br s, OH), 8.72 (1H, m, NH), 7.83 (2H, d, $^3J = 8.3$ Hz, H_e), 7.56 (2H, d, $^3J = 8.3$ Hz, H_d), 6.78 (1H, dd, $^3J = 17.7$ Hz, $^3J = 11.1$ Hz, H_a), 5.95 (1H, d, $^3J = 17.7$ Hz, H_b), 5.36 (1H, d, $^3J = 11.1$ Hz, H_c), 4.74 (1H, m, CHNH), 2.84 – 2.69 (2H, m, CH_2); **$^{13}\text{C NMR}$** (125 MHz, CDCl_3) 172.4 ($\text{CHC}=\text{O}$), 172.3 ($\text{CH}_2\text{C}=\text{O}$), 166.9 ($\text{C}=\text{O}$, vinyl benzoic acid), 141.5 ($\text{CCH}=\text{CH}_2$), 137.0 ($\text{CC}=\text{O}$), 134.2 ($\text{CH}=\text{CH}_2$), 128.5 (C_1), 126.9 (C_2), 116.2 ($\text{CH}=\text{CH}_2$), 50.1 (CHNH), 36.3 (CH_2); **ν_{max}** (neat/ cm^{-1}) 3314.3 (br, O-H), 2936.4, 2640.1 (w, Ar-H), 1698.5, 1644.9 (s, $\text{C}=\text{O}$), 1563.2, 1530.9, 1504.4 (s, $\text{C}=\text{C}$), 1416.6 (s, C-H bend), 1290.4, 1226.6 (s, N-C); **m/z** (Positive ESI) 286 ($[\text{M} + \text{Na}]^+$, 48%), 276 (88), 210 (100), 178 (32), 163 (19), 144 (32); **HRMS** found $[\text{M} + \text{Na}]^+$, 286.06800; $\text{C}_{13}\text{H}_{13}\text{NO}_5\text{Na}$ requires 286.06910.

3.13 1-(2-Aminoethyl)-3-phenylthiourea (118)¹⁴⁵

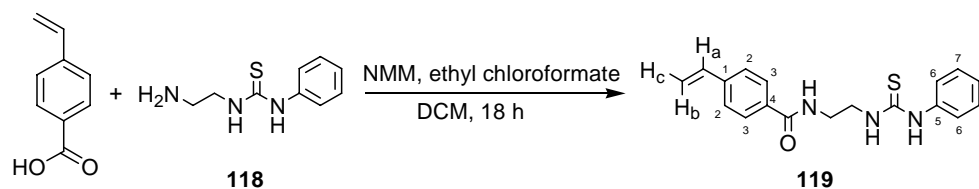


A solution of phenylisothiocyanate (2.70 g, 3.40 ml, 20.0 mmol) in benzene (5 ml) was added dropwise to a stirred solution of ethane-1,2-diamine (1.20 g, 1.34 ml, 20.0 mmol) in benzene (30 ml). The reaction mixture was stirred for 2 h at room temperature before it was quenched by the addition of 2 M HCl (80 ml). Solvent was removed under reduced pressure and the residue suspended in distilled water (30 ml). The reaction mixture was hot filtered and the filtrate basified by addition of solid NaOH to pH 12, during which time the product precipitated out as colourless crystalline solid (2.67 g, 68%).

m.p. 134 – 135 °C [lit. 136 – 137 °C];¹⁸⁴ **$^1\text{H NMR}$** (300 MHz, DMSO) 8.39 (2H,

br s, NH₂), 7.45 – 7.42 (2H, m, *o*-Ar-H), 7.32 – 7.31 (2H, m, *m*-Ar-H), 7.10 – 7.05 (1H, m, *p*-Ar-H), 4.38 (1H, br s, NH-Ph), 3.43 (2H, m, NHCH₂), 2.72 – 2.68 (2H, m, CH₂NH₂), 1.85 (1H, br s, NHCH₂); ¹³C NMR (75 MHz, DMSO) 180.4 (C=S), 138.2 (C-NH), 128.5 (*o*-Ar-C), 123.8 (*m*-Ar-C), 122.9 (*p*-Ar-C), 47.0 (CH₂NH), 42.9 (CH₂NH₂); ν_{\max} (neat/cm⁻¹) 3168.0 (m, N-H), 1590.3 (m, C=C), 1529.5 (s, N-H bend), 1490.4, 1320.5 (s, C-H bend), 1240.2 (m, N-C), 1040.3 (m, C=S); *m/z* (Positive CI-Methane) 196 ([M + H]⁺, 70%), 179 (75), 162 (84), 153 (37), 136 (100), 103 (58), 94 (67); HRMS found [M + H]⁺, 196.09107; C₉H₁₄N₃S requires 196.09084.

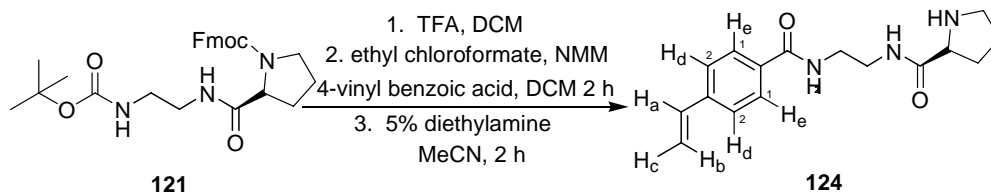
3.14 *N*-[2-(3-Phenylthioureido)ethyl]-4-vinylbenzamide (119)



NMM (0.38 g, 0.41 ml, 3.8 mmol) was added to a stirred solution of 4-vinylbenzoic acid (0.44 g, 3.0 mmol) in DCM (12 ml) at –15 °C. Ethyl chloroformate (0.33 g, 0.29 ml, 3.0 mmol) in DCM (5 ml) was added dropwise to the reaction mixture which was then stirred at this temperature for a further 30 mins. This was followed by the portionwise addition of 1-(2-aminoethyl)-3-phenylthiourea (0.59 g, 3.0 mmol). The reaction mixture was allowed to slowly warm to room temperature and stirred for 18 h. Distilled water (20 ml) was added and the DCM layer separated. The aqueous phase was extracted with DCM (3 × 40 ml) and the combined organic extracts were washed with sat. NaHCO₃ (100 ml), brine (100 ml), dried (MgSO₄) and filtered. Solvent was removed under reduced pressure and the crude product purified by flash column chromatography (SiO₂; EtOAc/petroleum spirit (40 – 60 °C); 1:1) to give a white solid (0.26 g, 27%).

m.p. 142 – 145 °C; **R_f** = 0.13 (SiO₂; EtOAc/petroleum spirit (40 – 60 °C); 1:1); **¹H NMR** (300 MHz, CDCl₃) 7.71 (1H, s, *NHP*h), 7.61 (1H, s, CH₂NHC=S), 7.47 – 7.19 (9H, m, ArH), 6.81 – 6.69 (1H, m, H_a), 5.83 (1H, d, ³*J* = 17.4 Hz, H_b), 5.36 (1H, d, ³*J* = 10.9 Hz, H_c), 4.13 – 4.02 (2H, m, CH₂NHCO), 3.78 – 3.66 (2H, m, CH₂NHC=S), 1.93 (1H, br s, NH); **¹³C NMR** (75 MHz, DMSO) 180.5 (C=S), 166.1 (C=O), 139.7 (C₅), 135.9, (C₁), 133.5 (CH=CH₂), 128.9 (C₄), 128.6 (C₇), 127.5 (C₃), 125.9 (C₂), 124.2 (C₆), 123.3 (C₈), 116.1 (CH=CH₂), 35.7 (CH₂NHCO), 30.7 (CH₂NHC=S); **ν_{max}** (neat/cm⁻¹) 3309.5 (m, N-H), 1633.8 (s, C=O), 1601.9 (m, C=C), 1543.4 (s, N-H bend), 1495.4, 1425.8 (m, C-H bend), 1309.7, 1277.1, 1207.2 (m, N-C), 1073.3 (m, C=S); ***m/z*** (Positive CI-Methane) 326 ([M + H]⁺, 100), 299 (9), 268 (13), 233 (23); **HRMS** found [M + H]⁺, 326.13259; C₁₈H₂₀N₃OS requires 326.13216.

3.15 (*S*)-2-Pyrrolidine-2-carboxylic acid [2-(4-vinyl-benzoylamino)ethyl] amide (124)



TFA (2 ml) was added to a cooled solution of (*S*)-(9*H*-fluoren-9-yl)methyl-2-{[2-(*tert*-butoxycarbonyl)ethyl]carbamoyl}pyrrolidine-1-carboxylate (3.23 g, 6.8 mmol) in DCM (10 ml) and stirred for 2 h. DCM was removed under reduced pressure and the excess TFA by co-evaporation with toluene. The product was used in the next step without further purification.

NMM (0.68 g, 0.74 ml, 6.8 mmol) was added to a stirred solution of 4-vinylbenzoic acid (1.00 g, 6.8 mmol) in DCM (20 ml) at –15 °C. Ethyl chloroformate (0.73 g, 0.20 ml, 2.0 mmol) in DCM (12 ml) was added dropwise and the reaction stirred at this temperature for 20 mins. A further portion of

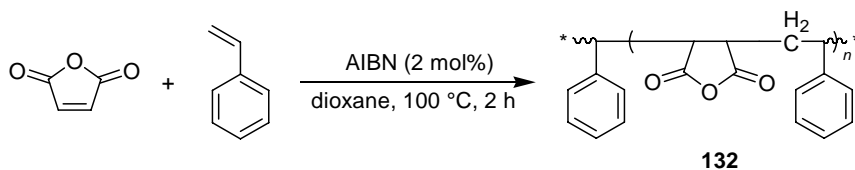
NMM (0.68 g, 0.74 ml, 6.8 mmol) was added, followed by portionwise addition of TFA salt of (*S*)-(9*H*-fluoren-9-yl)methyl-2- $\{[2-(tert\text{-butoxycarbonyl})ethyl] carbamoyl\}$ pyrrolidine-1-carboxylate prepared earlier. The reaction mixture was allowed to slowly warm to room temperature and left to stir for a further 2 h. Solvent was removed under reduced pressure and the residue partitioned between distilled water (20 ml) and EtOAc (20 ml). The EtOAc layer was separated and the aqueous layer was extracted with EtOAc (3 \times 30 ml). The combined organic layers were washed with dilute citric acid (20% aq. solution, 20 ml), sat. NaHCO₃ (40 ml), brine (40 ml), dried (MgSO₄) and filtered. Solvent was removed under reduced pressure and the crude product purified by flash column chromatography (SiO₂; MeOH/EtOAc; 1:24) to give the product as a colourless solid (1.77 g, 51%).

Deprotection of the Fmoc group was then carried out by suspending the product obtained in diethylamine/MeCN; 1:20 (20 ml) for 2 h at room temperature. The solvent was then removed under reduced pressure to yield the crude product which was purified by flash column chromatography (SiO₂; MeOH/DCM; 15:85) to give the product as an off-white solid (0.92 g, 47%).

m.p. 70 – 72 °C; **R_f** = 0.14 (SiO₂; MeOH/DCM; 15:85); **[α]_D²³** = – 15.6 (*c* 1, DMSO); **¹H NMR** (500 MHz, CDCl₃) 8.30 (1H, br s, NH(CH₂)₂NHPro), 7.78 (2H, d, ³*J* = 8.3 Hz, H_c), 7.66 (1H, br s, NH(CH₂)₂NHPro), 7.42 (2H, d, ³*J* = 8.3 Hz, H_d), 6.70 (1H, dd, ³*J* = 17.6 Hz, ³*J* = 10.9 Hz, H_a), 5.78 (1H, d, ³*J* = 17.6 Hz, H_b), 5.31 (1H, d, ³*J* = 10.9 Hz, H_c), 3.80 (1H, m, CH-NH), 3.57 – 3.47 (4H, m, NH(CH₂)₂NH), 2.95 (2H, m, CH₂(CH₂)₂CHNH), 2.69 (1H, br s, NH, Pro), 1.84 (2H, m, CH₂CHNH), 1.67 (2H, m, CH₂CH₂CHNH); **¹³C NMR** (125 MHz, CDCl₃) 176.8 (C=O, Pro), 167.5 (C=O, vinyl benzoic acid), 140.5 (CCH=CH₂), 136.1 (CH=CH₂), 133.2 (CC=O), 127.6 (C₁), 126.3 (C₂), 115.8 (CH=CH₂), 60.4 (CHNH), 47.1 (NHCH₂CH₂NHPro), 41.9 (NHCH₂CH₂NHPro), 38.9 (CH₂(CH₂)₂CHNH), 30.7 (CH₂CHNH), 26.0 (CH₂CH₂CHNH); **ν_{\max}** (neat/cm⁻¹) 3291.7, 3081.3 (br, N-H), 2970.7, 2871.3 (w, Ar-H), 1696.3 (s, C=O, vinyl benzoic acid), 1633.3 (s, C=O, Pro), 1529.4 (s, C=C), 1441.7, 1273.8 (s, C-H

bend), 1256.4 (s, N-C); m/z (Positive ESI) 310 ($[M + Na]^+$, 100%), 288 (67), 174 (26); **HRMS** found $[M + Na]^+$, 310.15290; $C_{16}H_{21}N_3O_2Na$ requires 310.15310.

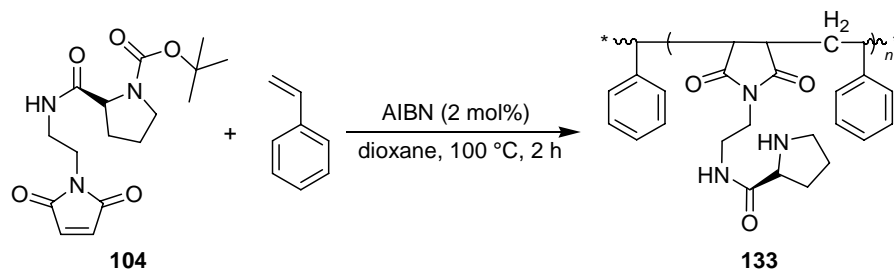
3.16 Maleic Anhydride – Styrene Co-polymer (132)¹³⁵



Maleic anhydride (1.96 g, 20.0 mmol), styrene (2.08 g, 20.0 mmol) and AIBN (66.00 mg, 2.0 mol%) were heated in dioxane (25 ml) at reflux for 2 h under an atmosphere of N_2 . The reaction mixture was allowed to cool and the polymer was precipitated out by addition of petroleum spirit (40 – 60 °C) to give a colourless solid (2.84 g, 70%).

m.p. 144 – 148 °C (T_g); ^{13}C NMR (75 MHz, solid state) 173.1 (C=O), 138.8 (C_q , Ar), 129.6 (CH, Ar), 67.5 (CHC=O), 53.1 (CHPh), 42.4 (CH_2); ν_{max} (neat/ cm^{-1}) 2925.4, 2863.8 (w, C-H), 1774.9, 1728.2 (s, C=O), 1454.3, 1255.0 (m, C-H bend).

3.17 Functionalised Maleimide (104) – Styrene Co-polymer (133)



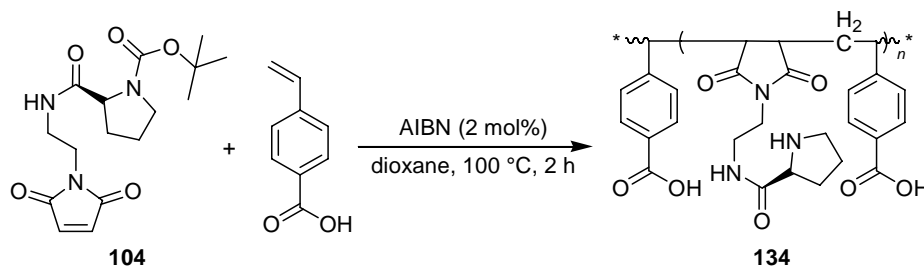
Co-polymerisation was carried out by modifying the method outlined by Charleux.¹⁴⁶ 2-[2-(2,5-dioxo-2,5-dihydropyrrol-1-yl)ethylcarbamoyl]pyrrolidine-

1-carboxylic acid *tert*-butyl ester (1.68 g, 5.0 mmol), styrene (0.52 g, 5.0 mmol) and AIBN (16.00 mg, 2.0 mol%) were heated in dioxane (15 ml) at reflux for 2 h under an atmosphere of N₂. The reaction mixture was allowed to cool and the polymer was precipitated out by addition of petroleum spirit (40 – 60 °C).

TFA (10 ml) was added to a cooled solution of the resultant polymer in DCM (24 ml) and stirred for 20 mins. DCM was removed under reduced pressure and the excess TFA by co-evaporation with toluene. Pyridine (10 ml) was added and the residue was washed with diethyl ether (Et₂O) (5 × 50 ml) and distilled water (5 × 50 ml) to yield the product as a light orange solid (1.17 g, 69%).

m.p. 180 – 185 °C (T_g); ¹³C NMR (75 MHz, solid state) 178.6 (C=O, maleimide), 169.3, 161.5 (C=ONH), 141.0 (C_q, Ar), 128.1 (CH, Ar), 59.7 (CHC=O), 40.5, 37.5, 30.7, 24.3, 9.6 (aliphatic); ν_{\max} (neat/cm⁻¹) 3256.5, 3082.4 (br, N-H), 2950.9, 2760.9 (w, C-H), 1770.3, 1667.9 (s, C=O), 1567.5 (m, C=C), 1489.8, 1401.0 (m, C-H bend), 1258.7 (m, N-C); $M_w/M_n = 1.18$, $M_n = 21139$.

3.18 Functionalised Maleimide (104) – 4-vinylbenzoic acid Co-polymer (134)



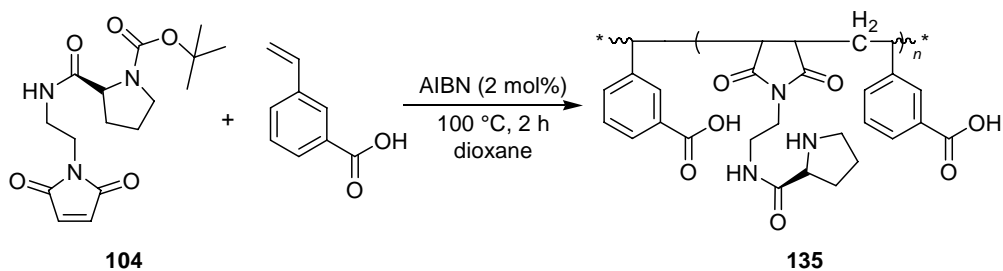
Co-polymerisation was carried out by modifying the method outlined by Charleux.¹⁴⁶ 2-[2-(2,5-dioxo-2,5-dihydropyrrol-1-yl)ethylcarbamoyl]pyrrolidine-1-carboxylic acid *tert*-butyl ester (1.68 g, 5.0 mmol), 4-vinylbenzoic acid (0.74 g, 5.0 mmol) and AIBN (16.00 mg, 2.0 mol%) were heated in dioxane (15 ml) at

reflux for 2 h under an atmosphere of N₂. The reaction mixture was allowed to cool and the polymer was precipitated out by addition of petroleum spirit (40 – 60 °C).

TFA (10 ml) was added to a cooled solution of the resultant polymer in DCM (24 ml) and stirred for 20 mins. DCM was removed under reduced pressure and the excess TFA by co-evaporation with toluene. Pyridine (10 ml) was added and the residue was washed with Et₂O (5 × 50 ml) and distilled water (5 × 50 ml) to yield the product as a light orange solid (1.04 g, 54%).

m.p. 98 – 100 °C (T_g); ¹³C NMR (75 MHz, solid state) 178.3 (C=O, maleimide), 169.7, (C=OOH), 162.6 (C=ONH), 143.1 (C_q, Ar), 130.4 (CH, Ar), 60.6 (CHC=O), 40.3, 31.1, 24.5 (aliphatic); **v**_{max} (neat/cm⁻¹) 3074.3 (br, O-H), 2952.1, 2569.9 (w, C-H), 1771.4, 1663.2, 1611.0 (s, C=O), 1575.5, 1547.0 (m, C=C), 1488.5, 1421.2, 1401.5 (m, C-H bend), 1258.8 (m, N-C), 1175.3, 1123.7 (s, C-O); **M**_w/**M**_n = 1.54, **M**_n = 2122.

3.19 Functionalised Maleimide (104) – 3-vinyl-benzoic acid Co-polymer (135)



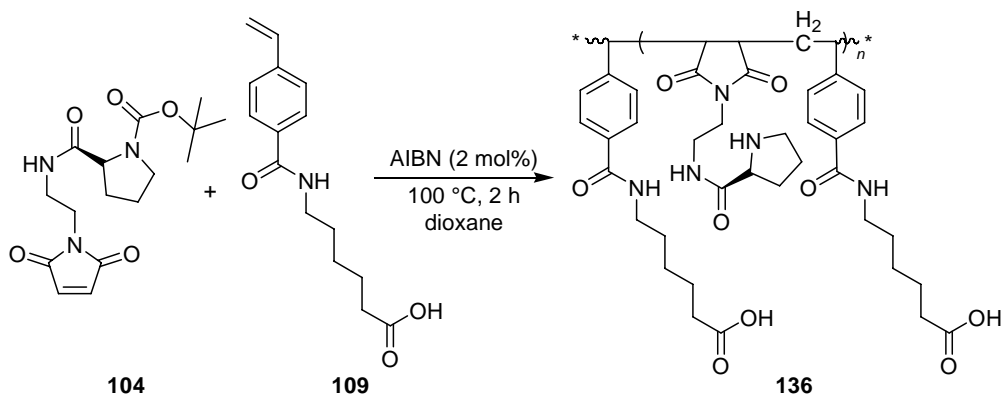
Co-polymerisation was carried out by modifying the method outlined by Charleux.¹⁴⁶ 2-[2-(2,5-dioxo-2,5-dihydropyrrol-1-yl)ethylcarbamoyl]pyrrolidine-1-carboxylic acid *tert*-butyl ester (1.68 g, 5.0 mmol), 3-vinylbenzoic acid (0.74 g, 5.0 mmol) and AIBN (16.37 mg, 2.0 mol%) were heated in dioxane (15 ml) at

reflux for 2 h under an atmosphere of N₂. The reaction mixture was allowed to cool and the polymer was precipitated out by addition of petroleum spirit (40 – 60 °C).

TFA (10 ml) was added to a cooled solution of the resultant polymer in DCM (24 ml) and stirred for 20 mins. DCM was removed under reduced pressure and the excess TFA by co-evaporation with toluene. Pyridine (10 ml) was added and the residue was washed with Et₂O (5 × 50 ml) and distilled water (5 × 50 ml) to yield the product as a pale yellow solid (0.77 g, 40%).

m.p. 144 – 147 °C (T_g); ¹³C NMR (75 MHz, solid state) 179.1 (C=O, maleimide), 170.3, (C=OOH), 161.6 (C=ONH), 141.5 (C_q, Ar), 131.1 (CH, Ar), 70.0 (CHC=O), 60.2 (CHPh), 40.8, 30.6, 25.1 (aliphatic); ν_{\max} (neat/cm⁻¹) 3083.9 (br, O-H), 2952.0 (w, C-H), 1770.8, 1670.5 (s, C=O), 1586.1 (m, C=C), 1489.8, 1434.8, 1401.8 (m, C-H bend), 1258.3 (m, N-C), 1172.2, 1132.2 (s, C-O); M_w/M_n = 1.84, M_n = 3788.

3.20 Functionalised Maleimide (104) – Functionalised Styrene (109) Copolymer (136)



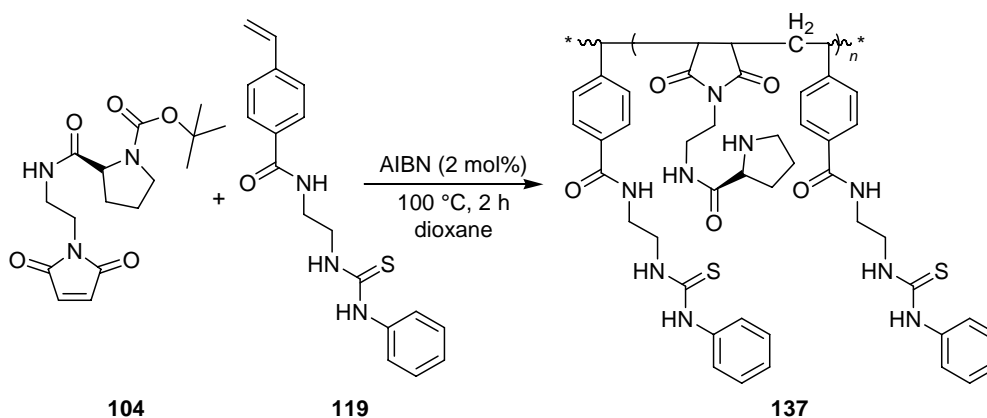
Co-polymerisation was carried out by modifying the method outlined by Charleux.¹⁴⁶ 2-[2-(2,5-dioxo-2,5-dihydropyrrol-1-yl)ethylcarbamoyl]pyrrolidine-

1-carboxylic acid *tert*-butyl ester (0.84 g, 2.5 mmol), 6-(4-vinylbenzoylamino)hexanoic acid (0.65 g, 2.5 mmol) and AIBN (8.00 mg, 2.0 mol%) were heated in dioxane (15 ml) at reflux for 2 h under an atmosphere of N₂. The reaction mixture was allowed to cool and the polymer was precipitated out by addition of petroleum spirit (40 – 60 °C).

TFA (10 ml) was added to a cooled solution of the resultant polymer in DCM (24 ml) and stirred for 20 mins. DCM was removed under reduced pressure and the excess TFA by co-evaporation with toluene. Pyridine (10 ml) was added and the residue was washed with toluene (5 × 50 ml) and petroleum spirit (40 – 60 °C) (5 × 50 ml) to yield the product as a yellow solid (0.84 g, 68%).

m.p. 160 – 165 °C (T_g); ¹³C NMR (75 MHz, solid state) 178.3 (C=O, maleimide), 169.7, (C=OOH), 162.2 (C=ONH), 144.1 (C_q, Ar), 128.4 (CH, Ar), 60.7 (CHC=O), 40.8, 26.0 (aliphatic); ν_{\max} (neat/cm⁻¹) 3271.6 (br, O-H), 3074.5 (w, N-H), 2941.8 (w, C-H), 1671.0 (s, C=O), 1546.5, 1503.7 (m, C=C), 1433.8, 1400.8, 1372.0 (m, C-H bend), 1180.7, 1126.2 (s, C-O); $M_w/M_n = 1.97$, $M_n = 2853$.

3.21 Functionalised Maleimide (104) – Functionalised Styrene (119) Copolymer (137)

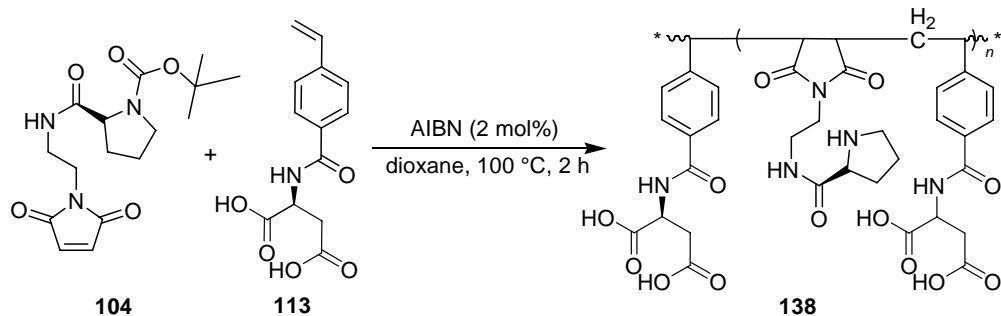


Co-polymerisation was carried out by modifying the method outlined by Charleux.¹⁴⁶ 2-[2-(2,5-dioxo-2,5-dihydropyrrol-1-yl)ethylcarbamoyl]pyrrolidine-1-carboxylic acid *tert*-butyl ester (0.51 g, 1.5 mmol), *N*-[2-(3-phenylthioureido)ethyl]-4-vinylbenzamide (0.49 g, 1.5 mmol) and AIBN (4.90 mg, 2.0 mol%) were heated in dioxane (15 ml) at reflux for 2 h under an atmosphere of N₂. The reaction mixture was allowed to cool and the polymer was precipitated out by addition of petroleum spirit (40 – 60 °C).

TFA (10 ml) was added to a cooled solution of the resultant polymer in DCM (24 ml) and stirred for 20 mins. DCM was removed under reduced pressure and the excess TFA by co-evaporation with toluene. Pyridine (10 ml) was added and the residue was washed with Et₂O (5 × 50 ml) and distilled water (5 × 50 ml) to yield the product as a yellow solid (0.55 g, 65%).

m.p. >230 °C (*T_g*); ¹³C NMR (75 MHz, solid state) 178.9 (C=O, maleimide), 169.4, (C=OOH), 162.3 (C=ONH), 157.5 (C=S), 141.0 (C_q, Ar), 128.4 (CH, Ar), 60.2 (CHC=O), 39.3, 25.5 (aliphatic); **v_{max}** (neat/cm⁻¹) 3322.8 (br, O-H), 2929.0, 2850.9 (m, C-H), 1672.0, 1626.0 (s, C=O), 1537.0 (m, C=C), 1498.0, 1434.8, 1400.0, 1311.5 (m, C-H bend), 1243.9 (m, N-C), 1088.3 (m, C=S); **M_w/M_n** (Sample was too insoluble for GPC analysis), **M_n** (Sample was too insoluble for GPC analysis).

3.22 Functionalised Maleimide (104) – Functionalised Styrene (113) Copolymer (138)

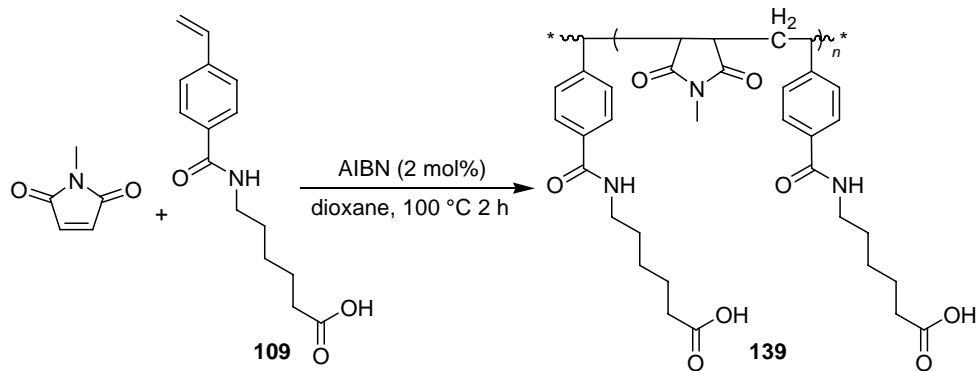


Co-polymerisation was carried out by modifying the method outlined by Charleux.¹⁴⁶ 2-[2-(2,5-Dioxo-2,5-dihydropyrrol-1-yl)ethylcarbamoyl]pyrrolidine 1-carboxylic acid *tert*-butyl ester (0.27 g, 0.8 mmol), (*S*)- 2-(4-vinylbenzoylamino)succinic acid (0.21 g, 0.8 mmol) and AIBN (2.60 mg, 2.0 mol%) were heated in dioxane (10 ml) at reflux for 2 h under an atmosphere of N₂. The reaction mixture was allowed to cool and the polymer was precipitated out by addition of petroleum spirit (40 – 60 °C).

TFA (10 ml) was added to a cooled solution of the resultant polymer in DCM (24 ml) and stirred for 20 mins. DCM was removed under reduced pressure and the excess TFA by co-evaporation with toluene. Pyridine (10 ml) was added and the residue was washed with Et₂O (5 × 50 ml) and distilled water (5 × 50 ml) to yield the product as an orange solid (0.28 g, 70%).

m.p. 95 – 97 °C (T_g); ¹³C NMR (150 MHz, solid state) 173.7 (C=O, maleimide), 171.9, 171.1 (C=OOH), 170.1 (C=O, amide), 138.0 (C_q, Ar), 133.0, 129.5, 128.7, 126.1 (CH, Ar), 118.9, 117.0, 115.0, 113.1 (C=C), 66.4 (CHC=O), 45.5, 35.8, 28.8 (aliphatic); **v**_{max} (neat/cm⁻¹) 3258.7 (br, O-H), 2942.4, 2558.5 (w, C-H), 1694.9 (s, C=O), 1544.8, 1502.4 (m, C=C), 1436.0, 1403.6, 1342.9 (m, C-H bend), 1147.7 (s, C-O).

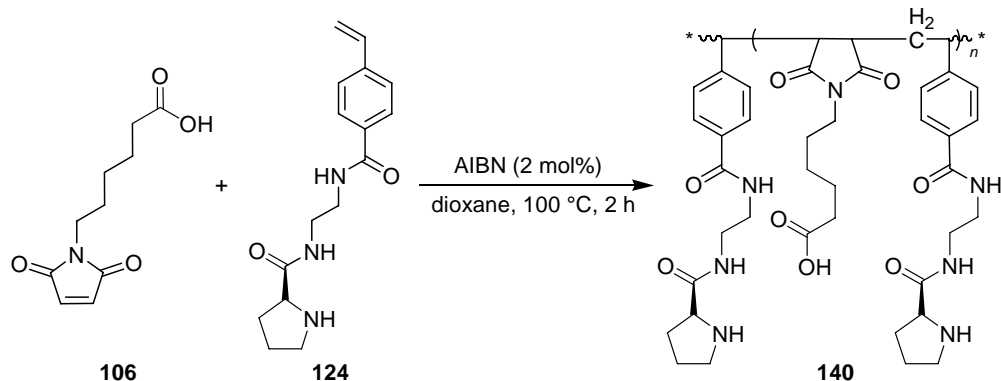
3.23 *N*-Methyl Maleimide – Functionalised Styrene (109) Co-polymer (139)



Co-polymerisation was carried out by modifying the method outlined by Charleux.¹⁴⁶ *N*-Methyl maleimide (0.11 g, 1.0 mmol), 6-(4-vinylbenzoylamino)hexanoic acid (0.26 g, 1.0 mmol) and AIBN (3.30 mg, 2.0 mol%) were heated in dioxane (15 ml) at reflux for 2 h under an atmosphere of N₂. The reaction mixture was allowed to cool and the polymer was precipitated out by addition of petroleum spirit (40 – 60 °C) to yield the product as a colourless solid (0.31 g, 83%).

m.p 166 – 170 °C (*T_g*); ¹³C NMR (150 MHz, solid state) 176.2 (C=O, maleimide), 165.8 (C=OOH), 146.6 (C_q, Ar), 133.5, 129.4, 128.4, 127.5, 126.1 (CH, Ar), 67.3 (CHC=O), 36.4, 28.9, 26.1, 24.3 (aliphatic); ν_{max} (neat/cm⁻¹) 3334.2 (br, O-H), 2935.6, 2362.9 (w, C-H), 1770.8, 1690.2, 1628.7 (s, C=O), 1545.6, 1502.7 (m, C=C), 1437.4, 1384.0, 1285.1 (m, C-H bend), 1191.9, 1163.5, 1130.1 (m, C-O).

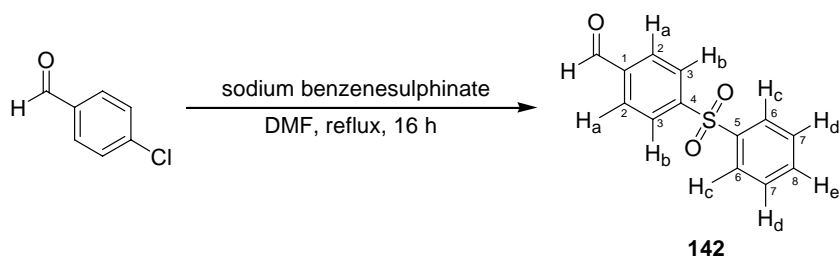
3.24 Functionalised Maleimide (106) – Functionalised Styrene (124) Co-polymer (140)



Co-polymerisation was carried out by modifying the method outlined by Charleux.¹⁴⁶ 6-(2,5-Dioxo-2,5-dihydro-pyrrol-1-yl)hexanoic acid (0.11 g, 0.5 mmol), (S)-2-pyrrolidine-2-carboxylic acid [2-(4-vinyl-benzoylamino)ethyl]amide (0.15 g, 0.5 mmol) and AIBN (1.70 mg, 2.0 mol%) were heated in dioxane (15 ml) at reflux for 2 h under an atmosphere of N₂. The reaction mixture was allowed to cool and the polymer was precipitated out by addition of petroleum spirit (40 – 60 °C) to give a dark orange solid (0.23 g, 92%).

m.p. 110 – 112 °C (T_g); **¹³C NMR** (150 MHz, solid state) 174.4 (C=O, maleimide), 166.0, (C=OOH), 139.7 (C_q, Ar), 135.9, 133.6, 128.0, 127.6, 126.0 (CH, Ar), 66.4 (CHC=O), 46.1, 33.4, 29.9, 26.8, 24.5, 24.0, 23.5 (aliphatic); **ν_{max}** (neat/cm⁻¹) 3322.8 (br, O-H), 2946.4, 2856.6 (m, C-H), 1692.1, 1640.9 (s, C=O), 1535.3, 1502.5 (m, C=C), 1438.4, 1402.6, 1365.0 (m, C-H bend), 1289.0, 1253.7 (m, N-C).

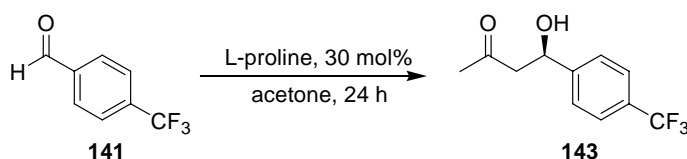
3.25 4-Benzenesulfonyl-benzaldehyde (142)¹⁸⁵



4-Chlorobenzaldehyde (3.00 g, 20.0 mmol) and sodium benzenesulphinate (3.60 g, 22.0 mmol) were dissolved in DMF (15 ml). The reaction mixture was then heated at reflux for 16 h, after which it was poured into a flask containing ice (40 g). The solid thus formed was collected and purified by flash column chromatography (SiO₂; EtOAc/petroleum spirit (40 – 60 °C); 1:1) to yield the product as a yellow crystalline solid (0.80 g, 16%).

m.p. 133 – 135 °C [lit. 132 – 133 °C];¹⁸⁵ **R_f** = 0.57 (SiO₂; EtOAc/petroleum spirit (40 – 60 °C); 1:1); **¹H NMR** (300 MHz, CDCl₃) 10.10 (1H, br s, CHO), 8.11 (2H, m, H_b), 7.95 (2H, m, H_a), 7.98 (2H, m, H_c), 7.63 – 7.51 (3H, m, H_d, H_e); **¹³C NMR** (125 MHz, CDCl₃) 192.1 (CHO), 148.1 (C₄), 141.9 (C₁), 140.5 (C₅), 135.2 (C₈), 131.7 (C₂), 131.0 (C₇), 129.7 (C₃), 129.3 (C₆); **ν_{max}** (neat/cm⁻¹) 1703.5 (s, C=O), 1593.8, 1578.2 (m, C=C), 1447.3, 1321.9 (m, C-H bend), 1198.8, 1153.8 (s, S=O); **m/z** (Positive Cl-Methane) 247 ([M + H]⁺, 100%), 213 (21), 169 (29), 167 (18); **HRMS** found [M + H]⁺, 247.04252; C₁₃H₁₁O₃S requires 247.04289.

3.26 (*R*)-4-Hydroxy-4-(4-trifluoromethyl-phenyl)butan-2-one (143)¹⁸⁶

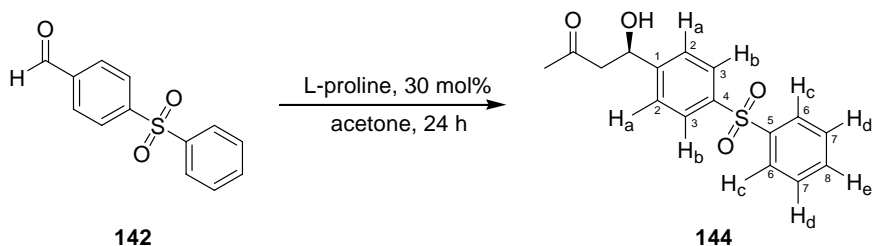


A suspension of 4-(trifluoromethyl)benzaldehyde (0.35 g, 2.0 mmol) and L-proline (0.07 g, 30 mol%) were stirred in acetone (10 ml) at room temperature for 24 h. Solvent was removed under reduced pressure and the residue purified by flash column chromatography (SiO₂; EtOAc/petroleum spirit (40 – 60 °C); 1:1) to yield the product as a colourless oil (0.28 g, 60%).

R_f = 0.53 (SiO₂; EtOAc/petroleum spirit (40 – 60 °C); 1:1); **¹H NMR** (500 MHz,

CDCl₃) 7.51 (2H, m, *o*-Ar), 7.47 (2H, m, *m*-Ar), 5.19 (1H, m, CH), 3.00 (1H, br s, OH), 2.78 (2H, m, CH₂), 2.18 (3H, s, CH₃); ¹³C NMR (125 MHz, CDCl₃) 208.8 (C=O), 146.8 (C-CF₃), 130.2 (C-CHOH), 129.1, 127.4 (Ar-C-H), 120.9 (CF₃), 69.2 (CH-OH), 51.8 (CH₂), 30.8 (CH₃); ν_{\max} (neat/cm⁻¹) 3418.8 (br, O-H), 2923.7, 2339.0 (m, C-H), 1712.4 (s, C=O), 1618.5 (m, Ar-CF₃), 1161.3 (s, C-O), 1109.9, 1065.6 (C-F); *m/z* (Positive CI-Methane) 233 ([M + H]⁺, 100%), 232 (62), 215 (36), 213 (60), 145 (17), 131 (20), 103 (51); HRMS found [M + H]⁺, 233.07738; C₁₁H₁₂F₃O₂ requires 233.07894.

3.27 (R)-4-Hydroxy-4-(4-benzenesulfonyl-phenyl)butan-2-one (144)

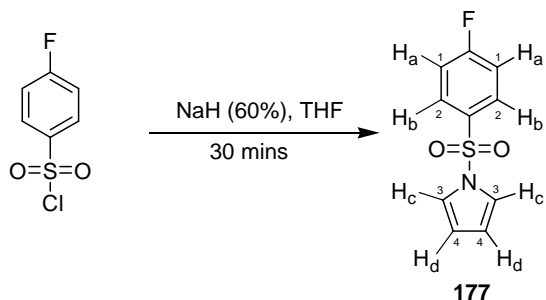


A suspension of 4-benzenesulfonyl-benzaldehyde (0.49 g, 2.0 mmol) and L-proline (0.07 g, 30 mol%) were stirred in acetone (10 ml) at room temperature for 24 h. Solvent was removed under reduced pressure and the residue purified by flash column chromatography (SiO₂; EtOAc/petroleum spirit (40 – 60 °C); 3:2) to yield the product as a white solid (0.33 g, 55%).

m.p. 81 – 83 °C; **R_f** = 0.21 (SiO₂; EtOAc/petroleum spirit (40 – 60 °C); 1:1); ¹H NMR (300 MHz, CDCl₃) 7.87 – 7.92 (4H, m, H_b, H_c), 7.55 – 7.46 (5H, m, H_a, H_d, H_e), 5.16 (1H, m, CH), 3.57 (1H, m, OH), 2.79 (2H, m, CH₂), 2.17 (3H, s, CH₃); ¹³C NMR (75 MHz, CDCl₃) 208.6 (C=O), 148.5 (C₁), 141.5 (C₅), 140.6 (C₄), 133.2 (C₈), 129.3 (C₇), 128.0 (C₂), 127.6 (C₃), 126.5 (C₆), 69.1 (CH), 51.6 (CH₂), 30.7 (CH₃); ν_{\max} (neat/cm⁻¹) 3535.8 (br, OH), 2900.0, 2327.5 (w, C-H), 1706.2 (s, C=O), 1599.2 (C=C), 1445.3, 1362.2, 1303.8 (m, C-H bend), 1153.1, 1104.9 (s, S=O); *m/z* (Positive ESI) 327 ([M + Na]⁺, 52%), 322 (98), 288 (56), 286 (100),

245 (22), 195 (20); **HRMS** found $[M + Na]^+$, 327.06760; $C_{16}H_{16}O_4SNa$ requires 327.06670.

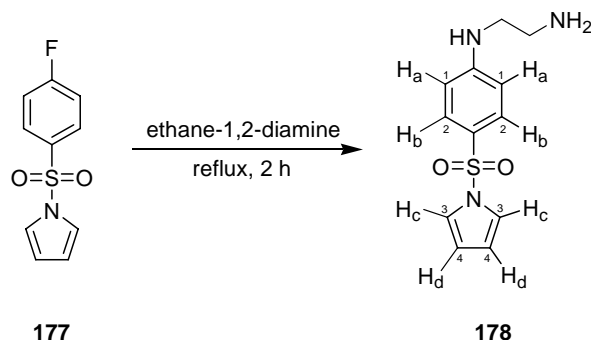
3.28 1-(4-Fluoro-benzenesulfonyl)-1H-pyrrole (177)



Pyrrole (1.00 g, 1.03 ml, 14.9 mmol) was added to a stirred solution of sodium hydride (0.74 g of a 60% dispersion in mineral oil, 18.6 mmol) in anhydrous tetrahydrofuran (THF) (50 ml) and stirred for 10 mins at room temperature, under an atmosphere of N_2 . 4-fluorobenzenesulfonyl chloride (2.90 g, 14.9 mmol) was then added and the reaction mixture stirred for 30 mins. Solvent was removed under reduced pressure and the crude product purified by recrystallisation from hexane to yield the product as a violet solid (2.27 g, 68%).

m.p. 104 – 105 °C (hexane); **1H NMR** (300 MHz, $CDCl_3$) 7.91 – 7.84 (2H, m, H_a), 7.21 – 7.14 (4H, m, H_b and H_c), 6.32 – 6.30 (2H, m, H_d); **^{13}C NMR** (75 MHz, $CDCl_3$) 165.7 (d, $^1J = 255.7$ Hz, C-F), 135.1 (C- SO_2), 129.7 (d, $^3J = 9.7$ Hz, C_2), 120.8 (C_3), 116.7 (d, $^2J = 22.8$ Hz, C_1), 114.0 (C_4); ν_{max} (neat/ cm^{-1}) 3137.4, 3108.4 (w, Ar-H), 2924.1 (s, N-C), 1588.4 (s, C=C), 1494.0, 1456.3, 1367.1 (s, C-H bend), 1172.8, 1154.5 (s, S=O), 538.1 (m, C-F); **m/z** (Positive CI-Methane) 226 ($[M + H]^+$, 100%), 175 (27), 129 (48); **HRMS** found $[M + H]^+$, 226.03345; $C_{10}H_9FNO_2S$ requires 226.03380.

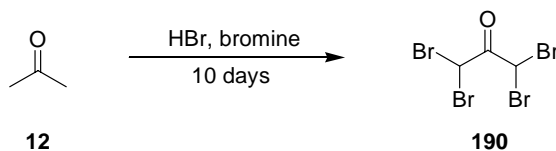
3.29 4-(1*H*-Pyrrol-1-ylsulfonyl)-*N*-(2-aminoethyl)benzenamine (178)



1-(4-Fluoro-benzenesulfonyl)-1*H*-pyrrole (0.50 g, 2.2 mmol) was heated under reflux in ethane-1,2-diamine (8 ml) for 2 h. Excess ethane-1,2-diamine was removed under reduced pressure to leave the product as an off-white solid (0.53 g, 89%).

m.p. 106 – 108 °C; **¹H NMR** (300 MHz, CDCl₃) 7.64 (2H, d, ³*J* = 8.9 Hz, H_a), 7.13 (2H, m, H_c), 6.55 (2H, d, ³*J* = 8.9 Hz, H_b), 6.24 (2H, m, H_d), 4.83 (1H, s, NH), 3.17 (2H, m, NHCH₂), 2.96 (2H, m, CH₂NH₂), 1.27 (2H, br s, NH₂); **¹³C NMR** (125 MHz, DMSO) 153.6 (C-NH), 129.0 (C-SO₂), 121.8 (C₁), 120.4 (C₃), 112.8 (C₂), 111.2 (C₄), 45.6 (NHCH₂), 40.4 (CH₂NH₂); **ν_{max}** (neat/cm⁻¹) 3371.7, 3314.9 (m, N-H), 3137.3, 2868.1 (w, Ar-H), 2842.0 (m, N-C), 1589.2, 1530.1 (s, C=C), 1451.6, 1344.3 (s, C-H bend), 1181.4, 1148.6 (s, S=O); ***m/z*** (Positive CI-Methane) 266 ([M + H]⁺, 100%), 199 (77); **HRMS** found [M + H]⁺, 266.09599; C₁₂H₁₆N₃O₂S requires 266.09632.

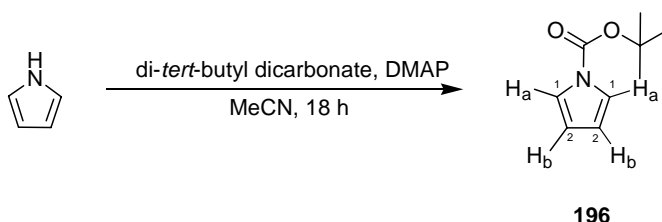
3.30 1,1,3,3-Tetrabromopropan-2-one (190)¹⁵⁷



HBr (5.10 ml, 445 mmol, 48% aqueous solution) was added at 0 °C to acetone (11.00 ml, 150 mmol), followed by dropwise addition of bromine (31.00 ml, 590.0 mmol) over 3 h and the resulting reaction mixture was stirred for 10 days at room temperature with exclusion of light. The reaction mixture was shock-frozen with liquid N₂ and left at room temperature for 2 h. The aqueous layer was then decanted and the residue was filtered. The solid cake was washed with ice-cold petroleum spirit (40 – 60 °C) (3 × 50 ml) to leave a colourless filtrate. The resultant solid was dried to afford the product as a colourless solid (7.40 g, 44%).

m.p. 33 – 36 °C [lit. 38 °C]; ¹⁵⁷**¹H NMR** (300 MHz, CDCl₃) 6.37 (2H, s, CH); ¹³**C NMR** (75 MHz, CDCl₃) 183.4 (C=O), 33.9 (CH); **ν_{max}** (neat/cm⁻¹) 1745.5 (s, C=O), 1267.1, 1141.8, 1085.8 (m, C-H), 570.9 (m, C-Br); **m/z** (EI) 373 ([M]⁺, 6%), 201 (33), 173 (26), 149 (7), 120 (21), 97 (38), 83 (48), 71 (53), 57 (100); **HRMS** found [M]⁺, 369.68391; C₃H₂Br₄O requires 369.68225.

3.31 Pyrrole-1-carboxylic acid *tert*-butyl ester (196)¹⁸⁷

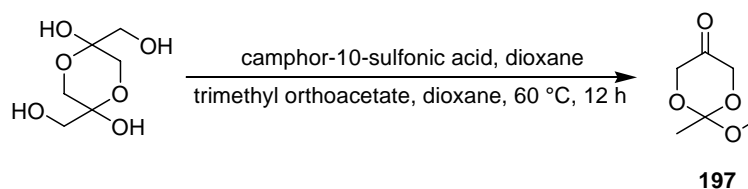


Di-*tert*-butyl dicarbonate (15.71 g, 72.0 mmol) and DMAP (0.88 g, 7.2 mmol) were added to a solution of pyrrole (4.83 g, 5.00 ml, 72.0 mmol) in acetonitrile (MeCN) (50 ml) and stirred for 18 h. Solvent was removed under reduced pressure and the dark residue purified by flash column chromatography (SiO₂; EtOAc/petroleum spirit (40 – 60 °C); 1:19) to yield the product as a light brown oil (9.69 g, 80%).

R_f = 0.74 (SiO₂; EtOAc/petroleum spirit (40 – 60 °C); 1:19); ¹**H NMR** (300 MHz, CDCl₃) 7.25 (2H, d, ³*J* = 4.7 Hz, H_a), 6.21 (2H, d, ³*J* = 4.7 Hz, H_b), 1.60 (9H, s,

CH₃); ¹³C NMR (75 MHz, CDCl₃) 148.9 (C=O), 119.9 (C-H_a), 111.8 (C-H_b), 83.3 (C(CH₃)₃), 27.9 (CH₃); ν_{\max} (neat/cm⁻¹) 3458.6, 3151.6 (w, N-H), 2980.4, 2935.7 (s, C-H), 1740.6 (s, C=O), 1472.2, 1340.0 (m, C-H bend), 1315.3, 1155.3 (s, C-O); *m/z* (EI) 167 ([M]⁺, 10%), 111 (22), 94 (21), 67 (46), 57 (100); HRMS found [M + H]⁺, 167.09406; C₉H₁₄NO₂ requires 167.09462.

3.32 2-Methoxy-2-methyl-[1,3]dioxan-5-one (197)¹⁵⁹



2,5-Bis-hydroxymethyl-[1,4]dioxane-2,5-diol (9.00g, 50.0 mmol) and camphor-10-sulfonic acid (CSA) (0.12 g, 1 mol%) in dioxane (400 ml) were heated at 60 °C for 20 mins. Trimethyl orthoacetate (124.00 g, 135.00 ml, 1058.0 mmol) was then added and the reaction mixture stirred for a further 12 h at this temperature. The reaction mixture was concentrated to ~40 ml and the product was obtained by distillation (54 °C at 3 mbar) as a colourless oil (8.28 g, 57%).

¹H NMR (300 MHz, CDCl₃) 4.19 (2H, d, ⁴J = 18.5 Hz, CH₂), 4.04 (2H, d, ⁴J = 18.5 Hz, CH₂), 3.25 (3H, s, OCH₃), 1.43 (3H, s, CCH₃); ¹³C NMR (75 MHz, CDCl₃) 204.3 (C=O), 112.2 (CCH₃), 67.3 (CH₂), 51.1 (OCH₃), 20.3 (CCH₃); ν_{\max} (neat/cm⁻¹) 2950.7, 2839.5 (m, C-H), 1740.0 (s, C=O), 1426.6, 1387.3, 1351.2 (m, C-H bend), 1246.3, 1150.3, 1104.4 (s, C-O); *m/z* (Positive CI-Methane) 147 ([M + H]⁺, 68%), 133 (28), 115 (100), 101 (24); HRMS found [M + H]⁺, 147.06538; C₆H₁₁O₄ requires 147.06573.

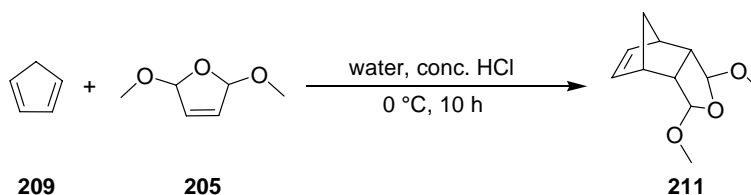
3.33 2-Triisopropylsilyloxypropenal (198)¹⁵⁸



2-Methoxy-2-methyl-[1,3]dioxan-5-one (0.87 g, 5.9 mmol) and triethylamine (0.90 g, 1.22 ml, 8.9 mmol) were stirred in benzene (10 ml) for 15 mins. Triisopropylsilyloxytriflate (TIPSOTf) (2.00 g, 1.75 ml, 6.5 mmol) was added over 5 mins and the reaction mixture heated at 50 °C for 12 h. Distilled water (25 ml) was added and the product extracted with Et₂O (3 × 25 ml). The combined organic layers were washed with brine (50 ml), dried (MgSO₄) and filtered. Solvent was removed under reduced pressure to give a brown residue. Purification by flash column chromatography (SiO₂; EtOAc/petroleum spirit (40 – 60 °C); 1:20) yielded the product as a colourless oil (0.47 g, 35%).

R_f = 0.38 (SiO₂; EtOAc/petroleum spirit (40 – 60 °C); 1:20); **¹H NMR** (300 MHz, CDCl₃) 9.33 (1H, s, CHO), 5.51 (1H, d, ²J = 1.67 Hz, CH=CH), 5.24 (1H, d, ²J = 1.67 Hz, CH=CH), 1.29 – 1.21 (3H, m, CH), 1.13 – 1.07 (18H, m, CH₃); **¹³C NMR** (75 MHz, CDCl₃) 189.4 (C=O), 156.3 (H₂C=C), 128.4 (H₂C=C), 17.7 (CH), 12.3 (CH₃); **ν_{max}** (neat/cm⁻¹) 2942.8, 2866.5 (s, C-H), 1713.1 (s, C=O), 1463.6 (s, C=C), 1383.2, 1367.2 (C-H bend), 1247.2 (C-O), 1052.3 (s, Si-C), 676.3 (s, Si-O); **m/z** (Positive CI-Methane) 229 ([M + H]⁺, 10%), 185 (80), 173 (26), 157 (99), 145 (22), 131 (100), 115 (23), 103 (20), 87 (9); **HRMS** found [M + H]⁺, 229.16275; C₁₂H₂₅O₂Si requires 229.16237.

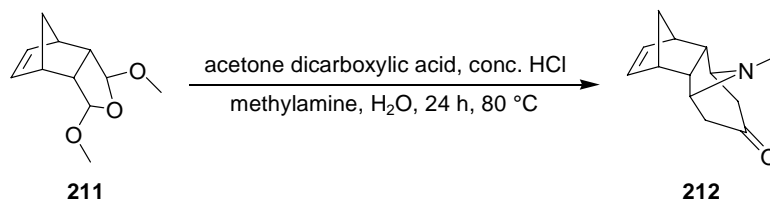
3.34 7-Oxabicyclo[2.2.1]heptene-endo-2,3-dicarboxylic anhydride (211)¹⁶³



2,5-Dimethoxyfuran (20.00 g, 153.7 mmol) was dissolved in distilled water (40 ml) and cooled to 0 °C in an ice bath for 10 mins. Freshly distilled cyclopentadiene (20.00 g, 302.6 mmol) and conc. HCl (0.8 ml) were added to the reaction mixture and stirred at this temperature for 10 h, after which it was allowed to warm to room temperature and stirred for a further 12 h. The organic layer was separated from the aqueous layer and the product was purified by distillation (117 – 120 °C at 12 mbar) to give a colourless crystalline solid (28.70 g, 95%).

m.p. 49 – 51 °C [lit. 52 °C]; ¹⁶³ **¹H NMR** (300 MHz, CDCl₃) 6.02 (2H, s, CH=CH), 4.41 (2H, s, CH-OCH₃), 3.24 (6H, s, CH₃), 2.83 (2H, m, CHCH=CH), 2.69 (2H, m, CHCH-OCH₃), 1.32 (1H, d, ²J = 8.2 Hz, CH₂), 1.20 (1H, d, ²J = 8.2 Hz, CH₂); **¹³C NMR** (75 MHz, CDCl₃) 135.3 (CH=CH), 108.8 (CH-OCH₃), 54.9 (OCH₃), 53.5 (CH₂), 51.4 (CHCH-OCH₃), 45.4 (CHCH=CH); **ν_{max}** (neat/cm⁻¹) 2967.9, 2890.8 (m, C-H), 1736.2, 1442.9 (m, C=C), 1465.3, 1376.9 (m, C-H bend), 1189.6, 1087.6 (s, C-O); **m/z** (Positive FAB) 219 ([M + Na]⁺, 100%), 203 (28), 191 (21), 181 (62), 173 (34), 165 (82); **HRMS** found [M + Na]⁺, 219.09908; C₁₁H₁₆O₃Na requires 219.09971.

3.35 *N*-Methyl-2,6-endimino-8,11-endomethylen-bicyclo[5.4.0]undecen-(9)-on-(4) (212)¹⁶³

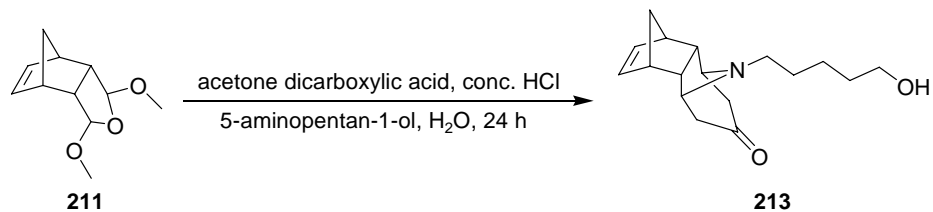


7-Oxabicyclo[2.2.1]heptene-endo-2,3-dicarboxylic anhydride (1.96 g, 10.0 mmol) and conc. HCl (0.44 ml) were dissolved in deoxygenated water (10 ml) and stirred under an atmosphere of N₂ for 20 mins. Methylamine hydrochloride (1.00 g, 14.8

mmol) in deoxygenated water (7 ml) and acetone dicarboxylic acid (1.66 g, 11.4 mmol) in deoxygenated water (17 ml) were then added along with disodium hydrogen phosphate (0.70 g). The reaction mixture began to effervesce immediately and the pH of the solution increased from 2.5 to 4.5 over the course of 24 h at room temperature. More conc. HCl (0.66 ml) was then added and the reaction mixture was heated at 80 °C for 1 h to complete decarboxylation. The reaction mixture was cooled to room temperature, made basic using 2 M NaOH solution and extracted with DCM (3 × 50 ml). The combined organic layers were dried (Na₂SO₄) and the solvent removed under reduced pressure. The crude product was purified by flash column chromatography (SiO₂; Et₂O/petroleum spirit (40 – 60 °C); 1:8) to yield the product as a colourless crystalline solid (0.82 g, 40%).

m.p. 86 – 89 °C [lit. 68 – 70 °C];¹⁶³ **R_f** = 0.25 (SiO₂; Et₂O/petroleum spirit (40 – 60 °C); 1:8); **¹H NMR** (500 MHz, CDCl₃) 6.05 (2H, s, CH=CH), 3.05, 2.82 (4H, m, CH₂C=O), 2.60 (2H, m, CHNCH₃), 2.32 (3H, s, CH₃), 2.28 (2H, m, CH=CHCH), 2.05, 2.02 (2H, m, CHCHNCH₃), 1.22, 1.11 (2H, m, CH=CHCHCH₂); **¹³C NMR** (125 MHz, CDCl₃) 210.7 (C=O), 133.8 (CH=CH), 60.8 (CHNCH₃), 51.2 (CHC=O), 50.2 (CH=CHCHCH₂), 46.5 (CHCHNCH₃), 43.9 (CH=CHCH), 32.2 (CH₃); **ν_{max}** (neat/cm⁻¹) 2956.4, 2928.5 (s, C-H), 1710.3 (s, C=O), 1571.2 (s, C=C), 1455.5, 1411.6, 1334.2 (s, C-H bend), 1161.5, 1132.9 (m, C-N); **m/z** (Positive FAB) 204 ([M + H]⁺, 100%), 154 (63); **HRMS** found [M + H]⁺, 204.13833; C₁₃H₁₈NO requires 204.13883.

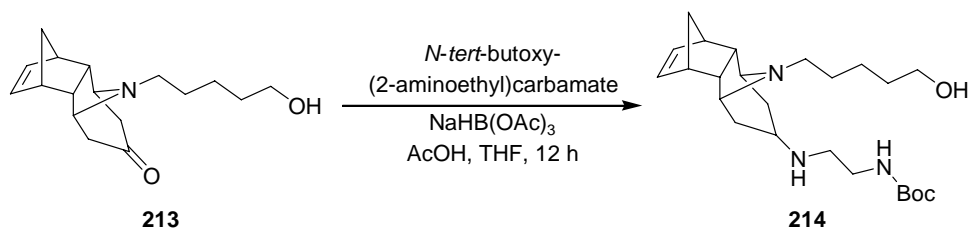
3.36 *N*-(5-Aminopentan-1-ol)-2,6-endimino-8,11-endomethylen-bicyclo[5.4.0]undecen-(9)-on-(4) (213)



7-Oxabicyclo[2.2.1]heptene-endo-2,3-dicarboxylic anhydride (13.18 g, 67.2 mmol) and conc. HCl (8 ml) were dissolved in deoxygenated water (50 ml) and stirred under an atmosphere of N₂ for 20 mins. 5-Aminopentan-1-ol (9.01 g, 87.4 mmol) and acetone dicarboxylic acid (14.93 g, 73.9 mmol) were then added. The reaction mixture began to effervesce immediately and the pH of the solution increased from 2.5 to 4.8 over the course of 24 h at room temperature. More conc. HCl (10 ml) was then added and the reaction mixture was stirred at room temperature for a further 12 h to complete decarboxylation. The reaction mixture was made basic using 2 M NaOH solution and extracted with DCM (3 × 50 ml). The combined organic layers were dried (Na₂SO₄) and the solvent removed under reduced pressure. The crude product was purified by flash column chromatography (SiO₂; Et₂O/petroleum spirit (40 – 60 °C); 1:1) to yield the product as an orange oil (11.10 g, 60%).

R_f = 0.38 (SiO₂; Et₂O/petroleum spirit (40 – 60 °C); 1:1); **¹H NMR** (300 MHz, CDCl₃) 5.91 (2H, s, CH=CH), 3.56 (2H, m, CH₂OH), 3.12 (2H, m, CH-N), 2.77 (2H, m, N-CH₂), 2.56 – 2.50 (4H, m, CH₂C=O), 2.22 (2H, m, CH=CHCH), 1.98 (2H, m, CH=CHCHCH), 1.52 (1H, br s, OH), 1.51 – 1.32 (6H, m, NCH₂(CH₂)₃CH₂OH), 1.17 – 1.06 (2H, m, CH=CHCHCH₂); **¹³C NMR** (75 MHz, CDCl₃) 211.3 (C=O), 134.0 (CH=CH), 62.7 (CHOH), 58.9 (CH-N), 51.4 (N-CH₂), 49.5 (CH₂C=O), 46.5 (CH=CHCHCH₂), 45.5 (CH=CHCHCH), 44.1 (CH=CHCH), 32.4, 28.0, 23.6 (NCH₂(CH₂)₃CH); **ν_{max}** (neat/cm⁻¹) 3417.1 (br, O-H), 2929.7 (s, C-H), 2861.3 (s, N-C), 1705.1 (s, C=O), 1411.8, 1351.7, 1334.6 (m, C-H bend), 1127.5, (m, C-O); **m/z** (Positive ESI) 276 ([M + H]⁺, 96%), 210 (100); **HRMS** found [M + H]⁺, 276.19730; C₁₇H₂₆NO₂ requires 276.19640.

3.37 Reductive Amination Product of 213 (214)

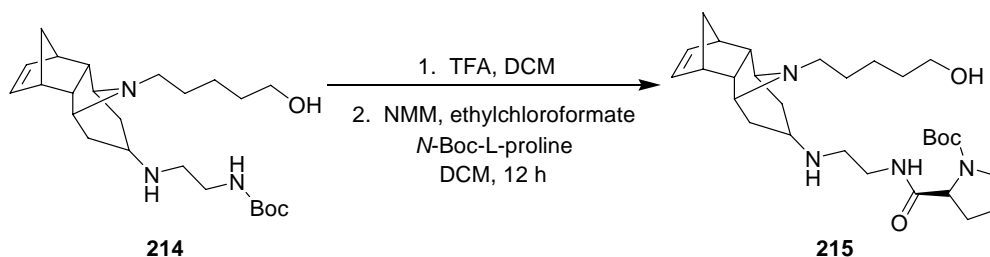


N-(5-Aminopentan-1-ol)-2,6-endimino-8,11-endomethylen-bicyclo[5.4.0]undecen-(9)-on-(4) (2.76 g, 10.0 mmol), *N*-tert-butoxy(2-aminoethyl)carbamate (1.88 g, 10.0 mmol) and acetic acid (AcOH) were dissolved in THF (65 ml) at room temperature under an atmosphere of N₂. Sodium triacetoxy borohydride (4.24 g, 20.0 mmol) was then added and stirred for 12 h. The reaction mixture was made basic using 2 M NaOH solution and extracted with DCM (3 × 60 ml). The combined organic layers were dried (Na₂SO₄) and the solvent removed under reduced pressure. The crude product was purified by flash column chromatography (SiO₂; MeOH/EtOAc); 2:8, 1% triethylamine) to yield the product as an orange oil (2.66 g, 63%).

R_f = 0.17 (SiO₂; MeOH/EtOAc); 2:8 with 1% triethylamine); **¹H NMR** (500 MHz, CDCl₃) 5.93 (2H, s, CH=CH), 5.33 (1H, br s, NHBoc), 4.40 (1H, m, CH-NH), 3.58 (2H, m, CH₂OH), 3.15 (2H, m, CH-N), 2.87 (2H, m, CH₂NHBoc), 2.83 (2H, m, CH₂CH₂NHBoc), 2.77 (2H, m, N-CH₂), 2.46 – 2.57 (4H, m, CH₂CH), 2.24 (2H, m, CH=CHCH), 2.10 (2H, m, CH=CHCHCH), 1.52 (1H, br s, OH), 1.58 – 1.22 (6H, m, NCH₂(CH₂)₃CH₂OH), 1.37 (9H, s, ^tBu), 1.19 – 1.08 (2H, m, CH=CHCHCH₂); **¹³C NMR** (125 MHz, CDCl₃) 156.3 (C=O), 134.1 (CH=CH), 75.8 (C(CH₃)₃), 62.5 (CHOH), 61.0 (CH-NH) 59.0 (CH-N), 50.9 (N-CH₂), 49.6 (CH₂CH₂NHBoc), 47.5 (CH₂NHBoc), 47.2 CH₂CH), 46.6 (CH=CHCHCH₂), 45.1 (CH=CHCHCH), 40.3 (CH=CHCH), 32.1, 28.4, 23.3 (NCH₂(CH₂)₃CH), 28.5 (C(CH₃)₃); **ν_{max}** (neat/cm⁻¹) 3302.2 (br, O-H), 2935.6 (s, C-H), 1694.7 (s, C=O), 1505.3, 1453.9 (m, N-H bend), 1391.4, 1365.8 (m, C-H bend), 1275.4 (m, C-N), 1250.2, 1168.6 (s, C-O); **m/z** (EI) 419 ([M]⁺, 9%), 289 (59), 260 (23), 234 (20), 220 (14), 194 (66), 168 (41), 154 (77), 131 (100), 113 (34), 94 (17), 80 (33);

HRMS found $[M]^+$, 419.31245; $C_{24}H_{41}N_3O_3$ requires 419.31424.

3.38 Tropane Alkaloid Derivative (215)

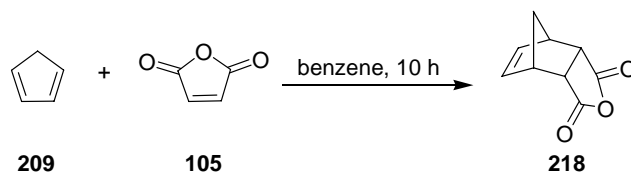


TFA (10 ml) was added to a cooled solution of **214** (4.80 g, 11.5 mmol) in DCM (24 ml) and stirred for 2 h. DCM was removed under reduced pressure and the excess TFA by co-evaporation with toluene. The product was used in the next step without further purification.

NMM (1.09 g, 1.18 ml, 10.8 mmol) was added to a stirred solution of *N*-Boc-L-proline (2.31 g, 10.8 mmol) in DCM (40 ml) at $-15\text{ }^{\circ}\text{C}$. Ethyl chloroformate (1.17 g, 1.03 ml, 10.8 mmol) in DCM (10 ml) was added dropwise and stirred at this temperature for 20 mins. A further portion of NMM (1.09 g, 1.18 ml, 10.8 mmol) was added, followed by portionwise addition of the TFA salt of **214** prepared earlier. The reaction mixture was allowed to warm to room temperature and left to stir for a further 12 h. Distilled water (50 ml) was added and the DCM layer separated. The aqueous phase was washed with DCM ($3 \times 40\text{ ml}$) and the combined organic layers washed with 0.5 M HCl (100 ml), sat. NaHCO_3 (100 ml) and brine (100 ml), dried (MgSO_4) and filtered. Solvent was removed under reduced pressure and the crude product was purified by flash column chromatography (SiO_2 ; MeOH/EtOAc); 2:8, 1% triethylamine) to yield the product as an orange oil (1.44 g, 26%).

$R_f = 0.11$ (SiO₂; MeOH/EtOAc); 2:8 with 1% triethylamine); $[\alpha]_D^{22} = -29.2$ (*c* 1, CHCl₃); ¹H NMR (500 MHz, CDCl₃) 5.96 (2H, s, CH=CH), 5.20 (1H, br s, NHC=O), 4.38 (1H, m, CH-NH), 4.20 (1H, br s, CH-NH), 3.99 (1H, m, CHNBoc), 3.48 (2H, m, CH₂OH), 3.35 (2H, CH₂NBoc), 3.21 (2H, m, CHNC(CH₂)₅OH), 2.86 (2H, m, CH₂NHC=O), 2.85 (2H, m, CH₂CH₂NHC=O), 2.78 (2H, m, NCH₂(CH₂)₄OH), 2.52 (4H, m, CH₂CHNH), 2.04 (2H, m, CH=CHCH), 1.91 (2H, m, CH=CHCHCH), 1.86 – 1.42 (10H, m, NCH₂(CH₂)₃CH₂OH, CH₂CH₂CHNBoc), 1.64 (1H, br s, OH), 1.30 (9H, s, ^tBu), 1.13 – 1.10 (2H, m, CH=CHCHCH₂); ¹³C NMR (125 MHz, CDCl₃) 178.5 (C=O, carbamate), 154.8 (C=O, amide), 137.0 (CH=CH), 75.6 (C(CH₃)₃), 61.5 (CHOH), 61.3 (CHNBoc), 61.0 (CH-NH), 60.3 (CHNC(CH₂)₅OH), 50.8 (NCH₂(CH₂)₄OH), 50.0 (CH₂NHC=O), 47.1 (CH₂CH₂NHC=O), 46.8 (CH₂CHNH), 46.3 (CH=CHCHCH₂), 44.9 (CH=CHCHCH), 44.3 (CH₂NBoc), 40.1 (CH=CHCH), 31.4, 28.4, 23.3 (NCH₂(CH₂)₃CH), 28.5 (C(CH₃)₃), 23.6 (CH₂CH₂CHNBoc), 14.2 (CH₂CH₂CHNBoc); ν_{\max} (neat/cm⁻¹) 3314.3 (br, O-H), 2977.1 (w, C-H), 2877.2 (w, N-C), 1678.3, 1594.3 (s, C=O), 1477.3, 1404.0 (s, N-H bend), 1366.4 (m, C-H bend), 1248.4 (m, C-N), 1163.2 (m, C-O); *m/z* (Positive Cl-Methane) 517 ([M + H]⁺, 100%), 289 (10), 260 (12), 160 (12); HRMS found [M + H]⁺, 517.37649; C₂₉H₄₉N₄O₄ requires 517.37538.

3.39 (1R, 2S, 6R, 7R)-4-Oxa-tricyclo[5.2.1.0^{2,6}]dec-8-ene-3,5-dione (218)¹⁸⁸

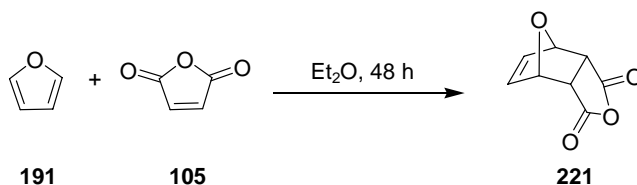


Maleic anhydride (80.00 g, 816.0 mmol) was dissolved in benzene (350 ml) and cooled to 0 °C. Freshly distilled cyclopentadiene (59.00 g, 900.0 mmol) was then added and the reaction mixture was allowed to warm to room temperature and stirred for 10 h. The precipitate thus formed was collected via filtration to give

the product as a colourless crystalline solid (130.90 g, 98%).

m.p. 162 – 164 °C [lit. 165 – 166 °C];¹⁸⁸ **¹H NMR** (300 MHz, CDCl₃) 6.30 (2H, s, CH=CH), 3.57 (2H, m, CHC=O), 3.51 (2H, m, CHCH=CH), 1.77. 1.57 (2H, d, ²J = 9.0 Hz, CH₂); **¹³C NMR** (125 MHz, DMSO) 172.4 (C=O), 135.5 (CH=CH), 52.4 (CH₂), 47.1 (CHCH=CH), 45.2 (CHC=O); **ν_{max}** (neat/cm⁻¹) 2981.4 (w, C=C), 1764.3 (s, C=O), 1333.3, 1228.6, 1087.8 (m, C-H bends); **m/z** (EI) 164 ([M]⁺, 36%), 150 (11), 137 (12), 136 (14), 131 (20), 119 (100), 113 (56), 99 (21); **HRMS** found [M]⁺, 164.04657; C₉H₈O₃ requires 164.04680.

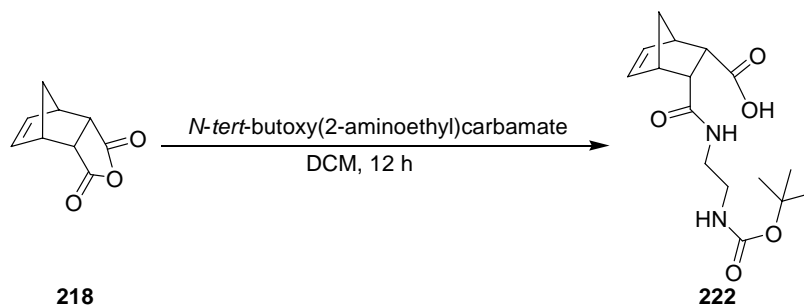
3.40 7-Oxabicyclo[2.2.1]heptene-endo-2,3-dicarboxylic anhydride (221)¹⁸⁹



Furan (9.38 g, 10.00 ml, 138.0 mmol) and maleic anhydride (2.50 g, 25.5 mmol) were stirred in Et₂O (5 ml) at room temperature for 48 h. The precipitate thus formed was collected via filtration to give the product as a colourless solid (3.16 g, 75%).

m.p. 122 – 125 °C [lit. 122 °C];¹⁸⁹ **¹H NMR** (300 MHz, CDCl₃) 6.57 (2H, s, CH=CH), 5.45 (2H, s, CH-O), 3.18 (2H, s, CHC=O); **¹³C NMR** (75 MHz, CDCl₃) 170.0 (C=O), 137.0 (CH=CH), 82.2 (CH-O), 48.7 (CHC=O); **ν_{max}** (neat/cm⁻¹) 3057.9, 2991.9 (w, C=C), 1781.6 (s, C=O), 1634.4 (m, C=C bend), 1431.6, 1309.9 (m, C-H bend), 1230.4, 1211.8 (s, C-O); **m/z** (Positive CI-Methane) 167 ([M + H]⁺, 46%), 139 (25), 127 (57), 113 (97), 99 (100); **HRMS** found [M + H]⁺, 167.03445; C₈H₇O₄ requires 167.03443.

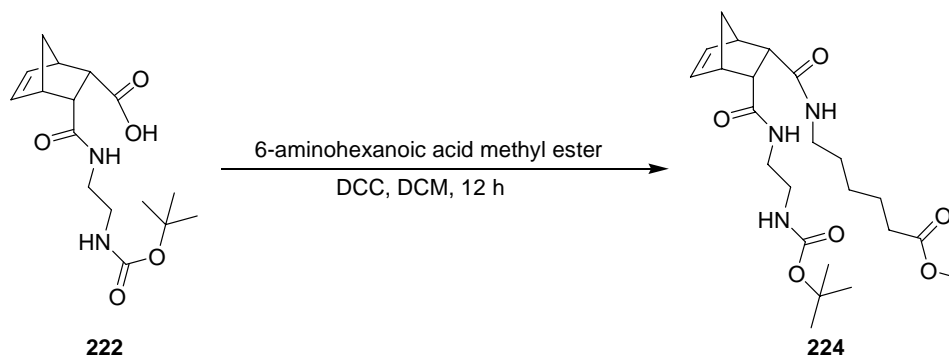
3.41 3-(2-*tert*-Butoxycarbonylamino-ethylcarbamoyl)bicyclo[2.2.1]hept-5-ene-2-carboxylic acid (222)



(1*R*, 2*S*, 6*R*, 7*R*)-4-Oxa-tricyclo[5.2.1.0^{2,6}]dec-8-ene-3,5-dione (0.82 g, 5.0 mmol) was added to *N-tert*-butoxy(2-aminoethyl)carbamate (0.80 g, 5.0 mmol) in anhydrous DCM (20 ml). The reaction mixture was stirred at room temperature for 12 h during which time a colourless precipitate was formed and was collected *via* filtration to give the product as a colourless solid (1.41 g, 87%).

m.p. 145 – 147 °C; **¹H NMR** (300 MHz, DMSO) 11.53 (1H, br s, COOH), 7.72 (1H, br s, CHC=ONH), 6.68 (1H, br s, NHBoc), 6.13 (1H, m, CH=CHCHCHCOOH), 5.95 (1H, m, CH=CHCHCHCOOH), 3.08 (2H, m, CH₂CH₂NHBoc), 2.99 (2H, m, CH₂NHBoc), 2.97 – 2.92 (4H, m, CH=CHCHCHC=O), 1.36 (9H, s, ^tBu), 1.24 (2H, m, CH=CHCHCH₂); **¹³C NMR** (75 MHz, DMSO) 173.5 (C=O, acid), 171.2 (C=O, amide), 155.5 (C=O, carbamate), 134.7 (HC=CHCHCHCOOH), 133.8 (HC=CHCHCHCOOH), 77.6 (C(CH₃)₃), 48.4 (CH₂NHBoc), 48.2 (CH₂CH₂NHBoc), 48.0 (CH=CHCHCH₂), 46.6 (CH=CHCHCHC=O), 45.3 (CH=CHCHCHC=O), 28.2 (CH₃); **ν_{max}** (neat/cm⁻¹) 3414.5 (br, OH), 3369.9 (s, N-H), 2974.6, 2946.2 (m, C-H), 1713.6 (s, C=O, acid), 1703.1 (s, C=O, amide), 1629.5 (s, C=O, carbamate), 1555.7, 1504.5 (m, N-H bend), 1451.7 (m, C=C), 1389.0, 1320.9, 1278.7, 1238.7 (m, C-H bend), 1164.5 (w, C-O); ***m/z*** (Positive FAB) 347 ([M + Na]⁺, 81%), 269 (100), 225 (30), 203 (72), 181 (20); **HRMS** found [M + Na]⁺, 347.15859; C₁₆H₂₄N₂O₅Na requires 347.15829.

3.42 6-{[3-(2-*tert*-Butoxycarbonylamino-ethylcarbamoyl)bicyclo[2.2.1]hept-5-ene-2-carbonyl]amino}hexanoic acid methyl ester (224)

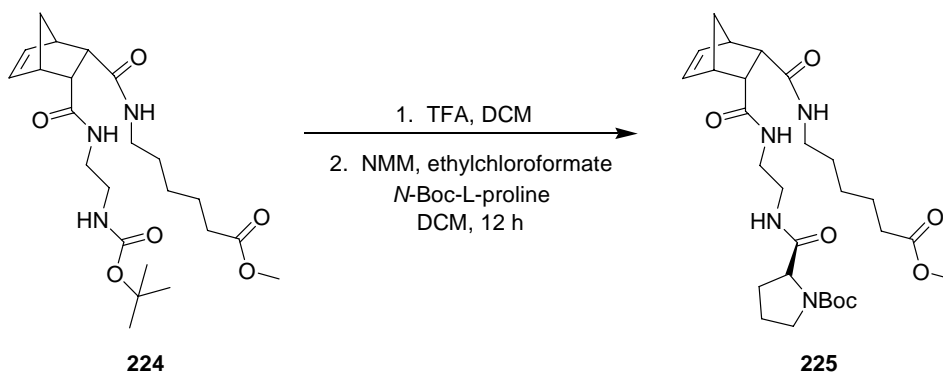


3-(2-*tert*-Butoxycarbonylamino-ethylcarbamoyl)bicyclo[2.2.1]hept-5-ene-2-carboxylic acid (3.56 g, 11.0 mmol) and 6-aminohexanoic acid methyl ester hydrochloride (2.00 g, 11.0 mmol) were suspended in anhydrous DCM (40 ml). To this DCC (2.70 g, 13.1 mmol) was added and stirred at room temperature for 12 h. The colourless by-product was removed by filtration and the organic phase was washed with 1 M HCl (50 ml), sat. NaHCO₃ (50 ml) and brine (50 ml). The combined organic layers were dried (MgSO₄) and filtered. Solvent was removed under reduced pressure to yield the crude product which was purified by flash column chromatography (SiO₂; MeOH/EtOAc; 1:49) to give product as a colourless solid (3.69 g, 74%).

m.p. 86 – 87 °C; **R_f** = 0.23 (SiO₂; MeOH/EtOAc; 1:49); **¹H NMR** (300 MHz, CDCl₃) 6.57 (1H, br s, NHCH₂CH₂NHBoc), 6.44 (1H, br s, NHCH₂CH₂NHBoc), 6.34 (1H, m, CH=CHCHCHC=ONH(CH₂)₂NH), 6.29 (1H, m, CH=CHCHCHC=ONH(CH₂)₂NH), 5.34 (1H, br s, NH(CH₂)₅COOMe), 3.61 (3H, s, CH₃), 3.21 – 3.07 (10H, m, NH(CH₂)₂NH, NHCH₂(CH₂)₄, CH=CHCHCHC=O), 2.23 (2H, t, ³J = 7.4 Hz, CH₂COOMe), 1.57 (2H, m, CH=CHCHCH₂), 1.42 – 1.21 (6H, CH₂(CH₂)₃CH₂), 1.39 (9H, s, ^tBu); **¹³C NMR** (75 MHz, CDCl₃) 174.0 (C=ONH(CH₂)₂NH), 173.4 (C=ONH(CH₂)₅), 172.8 (C=OOMe), 156.4 (C=OO^tBu), 135.6 (CH=CHCHCHC=ONH(CH₂)₂NH), 135.4

(CH=CHCHCHC=ONH(CH₂)₂NH), 79.2 (C(CH₃)₃), 51.9 (COOCH₃), 51.5 (NHCH₂CH₂NHBoc), 50.9 (NHCH₂CH₂NHBoc), 47.4 (NHCH₂(CH₂)₄), 47.1 (CH=CHCHCH₂), 40.2 (CH=CHCHCHC=ONH(CH₂)₂NH), 40.0 (CH=CHCHCHC=ONH(CH₂)₅), 39.2 (CH=CHCHCHC=ONH(CH₂)₂NH), 33.8 (CH=CHCHCHC=ONH(CH₂)₅), 30.9 (CH₂COOMe), 29.1, 26.4, 24.5 (NHCH₂(CH₂)₃CH₂COOMe), 28.4 (C(CH₃)₃); ν_{\max} (neat/cm⁻¹) 3302.4, 3067.2 (s, N-H), 2963.0, 2934.9, 2869.2 (m, C-H), 1739.4, 1691.3, 1656.2 (s, C=O), 1520.4 (s, C=C), 1468.3, 1437.1, 1364.8 (m, C-H bend), 1251.3, 1224.7 (m, C-N), 1161.4, 1114.1 (m, C-O); *m/z* (Positive FAB) 474 ([M + Na]⁺, 100%), 308 (23); **HRMS** found [M + Na]⁺, 474.25732; C₂₃H₃₇N₃O₆Na requires 474.25799.

3.43 (2S)-2-(2-{[3-(5-Methoxycarbonyl-pentylcarbamoyl)bicyclo[2.2.1]hept-5-ene-2-carbonyl]amino}ethylcarbamoyl)pyrrolidino-1-carboxylic acid *tert*-butyl ester (225)



TFA (2 ml) was added to a cooled solution of 6-{[3-(2-*tert*-butoxycarbonylamino-ethylcarbamoyl)bicyclo[2.2.1]hept-5-ene-2-carbonyl]amino}hexanoic acid methyl ester (2.00 g, 4.4 mmol) in DCM (10 ml) and stirred for 2 h. DCM was removed under reduced pressure and the excess TFA by co-evaporation with toluene. The product was used in the next step without further purification.

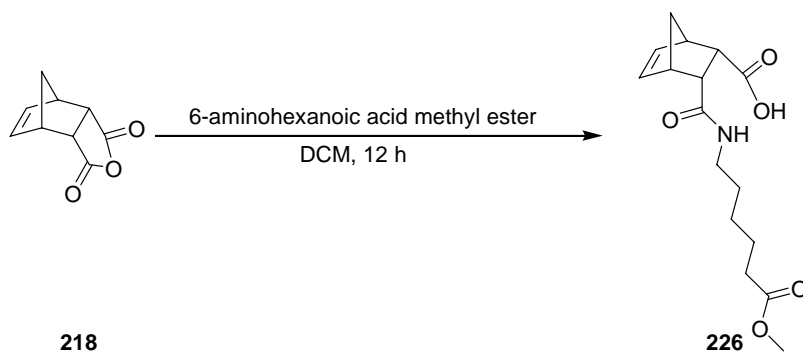
NMM (0.50 g, 0.54 ml, 4.9 mmol) was added to a stirred solution of *N*-Boc-L-

proline (1.05 g, 4.9 mmol) in DCM (20 ml) at $-15\text{ }^{\circ}\text{C}$. Ethyl chloroformate (0.53 g, 0.47 ml, 4.9 mmol) in DCM (5 ml) was added dropwise and stirred at this temperature for 20 mins. A further portion of NMM (0.50 g, 0.54 ml, 4.9 mmol) was added, followed by portionwise addition of the TFA salt of [2.2.1]hept-5-ene-2-carbonyl]-amino}hexanoic acid methyl ester prepared earlier. The reaction mixture was allowed to warm to room temperature and left to stir for a further 12 h. Distilled water (50 ml) was added and the DCM layer separated. The aqueous phase was extracted with DCM (3×40 ml) and the combined organic layers washed with 0.5 M HCl (20 ml), sat. NaHCO_3 (20 ml) and brine (20 ml), dried (MgSO_4) and filtered. Solvent was removed under reduced pressure and the crude product was purified by flash column chromatography (SiO_2 ; MeOH/EtOAc); 1:9) to yield the product as an orange oil (0.56 g, 23%).

$R_f = 0.52$ (SiO_2 ; MeOH/EtOAc; 1:4); $^1\text{H NMR}$ (500 MHz, CDCl_3) 7.09 (1H, br s, $\text{NHCH}_2\text{CH}_2\text{NHPro}$), 6.62 (1H, br s, $\text{NHCH}_2\text{CH}_2\text{NHPro}$), 6.34 (1H, m, $\text{CH}=\text{CHCHCHCHC}=\text{ONH}(\text{CH}_2)_2\text{NH}$), 6.28 (1H, m, $\text{CH}=\text{CHCHCHCHC}=\text{ONH}(\text{CH}_2)_2\text{NH}$), 6.12 (1H, br s, $\text{NH}(\text{CH}_2)_5\text{COOMe}$), 4.12 (1H, m, CH-NBoc), 3.44 (3H, s, COOCH_3), 3.32 (2H, m, $\text{NHCH}_2\text{CH}_2\text{Pro}$), 3.21 (2H, m, $\text{NHCH}_2\text{CH}_2\text{NHPro}$), 3.19 – 3.07 (8H, m, $\text{CH}=\text{CHCHCHC}=\text{O}$, $\text{CH}_2\text{-N}$, $\text{CH}_2(\text{CH}_2)_4$), 2.27 (2H, t, $^3J = 2.7$ Hz, CH_2COOMe), 2.11 – 1.89 (4H, m, $(\text{CH}_2)_2\text{CH-N}$), 1.57 (2H, m, $\text{CH}=\text{CHCHCH}_2$), 1.43 (9H, s, ^tBu), 1.28 – 1.26 (6H, $\text{CH}_2(\text{CH}_2)_3\text{CH}_2$); $^{13}\text{C NMR}$ (125 MHz, CDCl_3) 174.1 ($\text{C}=\text{ONH}(\text{CH}_2)_2\text{NHPro}$), 173.5 ($\text{C}=\text{ONH}(\text{CH}_2)_5$), 172.7 ($\text{C}=\text{OOMe}$), 156.3 ($\text{C}=\text{OO}^t\text{Bu}$), 135.5 ($\text{CH}=\text{CHCHCHC}=\text{ONH}(\text{CH}_2)_2\text{NHPro}$), 134.2 ($\text{CH}=\text{CHCHCHC}=\text{ONH}(\text{CH}_2)_2\text{NHPro}$), 80.2 ($\text{C}(\text{CH}_3)_3$), 60.6 (CH-N), 52.3 (COOCH_3), 51.8 ($\text{NHCH}_2\text{CH}_2\text{NHPro}$), 51.6 ($\text{NHCH}_2\text{CH}_2\text{NHPro}$), 50.1 ($\text{NHCH}_2(\text{CH}_2)_4$), 47.4 ($\text{CH}_2\text{-N}$), 47.0 ($\text{CH}=\text{CHCHCH}_2$), 46.9 ($\text{CH}=\text{CHCHCHC}=\text{ONH}(\text{CH}_2)_2\text{NH}$), 40.0 ($\text{CH}=\text{CHCHCHC}=\text{ONH}(\text{CH}_2)_5$), 39.9 ($\text{CH}=\text{CHCHCHC}=\text{ONH}(\text{CH}_2)_2\text{NH}$), 39.4 ($\text{CH}=\text{CHCHCHC}=\text{ONH}(\text{CH}_2)_5$), 39.3 (CH_2COOMe), 38.0 33.9, 29.6 ($\text{NHCH}_2(\text{CH}_2)_3\text{CH}_2\text{COOMe}$), 29.4 ($\text{CH}_2\text{CH-N}$), 28.5 ($\text{C}(\text{CH}_3)_3$), 24.5 ($\text{CH}_2\text{CH}_2\text{CH-N}$); ν_{max} (neat/ cm^{-1}) 3324.5, 3001.9 (m, N-H), 2973.5, 2870.4 (m, C-H), 1769.6, 1695.4, 1681.8, 1659.9 (s, C=O), 1542.0 (s,

C=C), 1478.1, 1394.6, 1316.1(m, C-H bend), 1233.2, 1280.4 (m, C-N), 1189.4, 1161.6, 1119.6 (s, C-O); *m/z* (EI) 549 ([M + H]⁺, 8%), 449 (26), 292 (28), 226 (37), 170 (23), 146 (17), 114 (100), 91 (37); **HRMS** found [M + H]⁺, 548.32112; C₂₈H₄₅N₄O₇ requires 548.32045.

3.44 3-(5-Methoxycarbonyl-pentylcarbamoyl)bicyclo[2.2.1]hept-5-ene-2-carboxylic acid (226)

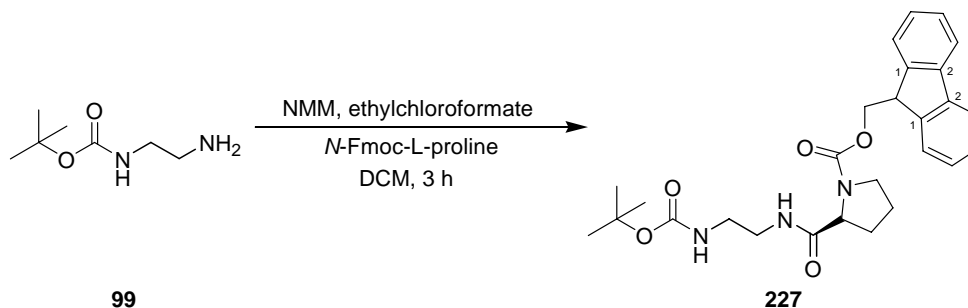


(1*R*, 2*S*, 6*R*, 7*R*)-4-Oxa-tricyclo[5.2.1.0^{2,6}]dec-8-ene-3,5-dione (6.60 g, 40.0 mmol) was added to 6-aminohexanoic acid methyl ester hydrochloride (9.00 g, 50.0 mmol) in anhydrous DCM (80 ml) and stirred at room temperature for 12 h. Solvent was then removed under reduced pressure and the residue was dissolved in sat. NaHCO₃ (50 ml). The aqueous layer was washed with EtOAc (3 × 20 ml) and then acidified using 2 M HCl. The aqueous layer was extracted with EtOAc (3 × 50 ml), dried (MgSO₄) and filtered. Solvent was removed under reduced pressure to give the product as a pale yellow oil (8.73 g, 71%).

¹H NMR (300 MHz, CDCl₃) 10.65 (1H, br s, COOH), 6.48 (1H, t, ³*J* = 5.6 Hz, NH), 6.36 (1H, m, CH=CHCHCHCOOH), 6.12 (1H, m, CH=CHCHCHCOOH), 3.64 (3H, s, CH₃), 3.23 (2H, m, NHCH₂), 3.16 (2H, m, CH=CHCHCHC=O), 3.07 (2H, m, CH=CHCHCHC=O), 2.30 (2H, t, ³*J* = 6.1 Hz, CH₂COOMe), 1.59 (2H, m, CH=CHCHCH₂), 1.48 – 1.30 (6H, m, NHCH₂(CH₂)₃CH₂COOMe); **¹³C NMR** (75 MHz, CDCl₃) 176.2 (C=O, acid), 174.4 (C=O, amide), 173.7 (C=O, ester), 136.4

(CH=CHCHCHCOOH), 133.9 (CH=CHCHCHCOOH), 51.6 (CH₃), 50.2 (NHCH₂), 49.7 (CH=CHCHCH₂), 49.1 (CHCOOH), 48.0 (CH=CHCHCHCOOH), 47.0 (CH=CHCHCHC=ONH), 46.1 (CH=CHCHCHC=ONH), 39.5 (CH₂COOMe), 33.9, 28.8, 26.3 (NHCH₂(CH₂)₃CH₂COOMe); ν_{\max} (neat/cm⁻¹) 3448.3 (br, O-H), 2946.4, 2868.1 (m, C-H), 1769.1 (s, C=O, acid), 1733.8 (s, C=O, amide), 1690.1 (s, C=O, ester), 1435.9 (m, C=C), 1397.4, 1337.0 (m, C-H bend), 1148.8, 1169.1 (s, C-O); *m/z* (Positive FAB) 332 ([M + Na]⁺, 61%), 314 (100), 292 (64), 260 (39), 248 (62), 227 (21), 205 (19), 194 (51), 176 (87), 166 (13), 154 (25); **HRMS** found [M + Na]⁺, 332.14766; C₁₆H₂₃NO₅Na requires 332.14738.

3.45 (S)-(9H-Fluoren-9-yl)methyl-2-([2-(*tert*-butoxycarbonyl)ethyl] carbamoyl)pyrrolidine-1-carboxylate (227)

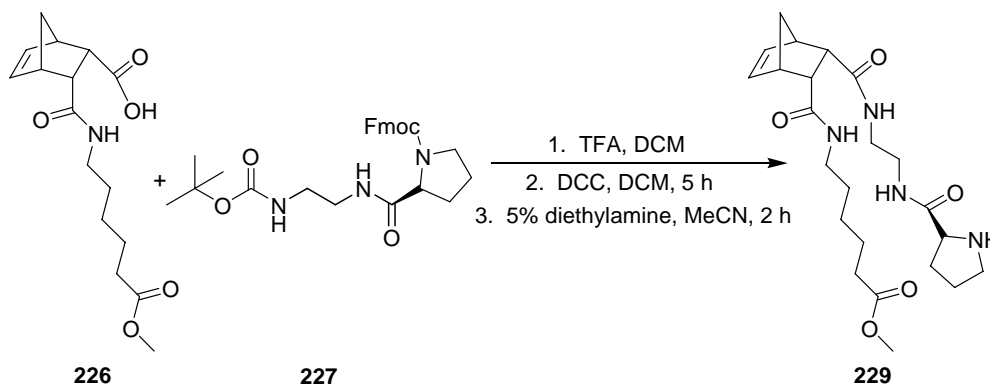


NMM (1.77 g, 1.90 ml, 17.5 mmol) was added to a stirred solution of *N*-Fmoc-L-proline (5.89 g, 17.5 mmol) in DCM (15 ml) at -15 °C. Ethyl chloroformate (1.90 g, 1.70 ml, 17.5 mmol) in DCM (10 ml) was added dropwise and stirred at this temperature for 20 mins. This was followed by portionwise addition of *N*-*tert*-butoxy(2-aminoethyl)carbamate (2.80 g, 17.5 mmol) in DCM (7 ml). The reaction mixture was allowed to warm to room temperature and left to stir for a further 3 h. Distilled water (50 ml) was added and the DCM layer separated. The aqueous phase was extracted with DCM (3 × 40 ml) and the combined organic layers washed with 0.5 M HCl (50 ml), sat. NaHCO₃ (50 ml) and brine (50 ml), dried (MgSO₄) and filtered. Solvent was removed under reduced pressure and the

crude product was purified by flash column chromatography (SiO₂; EtOAc/petroleum spirit (40 – 60 °C); 4:1) to yield the product as an off-white solid (8.32 g, 99%).

m.p. 48 – 50 °C; **R_f** = 0.33 (SiO₂; EtOAc/petroleum spirit (40 – 60 °C); 4:1); **[α]_D²³** = – 32.0 (*c* 1, CHCl₃); **¹H NMR** (500 MHz, CDCl₃) 7.91 (1H, br s, *NH*Pro), 7.75 – 7.26 (8H, m, Ar-H), 6.97 (1H, br s, *NH*Boc), 5.15 (1H, m, COOCH₂CH), 4.44 (1H, m, CH-N), 4.40 (2H, m, COOCH₂), 3.54 (2H, m, CH₂-N), 3.29 (2H, t, ³*J* = 5.8 Hz, CH₂*NH*Pro), 3.16 (2H, ³*J* = 5.8 Hz, CH₂*NH*Boc), 2.11 – 1.83 (4H, m, CH₂CH₂CH-N), 1.41 (9H, s, ^tBu); **¹³C NMR** (125 MHz, CDCl₃) 175.6 (*NHC=O*CH), 156.6 (*C=O*OCH₂), 156.0 (*C=O*O^tBu), 143.4 (*C*₁), 138.1 (*C*₂), 128.8, 128.0, 127.8, 127.1, 125.2, 124.4, 121.1, 120.1 (Ar-C), 79.4 (COOCH₂), 67.7 (*C*(CH₃)₃), 60.5 (CH-N), 47.3 (CH₂*NH*Boc), 41.4 (CH₂*NH*Pro), 40.3 (CH₂-N), 39.5 (COOCH₂CH), 28.4 (^tBu), 26.4 (CH₂CH-N), 19.5 (CH₂CH₂CH-N); **ν_{max}** (neat/cm⁻¹) 3329.0 (br, N-H), 2975.9, 2878.7 (m, C-H), 1692.5 (s, C=O), 1520.9 (m, C=C), 1450.2, 1417.7, 1364.8 (m, C-H bend), 1248.5 (m, C-N), 1167.6 (m, C-O); ***m/z*** (Positive ESI) 502 ([*M* + Na]⁺, 28%), 436 (43), 380 (37), 355 (34), 299 (18), 258 (34), 202 (100), 158 (18); **HRMS** found [*M* + Na]⁺, 502.22950; C₂₇H₃₃N₃O₅Na requires 502.23180.

3.46 (2S)-2-6-[(3-{2-[(Pyrrolidine-2-carbonyl)amino]ethylcarbamoyl} bicyclo[2.2.1]hept-5-ene-2-carbonyl)amino]hexanoic acid methyl ester (229)



TFA (10 ml) was added to a cooled solution of (*S*)-(9*H*-fluoren-9-yl)methyl-2-{{2-(*tert*-butoxycarbonyl)ethyl}carbamoyle}pyrrolidine-1-carboxylate (7.75 g, 16.2 mmol) in DCM (40 ml) and stirred for 2 h. DCM was removed under reduced pressure and the excess TFA by co-evaporation with toluene. The product was used in the next step without further purification.

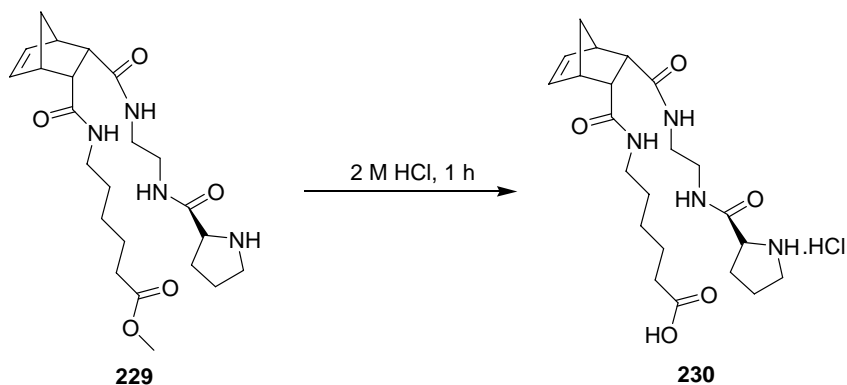
3-(5-Methoxycarbonyl-pentylcarbamoyle)bicyclo[2.2.1]hept-5-ene-2-carboxylic acid (5.00 g, 16.2 mmol) and the TFA salt of (*S*)-(9*H*-fluoren-9-yl)methyl-2-{{2-(*tert*-butoxycarbonyl)ethyl}carbamoyle}pyrrolidine-1-carboxylate prepared earlier were dissolved in anhydrous DCM (40 ml). To this DCC (5.00 g, 24.3 mmol) was added and stirred at room temperature for 5 h. The colourless by-product was removed by filtration and the organic phase was washed with 1 M HCl (50 ml), sat. NaHCO₃ (50 ml) and brine (50 ml). The combined organic layers were dried (MgSO₄) and filtered. Solvent was removed under reduced pressure to yield the crude product which was purified by flash column chromatography (SiO₂; MeOH/EtOAc; 3:22) to give product as a yellow solid (5.21 g, 47%).

Deprotection of the Fmoc group was then carried out by suspending the product obtained in diethylamine/MeCN; 1:20 (20 ml) for 2 h. at room temperature. The solvent was then removed under reduced pressure to yield the crude product which was purified by flash column chromatography (SiO₂; MeOH/DCM; 1:4) to give the product as a yellow oil (3.21 g, 92%).

R_f = 0.42 (SiO₂; MeOH/DCM; 1:4); **¹H NMR** (500 MHz, CDCl₃) 7.96 (1H, br s, NHCH₂CH₂NHPro), 6.81 (1H, br s, NHCH₂CH₂NHPro), 6.42 (1H, m, CH=CHCHCHC=ONH(CH₂)₂NH), 6.28 (1H, m, CH=CHCHCHC=ONH(CH₂)₂NH), 6.18 (1H, br s, NH(CH₂)₅COOMe), 3.81 (1H, m, CH-NH), 3.48 (3H, s, CH₃), 3.26 – 3.21 (6H, m, NH(CH₂)₂NH, NHCH₂(CH₂)₄), 3.13 – 3.04 (6H, m, CH=CHCHCHC=O, CH₂(CH₂)₂CHNH), 2.47 (1H, br s, NH, Pro), 2.30 (2H, t, ³J = 7.4 Hz, CH₂COOMe), 2.14, 1.89 (2H, m, CH=CHCHCH₂), 1.75 (2H, m, CH₂CHNH), 1.61 (2H, m, CH₂CH₂COOMe), 1.43 – 1.30 (6H, NHCH₂(CH₂)₂(CH₂)₂, CH₂CH₂CHNH); **¹³C NMR** (150 MHz,

CDCl₃) 175.8 (C=ONH(CH₂)₂NHPro), 174.2 (C=ONH(CH₂)₅), 173.5 (C=O, Pro), 172.6 (C=OOMe), 136.6 (CH=CHCHCHC=ONH(CH₂)₂NHPro), 135.6 (CH=CHCHCHC=ONH(CH₂)₂NHPro), 60.6 (CH-NH), 51.7 (COOCH₃), 50.1 (NHCH₂CH₂NHPro), 47.5 (NHCH₂CH₂NHPro), 47.2 (NHCH₂(CH₂)₄), 47.1 (CH₂(CH₂)₂CHNH), 47.0 (CH=CHCHCH₂), 40.4 (CH=CHCHCHC=O), 39.5 (CH=CHCHCHC=O), 38.9 (CH₂COOMe), 34.0 (NHCH₂CH₂(CH₂)₃), 30.6 (CH₂CHNH), 29.2, 26.5 (NH(CH₂)₂(CH₂)₂CH₂), 26.2 (CH₂CH₂CHNH); ν_{\max} (neat/cm⁻¹) 3270.1, 3069.9 (br, N-H), 2940.4, 2868.2 (m, C-H), 1735.1, 1646.9 (s, C=O), 1532.8 (m, C=C), 1435.0, 1365.4, 1337.5 (s, C-H bend), 1256.5, 1229.2 (m, C-N), 1163.3, 1105.6 (s, C-O); *m/z* (Positive ESI) 449 ([M + H]⁺, 100%), 383 (72), 292 (19), 238 (33), 226 (28); **HRMS** found [M + H]⁺, 449.27720; C₂₃H₃₇N₄O₅ requires 449.27640.

3.47 (2S)-2-6-[(3-{2-[(Pyrrolidine-2-carbonyl)-amino]ethylcarbamoyl} bicyclo[2.2.1]hept-5-ene-2-carbonyl)amino]hexanoic acid; hydrochloride (230)

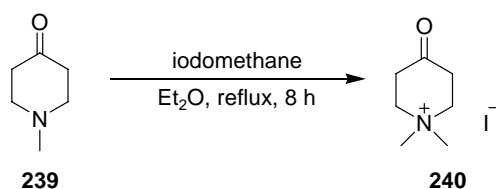


(2S)-2-6-[(3-{2-[(Pyrrolidine-2-carbonyl)amino]ethylcarbamoyl} bicyclo[2.2.1]hept-5-ene-2-carbonyl)amino]hexanoic acid methyl ester (1.00 g, 2.2 mmol) was stirred in 2 M HCl (10 ml) for 1 h. Excess 2 M HCl was removed by freeze drying to give the product as a yellow oil (1.03 g, 99%).

¹H NMR (500 MHz, DMSO) 10.20 (1H, br s, OH), 8.59 (1H, br s,

$\text{NHCH}_2\text{CH}_2\text{NHPro}$), 8.32 (1H, br s, $\text{NHCH}_2\text{CH}_2\text{NHPro}$), 6.44 (1H, m, $\text{CH}=\text{CHCHCHCHC}=\text{ONH}(\text{CH}_2)_2\text{NH}$), 6.22 (1H, m, $\text{CH}=\text{CHCHCHCHC}=\text{ONH}(\text{CH}_2)_2\text{NH}$), 6.05 (1H, br s, $\text{NH}(\text{CH}_2)_5\text{COOH}$), 4.10 (1H, m, CH-NH), 3.23 – 3.16 (6H, m, $\text{NH}(\text{CH}_2)_2\text{NH}$, $\text{NHCH}_2(\text{CH}_2)_4$), 3.14 – 2.96 (6H, m, $\text{CH}=\text{CHCHCHC}=\text{O}$, $\text{CH}_2(\text{CH}_2)_2\text{CHNH}$), 2.49 (1H, br s, NH, Pro), 2.24 (2H, t, $^3J = 7.4$ Hz, CH_2COOMe), 2.15 (2H, m, $\text{CH}=\text{CHCHCH}_2$), 1.85 (2H, m, CH_2CHNH), 1.45 (2H, m, $\text{CH}_2\text{CH}_2\text{COOH}$), 1.34 – 1.20 (6H, $\text{NHCH}_2(\text{CH}_2)_2(\text{CH}_2)_2$, $\text{CH}_2\text{CH}_2\text{CHNH}$); ^{13}C NMR (125 MHz, CDCl_3) 175.4 ($\text{C}=\text{ONH}(\text{CH}_2)_2\text{NHPro}$), 173.3 ($\text{C}=\text{ONH}(\text{CH}_2)_5$), 173.0 ($\text{C}=\text{O}$, Pro), 172.7 ($\text{C}=\text{OOH}$), 135.0 ($\text{CH}=\text{CHCHCHC}=\text{ONH}(\text{CH}_2)_2\text{NHPro}$), 134.4 ($\text{CH}=\text{CHCHCHC}=\text{ONH}(\text{CH}_2)_2\text{NHPro}$), 58.9 (CH-NH), 51.8 ($\text{NHCH}_2\text{CH}_2\text{NHPro}$), 51.2 ($\text{NHCH}_2\text{CH}_2\text{NHPro}$), 49.5 ($\text{NHCH}_2(\text{CH}_2)_4$), 45.4 ($\text{CH}_2(\text{CH}_2)_2\text{CHNH}$), 45.3 ($\text{CH}=\text{CHCHCH}_2$), 39.8 ($\text{CH}=\text{CHCHCHC}=\text{O}$), 39.5 ($\text{CH}=\text{CHCHCHC}=\text{O}$), 38.2 (CH_2COOH), 33.6 ($\text{NHCH}_2\text{CH}_2(\text{CH}_2)_3$), 29.4 (CH_2CHNH), 28.4, 25.9 ($\text{NH}(\text{CH}_2)_2(\text{CH}_2)_2\text{CH}_2$), 25.8 ($\text{CH}_2\text{CH}_2\text{CHNH}$); ν_{max} (neat/ cm^{-1}) 3363.9 (br, OH), 3226.2 (br, N-H), 2943.6 (m, C=C), 1437.2, 1397.3, 1335.9 (s, C-H bend), 1239.7 (m, C-N), 1186.1, 1105.5 (s, C-O); m/z (Positive ESI) 435 ($[\text{M} + \text{H}]^+$, 100%), 417 (46), 310 (22), 296 (95); HRMS found $[\text{M} + \text{H}]^+$, 435.26210; $\text{C}_{22}\text{H}_{35}\text{N}_4\text{O}_5$ requires 435.26070.

3.48 1,1-Dimethyl-4-oxo-piperidinium iodide (240)¹⁹⁰

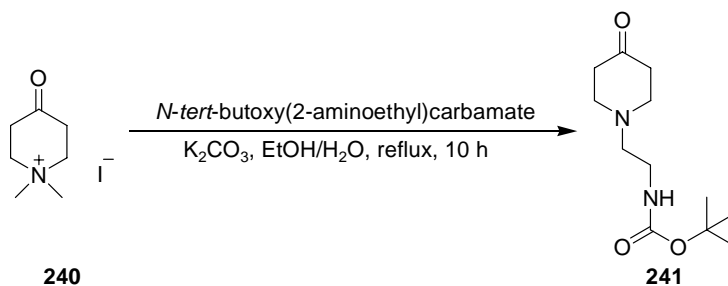


N -Methylpiperidine (3.00 g, 26.5 mmol) was added to anhydrous Et_2O (60 ml) and stirred under an atmosphere of N_2 for 20 mins. Iodomethane (4.00 g, 1.74 ml, 28.0 mmol) was then added dropwise and the reaction stirred at room temperature for 2 h and then heated at reflux for 8 h. The precipitate thus formed was

collected via filtration to give the product as a colourless solid (6.10 g, 90%).

m.p. 180 – 185 °C [lit. 186 – 188 °C];¹⁹⁰ **¹H NMR** (300 MHz, D₂O) 3.41 (4H, m, CH₂N⁺(CH₃)₂), 3.09 (6H, s, CH₃), 2.25 (4H, m, CH₂C=O); **¹³C NMR** (125 MHz, DMSO) 201.8 (C=O), 60.0 (CH₂N⁺(CH₃)₂), 50.9 (CH₂C=O), 35.1 (CH₃); **ν_{max}** (neat/cm⁻¹) 3340.5, 3215.0 (s, C-H), 1729.4 (s, C=O), 1457.8, 1323.7, 1193.0 (m, C-H bend); **m/z** (EI) 128 ([M]⁺, 100%), 113 (6), 98 (5); **HRMS** found [M]⁺, 128.10727; C₇H₁₄NO requires 128.10699.

3.49 [2-(4-Oxo-piperidin-1-yl)-ethyl]carbamic acid *tert*-butyl ester (241)



N-*tert*-Butoxy(2-aminoethyl)carbamate (0.20 g, 1.3 mmol) and K₂CO₃ (0.86 g, 6.3 mmol) were dissolved in a mixture of ethanol (EtOH) (17 ml) and distilled water (9 ml) and heated at reflux for 1 h. 1,1-Dimethyl-4-oxo-piperidinium iodide (0.80 g, 3.1 mmol) was then added dropwise to the reaction mixture and heated at reflux for a further 10 h. EtOH was then removed under reduced pressure and the aqueous layer was extracted with Et₂O (3 × 50 ml). The combined organic layers were dried (MgSO₄) and filtered. Solvent was removed under reduced pressure to give an orange residue. Purification by flash column chromatography (SiO₂; MeOH/EtOAc; 1:9) yielded the product as a pale yellow oil (0.28 g, 89%).

R_f = 0.40 (SiO₂; MeOH/EtOAc); 1:9); **¹H NMR** (400 MHz, CDCl₃) 4.96 (1H, br s, NH), 3.27 (2H, m, CH₂NH), 2.76 (4H, t, ³*J* = 6.4 Hz, CH₂CH₂C=O), 2.57 (2H, t, ³*J* = 5.8 Hz, CH₂CH₂NH), 2.45 (4H, t, ³*J* = 6.4 Hz, CH₂C=O), 1.46 (9H, s, ^tBu);

^{13}C NMR (125 MHz, CDCl_3) 208.9 (C=O, ketone), 156.0 (C=O, carbamate), 79.4 ($\text{C}(\text{CH}_3)_3$), 56.3 ($\text{CH}_2\text{CH}_2\text{NH}$), 52.9 ($\text{CH}_2\text{CH}_2\text{C}=\text{O}$), 41.2 (CH_2NH), 37.8 ($\text{CH}_2\text{C}=\text{O}$), 28.5 (CH_3); ν_{max} (neat/ cm^{-1}) 3356.4 (s, N-H), 2973.5, 2811.1 (m, C-H), 1708.6 (s, C=O), 1516.9 (s, N-H bend), 1365.0, 1249.4, 1168.7 (m, C-H bend), 1134.8 (m, C-O); m/z (Positive FAB) 265 ($[\text{M} + \text{Na}]^+$, 94%), 243 (48), 187 (100), 165 (25); HRMS found $[\text{M} + \text{Na}]^+$, 265.15205; $\text{C}_{12}\text{H}_{22}\text{N}_2\text{O}_3\text{Na}$ requires 265.15281.

3.50 7-Benzyl-9-oxo-3,7-diaza-bicyclo[3.3.1]nonane-3-carboxylic acid *tert*-butyl ester (244)¹⁹¹



A solution of 1-Boc-piperidin-4-one (2.00 g, 10.0 mmol), benzylamine (1.11 g, 10.3 mmol) and acetic acid (0.57 ml, 10.0 mmol) in anhydrous MeOH (50 ml) was added dropwise over a period of 1 h at 65 °C to a suspension of paraformaldehyde (0.66 g, 22.1 mmol) in anhydrous MeOH (40 ml). A further portion of paraformaldehyde (0.66 g, 22.1 mmol) was added and the reaction mixture was stirred for 1 h at 65 °C and then left to cool to room temperature. Distilled water (400 ml) and 1 M NaOH (20 ml) were then added and the aqueous phase was extracted with Et_2O (3×200 ml). The combined organic layers were dried (MgSO_4) and solvent was removed under reduced pressure. The crude product was purified by flash column chromatography (SiO_2 ; EtOAc/petroleum spirit (40 – 60 °C); 3:1) to give the product as a yellow solid (2.48 g, 75%).

R_f = 0.50 (SiO_2 ; EtOAc/petroleum spirit (40 – 60 °C); 3:2); ^1H NMR (300 MHz,

CDCl₃) 7.33 – 7.22 (5H, m, Ph), 4.57, 4.40 (2H, d, ²J = 8.0 Hz, CH₂_{eq}NBoc), 3.52, 3.45 (2H, d, ²J = 7.8 Hz, CH₂Ph), 3.35, 3.27 (2H, d, ²J = 8.0 Hz, CH₂_{ax}NBoc), 3.18, 3.14 (2H, d, ²J = 6.7 Hz, CH₂_{eq}NCH₂Ph), 2.71, 2.64 (2H, d, ²J = 6.7 Hz, CH₂_{ax}NCH₂Ph), 2.43, 2.39 (2H, s, CHCH₂N), 1.53 (9H, s, ^tBu); ¹³C NMR (125 MHz, CDCl₃) 213.6 (CHC=O), 154.8 (C=O, carbamate), 137.5 (C-CH₂), 129.8, 129.1, 128.8, 128.4, 127.3 (CH, Ph), 80.1 (C(CH₃)₃), 61.9 (CH₂Ph), 59.1, 58.7 (CH₂NCH₂Ph), 50.5, 49.8 (CH₂NBoc), 47.6 (CHC=O), 28.6 (C(CH₃)₃); **ν**_{max} (neat/cm⁻¹) 2975.0, 2932.9 (w, C=C), 2864.2, 2800.3 (w, C-H), 1732.3 (s, C=O, ketone), 1689.3 (s, C=O, carbamate), 1494.7, 1475.4 (w, C=C bend), 1454.6, 1420.2 1364.6 (m, C-H bends), 294.7, 1234.8 (m, C-N), 1165.4, 1124.1 (s, C-O); **m/z** (Positive FAB) 353 ([M + Na]⁺, 100%), 331 (30), 318 (13), 273 (76), 253 (77), 229 (53), 208 (27), 186 (56); **HRMS** found [M + Na]⁺, 353.18454; C₁₆H₂₆N₂O₃Na requires 353.18410.

References

1. Voet, D.; Voet, J. G. *Biochemistry*; J. Wiley & Sons: Hoboken, NJ, 2004.
2. Copeland, R. A. *Enzymes, a practical introduction to structure, mechanism, and data analysis*; Wiley-VCH: New York, 2000.
3. Pauling, L. *Nature* **1948**, *161*, 707.
4. Blow, D. M. *Acc. Chem. Res.* **1976**, *9*, 145.
5. Blow, D. M.; Birktoft, J. J.; Hartley, B. S. *Nature* **1969**, *221*, 337.
6. Davis, A. M.; Teague, S. J. *Angew. Chem., Int. Ed.* **1999**, *38*, 737.
7. Mader, M. M.; Bartlett, P. A. *Chem. Rev.* **1997**, *97*, 1281-1302.
8. Heginbotham, L.; Mackinnon, R. *Neuron* **1992**, *8*, 483.
9. Motherwell, W. B.; Bingham, M. J.; Six, Y. *Tetrahedron* **2001**, *57*, 4663.
10. Fersht, A. R.; Shi, J. P.; Knill-Jones, J.; Lowe, D. M.; Wilkinson, A. J.; Blow, D. M.; Brick, P.; Carter, P.; Waye, M. M. Y.; Winter, G. *Nature* **1985**, *314*, 235.
11. Rockwell, A.; Melden, M.; Copeland, R. A.; Hardman, K.; Decicco, C. P.; DeGrado, W. F. *J. Am. Chem. Soc.* **1996**, *118*, 10337.
12. Rosales, C.; Brown, E. J. *J. Biol. Chem.* **1992**, *267*, 1443.
13. Ma, J. C.; Dougherty, D. A. *Chem. Rev.* **1997**, *97*, 1303.
14. Kirby, A. J. *Angew. Chem., Int. Ed.* **1996**, *35*, 707.
15. Zimmerman, H. E.; Traxler, M. D. *J. Am. Chem. Soc.* **2002**, *79*, 1920.
16. Kimura, E.; Gotoh, T.; Koike, T.; Shiro, M. *J. Am. Chem. Soc.* **1999**, *121*, 1267.
17. Lorentzen, E.; Siebers, B.; Hensel, R.; Pohl, E. *Biochemistry* **2005**, *44*, 4222.
18. Plater, A. R.; Zgiby, S. M.; Thomson, G. J.; Qamar, S.; Wharton, C. W.; Berry, A. *J. Mol. Biol.* **1999**, *285*, 843.
19. List, B.; Lerner, R. A.; Barbas, C. F. *J. Am. Chem. Soc.* **2000**, *122*, 2395.
20. Seebach, D.; Boes, M.; Naef, R.; Schweizer, W. B. *J. Am. Chem. Soc.*

-
- 1983, 105, 5390.
21. Rizzi, G. P. *J. Org. Chem.* **1970**, 35, 2069.
 22. Hoang, L.; Bahmanyar, S.; Houk, K. N.; List, B. *J. Am. Chem. Soc.* **2003**, 125, 16.
 23. Arno, M.; Domingo, L. R. *Theor. Chem. Acc.* **2002**, 108, 232.
 24. Pan, Q.; Zou, B.; Wang, Y.; Ma, D. *Org. Lett.* **2004**, 6, 1009.
 25. Patel, S. K.; Murat, K.; Py, S.; Vallee, Y. *Org. Lett.* **2003**, 5, 4081.
 26. Benaglia, M.; Cinquini, M.; Cozzi, F.; Puglisi, A.; Celentano, G. *Adv. Synth. Catal.* **2002**, 344, 533.
 27. Liu, Y. X.; Sun, Y. N.; Tan, H. H.; Liu, W.; Tao, J. C. *Tetrahedron: Asymmetry* **2007**, 18, 2649.
 28. Font, D.; Sayalero, S.; Bastero, A.; Jimeno, C.; Pericas, M. A. *Org. Lett.* **2008**, 10, 337.
 29. Gruttadauria, M.; Giacalone, F.; Marculescu, A. M.; Noto, R. *Adv. Synth. Catal.* **2008**, 350, 1397.
 30. Tang, Z.; Yang, Z. H.; Cun, L. F.; Gong, L. Z.; Mi, A. Q.; Jiang, Y. Z. *Org. Lett.* **2004**, 6, 2285.
 31. Revell, J. D.; Wennemers, H. *Tetrahedron* **2007**, 63, 8420.
 32. Raj, M.; Vishnumaya; Ginotra, S. K.; Singh, V. K. *Org. Lett.* **2006**, 8, 4097.
 33. Guizzetti, S.; Benaglia, M.; Raimondi, L.; Celentano, G. *Org. Lett.* **2007**, 9, 1247.
 34. Berkessel, A.; Koch, B.; Lex, J. *Adv. Synth. Catal.* **2004**, 346, 1141.
 35. Tang, Z.; Cun, L. F.; Cui, X.; Mi, A. Q.; Jiang, Y. Z.; Gong, L. Z. *Org. Lett.* **2006**, 8, 1263.
 36. Chen, J. R.; Li, X. Y.; Xing, X. N.; Xiao, W. J. *J. Org. Chem.* **2006**, 71, 8198.
 37. Tzeng, Z. H.; Chen, H. Y.; Huang, C. T.; Chen, K. *Tetrahedron Lett.* **2008**, 49, 4134.
 38. Torii, H.; Nakadai, M.; Ishihara, K.; Saito, S.; Yamamoto, H. *Angew. Chem., Int. Ed.* **2004**, 43, 1983.
-

-
39. Kim, W.; McMillan, R. A.; Snyder, J. P.; Conticello, V. P. *J. Am. Chem. Soc.* **2005**, *127*, 18121.
 40. List, B. *Tetrahedron* **2002**, *58*, 5573.
 41. Inoue, T.; Weber, C.; Fujishima, A.; Honda, K. *Bull. Chem. Soc. Jpn.* **1980**, *53*, 334.
 42. Komiyama, M.; Hirai, H. *Chem. Lett.* **1980**, 1251.
 43. Shokat, K.; Uno, T.; Schultz, P. G. *J. Am. Chem. Soc.* **1994**, *116*, 2261.
 44. Breslow, R.; Nesnas, N. *Tetrahedron Lett.* **1999**, *40*, 3335.
 45. Tastan, P.; Akkaya, E. U. *J. Mol. Catal. A: Chem.* **2000**, *157*, 261.
 46. Yu, J. X.; Zhao, Y. Z.; Holterman, M. J.; Venton, D. L. *Bioorg. Med. Chem. Lett.* **1999**, *9*, 2705.
 47. Mattei, P.; Diederich, F. *Angew. Chem., Int. Ed.* **1996**, *35*, 1341.
 48. Haring, D.; Distefano, M. D. *Bioconjugate Chem.* **2001**, *12*, 385.
 49. Villiers, A. *C. R. Hebd. Seances Acad. Sci.* **1891**, *112*, 536.
 50. Schardinger, F.; Unters, Z. *Nahrungs-Genussmittel Gebrauchsgegenstande* **1903**, *6*, 865.
 51. Li, S.; Purdy, W. C. *Chem. Rev.* **1992**, *92*, 1457.
 52. Consonni, R.; Recca, T.; Dettori, M. A.; Fabbri, D.; Delogu, G. *J. Agric. Food Chem.* **2004**, *52*, 1590.
 53. Yuan, D. Q.; Dong, S. D.; Breslow, R. *Tetrahedron Lett.* **1998**, *39*, 7673.
 54. Rideout, D. C.; Breslow, R. *J. Am. Chem. Soc.* **1980**, *102*, 7816.
 55. Hudlicky, T.; Butora, G.; Fearnley, S. P.; Gum, A. G.; Persichini, P. J.; Stabile, M. R.; Merola, J. S. *J. Chem. Soc., Perkin Trans. 1* **1995**, 2393.
 56. Zoh, K. D.; Lee, S. H.; Suh, J. *Bioorg. Chem.* **1994**, *22*, 242.
 57. Kuroda, Y.; Hiroshige, T.; Sera, T.; Shiroiwa, Y.; Tanaka, H.; Ogoshi, H. *J. Am. Chem. Soc.* **1989**, *111*, 1912.
 58. Kuroda, Y.; Hiroshige, T.; Sera, T.; Ogoshi, H. *Carbohydr. Res.* **1989**, *192*, 347.
 59. Kuroda, Y.; Egawa, Y.; Seshimo, H.; Ogoshi, H. *Chem. Lett.* **1994**, 2361.
-

-
60. Kuroda, Y.; Hiroshige, T.; Ogoshi, H. *J. Chem. Soc., Chem. Commun.* **1990**, 1594.
 61. Breslow, R.; Kool, E. *Tetrahedron Lett.* **1988**, 29, 1635.
 62. Hilvert, D.; Breslow, R. *Bioorg. Chem.* **1984**, 12, 206.
 63. Breslow, R.; Dong, S. D. *Chem. Rev.* **1998**, 98, 1997.
 64. Cram, D. J.; Cram, J. M. *Acc. Chem. Res.* **1971**, 4, 204.
 65. Habicher, T.; Diederich, F.; Gramlich, V. *Helv. Chim. Acta* **1999**, 82, 1066.
 66. Mattei, P.; Diederich, F. *Helv. Chim. Acta* **1997**, 80, 1555.
 67. Tamchang, S. W.; Jimenez, L.; Diederich, F. *Helv. Chim. Acta* **1993**, 76, 2616.
 68. Breslow, R.; Yang, J.; Yan, J. *Tetrahedron* **2002**, 58, 653.
 69. Kang, J.; Santamaria, J.; Hilmersson, G.; Rebek, J. *J. Am. Chem. Soc.* **1998**, 120, 7389.
 70. Laschat, S. *Angew. Chem., Int. Ed.* **1996**, 35, 289.
 71. Ichihara, A.; Oikawa, H. *Biosci. Biotechnol., Biochem.* **1997**, 61, 12.
 72. Darbre, T.; Dubs, C.; Rusanov, E.; Stoeckli-Evans, H. *Eur. J. Inorg. Chem.* **2002**, 3284.
 73. Clyde-Watson, Z.; Vidal-Ferran, A.; Twyman, L. J.; Walter, C. J.; McCallien, D. W. J.; Fanni, S.; Bampos, N.; Wylie, R. S.; Sanders, J. K. M. *New J. Chem.* **1998**, 22, 493.
 74. Marty, M.; Clyde-Watson, Z.; Twyman, L. J.; Nakash, M.; Sanders, J. K. M. *Chem. Commun.* **1998**, 2265.
 75. Sanders, J. K. M. *Pure Appl. Chem.* **2000**, 72, 2265.
 76. Jencks, W. P. *Catalysis in chemistry and enzymology*; McGraw-Hill: New York, 1969.
 77. Tramontano, A.; Janda, K. D.; Lerner, R. A. *Science* **1986**, 234, 1566.
 78. Pollack, S. J.; Jacobs, J. W.; Schultz, P. G. *Science* **1986**, 234, 1570.
 79. Wagner, J.; Lerner, R. A.; Barbas, C. F. *Science* **1995**, 270, 1797.
 80. List, B.; Shabat, D.; Barbas, C. F.; Lerner, R. A. *Chem. Eur. J.* **1998**, 4, 881.
-

-
81. Zhu, X. Y.; Tanaka, F.; Hu, Y. F.; Heine, A.; Fuller, R.; Zhong, G. F.; Olson, A. J.; Lerner, R. A.; Barbas, C. F.; Wilson, I. A. *J. Mol. Biol.* **2004**, *343*, 1269.
 82. Karlstrom, A.; Zhong, G.; Rader, C.; Larsen, N. A.; Heine, A.; Fuller, R.; List, B.; Tanaka, F.; Wilson, I. A.; Barbas, C. F.; Lerner, R. A. *PNAS* **2000**, *97*, 3878.
 83. Matsui, J.; Nicholls, I. A.; Karube, I.; Mosbach, K. *J. Org. Chem.* **1996**, *61*, 5414.
 84. Oh, S.; Chang, W.; Suh, J. *Bioorg. Med. Chem. Lett.* **2001**, *11*, 1469.
 85. Slade, C. J.; Vulfson, E. N. *Biotechnol. Bioeng.* **1998**, *57*, 211.
 86. Peissker, F.; Fischer, L. *Bioorg. Med. Chem.* **1999**, *7*, 2231.
 87. Liu, J. Q.; Luo, G. M.; Gao, S. J.; Zhang, K.; Chen, X. F.; Shen, J. C. *Chem. Commun.* **1999**, 199.
 88. Ozawa, S.; Klibanov, A. M. *Biotechnol. Lett.* **2000**, *22*, 1269.
 89. Berkovich-Berger, D.; Lemcoff, N. G. *Chem. Commun.* **2008**, 1686.
 90. Cordes, E. H.; Bull, H. G. *Chem. Rev.* **1974**, *74*, 581.
 91. Sulzbacher, M.; Bergmann, E.; Pariser, E. R. *J. Am. Chem. Soc.* **1948**, *70*, 2827.
 92. Fife, T. H.; Jao, L. K. *J. Org. Chem.* **1965**, *30*, 1492.
 93. Lemcoff, N. G.; Fuchs, B. *Org. Lett.* **6-2-2002**, *4*, 731-734.
 94. Larsson, R.; Ramstrom, O. *Eur. J. Org. Chem.* **2006**, 285.
 95. Bunyapaiboonsri, T.; Ramstrom, O.; Lohmann, S.; Lehn, J. M.; Peng, L.; Goeldner, M. *Chembiochem* **2001**, *2*, 438.
 96. Bunyapaiboonsri, T.; Ramstrom, H.; Ramstrom, O.; Haiech, J.; Lehn, J. M. *J. Med. Chem.* **2003**, *46*, 5803.
 97. Ramstrom, O.; Lohmann, S.; Bunyapaiboonsri, T.; Lehn, J. M. *Chem. Eur. J.* **2004**, *10*, 1711.
 98. Otto, S.; Furlan, R. L. E.; Sanders, J. K. M. *J. Am. Chem. Soc.* **2000**, *122*, 12063.
 99. Ramstrom, O.; Lehn, J. M. *Chembiochem* **2000**, *1*, 41.
 100. Erlanson, D. A.; Lam, J. W.; Wiesmann, C.; Luong, T. N.; Simmons, R. L.;
-

-
- Delano, W. L.; Choong, I. C.; Burdett, M. T.; Flanagan, W. M.; Lee, D.; Gordon, E. M.; O'Brien, T. *Nat. Biotechnol.* **2003**, *21*, 308.
101. Hioki, H.; Still, W. C. *J. Org. Chem.* **1998**, *63*, 904.
102. Furlan, R. L. E.; Cousins, G. R. L.; Sanders, J. K. M. *Chem. Commun.* **2000**, 1761.
103. Eliseev, A. V.; Nelen, M. I. *Chem. Eur. J.* **1998**, *4*, 825.
104. Cardullo, F.; Calama, M. C.; Snellink-Ruel, B. H. M.; Weidmann, J. L.; Bielejewska, A.; Fokkens, R.; Nibbering, N. M. M.; Timmerman, P.; Reinhoudt, D. N. *Chem. Commun.* **2000**, 367.
105. McNaughton, B. R.; Gareiss, P. C.; Miller, B. L. *J. Am. Chem. Soc.* **2007**, *129*, 11306.
106. Menger, F. M.; Eliseev, A. V.; Migulin, V. A. *J. Org. Chem.* **2002**, *60*, 6666.
107. Menger, F. M.; West, C. A.; Ding, J. *Chem. Commun.* **1997**, 633.
108. De Kok, P. M. T.; Bastiaansen, L. A. M.; Van Lier, P. M.; Vekemans, J. A. J. M.; Buck, H. M. *J. Org. Chem.* **1989**, *54*, 1313.
109. Kofoed, J.; Darbre, T.; Reymond, J. L. *Org. Biomol. Chem.* **2006**, *4*, 3268.
110. Reetz, M. T. *Angew. Chem., Int. Ed.* **2001**, *40*, 284.
111. Mihovilovic, M.; Lee, J. E. *Biotechniques* **1989**, *7*, 14.
112. Arnold, F. H. *Acc. Chem. Res.* **1998**, *31*, 125.
113. Wells, J. A.; Vasser, M.; Powers, D. B. *Gene* **1985**, *34*, 315.
114. Stemmer, W. P. C. *Nature* **1994**, *370*, 389.
115. Reetz, M. T. *Tetrahedron* **2002**, *58*, 6595.
116. Zhao, H.; Arnold, F. H. *Protein Eng.* **1999**, *12*, 47.
117. Agresti, J. J.; Kelly, B. T.; Jäschke, A.; Griffiths, A. D. *PNAS* **2005**, *102*, 16170.
118. Bornscheuer, U. T.; Altenbuchner, J.; Meyer, H. H. *Bioorg. Med. Chem.* **1999**, *7*, 2169.
119. Joo, H.; Lin, Z.; Arnold, F. H. *Nature* **1999**, *399*, 670.
120. Joo, H.; Arisawa, A.; Lin, Z. L.; Arnold, F. H. *Chemistry & Biology* **1999**,
-

6, 699.

121. Reetz, M. T.; Wu, S. *Chem. Commun.* **2008**, 5499.
122. Reetz, M. T.; Kahakeaw, D.; Lohmer, R. *Chembiochem* **2008**, *9*, 1797.
123. Reetz, M. T.; Sanchis, J. *Chembiochem* **2008**, *9*, 2260.
124. Reetz, M. T.; Carballeira, J. D.; Peyralans, J.; Hobenreich, H.; Maichele, A.; Vogel, A. *Chem. Eur. J.* **2006**, *12*, 6031.
125. Carballeira, J. D.; Krumlinde, P.; Bocola, M.; Vogel, A.; Reetz, M. T.; Backvall, J. E. *Chem. Commun.* **2007**, 1913.
126. Clouthier, C. M.; Kayser, M. M.; Reetz, M. T. *J. Org. Chem.* **2006**, *71*, 8431.
127. Reetz, M. T.; Carballeira, J. D. *Nat. Protocols* **2007**, *2*, 891.
128. Motherwell, W. B.; Atkinson, C. E.; Aliev, A. E.; Wong, S. Y. F.; Warrington, B. H. *Angew. Chem., Int. Ed.* **2004**, *43*, 1225.
129. Atkinson, C. A. *PhD Thesis*; University of London, 2001.
130. Fielding, L. *Tetrahedron* **2000**, *56*, 6151.
131. Atkinson, C. E.; Aliev, A. E.; Motherwell, W. B. *Chem. Eur. J.* **2003**, *9*, 1714.
132. Wu, D.; Chen, A.; Johnson, C. S. *J. Magn. Reson.* **1995**, *115*, 260.
133. Fersht, A. *Structure and Mechanism in Protein Science: A Guide to Enzyme Catalysis and Protein Folding*; W. H. Freeman, New York, 2000.
134. Smiljanic, E. *PhD Thesis*; University of London, 2006.
135. Davies, M. C.; Dawkins, J. V.; Hourston, D. J. *Polymer* **2005**, *46*, 1739.
136. Antczak, C.; Bauvois, B.; Monneret, C.; Florent, J. C. *Bioorg. Med. Chem.* **2001**, *9*, 2843.
137. Nune, S. K. *Synlett* **2003**, 1221.
138. Mattingly, P. *Synthesis* **1990**, 366.
139. Kopka, K.; Wagner, S.; Riemann, B.; Law, M. P.; Puke, C.; Luthra, S. K.; Pike, V. W.; Wichter, T.; Schmitz, W.; Schober, O.; Schäfers, M. *Bioorg. Med. Chem.* **2003**, *11*, 3513.

-
140. Wakisaka, K.; Arano, Y.; Uezono, T.; Akizawa, H.; Ono, M.; Kawai, K.; Ohomomo, Y.; Nakayama, M.; Saji, H. *J. Med. Chem.* **1997**, *40*, 2643.
141. Ede, N. J.; Tregear, G. W.; Haralambidis, J. *Bioconjugate Chem.* **1994**, *5*, 373.
142. Lin, Y. M.; Miller, M. J. *J. Org. Chem.* **2001**, *66*, 8282.
143. Miyabe, H.; Takemoto, Y. *Bull. Chem. Soc. Jpn.* **2008**, *81*, 785.
144. Lee, J.; Lee, J.; Kim, J.; Kim, S. Y.; Chun, M. W.; Cho, H.; Hwang, S. W.; Oh, U.; Park, Y. H.; Marquez, V. E.; Beheshti, M.; Szabo, T.; Blumberg, P. M. *Bioorg. Med. Chem.* **2001**, *9*, 19.
145. Zlatušková, P.; Stibor, I.; Tkadlecová, M.; Lhoták, P. *Tetrahedron* **2004**, *60*, 11383.
146. Chernikova, E.; Terpugova, P.; Bui, C.; Charleux, B. *Polymer* **2003**, *44*, 4101.
147. Fessner, W. D.; Schneider, A.; Held, H.; Sinerius, G.; Walter, C.; Hixon, M.; Schloss, J. V. *Angew. Chem., Int. Ed.* **1996**, *35*, 2219.
148. Dreyer, M. K.; Schulz, G. E. *J. Mol. Biol.* **1993**, *231*, 549.
149. Chen, Z.; Trudell, M. L. *Chem. Rev.* **1996**, *96*, 1179.
150. Altenbach, H. J.; Blech, B.; Marco, J. A.; Vogel, E. *Angew. Chem., Int. Ed.* **1982**, *21*, 778.
151. Rajakumar, P.; Kannan, A. *Indian J. Chem., Sect B* **1993**, *32B*, 1275.
152. Drew, M. G. B.; George, A. V.; Isaacs, N. S.; Rzepa, H. S. *J. Chem. Soc., Perkin Trans. 1* **1985**, 1277.
153. Jones, R. A. *Pyrrroles*; Wiley: New York, 1990.
154. Leung-Toung, R.; Liu, Y.; Muchowski, J. M.; Wu, Y. L. *J. Org. Chem.* **1998**, *63*, 3235.
155. Jung, M. E.; Rohloff, J. C. *J. Chem. Soc., Chem. Commun.* **1984**, 630.
156. Aberle, N. S.; Ganesan, A.; Lambert, J. N.; Saubern, S.; Smith, R. *Tetrahedron Lett.* **2001**, *42*, 1975.
157. Kim, H.; Hoffmann, H. M. R. *Eur. J. Org. Chem.* **2000**, 2195.
158. Harmata, M.; Sharma, U. *Org. Lett.* **2000**, *2*, 2703.
-

-
159. Muller, S. N.; Batra, R.; Senn, M.; Giese, B.; Kisel, M.; Shadyro, O. *J. Am. Chem. Soc.* **1997**, *119*, 2795.
160. Berdini, V.; Cesta, M. C.; Curti, R.; D'Anniballe, G.; Bello, N. D.; Nano, G.; Nicolini, L.; Topai, A.; Allegretti, M. *Tetrahedron* **2002**, *58*, 5669.
161. Neipp, C. E.; Martin, S. F. *Tetrahedron Lett.* **2002**, *43*, 1779.
162. Zhao, L.; Johnson, K. M.; Zhang, M.; Flippen-Anderson, J.; Kozikowski, A. P. *J. Med. Chem.* **2000**, *43*, 3283.
163. Alder, K.; Betzing, H.; Heimbach, K. *Liebigs Annalen* **1960**, *638*, 187.
164. Kashima, C.; Harada, K.; Fujioka, Y.; Maruyama, T.; Omote, Y. *J. Chem. Soc., Perkin Trans. 1* **1988**, 535.
165. Chen, L. G.; Gill, G. B.; Pattenden, G.; Simonian, H. *J. Chem. Soc., Perkin Trans. 1* **1996**, 31.
166. Leanza, W. J.; Becker, H. J.; Rogers, E. F. *J. Am. Chem. Soc.* **1953**, *75*, 4086.
167. Mancuso, A. J.; Huang, S. L.; Swern, D. *J. Org. Chem.* **1978**, *43*, 2480.
168. Dalcanale, E.; Montanari, F. *J. Org. Chem.* **1986**, *51*, 567.
169. Ranganathan, D.; Haridas, V.; Kurur, S.; Thomas, A.; Madhusudanan, K. P.; Nagaraj, R.; Kunwar, A. C.; Sarma, A. V. S.; Karle, I. L. *J. Am. Chem. Soc.* **1998**, *120*, 8448.
170. Delatorre, B. G.; Torres, J. L.; Bardaji, E.; Clapes, P.; Xaus, N.; Jorba, X.; Calvet, S.; Albericio, F.; Valencia, G. *J. Chem. Soc., Chem. Commun.* **1990**, 965.
171. Fleming, I.; Kindon, N. D.; Sarkar, A. K. *Tetrahedron Lett.* **1987**, *28*, 5921.
172. Madan, R.; Srivastava, A.; Anand, R. C.; Varma, I. K. *Prog. Polym. Sci.* **1998**, *23*, 621.
173. Blackwell, H. E.; O'Leary, D. J.; Chatterjee, A. K.; Washenfelder, R. A.; Bussmann, D. A.; Grubbs, R. H. *J. Am. Chem. Soc.* **1999**, *122*, 58.
174. Dias, E. L.; Nguyen, S. T.; Grubbs, R. H. *J. Am. Chem. Soc.* **1997**, *119*, 3887.
175. Belderrain, T. R.; Grubbs, R. H. *Organometallics* **2-9-1997**, *16*, 4001.
176. Liaw, D. J.; Huang, C. C.; Hong, S. M. *J. Polym. Sci., Part A: Polym. Chem.* **2006**, *44*, 6287.
-

-
177. Phuan, P. W.; Ianni, J. C.; Kozlowski, M. C. *J. Am. Chem. Soc.* **2004**, *126*, 15473.
178. Spieler, J.; Huttenloch, O.; Waldmann, H. *Eur. J. Org. Chem.* **2000**, 391.
179. Lesma, G.; Danieli, B.; Passarella, D.; Sacchetti, A.; Silvani, A. *Tetrahedron: Asymmetry* **2003**, *14*, 2453.
180. Dutton, J. K.; Knox, J. H.; Radisson, X.; Ritchie, H. J.; Ramage, R. *J. Chem. Soc., Perkin Trans. 1* **1995**, 2581.
181. Keller, O.; Rudinger, J. *Helv. Chim. Acta* **1975**, *58*, 531.
182. Banerjee, S. R.; Schaffer, P.; Babich, J. W.; Valliant, J. F.; Zubieta, J. *Dalton Trans.* **2005**, 3886.
183. Omata, K.; Aoyagi, S.; Kabuto, K. *Tetrahedron: Asymmetry* **2004**, *15*, 2351.
184. Stoutland, O. L. I. V.; Helgen, L. O. N.; Agre, C. *J. Org. Chem.* **1959**, *24*, 818.
185. Ulman, A.; Urankar, E. *J. Org. Chem.* **1989**, *54*, 4691.
186. Mosse, S.; Alexakis, A. *Org. Lett.* **2006**, *8*, 3577.
187. Davies, H. M. L.; Saikali, E.; Huby, N. J. S.; Gilliatt, V. J.; Matasi, J. J.; Sexton, T.; Childers, S. R. *J. Med. Chem.* **1994**, *37*, 1262.
188. Bargiband, R. F.; Winston, A. *Tetrahedron* **1972**, *28*, 1427.
189. Politis, J. K.; Nemes, J. C.; Curti, M. D. *J. Am. Chem. Soc.* **2001**, *123*, 2537.
190. Thompson, M. D.; Holt, E. M.; Berlin, K. D.; Scherlag, B. J. *J. Org. Chem.* **1985**, *50*, 2580.
191. Huttenloch, O.; Laxman, E.; Waldmann, H. *Chem. Eur. J.* **2002**, *8*, 4767.
-